Analysis of senescence-like growth arrest induced by RUNX1 and its fusion derived oncoproteins

Kamil K Wolyniec

A thesis submitted for the degree of Doctor of Philosophy

UNIVERSITY of GLASGOW

Molecular Oncology Laboratory
Institute of Comparative Medicine
Faculty of Veterinary Medicine
University of Glasgow

November 2008

Table of contents

List of tables

List of figures

Abbreviations

AML	Acute myeloid leukaemia
AGM	Aorta-gonad-mesonephros
ARF	Alternative Reading Frame
ATP	Adenosine triphosphate
ATR	A-T Rad3-related protein
ATM	Ataxia telangiectasia mutated
B-ALL	B cell acute lymphoblastic leukaemia
bp	Base pairs
BrdU	Bromodeoxyuridine
BSA	Bovine serum albumin
CBF	Core binding factor
CDK	Cyclin dependent kinase
CDKI	Cyclin dependent kinase inhibitor
CHK	Checkpoint
° C	Degree centigrade
DAPI	Diamidino-2-phenylindole
DCF	Dichloro fluorescein
DNA	Deoxyribonucleic acid
DDR	DNA damage response
ddH_2O	Double distilled water
DSB	Double strand breaks
DNMT	DNA methyl transferase
DMEM	Dulbecco's modified eagle's medium
DMSO	Dimethyl sulphoxide
ENU	Ethyl nitrosourea
ECL	Enhanced chemiluminescence
ERK	Extracellular signlal regulated kinase
ETS	E twenty six family of transcription factors
FACS	Fluorescence activated cell sorting

FCS	Foetal calf serum
FPD	Familial platelet disorder
g	Gram
GM-CSF	Granulocyte monocyte colony stimulating factor
HDAC	Histone deacetylase
HEL	Human erythroleukaemic line
HLH	Human Embryonic Kidney Cells
HPV	Human papillomavirus
HRP	Horseradish peroxidase
HSC	Haematopoietic stem cells
IL	Interleukin
Kb	Kilobase pairs
kDa	Kilodaltons
L	Litre
µg	Microgram
µl	Microlitre
mg	Milligram
ml	Millilitre
mM	Millimolar
mRNA	Messenger ribonucleic acid
MAPK	Mitogen activated protein kinase
MDM	Murine double minute
MDS	Myelodysplastic syndrome
MEF	Murine embryonic fibroblasts
MEK	MAP-ERK kinase
MINK	Misshapen/NIK-Related Kinase
MKK	Mitogen activated protein kinase kinase
Mo-MuLV	Moloney murine leukaemia virus
MYH	Myosin heavy chain
NAC	N-acetyl cystein
nCoR	Nuclear receptor corepressor
PAGE	Polyacrylamide gel electrophoresis

PBS	Phosphate buffered saline
PCNA	Proliferating cell nuclear antigen
PCR	Polymerase chain reaction
PEBP	Polyomavirus enhancer binding protein
PKC	Protein kinase C
PML	Promyleocytic leukemia
Rb	Retinoblastoma protein
ROS	Reactive oxygen species
RNase	Ribonuclease
RUNX	Runt related transcription factor
RNA	Ribonucleic acid
SA-ß-Gal	Senescence associated beta galactosidase
SAHF	Senescence associated heterochromatin foci
SDF	Senescence associated DNA damage foci
SDS	Sodium dodecyl sulphate
shRNA	Small hairpin RNA
STASIS	Stress or aberrant signaling induced senescence
SV40	Simian Virus 40
TGF	Transforming growth factor
TLE	Transducin like enhancer of split
UTR	Upstream terminal region
UV	Ultraviolet
WARTS	WTS/large tumour-suppressor 1 mitotic kinase
WT	Wild type
YAP	Yes associated protein

Acknowledgements

I would like to thank all the people that have had a substantial influence on my life and who inspired me over years.

I would like to express my deepest gratitude to my principal investigators, Professor Jim Neil and Professor Ewan Cameron who provided me with the opportunity to work on the exciting project allowing me a profound exploration of my scientific passion.

For the great kindness and understanding, never ending support and patience, excellent technical assistance and every day lab-chats if not to mention cake parties I would like to thank all the members of Molecular Oncology Laboratory, especially my laboratory supervisor Dr. Sandra Wotton, Dr. Anna Kilbey, Alma Jenkins, Dr. Monica Stewart and Dr. Karen Blyth.

I would like to thank our collaborators Prof. Gordon Peters (Cancer Research UK, London Research Institute, London) and Prof. Carol Stocking (Heinrich-Pette-Institute, Hamburg, Germany) who kindly provided us with cells and retroviral constructs.

My appreciation also goes to Dr. Tina Rich (Institute of Comparative Medicine, University of Glasgow) and members of Retroviral Pathogenesis lab (Institute of Comparative Medicine, University of Glasgow) for all the chats and fruitful discussions.

Special regards go to all my beautiful friends, in particular new friends that I made in Glasgow without whom these 3 years in Scotland would not be so intense and colourful: Neil, Franck and the rest of Irish folks, ‘Roxborough family’, Ben Bike, nimble capoeristas…

Warm Hugs to my great family for all the love and Paulinka for the lesson of life.

I dedicate this dissertation to my lovely mum and dad.

Author's declaration

I declare that the work described in this thesis was carried out personally in Molecular Oncology Laboratory, Institute of Comparative Medicine, University of Glasgow unless otherwise stated, and has not been submitted in full or in part for consideration for any other degree or qualification.

_____

Kamil K Wolyniec

November 2008

Abstract

Cellular senescence is an end point of a signal transduction programme leading to irreversible cell cycle arrest accompanied by characteristic alterations to cell morphology, biochemical properties and gene expression profile. This phenotype can be triggered by a variety of stimuli including telomere shortening, DNA damage or activated oncogenes. Senescence is now recognised as a tumour suppressor mechanism mediated by p53 and pRB pathways which act to prevent the proliferation of cells that are at risk of tumourigenic transformation.

RUNX1 is a transcription factor essential for definitive hematopoiesis and is frequently targeted in human leukaemias by chromosomal rearrangements. RUNX1 has been also demonstrated to act as a dominant oncogene in mice and the ectopic expression of RUNX1 in murine embryonic fibroblasts has been shown to cause senescence.

The central aim of this study was to investigate the mechanism of senescence induction by RUNX1 and its fusion derived leukaemogenic oncoproteins in primary fibroblasts.

My work showed that RUNX1 induces a strong senescence-like response in murine and human primary fibroblasts that requires intact DNA binding, CBFß interaction and C-terminal transcriptional activation/repression domains. However, surprising differences were found between the major RUNX1 fusion oncoprotein derivatives. The N-terminal fusion protein TEL-RUNX1 fails to induce senescence despite retention of a virtually full-length RUNX1 moiety, while the senescence-inducing potential is exaggerated in the truncated C-terminal fusion protein RUNX1-ETO (AML1-ETO). The potential to drive senescence is retained by the deletion mutant RUNX1-ETOΔ469 which lacks critical corepressor binding sites suggesting that the repression of target genes may be a primary mechanism implicated in RUNX1-ETO induced senescence. Interestingly, CBFß-MYH11 fusion oncoprotein that affects RUNX1 indirectly by targeting CBFß can also induce senescence when ectopically expressed in human primary cells. The RUNX1 and RUNX1-ETO induced senescent phenotypes differ from archetypal H-Ras^{V12} as arrest occurs without a preliminary phase of proliferation and the arrested cells lack prominent foci of DNA strand breaks and chromatin condensation. Notably however, RUNX1 and RUNX1-ETO display

differences in their potency and the extent of engagement of p53 and Rb effector pathways. RUNX1-ETO is highly dependent on p53 function and unlike RUNX1 drives senescence in cells lacking intact p16Ink4a. RUNX1-ETO appears to exert its unique effects through potent induction of reactive oxygen species and p38MAPK phosphorylation. These findings illustrate the heterogeneous manifestations of senescence-like growth arrest and elucidate the distinctive biology and oncogenic properties of RUNX1 and its fusion derivatives.

Chapter 1

1 Introduction

1.1 Characteristics of RUNX transcription factors

The RUNX (Runt-related transcription factor) genes encode the DNA-binding α-chain partners of the CBF (core binding factor) complexes that play crucial lineage-specific roles in cell proliferation and differentiation. The Runx proteins form heterodimers with a non-DNA-binding partner, CBFβ that is encoded by a single gene in mammals and lacks intrinsic DNA binding activity but profoundly enhances the affinity of its α-chain partner for DNA and confers stability on the complex(Blyth et al 2005; Ito 2004; Ogawa et al 1993a; Ogawa et al 1993b; Wang et al 1993).

The *Drosophila* regulatory gene *runt*, which functions in establishing segmentation patterns during embryogenesis as well as in sex determination and neurogenesis, was the first member of RUNX family to be identified twenty years ago (Duffy et al 1991; Duffy and Gergen 1991; Gergen and Butler 1988). Other invertebrate species with well-characterized RUNX transcription factors include the nematode *Caenorhabditis elegans* and the sea urchin S*trongylocentrotus purpuratus* (Nam et al 2002; Robertson et al 2002). Some lower organisms have only a single RUNX gene but in vertebrates multiplication of RUNX genes through gene duplication has occurred (Rennert et al 2003). Three highly conserved human and mouse RUNX genes: *RUNX1, RUNX2 and RUNX3* were identified and localized on human chromosomes 21, 6 and 1 and on mouse chromosomes 16, 17 and 4, respectively (Avraham et al 1995; Bae et al 1994; Calabi et al 1995; Levanon et al 1994). The three mammalian RUNX genes share extensive homology, which is also found in paralogous genes, *CLIC* and *DSCR,* that are adjacent to RUNX loci (Eggers et al 2002; Levanon et al 2001; Levanon et al 2003b) (Figure 1.1). All three mammalian RUNX genes are transcriptionally regulated by two independent promoter regions, P1 (distal) and P2 (proximal) that encode isoforms with distinct amino-terminal sequences (Levanon and Groner 2004) (Figure 1.1).

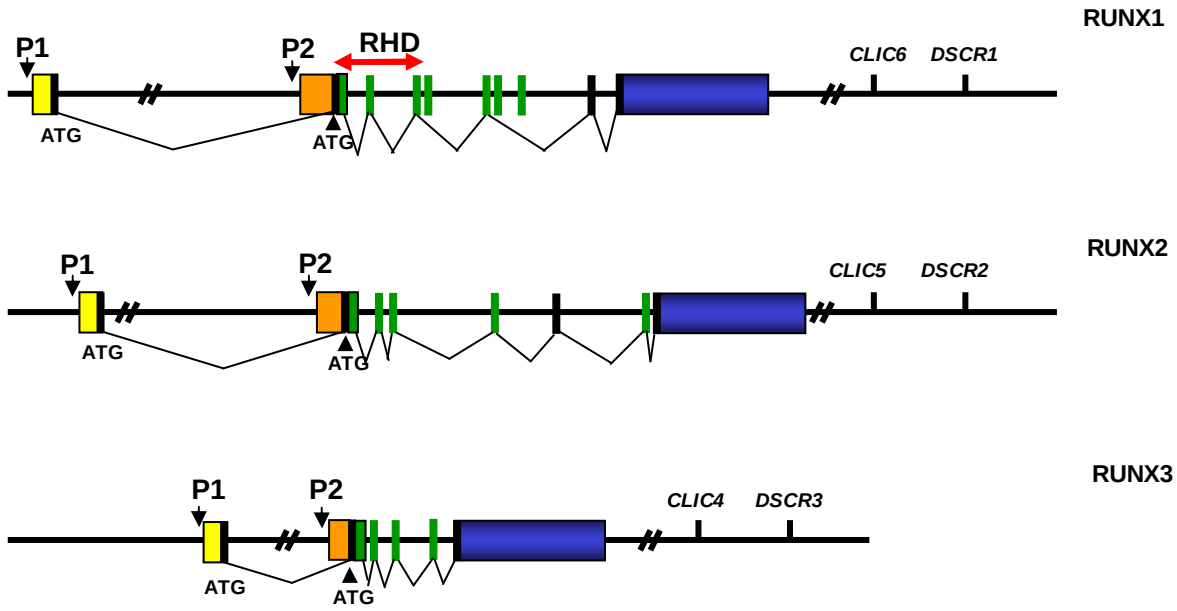

Figure 1.1 Genomic organization of the human RUNX genes

The two promoters P1 and P2 and initiator ATGs are indicated. 5'UTR are in yellow and orange and 3'UTR are in blue. Common exons are shown in similar colour and conserved neighbouring genes (CLIC and DSCR) are depicted

The most highly conserved feature of the RUNX proteins is the 128-amino-acid Runt domain that functions in DNA binding, protein-protein interactions, ATP binding and which also contributes to nuclear localisation (Crute et al 1996; Kagoshima et al 1993; Kanno et al 1998a). The runt domain lies in the N-terminal half of the protein. Structural analysis has revealed that this domain forms an S-type immunoglobulin fold which has also been identified in the 3-dimensional structure of the DNA binding domains of transcription factors such as p53, NF-κB, NFAT, STAT, and the T-box proteins (Figure 1.2) (Berardi et al 1999; Nagata et al 1999). Outside the runt domain there is less sequence similarity between family members, although the similarity in amino acid composition is evident. The carboxy-terminal regions of RUNX proteins tend to be rich in proline, serine and threonine (PST) and regions of homology can be noticed in the functionally defined transactivation/inhibitory domains, nuclear-matrix-attachment signal and in the C-terminal VWRPY motif that functions as a recruitment motif for the Groucho/TLE family of corepressors (Aronson et al 1997; Levanon et al 1994; Zeng et al 1997). The RUNX proteins bind directly to target genes and activate or repress transcription depending on the context (Otto et al 2003; Speck and

Gilliland 2002). The DNA-binding affinity of RUNX alpha chains is increased substantially via co-interaction with the non-DNA-binding β-chain cofactor which binds to the runt domain (Ogawa et al 1993a; Ogawa et al 1993b; Wang et al 1993) and could be also potentially regulated by other cofactors and by chromatin structure.

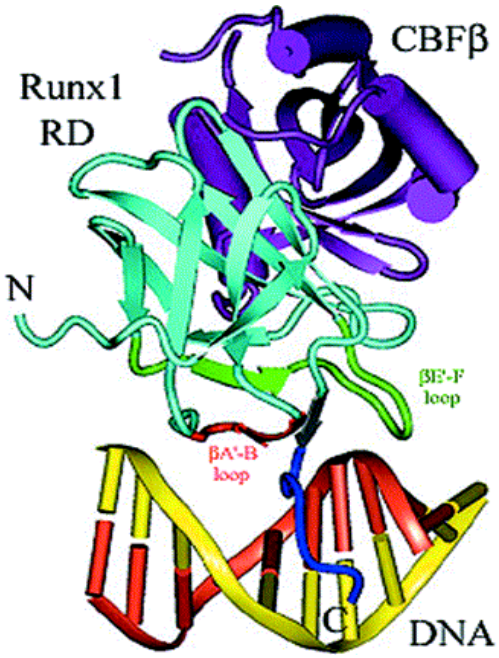

Figure 1.2 Structure of the RUNX1 Runt domain-CBFβ-DNA complex

DNA is shown in red and yellow. CBFβ is shown in magenta and the RUNX1 Runt domain in cyan. Runt domain loops in the major groove are coloured blue (C-terminal loop) and red (βA'-B loop), whereas the loop contacting the minor groove is shown in green (βE'-F loop) (Zhang et al 2003c)

The RUNX proteins are key regulators of major developmental pathways and their expression is tightly regulated, leading to highly specific spatio-temporal expression patterns which when disrupted lead to various defects. RUNX1 is required for definitive haematopoiesis and is frequently mutated in human leukaemia (Speck and Gilliland 2002). RUNX2 is essential for osteogenesis and its haploinsufficiency is associated with cleidocranial dysplasia in humans (Komori et al 1997; Otto et al 2002). More recently, RUNX3 was shown to control some aspects of neurogenesis and thymopoiesis as well as play a role in the control of cell proliferation and apoptosis in the gastric epithelium (Inoue et al 2003; Levanon et al 2002; Levanon et al 2003a; Taniuchi et al 2002; Woolf et al 2003). RUNX3 is also frequently methylated in human gastric cancers (Li et al 2002). A growing body of evidence implicates RUNX genes as tumour suppressors in some cancers, where inactivating mutations, gene deletions or hypermethylation occur. On the other hand transcriptional activation of all three RUNX genes by retroviral insertional mutagenesis in lymphoma-prone CD2-MYC transgenic mice has revealed their dominant oncogenic potential. A common result of these insertions was found to be the overexpression of structurally intact RUNX gene products (Blyth et al 2001; Stewart et al 1996; Stewart et al 1997; Stewart et al 2002; Wotton et al 2002).

1.2 Nomenclature of RUNX proteins

To avoid unnecessary confusion, an ad-hoc nomenclature committee on Runt-domain proteins, has proposed the unified terms RUNX1, RUNX2, RUNX3 (the homologous genes in mouse are Runx1, Runx2, Runx3, respectively) that refer to transcriptional factors which had previously been described by multiple terms (van Wijnen et al 2004). RUNX1 has previously been designated by different names: AML1 (acute myeloid leukemia 1), PEBP2αB (polyoma virus enhancer-binding protein 2αB) and CBFA2 (core-binding factor α2). RUNX2 could be found under names such as: AML3, PEBP2αA, CBFA1. Finally RUNX3 was known in the literature as: AML2, PEBP2αC, CBFA3.

1.3 Transcriptional regulation by RUNX1

There are three major isoforms of the RUNX1 protein that are produced by alternative splicing: AML1c (RUNX1-P1), AML1b (RUNX1-P2) and AML1a that have been reported so far (Meyers et al 1993; Miyoshi et al 1991; Miyoshi et al 1995) (Figure 1.3). AML1b (453 amino acid) and AML1c (480 amino acid) contain the runt homology domain as well as a proline-, serine- and threonine-rich (PST) region which is a putative transcriptional activation domain (Bae et al 1994). The difference in length between AML1b and AML1c arises from the use of two different promoters: AML1b is transcribed from proximal-P2 (MRIPV) promoter whereas AML1c is transcribed from distal-P1 (MASDS) promoter. The shorter 250 amino acid AML1a protein lacks the C-terminus including transactivation domain (PST region) but has a unique nine amino acids at its C-terminal end due to alternative splicing and can act as a competitive inhibitor of RUNX1 (Miyoshi et al 1991; Niitsu et al 1997; Tanaka et al 1995). For example it was reported that overexpression of AML1a blocks differentiation and promotes proliferation of murine myeloid cell line, whereas RUNX1 has the opposite effect of promoting differentiation and arresting proliferation (Tanaka et al 1995). RUNX1 binds to consensus sequence (PyGPyGGT, where Py is a pyrimidine) termed PEBP1 site, that was originally identified in polyomaviral and retroviral core enhancer elements (Kamachi et al 1990; Wang and Speck 1992).

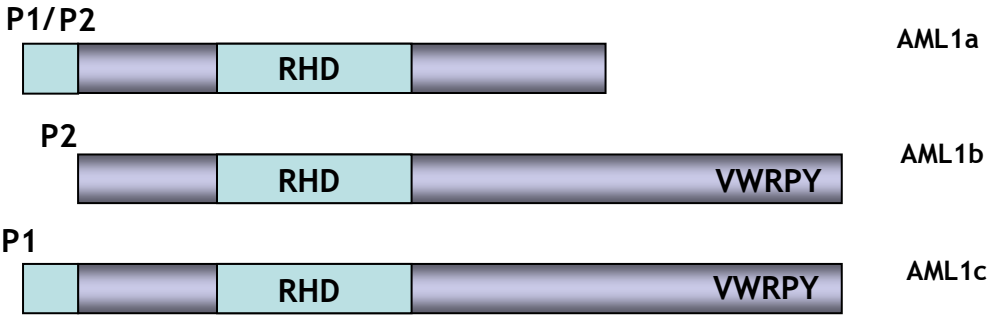

Figure 1.3 Structure of AML1a, AML1b and AML1c

RHD is the Runt homology domain, VWRPY indicates the C-terminal Groucho binding motif of RUNX1 family members, P1 –distal promoter, P2 –proximal promoter

1.3.1 Transcriptional activation

Most of the genes that have been shown to be activated by RUNX1 are involved in haematopoiesis i.e. T-cell and B-cell antigen receptor subunits (Erman et al 1998; Prosser et al 1992; Redondo et al 1992; Wang et al 1993), interleukin 3 (Uchida et al 1997), granulocyte-macrophage colony-stimulating factor (Hohaus et al 1995; Takahashi et al 1995), neutrophil elastase (Nuchprayoon et al 1994), myeloperoxidase (Britos-Bray and Friedman 1997; Nuchprayoon et al 1994) and granzyme B (Wargnier et al 1995). Because RUNX1 binding sites are necessary but not sufficient for transcriptional activation, this has led to the hypothesis that RUNX1 is an orchestrator of assembly of transcriptional activation complexes (Figure 1.4). The mechanism proposed for activation by the RUNX1/CBFβ complex is that it recruits coactivators such as p300/CBP (p300/CREB-binding protein), yes-associated protein (YAP) and ALY (Bruhn et al 1997; Kitabayashi et al 1998; Yagi et al 1999). These coactivators do not bind DNA directly, but stimulate transcription by acetylating histones and/or recruiting the RNA polymerase II transcription-initiating complex. However, the RUNX1/CBFβ complex is regarded as a relatively inefficient transcriptional activator and requires synergistic cooperation with other transcription factors. In this regard RUNX1 binding sites are frequently adjacent to binding sites of of Myb, Ets, AP-1 and C/EBP factors and RUNX1 cooperates with these transcription factors to activate transcription (Frank et al 1995; Hernandez-Munain and

Krangel 1994; Mao et al 1999; Petrovick et al 1998; Sun et al 1995; Zhang et al 1996).

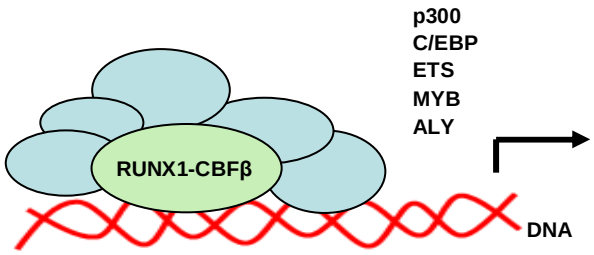

Figure 1.4 RUNX1 as an organizer of trancriptional activation

RUNX1-CBFβ complex binds to the consensus sequence and interacts with coactivators (p300, C/EBP, ETS, MYB, ALY, AP-1) to initiate transcriptional activation

1.3.2 Transcriptional repression

Paradoxically, RUNX1 can also be a context-dependent transcriptional repressor, although this function of RUNX1 remains largely enigmatic. The CD4 gene is probably the best characterised example of RUNX1 mediated transcriptional repression that occurs during T lymphocyte development. RUNX1 binds the silencer and represses CD4 transcription in immature thymocytes (Taniuchi et al 2002). The other mechanism has been recently proposed whereby RUNX1 binds positive transcription elongation factor b (P-TEFb) and represses transcriptional elongation by RNA polymerase II (Jiang et al 2005). Another example is the transcriptional repression of $p21^{WAF1}$ promoter in NIH3T3 and HEL cells (human erythroleukaemic cell line) (Lutterbach et al 2000). Interestingly, RUNX1 mediated repression of $p21^{WAF1}$ in these cells was independent of the Groucho interaction motif but required two C-terminal domains of RUNX1 (amino acids 208-237 and amino acids 290-387). One of these domains (amino acids 208-237) is adjacent to the runt domain and is required for interaction with the mSin3A and mSin3B corepressor proteins. However, the association with mSin3 was shown to be necessary but not sufficient for potent repression, since the other mutant (amino acids 290-387) that is still able to bind mSin3, was not found to be an efficient repressor (Lutterbach et al 2000). It is plausible that there could

be several different mechanisms of gene repression by RUNX1. In general, it has been proposed that the repressive property of RUNX1 is attributed to the recruitment of transcriptional corepressors such as histone deacetylases (HDACs), transducing-like enhancer of split (TLE), nuclear receptor corepressor (nCoR), mSin3 and SUV39H1 (Figure 1.5) (Aronson et al 1997; Chakraborty et al 2003; Durst and Hiebert 2004; Lutterbach et al 2000; Reed-Inderbitzin et al 2006).

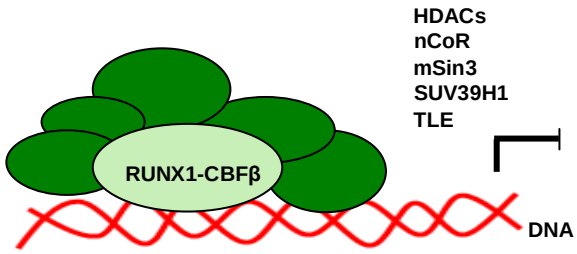

Figure 1.5 RUNX1 as an organizer of transcriptional repression
RUNX1-CBFβ complex binds to the consensus sequence and interacts with corepressors (HDACs, nCoR, mSin3, SUV39H1, TLE) to initiate transcriptional repression

If RUNX1 is capable of both transcription repression and activation it is of particular interest to understand the mechanism that converts RUNX1 from an activator to a repressor of transcription. Although an extensive survey in various cell types has not as yet been reported there is some evidence that repression by RUNX1 could be cell type and tissue specific. It has been shown that although RUNX1 represses $p21^{WAF1}$ in NIH3T3 cells and HEL human erythroleukaemia cells it actually activates its promoter in K562 human myeloid cell line (Lutterbach et al 2000). It seems that the factors determining the outcome of transcription (repression or transactivation) of a target gene involve promoter-specific features such as the proximity of binding sites for co-activators or co-repressors as well as availability of such cofactors in the nucleus. In addition, postranslational modifications such as phosphorylation (Tanaka et al 1996) or acetylation (Yamaguchi et al 2004) may contribute to the regulation of RUNX1 activity. The proposed model hypothesizes that binding of RUNX1 to activating factors such as p300 promotes expression whereas loss of p300 interaction and

subsequent binding to mSin3 proteins or Groucho family members leads to repression.

1.4 Role of RUNX1 in haematopoiesis

1.4.1 Foetal haematopoiesis

It was suggested that RUNX1 may be a master regulator of haematopoiesis when it became clear that there is a large number of chromosomal translocations targeting RUNX1 that are associated with leukaemias (Blyth et al 2005). However, the evidence supporting the crucial role of RUNX1 in developmental haematopoiesis came from the analysis of the phenotype of RUNX1 null mice. These animals are chararacterized by normal morphogenesis and yolk-sac derived primitive erythropoesis, however they lack definitive haematopoietic progenitors in the yolk sac and foetal liver (Okuda et al 1996; Wang et al 1996a). Foetal liver cells from RUNX1 null embryo are unable to differentiate into any of haematopoietic lineages although this is not due to a defect in the foetal liver microenvironment (Okuda et al 1996; Wang et al 1996a). RUNX1 is also essential for the generation of functional haematopoietic stem cells (HSCs) and immature progenitors (Cai et al 2000). RUNX1 deficient mice die due to haemorrhaging (Okuda et al 1996; Wang et al 1996a). The dosage of RUNX1 during foetal haematopoiesis is critical. RUNX1 heterozygous embryos show earlier appearance of HSCs in the yolk sac on embryonic day 10 and a premature extinction of HSC in the aorta-gonad-mesonephros (AGM) (Cai et al 2000) while $RUNX1^{+/-}$ animals have reduced numbers of myeloid and erythroid progenitors (Wang et al 1996a). Interestingly $RUNX1^{-/-}$ and $CBF\beta^{-/-}$ embryos have significantly overlapping phenotypes implying that the physiological effects of these two proteins are executed by RUNX1/CBFβ complexes, however other independent roles cannot be ruled out (Niki et al 1997; Sasaki et al 1996; Wang et al 1996b).

1.4.2 Adult haematopoiesis

The role of RUNX1 in adult haematopoiesis has been assessed in inducible gene targeting systems (conditional KO model, by f=floxed/Cre method) in the progeny of $RUNX1^{f/-}$ mice crossed to Mx-Cre transgenic mice (Ichikawa et al 2004). Examination of bone marrow in adult animals revealed that

haematopoietic progenitors remained intact in contrast with dramatic effects in the fetus. Moreover, RUNX1 deletion provides a proliferative adavantage to haematopoietic progenitors, as evidenced by an increased $Lin^{-}c\text{-}Kit^{+}Sca1^{+}CD34^{-}$ population in bone marrow and increased colony formation *in vitro* (Ichikawa et al 2004). However, RUNX1 has been implicated in adult megakaryocytic maturation and T-lymphocyte and B-lymphocyte differentiation. An analogous approach involving thymocyte-specific deletion of the RUNX1 gene has been undertaken to investigate the effects of RUNX1 in T-cell development. The progeny of $RUNX1^{fl/fl}$ mice crossed with Lck-Cre showed incomplete suppression of CD4 molecule in $CD4^{-}CD8^{-}$ double negative (DN) thymocytes, and incomplete up-regulation of CD8 molecule in $CD4^{+}CD8^{+}$ double positive (DP) thymocytes (Taniuchi et al 2002). This represents a further case whereby RUNX1 is engaged in both gene activation (CD8) and gene repression (CD4). It was also shown in other studies that a hemizygous level of RUNX1 allows inefficient transition from DP thymocytes to more mature $CD4^{+}CD8^{-}$ or $CD4^{-}CD8^{+}$ single-positive thymocytes (SP) (Hayashi et al 2000). Conversely, in RUNX1 over-expressing mice, an increase in the population of $CD4^{-}CD8^{+}$ thymocytes was observed (Hayashi et al 2001).

1.5 RUNX1 and leukaemia

1.5.1 Loss-of-function

The first implication that RUNX1 loss of function may play important role in leukaemogenesis was provided by the discovery that RUNX1 is involved in two common chromosomal translocations t(8;21) in acute myeloid leukaemia (AML) (Erickson et al 1992; Miyoshi et al 1991; Nisson et al 1992) and t(12;21) in pediatric B-cell precursor acute lymphoblastic leukaemia (B-ALL) (Golub et al 1995; Romana et al 1995). RUNX1 chimeric proteins arising from translocations have been reported to have dominant negative activity with respect to the wild-type gene product. Both RUNX1-ETO and TEL-RUNX1 have been demonstrated to recruit corepressors and actively repress transcription of RUNX1 target genes (Frank et al 1995; Gelmetti et al 1998; Hiebert et al 1996; Meyers et al 1995; Uchida et al 1999). Further evidence for antagonistic function of the fusion proteins was provided by the phenotype of RUNX1-ETO knock-in mice which

resembled RUNX1-knockouts (Okuda et al 1998; Yergeau et al 1997). Finally, in a retrospective study, sporadic point muations of RUNX1 were frequently found in myeloblastic leukaemia patients (Osato et al 1999) and subsequent studies found a high incidence of point mutations in the Runt domain of RUNX1 in three types of leukaemia: AML M0 subtype, MDS-AML, and secondary therapy related MDS/AML. Interestingly AML M0 mutations were predominantly biallelic suggesting selection for loss of function (Osato 2004; Preudhomme et al 2000). Moreover, monoallelic mutations underlie the hereditary condition familial platelet disorder (FPD), which predisposes to AML (Osato 2004; Song et al 1999). Despite the fact that loss of a second allele has not been observed in AML derived from FPD families so far, transdominant inhibition of the normal product could be considered as an alternative explanation. These observations highlight at least to some extent the concept of RUNX1 as a tumour suppressor where lower RUNX1 activity appears to correlate with a higher risk of developing leukaemia. Therefore, loss-of-function of RUNX1 is considered to be a common underlying mechanism for RUNX1-related leukaemias. However, a growing body of evidence suggests that RUNX1 alteration *per se* does not readily drive leukaemia and that additional genetic changes, 'second hits' are required for full-blown malignancy. Activation of the RAS pathway is one of the most common cooperating lesions in RUNX1 associated leukaemias. The RAS gene family and its upstream receptor tyrosine kinases such as c-Kit and FLT3 are frequently mutated in these types of leukaemias (Christiansen et al 2005; Goemans et al 2005; Speck and Gilliland 2002; Yamashita et al 2005). Interestingly, it has been recently shown that RUNX1 insufficiency in hematopoetic stem cells suppresses oncogenic N-RAS-induced effects such as apoptosis, senescence and differentiation (Motoda et al 2007). Therefore it seems that in this context RUNX1 is a part of a fail-safe mechanism that constrains neoplastic transformation.

1.5.2 Gain-of-function

On the other hand, strong evidence supporting the notion that RUNX1 act as a dominant oncogene came from *in vivo* mouse model insertional mutagenesis studies. RUNX1 together with other members of the family was identified as a common integration side in Mo-MuLV accelerated tumours in the CD2-MYC

transgenic model of lymphoma susceptible mice. This viral integration resulted in overexpression of intact RUNX genes (Blyth et al 2001; Stewart et al 1996; Stewart et al 1997; Stewart et al 2002; Wotton et al 2002). In addition, more than a decade ago it was reported that ectopic expression of RUNX1 P2 in 3T3 fibroblasts promotes transformation (Kurokawa et al 1996). Surprisingly, similar subsequent studies where RUNX1 P1 was used instead did not confirm this observation (Frank et al 1999). Recently, however, it has been shown in our laboratory that in p53 null MEFs, RUNX1 P1 has apparent pro-oncogenic effect on cells, including cytoskeletal reorganisation, reduced contact inhibition at confluence and accelerated tumour expansion *in vivo* (Wotton et al 2004). Moreover, the RUNX1 locus is also involved in genetic amplification in a number of cases in B-ALL and there are some speculations that increased dosage of RUNX1 in Down's syndrome patients predisposes them to acute megakaryocytic leukaemia (AMKL) (Osato and Ito 2005; Speck and Gilliland 2002).

1.6 Chromosomal translocations that involve CBF

CBFs are common target of gene rearrangements that are linked to human leukaemias. More than 30 different chromosomal translocations have been described that involve either RUNX1 or CBFβ. Of these the most common are t(8;21), inv(16) and t(12; 21). These translocations generate chimeric fusion oncoproteins that share common repressive functions with respect to wild type RUNX1 (Figure 1.6) (Blyth et al 2005).

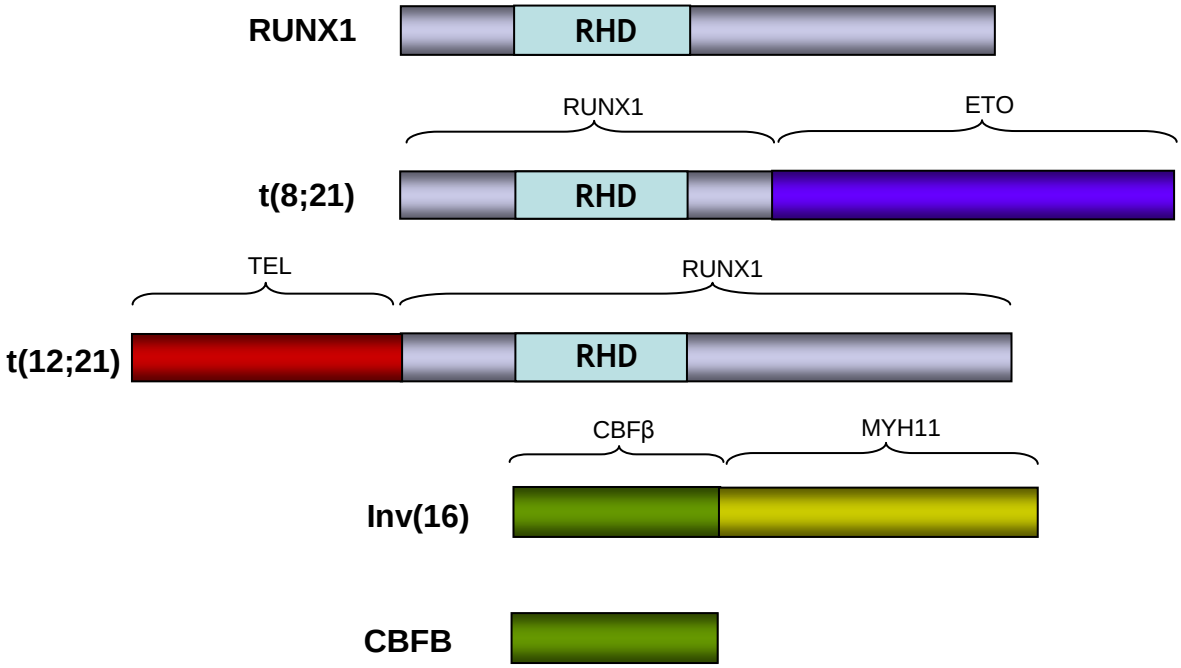

Figure 1.6 Schematic representation of three major fusion oncoproteins arising from chromosomal rearrangements targeting CBF and RUNX1

1.6.1 RUNX1-ETO in t(8; 21)

The t(8;21) translocation was the first to be discovered and is the most frequent translocation found in AML, accounting for 10-20% cases (Miyoshi et al 1991). The RUNX1-ETO chimeric protein (752 amino acids) is produced by the fusion of the N-terminal portion of the RUNX1 protein, including the Runt domain, with the heterologous partner protein, ETO (also known as MTG8 or CBFA2T1) that lacks the first 30 amino acid residues. ETO is an ubiquitously expressed nuclear protein engaged in transcriptional repression through interaction with corepressors such as the N-CoR complex, mSin3A and HDACs (Lutterbach et al 1998). Two molecular characteristics of the RUNX1-ETO fusion protein provide clues to its leukaemogenic potential. First, RUNX1-ETO retains the DNA binding Runt domain and heterodimerises with CBFβ and therefore binds to specific DNA sequences with high affinity. In fact, heterodimerisation with CBFβ is more stable with RUNX1-ETO than with wild-type RUNX1 (Tanaka et al 1998). Second, the adjacent ETO partner efficiently recruits multiple transcriptional repressor complexes (Gelmetti et al 1998). The resulting strong DNA-binding constitutive

repressor molecule can cause perturbations in gene expression which may trigger the transformation of haematopoietic cells. For instance, RUNX1-ETO represses such critical transcription factors as PU.1, C/EBPα, NF-1 (Burel et al 2001; Vangala et al 2003; Westendorf et al 1998; Yang et al 2005). Interestingly, in some cases RUNX1-ETO has been reported to enhance the expression of genes such as C/EBPε, c-Jun or anti-apoptotic Bcl-2 (Elsasser et al 2003; Klampfer et al 1996; Shimizu et al 2000). The ability of RUNX1-ETO to affect normal RUNX1 function was first shown in transient transfection assays, which demonstrated that RUNX1-ETO can function as a dominant negative regulator of RUNX1 mediated transcriptional activation (Frank et al 1995; Meyers et al 1995). Consistent with a negative effect on RUNX1 function, RUNX1-ETO has been shown to block the differentiation of myeloid progenitor cell lines and the ability of RUNX1 to activate myeloid specific promoters (Kitabayashi et al 1998; Westendorf et al 1998). Evidence for *in vivo* dominant negative activity of the fusion protein was provided by RUNX1-ETO knock-in experiments, which showed that mice heterozygous for RUNX1-ETO had a similar phenotype as RUNX1 knock-out mice (Okuda et al 1998; Yergeau et al 1997). Further attempts to express the fusion gene in adult mice using a tetracycline-inducible system, a conditional RUNX1-ETO knock in system, or a myeloid-specific promoter, all failed to induce spontaneous leukaemia (Higuchi et al 2002; Rhoades et al 2000; Yuan et al 2001), although RUNX1-ETO expression consistently enhanced the proliferation of HSCs and increased progenitor cell self-renewal capacity. In another study where stem cells were transduced with RUNX1-ETO and transplanted into lethally irradiated recipient animals, the stem cell compartment expanded dramatically (de Guzman et al 2002). Similarly direct targeting of RUNX1-ETO expression to stem cells by using the SCA-1 promoter enhanced myeloid progenitor expansion (Fenske et al 2004). These experiments suggest that AML-ETO can promote the expansion of a susceptible compartment that ultimately would acquire additional 'hits' leading to disease. Therefore it has become obvious that the RUNX1-ETO fusion protein does not cause leukaemia alone and requires additional cooperating events to induce leukaemogenesis in mice. RUNX1-ETO was analysed in the context of cooperating mutations in animals expressing RUNX1-ETO which were mutagenised with the alkylating agent N-ethyl-N-nitrosourea (ENU). In two independent systems, these

mice developed myeloid leukaemia at frequencies greater than ENU-treated WT mice (Yuan et al 2001; Higuchi et al 2002). In addition, retroviral transduction and haematopoietic cell transplantation experiments with $p21^{WAF1}$-deficient cells showed that RUNX1-ETO is able to promote leukaemogenesis in the absence of $p21^{WAF1}$ (Peterson et al 2007). Moreover, retroviral expression of a truncated form of RUNX1-ETO with a deleted C-terminal NcoR/SMRT-interacting region in bone marrow cells resulted in rapid onset of leukaemia in transplant recipient mice (Yan et al 2004) RUNX1-ETO was also shown to transform NIH3T3 cells through activation of AP-1 (Frank et al 1999). Paradoxically, RUNX1-ETO has an inhibitory effect on cell proliferation (Burel et al 2001) and overexpression of RUNX1-ETO reduces expression of target genes, including cyclin D3 and CDK4 (Bernardin-Fried et al 2004; Burel et al 2001; Lou et al 2000). The cellular consequence is impairment in the transition from G1 to S phase and slower proliferation. Therefore, the requirement for cooperating lesions that interfere with this block is not surprising.

1.6.2 TEL-RUNX1 in t(12; 21)

TEL-RUNX1 is generated by the t(12; 21) chromosomal translocation, which occurs in approximately 25% of cases of childhood common B-cell precursor acute lymphoblastic leukaemia (Golub et al 1995). In the TEL-RUNX1 fusion protein (794 amino acids), the N-terminus of TEL (336 residues) is fused to nearly all of the RUNX1 protein, including the Runt domain and the entire C-terminal portion. TEL (also ETV6) is a member of Ets family of transcription factors that have the Ets DNA binding domain at the C-terminus and a protein-binding helix-loop-helix (HLH) domain at the N-terminus. The Runt domain of TEL-RUNX1 can form a heterodimer with CBFß and specifically bind to target sequences but despite having the entire C-terminal region of RUNX1, this fusion protein generally represses the reporter activities and antagonises RUNX1-driven transactivation (Fears et al 1997; Hiebert et al 1996; Meyers et al 1993). This repressor property is attributed to the recruitment of HDACs and N-CoR by the TEL moiety and the recruitment of mSin3a by both TEL and RUNX1 (Fenrick et al 1999; Guidez et al 2000). The RUNX1 moiety is capable of recruiting transcriptional coactivators as well as repressors, however the generation of the fusion protein seems to increase the overall affinity towards corepressors and

subsequent constitutive repressor complex stability (Guidez et al 2000). TEL-RUNX1 may also suppress not only the normal function of RUNX1 but also TEL through HLH-mediated heterodimerisation (Gunji et al 2004). Wild-type TEL function is known to be essential for establishing haematopoiesis in the bone marrow (Wang et al 1998), therefore its disruption by the chimeric protein may also contribute to leukaemogenesis. The role of TEL-RUNX1 in inducing leukaemia has been assessed in mice. TEL-RUNX1 expressed under the control of immunoglobulin heavy chain enhancer/promoter did not cause leukaemia in mice (Andreasson et al 2001). However, retroviral delivery of TEL-RUNX1 into bone marrow strongly collaborated with deficiency in $p16^{INK4a}$ as well as $p19^{ARF}$ in promoting leukaemogenic transformation (Bernardin et al 2002b). A detailed analysis using similar experimental system showed that TEL-RUNX1 inhibits B-cell differentiation, leading to an accumulation of early B-cell progenitors and a corresponding deficit of mature B-cells (Morrow et al 2004; Tsuzuki et al 2004).

1.6.3 CBFβ-MYH11 in Inv(16)

The Inv(16) does not involve the RUNX1 locus directly but instead creates the CBFβ-MYH11 (smooth muscle myosin heavy chain) fusion protein that also inhibits RUNX1-dependent transactivation (Kanno et al 1998b; Lutterbach et al 1999). Inv(16) is a common chromosomal inversion event in myelomonocytic leukaemias (M4Eo). A model that has been proposed as an explanation of the mechanism of repression assumes that CBFβ-MYH11 binds to its RUNX1 α-chain partner with increased affinity, and might directly suppress or sequester RUNX1 in the cytoplasm (Adya et al 1998; Kanno et al 1998b; Lutterbach et al 1999). Thus CBFβ-MYH11 would be predicted to interfere with RUNX1 transcriptional activity. However, CBFβ-MYH11 cooperated with RUNX1 to repress the $p21^{WAF1}$ promoter, suggesting that it is present and functional in the nucleus. A repression domain in the MYH11 fragment of fusion was identified and CBFβ-MYH11 was found to interact with mSin3, but only when RUNX1 was coexpressed, indicating that RUNX1 is bridging the interaction between CBFβ-MYH11 and mSin3 protein (Lutterbach et al 1999). Furthermore, a strong argument for dominant-negative function of CBFβ-MYH11 was obtained from the analysis of the phenotype of Inv(16) knock-in mice, which recapitulates *RUNX1* and *CBFβ* homozygous knock-out phenotypes (Castilla et al 1996). The development of an

Inv(16) animal model in which to test the mechanism of pro-leukaemogenic action of CBFβ-MYH11 has been extremely difficult. Previous murine models of the Inv(16) have involved the expression of CBFβ-MYH11 coupled with ENU (N-ethyl N-nitrosourea) mutagenesis, retroviral insertional mutagenesis (Castilla et al 1999; Castilla et al 2004), the removal of two tumour suppressors (Yang et al 2002) or the coexpression of oncogenes (Bernardin et al 2002a; Kogan et al 1998). However, only the use of chimeric mice carrying a knock in Inv(16) allele plus random mutagenesis yielded an AML that mimicked the human disease (Castilla et al 1999, Castilla et al 2004). In a recent study it has been reported that Inv(16) cooperates with $p19^{ARF}$ haploinsufficiency to induce AML (Moreno-Miralles et al 2005).

1.7 Cellular senescence and its impact on aging and cancer

At one time it was believed that cells could proliferate indefinitely and that the maintenance of a cell culture was just a question of finding the right conditions. This idea was radically changed more than 40 years ago by the outstanding work of Hayflick (Hayflick 1965) which demonstrated that for most normal cells proliferation has an end, despite optimal culturing conditions. When mammalian cells are isolated from tissue and cultured, they undergo a limited number of population doublings and then arrest (having reached the 'Hayflick limit'). The process underlying this observation is known as replicative senescence. The discovery of senescence led to two important hypotheses that were proposed to explain its physiological relevance. The first was related to the fact that cancer cells are immortalised and therefore proliferate indefinitely in culture. Hence, cellular senescence was suggested to be a tumour suppressive mechanism. The second hypothesis originated from the fact that tissue regenerative capacity diminishes with age. In this context, cellular senescence was proposed to mimic aging at a single cell level (Campisi 2005). Four decades of subsequent intensive research have unravelled the primary mechanisms by which cellular senescence occurs and have shed light on central aspects of organismal aging and cancer (Campisi 2005). Furthermore, it is now evident that cellular senescence, like apoptosis, is an important biological stress response

programme that can be triggered by various stimuli. Finally, it is clear that there are marked differences among species in the propensity of cells to spontaneously escape senescence and acquire an immortal replicative lifespan. In this regard rodent cells are much more prone to spontaneous immortalization than human cells (Itahana et al 2004; Sherr and DePinho 2000).

1.8 The signals initiating cellular senescence

Senescence-inducing signals can originate from telomeric (intrinsic) or non-telomeric (extrinsic) sources (Figure 1.7) (Itahana et al 2004). Senescence mediated by non-telomeric signals is termed “premature senescence”, “accelerated senescence” or “extrinsic senescence”. Another term: stress- or aberrant signalling senescence (STASIS) has been suggested to convey the notion that cells engage a common senescence-like arrest mechanism in response to diverse stimuli (Drayton and Peters 2002). Both telomere-based and non-telomere-based growth arrest may be due in part to repression of genes required for cell cycle progression and upregulation of growth inhibitory genes. The existence of non-telomere-induced senescence was anticipated by the behaviour of primary murine cells in culture. Normal mouse cells, like normal human cells, have a finite replicative potential. However, their replicative lifespan is substantially shorter than that of human cells (10-15 population doublings compared to 50-70) despite murine fibroblasts having very long telomeres (~60kb versus ~12kb) and in some cases expressing telomerase (Itahana et al 2004; Sherr and DePinho 2000). Thus, it is unlikely that the replicative senescence of primary mouse fibroblasts is due to telomere shortening. It has been proposed that the senescence phenomenon in primary mouse cells is due to a stress response to culture conditions (Sherr and DePinho 2000) which can be abrogated by decreasing the oxygen concentration used in culturing these cells (Parrinello et al 2003). These observations have led to the hypothesis that rodent cells repair DNA damage much less efficiently than human cells and are thus much more sensitive to a variety of agents or conditions that produce oxidative stress (Parinello et al 2003). It is now apparent that a diverse spectrum of stress signals can elicit a senescence response. Of most importance are certain types of DNA damage, including DNA breaks and oxidative lesions (Chen et al 1995; Robles and

Adami 1998). It seems that cells may senesce when the damage is irreparable or is likely to impair the DNA repair machinery. Interestingly, many normal cells undergo senescence when they overexpress certain oncoproteins. The activated components of RAS-RAF-MEK signalling cascade (Lin et al 1998; Serrano et al 1997; Zhu et al 1998) were the first oncogenic inducers of premature senescence to be identified. A common feature of these non-telomeric inducers of cellular senescence is their potential to cause or facilitate tumourigenic transformation. It is not surprising, then, that overexpression of certain tumour suppressor genes also causes normal cells to undergo rapid premature senescence. Tumour suppressors that strongly induce this phenotype include $p16^{INK4a}$ cyclin-dependent kinase inhibitor (CDKI), $p21^{WAF1}$, p27 (McConnell et al 1998), $p14^{ARF}$ (Dimri et al 2000) and PML (Ferbeyre et al 2000). Moreover, cells can senesce in response to epigenetic changes to chromatin organisation, for example those caused by pharmacological agents or altered expression of proteins that modify DNA or histones (i.e. histone deacetylase inhibitors) (Neumeister et al 2002; Ogryzko et al 1996).

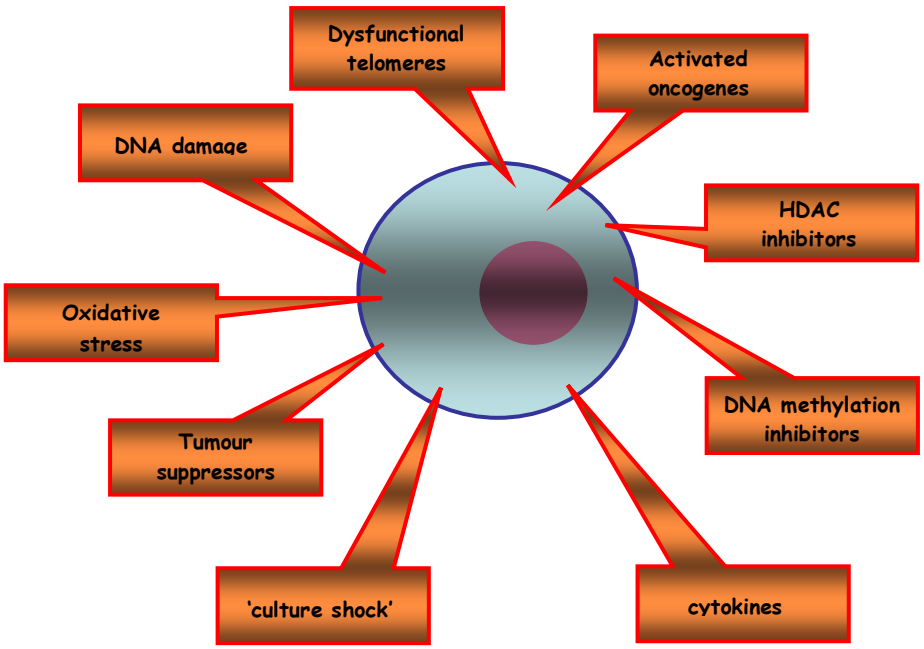

Figure 1.7 Cellular senescence is triggered by wide spectrum of stimuli
Telomere shortening as well as non-telomeric signals such as DNA damaging agents, oncogenic signalling, oxidative stress, overexpression of tumour suppressors, cytokines, HDAC and DNMT inhibitors, and undefined stress signals ('culture shock') induce senescence

1.8.1 Telomere attrition

Telomere shortening is a universal mechanism that limits the proliferative potential of normal cells (lacking endogenous telomerase) following extensive cell divisions. The role of telomere exhaustion in the suppression of tumourigenesis *in vivo* by initiating cellular senescence has been demonstrated recently (Cosme-Blanco et al 2007; Feldser and Greider 2007). It is believed that telomere erosion beyond a certain limit triggers a DNA damage response, thereby activating a checkpoint, resulting in growth arrest. Recent investigations provide some evidence that signals induced by the telomere dysfunction appear to be similar to those induced by double strand DNA breaks and that inactivation of the checkpoint kinases (CHK) can reinstate S phase progression in senescent cells (Gire et al 2004; d'Adda di Fagagna et al 2003). Other studies suggested that telomere shortening-induced senescence is a DNA damage response mediated by the ATM/ATR-p53-p21 pathway (Herbig et al 2004). Cells that fail to senesce and continue to proliferate despite dysfunctional telomeres develop chromosomal aberrations, which can result in malignant transformation (Artandi and DePinho 2000).

1.8.2 DNA damage

If cellular senescence induced by attrition of telomeres is a DNA damage response, then the DNA damaging agents should also be able to provoke cellular senescence. In fact this seems to be the case since DNA damaging agents that influence the integrity of the genome can trigger senescence. The direct DNA damaging of DNA caused by sublethal doses of irradiation or by treatment with chemotherapeutic drugs (like etoposide or cyclophosphamide) can induce senescence. Interestingly, such agents induce senescence in normal cells as well as in some tumour cells, both in culture and *in vivo* (Di Leonardo et al 1994; Roninson 2003; Schmitt et al 2002; Shay and Roninson 2004; Te Poele et al 2002; Wahl and Carr 2001). Such damage can either cause cell death or reversible cell-cycle arrest, depending on the type of agent or the dose administered, and the type of cell treated (Wahl and Carr 2001). Disruption of DNA repair genes such as Brca1, Xrcc4, DNA ligase IV and others in mice induces the premature senescence of MEFs cultured from these animals and symptoms of premature aging in the mice themselves (Frank et al 2000; Gao et al 2000; Ongusaha et al

2003). Many of these senescent phenotypes can be rescued by p53 inactivation indicating a pivotal role for p53 in DNA-damage induced senescence (Frank et al 2000; Gao et al 2000; Ongusaha et al 2003). Moreover, cancer cells that retain intact p53 are much more susceptible to senescence in response to chemotherapy at least in cell culture and mouse models (Roberson et al 2005; Roninson 2003; Schmitt et al 2002; Shay and Roninson 2004; Te Poele et al 2002).

1.8.3 Oxidative stress

Oxidative stress and the accumulation of intracellular reactive oxygen species (ROS) play crucial roles in the induction of senescence. Human fibroblasts undergo premature senescence when grown in high ambient oxygen conditions, but their proliferative lifespan can be substantially extended when cultured in low ambient oxygen (2-3%) which more closely resembles physiological oxygen levels (Chen et al 1995). The senescence of MEFs has also been linked oxidative stress in culture. When these cells are grown in 3% oxygen instead of 20%, senescence is greatly delayed or prevented altogether (Parrinello et al 2003). Moreover, MEFs that are propagated in 20% oxygen suffer from a high level of DNA damage that is much more apparent than in human cells grown in the same conditions (Busuttil et al 2003; Parrinello et al 2003). This indicates that human cells cope with the oxidative stress much more efficiently than murine cells either due to ability to neutralize ROS or to detect and repair DNA lesions. Increase of intracellular ROS levels through hydrogen peroxide treatment or through the inhibition of ROS scavenging enzymes (e.g. superoxide dismutase Sod1) causes premature senescence (Blander et al 2003; Chen et al 1998). Internal ROS can not only damage cellular components through the oxidation of DNA, proteins and lipids but can also act as second messengers in specific signal transduction pathways (Halliwell 2007). There is some evidence that oxidative stress-induced senescence, like telomere dysfunction operates through the p53-p21-Rb axis. This idea is supported by the observation that a reduced ambient oxygen level reduces the proportion of pre-senescent p21-expressing cells without any effect on p16-expressing cells (Itahana et al 2003). However, other studies indicate that oxidative stress can induce p16, possibly through the action

of p38 MAPK, a member of the stress-activated protein kinase family (Iwasa et al 2003).

1.8.4 Oncogene activation

Proto-oncogenes are genes that have the potential to transform cells when mutated or overexpressed usually in cooperation with other accompanying mutations. The expression of oncogenes in primary cells triggers defence responses that prevent their uncontrolled proliferation. Some oncogenes such as c-Myc or adenovirus E1A induce apoptosis whereas others such as activated Ras (H-Ras^{V12}) trigger a permanent arrest that is reminiscent of replicative senescence (de Stanchina et al 1998; Serrano et al 1997; Zindy et al 1998). Prototypical Ras-driven senescence has been extensively studied over the last decade in various human and mouse cell systems and has been shown to occur in epithelial cells of human and mouse origin as well as fibroblasts (Jones et al 2000; Lin and Lowe 2001; Serrano et al 1997). These studies have yielded a wealth of information about the molecular pathways relevant to oncogenesis. The tumour suppressor p16INK4a which inactivates D-type cyclins and p19^{ARF} (p19^{ARF}(mouse) = p14^{ARF}(human)) which activates p53 together with general cell cycle regulators pRb, p107 and p130, play key roles in Ras-induced senescence (Dannenberg et al 2000; Jones et al 2000; Lin et al 1998; Palmero et al 1998; Sage et al 2000; Serrano et al 1997). In mouse cells, induction of senescence by RAS occurs through the p19^{ARF}-p53 pathway. Targeted mutations that exclusively disrupt p16^{INK4a} but not p19^{ARF} have revealed that p16^{INK4a} is a less potent tumour suppressor in the mouse and that p16^{INK4a} null MEFs are susceptible to Ras-induced senescence whereas p19^{ARF} null cells are not (Krimpenfort et al 2001; Sharpless et al 2001). In contrast to MEFs, in human fibroblasts p16^{INK4a} seems to have a more prominent role than p14^{ARF}. It has been reported that Ras-mediated senescence in human diploid fibroblasts occurs independently of p14^{ARF} (Wei et al 2001) and human fibroblasts with biallelic mutation in p16^{INK4a} (Leiden cells) are resistant to RAS induced senescence (Brookes et al 2002). Other members of the RAS signalling pathway (for example, RAF, MEK, MOS and BRAF) as well as other oncoproteins such as nuclear protein E2F or tyrosine kinase receptor erbB2, were shown to cause premature senescence through engagement of

various pathways (Bartkova et al 2006; Dimri et al 2000; Lazzerini et al 2005; Lin et al 1998; Michaloglou et al 2005; Trost et al 2005; Zhu et al 1998).

1.8.5 Other inducers of cellular senescence

There are also other less well understood cellular senescence initiating signals. Chemical histone deacetylase inhibition, which involves decondensation of chromatin and formation of euchromatin was found to induce senescence in primary fibroblasts of murine and human origin (Munro et al 2004; Ogryzko et al 1996). Interestingly, whereas in human cells the $p16^{INK4a}$-pRb pathway is critical for this response, in murine cells p53 pathway is more important (Munro et al 2004). Inhibition of DNA methyl transferase (DNMT) with 5-azacytidine also results in senescence-like growth arrest (Weller et al 1993). Intriguingly, prolonged signalling by the anti-proliferative cytokine, interferon-β can induce ROS accumulation, DNA damage response and p53-dependent senescence (Moiseeva et al 2006). Likewise, chronic signalling by TGF-β promotes senescence in normal and cancer cells (Katakura et al 1999; Vijayachandra et al 2003; Zhang and Cohen 2004). Finally, a phenomenon known as 'culture shock' can induce senescence by a p16-dependent but telomere-independent route. Human keratinocytes and mammary epithelial cells spontaneously express p16 and enter premature senescence with long telomeres under standard *in vitro* culture conditions. These effects can be reversed by culturing cells on fibroblastic feeder layers suggesting that inadequate growth conditions also causes senescence and supporting the notion that senescence is a cellular stress response programme (Ramirez et al 2001).

1.9 Characteristics of senescent cells

Cellular senescence, originally defined as proliferative arrest that occurs in normal cells after a limited number of cell divisions (cell aging, replicative senescence), has now become regarded more generally as a biological programme of signal transduction leading to terminal, irreversible growth arrest, accompanied by a distinct set of alterations in the cellular phenotype (Dimri 2005). Cells that undergo senescence cannot divide even if stimulated by mitogens but they remain metabolically and synthetically active and display

dramatic changes in chromatin structure and gene expression. This is accompanied by characteristic and easily observed changes in morphology such as an enlarged and flattened cell shape with increased granularity and formation of intracellular vacuoles (Campisi 2001; Dimri et al 1995). Senescence has been most widely studied in fibroblasts *in vitro* but is also well-defined in melanocytes and epithelial cells as well as cancer cells (Jones et al 2000; Lin and Lowe 2001; Michaloglou et al 2005, Olsen et al 2002; Serrano et al 1997; Shay and Roninson, 2004). Other cell types suggested to undergo senescence include haematopoetic and neural progenitors (Geiger and Van Zant 2002; Palmer et al 2001). The most widely used marker for senescent cells is senescence-associated-β-galactosidase (Dimri et al 1995). The senescent phenotype also entails type specific changes. Some senescent cells, for example human fibroblasts but not endothelial cells, become resistant to apoptosis (Hampel et al 2004). In addition, senescent fibroblasts secrete proteins that can influence the tissue microenvironment (Chang et al 2002; Mason et al 2004; Shelton et al 1999; Trougakos et al 2006; Zhang et al 2003a) as well as inflammatory cytokines such as IL-6 (Kuilman et al 2008). Interestingly, paracrine factors produced by senescent cells have major effects on the growth and survival of tumour cells (Krtolica et al 2001). Hence, senescence should not be viewed as merely the end point in a cell's life cycle but rather as a physiological state determined by the homeostatic programmes of an organism.

1.9.1 Growth arrest

Somatic cell cycles consist of alternating DNA synthetic (S) and mitotic (M) phases, separated by gap phases (G1 and G2) (Figure 1.8). Senescent cells are unable to progress through the cell cycle and usually arrest growth with G1 DNA content. Once arrested they cannot be stimulated to resume proliferation by physiological mitogens. This is primarily caused by upregulation of cell cycle inhibitors and chromatin condensation (Campisi 2005; Narita et al 2003). The preferred theories emphasising G1 arrest have been overthrown by several reports that have shown that cellular senescence can be also associated with G2M arrest. For example, a defect in the stress signalling kinase MKK7 caused G2M arrest (Wada et al 2004) and also overexpression of oncogenic RAF results in a preferential accumulation in the G2M phase of the cell cycle (Zhu et al 1998).

Although earlier studies of H-RAS^{V12} induced senescence have described predominant G1 arrest, recent work from our laboratory has revealed a stronger block in G2M, and an increased number of cells with a 4N DNA content (Kilbey et al 2007).

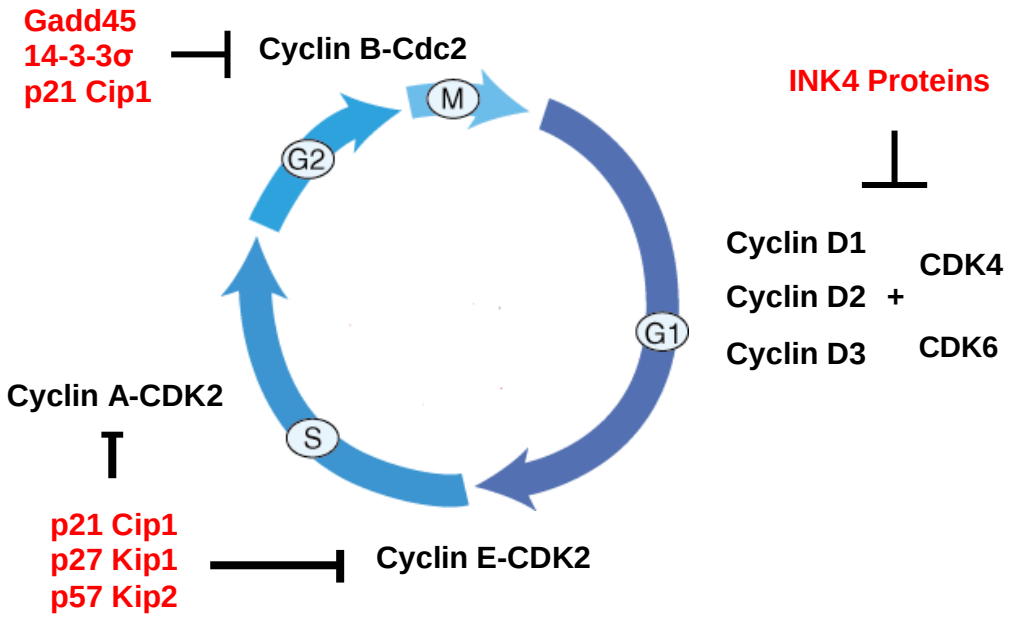

Figure 1.8 Schematic diagram of checkpoints in the eukaryotic cell cycle

The cell cycle consists of alternating S phase (DNA synthesis) and M phase (mitosis), separated by two gap phases G1 and G2. Cyclin D-dependent kinases (CDKs) accumulate in response to mitogenic signals and initiate the phosphorylation of pRb, a process that is completed by cyclin E-cdk2. Once cells enter S phase, cyclin E is degraded and cyclin A enters into complexes with cdk2. Cyclin B-Cdc2 mediates G2/M transition. INK4 proteins (p16INK4a, p15INK4b, p18INK4c, p19INK4d) oppose the activities of the various cyclin D-dependent kinases, whereas Cip/Kip proteins (p21Cip1, p27Kip1, p57Kip2) specifically inhibit cyclin E-cdk2 and cyclin A-cdk2. Gadd45, 14-3-3σ and p21Cip1 interefere with cyclin B-Cdc2.

1.9.2 Altered gene expression

Cells that undergo senescence show dramatic changes in gene expression patterns, especially cell-cycle inhibitors which are activated and cell cycle progression genes that are downregulated (Trougakos et al 2006; Zhang et al 2003a). $p16^{INK4a}$ and $p21^{WAF1}$, which are governed by two tumour suppressors, p53 and pRb respectively, are the most common cell cycle inhibitors that are expressed in senescent cells (Campisi 2005). P53 and pRb are often dysfunctional in cancer (Sherr and McCormick 2002). $p21^{WAF1}$ is a direct downstream target of p53, whereas induction of $p16^{INK4a}$ remains poorly understood, although transcription factors of the Jun, Ets and Id families together with polycomb group proteins, Bmi, have been implicated in the regulation of *INK4a* expression, thereby governing cellular senescence (Lowe and Sherr 2003; Gil and Peters 2006). Ultimately, $p16^{INK4a}$ and $p21^{WAF1}$ maintain pRb in a hypophosphorylated, active state (Lowe and Sherr 2003). Repressed genes during senescence include replication-dependent histones, c-FOS, cyclin A, cyclin B and PCNA (proliferating cell nuclear antigen) (Narita et al 2003; Pang and Chen 1994; Serrano et al 1997; Seshadri and Campisi 1990). The repression of some of these genes is believed to reflect pRb mediated inactivation of E2F target genes and pRb-dependent epigenetic chromatin reorganisation and formation of discrete foci termed senescence-associated heterochromatin foci (SAHF) within the nucleus (Narita et al 2005).

1.9.3 Senescence markers

The extensive study of senescence has yielded several markers that are useful for the detection of this phenotype not only *in vitro* but more importantly *in vivo*. Senescent cells do not replicate their DNA, which can be detected by the lack of incorporation of 3H-thymidine or BrdU. Alternatively, immunostaining for PCNA or Ki-67 can be performed. SA-β-gal staining serves as a reliable and extensively used marker. In addition, components of two main pathways involved in senescence: ARF-p53 and $p16^{INK4a}$-pRb are now used to identify senescent cells (Campisi 2005). Recently, the Serrano group has reported new markers that could help to describe senescence *in vivo* e.g. $p15^{INK4b}$, DCR2 and DEC1 (Collado and Serrano 2006). Senescent cells can also be detected by cytological markers: formation of SAHF (senescence-associated heterochromatin

foci) and senescence associated DNA-damage foci (SDFs) (Bartkova et al 2006; DiMicco et al 2006; Mallette et al 2007; Narita et al 2003)

1.9.3.1 Senescence-associated β-galactosidase

The most widely used assay for senescence cells is the cytochemical detection of β-galactosidase activity at pH 6, termed senescence-associated β-galactosidase (SA-β-Gal) (Dimri at al 1995). Most cells express a lysosomal β-Gal that is optimally active at about pH 4 and either pre-senescent or senescent cells stain equally when assayed at pH 4, but only senescent cells stain for β-Gal activity at pH 6. Neither pre-senescent nor senescent cells stain at pH 7.5 which is the optimum for bacterial β-Gal enzyme (Dimri at al 1995). β-galactosidase activity reflects increased lysosomal biogenesis (Kurz et al 2000). It has been recently reported that SA-β–Gal is expressed from *GLB1*, the gene encoding lysosomal beta-D-galactosidase and that downregulation of this gene by RNAi did not prevent cellular senescence indicating that SA-β–Gal is not required for cells to undergo senescence (Lee et al 2006). There is also evidence for a positive SA-β–Gal reaction in settings of cellular stress that are unrelated to senescence such as serum withdrawal or high confluency in culture dish (Severino et al 2000). Although SA-β–Gal is not necessary for senescence it is still a useful and extensively used assay for detection of senescent phenotypes.

1.9.3.2 Senescence-associated heterochromatin foci (SAHF)

When stained with DAPI (4'-6-Diamidino-2-phenylindole) or PI (propidium iodide) normal human cells exhibit a relatively even distribution of DNA across the cell nucleus. However most of the senescent cells undergo dramatic chromatin condensation which can be visualised by staining with DAPI as bright, punctate DNA foci (Narita et al 2003). SAHF are characterised by the presence of certain heterochromatin-asscociated histone modifications (for example, hypoacetylation of histones or methylation of Lys9 of histone H3 - H3K9Me) and bound heterochromatin proteins (e.g. HP1, heterochromatin protein 1) (Narita et al 2003) as well as loss of the linker histone H1 and enrichment in histone variant macroH2A and HMGA proteins (Funayama et al 2006; Narita et al 2006; Zhang et al 2005). The molecular mechanism of SAHF assembly is very complex and still largely unexplored but histone chaperones, ASF1a and HIRA together with PML

bodies play a critical role in this process (Figure 1.9) (Adams 2007). SAHF are believed to reflect p16-pRB mediated silencing of E2F target genes involved in cell cycling (Narita et al 2003). In mice, pericentric heterochromatin is much more prominent than in human cells and therefore it can be mistaken for SAHF (Adams 2007). Whether SAHF always occur in response to various stimuli and how exactly they are formed are questions that remain to be answered. It seems that not all cells have equal propensity to form SAHF. For instance WI-38 and IMR90 lung embryonic fibroblasts and primary melanocytes accumulate pronounced SAHF, whereas BJ foreskin fibroblasts form less marked SAHF (Adams 2007). It is very possible that the nature of pro-senescent stimuli may account for the SAHF occurrence, for example, STAT5A does not promote obvious SAHF formation (Hemann and Narita 2007).

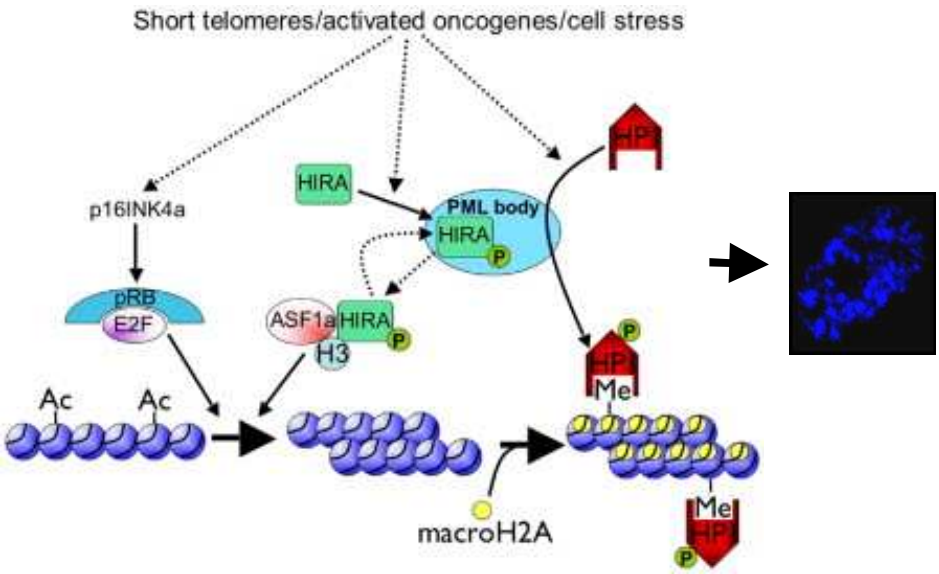

Figure 1.9 A model of SAHF formation in senescent human cells

The HIRA/ASF1a complex cooperates with p16INK4a/pRB pathway to drive chromatin condensation. HP1 and macroH2A are deposited into SAHF. HIRA and HP1 transiently localise to PML bodies where are activated through phosphorylation (adapted from Adams 2007)

1.9.3.3 Senescence-associated DNA-damage foci (SDF)

As discussed before, telomere uncapping can trigger a DNA damage response that results in senescence-like growth arrest (d'Adda di Fagagna et al 2003; Herbig et al 2004). In addition γ-irradiation and genotoxic drugs can also drive cellular senescence through DNA damage response pathways (Schmitt et al 2002; Wahl and Carr 2001). Interestingly, oncogenes such as H-RAS^{V12}. MOS, Cdc6 or STAT5a induce DNA double strand breaks (DSBs) and a DNA damage response due to replication stress that engages activation of ATM/ATR, CHK2 and CHK1 (Bartkova et al 2006; Di Micco et al 2006; Mallette et al 2007). SDFs can be detected in senescent cells from mice and humans and contain proteins that are involved in DNA damage such as γ-H2AX, 53BP1, MDC1 and NBS1 (Bartkova et al 2006; d'Adda di Fagagna et al 2003; DiMicco et al 2006; Herbig et al 2004). Importantly, it seems that not all oncogenes effectively induce DNA damage (Hemann and Narita 2007) and the role of SDF as a general marker of senescence remains to be investigated further.

1.10 Signalling pathways in cellular senescence

1.10.1 p53 and pRb, two master regulators of senescence

Regardless of the senescence initiating signals, tumour suppressor pathways are critical for initiation and maintenance of the senescent phenotype in human and mouse cells. These pathways are controlled by the tumour suppressor proteins p53 and pRB with a wide range of upstream regulators and downstream effectors (Figure 1.10). It was in the early 90s when Shay and colleagues identified p53 and pRB as two principal regulators of senescence (Shay et al 1991) and since then the molecular networks regulated by these proteins have become a subject of extensive research. Various studies have examined the relative functions of p53 and pRB in the initiation of senescence by assessing the outcomes of their inactivation. Numerous methods have been used to this end, for example: ectopic expression of SV40 large T-antigen and the human papilloma virus E6 and E7 oncoproteins (Shay et al 1991), germline homologous recombination in the mouse (Dannenberg et al 2000; Sage et al 2000], somatic homologous recombinations in human cells (Brown et al 1997) or RNAi knock-down models (Wei et al 2003). In mouse embryo fibroblasts, disruption of p53 alone is

sufficient to prevent senescence (Dirac and Bernards 2003). Likewise, inactivation of pRb gene together with other members of Rb family such as p107 and p130, but not pRb alone, is sufficient to escape senescence (Dannenberg et al 2000; Sage et al 2003). This implies that both p53 and the Rb family are required for the induction of senescence. P53 and pRb were also found to be necessary for the maintenance of the senescent state because inactivation of either of these genes in senescent MEFs was enough for proliferation to resume (Dirac and Bernards, 2003; Sage et al 2003). These observations suggested a model of linear signalling, whereby a stress signal activates p53 which in turn activates pRb. The $p21^{WAF1}$ protein, an inhibitor of cyclin E/Cdk2 complexes which is a direct transcriptional target of p53 was proposed to act as a linking chain between these two pathways. However, p21 null MEFs undergo RAS induced senescence (Pantoja and Serrano 1999), therefore exactly how the signal is transduced remains elusive. Unlike the behaviour of mouse cells, the inactivation of both p53 and pRb is essential to prevent the onset of replicative senescence in human cells (Smogorzewska and de Lange 2002), whereas disruption of only one of these proteins only delays the onset of senescence. This indicates that in human cells, p53 and pRb operate in two parallel pathways. A degree of complexity arises from other studies where it has been demonstrated that inactivation of either p53 or pRb by somatic homologous recombination in human lung fibroblasts allows bypass of senescence, suggesting that a linear model could be also applicable to human cells in some contexts (Wei et al 2003). This idea is supported by the fact that abrogation of $p21^{WAF1}$ by homologous recombination is sufficient to prevent replicative senescence in human fibroblasts (Brown et al 1997).

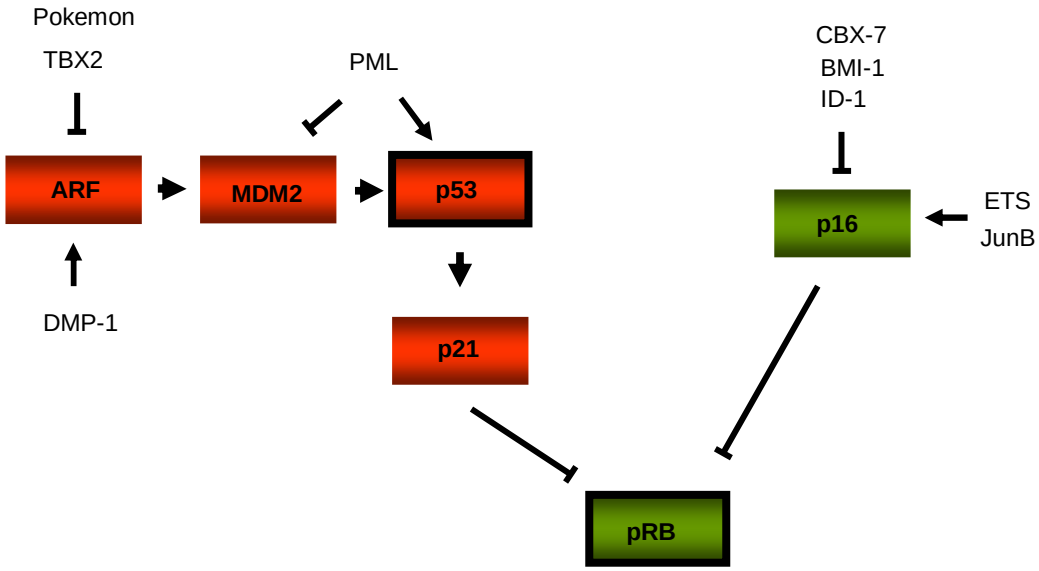

Figure 1.10 Control of cellular senescence by p53 and pRB pathway

Shown here are pathways that are activated by senescence-inducing signals. The model assumes linear crosstalk between the p53 pathway (red) and the pRB pathway (green). Positive and negative regulators of these two pathways are indicated and the effects of their action illustrated by arrows(→ - positive effect; ⊣ - negative effect)

1.10.1.1 pRb

It is well established that pRb is constitutively hypophosphorylated (in its active state) in senescent cells and there is a growing body of evidence that this is achieved at least to some extent by $p16^{INK4a}$. The $p16^{INK4a}$, an inhibitor of CDK4/CDK6/Cyclin D complex activity, is upregulated during either replicative senescence or premature senescence in human fibroblasts (Alcorta et al 1996; Serrano et al 1997; Stein et al 1999). Therefore, it has been proposed that $p16^{INK4a}$ prevents phosphorylation of pRb resulting in its activation. Consistent with this hypothesis, $p16^{INK4a}$ and its upstream regulators such as Bmi-1, CBX7, JunB, ID1 and Ets-1 regulate senescence in a pRb-dependent fashion (Gil et al 2004; Itahana et al 2003; Ohtani et al 2001; Passegue and Wagner 2000). Moreover, inactivation of $p16^{INK4a}$ in human cells causes a delay in the onset of replicative senescence, quite significantly in some cases (Brookes et al 2004) and p16 deficient human fibroblasts are resistant to RAS induced senescence (Brookes et al 2002). However, whereas in certain fibroblastic strains such as the

frequently used WI-38 strain, $p16^{INK4a}$ is clearly upregulated, in the other strains such as BJ fibroblasts, $p16^{INK4a}$ is only minimally expressed (Itahana et al 2003). Intriguingly, fibroblasts with low or undetectable $p16^{INK4a}$ levels, in contrast those with high $p16^{INK4a}$ expression levels, can be induced to re-enter cell cycle by inactivation of p53 (Beausejour et al 2003). Interestingly SAHF which are known to be responsible for the irreversibility of senescence are present only in human fibroblasts that contain high levels of $p16^{INK4a}$ (Narita et al 2003). In view of recent studies, it is plausible that there might be CDK inhibitors other than $p16^{INK4a}$, playing a surrogate role in the regulation of pRb. Using a $p16^{INK4a}$ knock-down strategy, it was shown that $p16^{INK4a}$ inactivation is not functionally equivalent to pRb inactivation (Wei et al 2003). Given that $p21^{WAF1}$ overexpression in human fibroblasts results in premature senescence (McConnel et al 1998) and its induction can also lead to the inhibition of pRb phosphorylation by suppressing CDK2/Cyclin E activity, $p16^{INK4a}$ and $p21^{WAF1}$ may cooperate in maintaining pRb in the active state during cellular senescence.

1.10.1.2 p53

p53 is considered to be a guardian of the genome and depending on the severity of the damage it can activate genetic programmes that stop cell proliferation transiently (G1 and G2 arrest) or permanently (senescence), or eliminate the cell (apoptosis). The signals that induce a DNA damage response such as ionizing radiation or telomere dysfunction induce senescence primarily via the p53 pathway. p53 activity, and in some cases protein level, increases when cells undergo senescence (Itahana et al 2001). The mechanisms responsible for this are incompletely understood, but some molecular details are emerging. One cause of p53 activation appears to be an increase in the expression of ARF (p14ARF in human; p19ARF in mouse), a tumour suppressor encoded by the *INK4a-ARF* locus. It stimulates p53 activity due to sequestration of HMDM2 (MDM2 in mice), an E3 ubiquitin ligase that targets p53 for proteosome-mediated degradation. Thus, ARF prevents negative-feedback regulation of p53 by MDM2 (Bringold and Serrano 2000; Gil and Peters 2006). ARF is upregulated in cultured senescent murine cells as well as during premature senescence induced by $H\text{-}RAS^{V12}$ and has been reported to be absolutely required for telomeric and non-telomeric senescence in MEFs (Kamijo et al 1997; Kamijo et al 1999; Sharpless et

al 2004). In human cells the role of ARF is more complicated. For example it has been proven to be a critical regulator of E2F induced senescence (Dimri et al 2000; Wei et al 2001) but not H-RAS^{V12} induced senescence in human primary fibroblasts (Wei et al 2001). ARF can be transcriptionally activated by DMP1, a transcription factor that was found to be essential in RAS-RAF-ARF signalling in murine cells (Inoue et al 2000; Sreeramaneni et al 2005). ARF can be also negatively regulated by TBX2 and Pokemon that can bind to the ARF promoter and repress its transcription (Jacobs et al 2000; Maeda et al 2005). Another cause for the increase in p53 activity is reported to be the promyelocytic leukaemia (PML) tumour suppressor. PML is upregulated in replicatively senescent cells and mediates premature senescence in response to oncogenic H-RAS^{V12} by interaction with CBP/p300 acetyltransferase and acetylation of p53 and its stimulation (Ferbeyre et al 2000; Pearson et al 2000). PML was also found to bind to MDM2 and sequester it into the nucleolus (Bernardi et al 2004).

1.10.2 Reactive oxygen species as signal transducer in cellular senescence

The results discussed earlier in this chapter in the section 'oxidative stress' (1.8.3) suggest that oxygen concentration limits cellular lifespan *in vitro* by induction of cellular senescence. The relationship between intracellular oxidants and the senescent programme has been strengthened by the observation that treatment with sub-lethal doses of hydrogen peroxide can trigger certain primary cells to rapidly enter senescence (Chen and Ames 1994; Chen et al 1998; Frippiat et al 2002). Molecular analysis of these hydrogen peroxide treated cells revealed a predominant G1 arrest with an increase in p53 protein levels and increased p53 activity, accompanied by subsequent upregulation of p21^{WAF1} (Chen et al 1998). Interestingly, an increase in the expression of a subset of p38 MAPK-dependent genes in H_20_2-induced premature senescence was identified suggesting a link between reactive oxygen species (ROS) and p38 activation (Zdanov et al 2006). A strong argument supporting the role of ROS in mediating senescence stems from the fact that overexpression of H-RAS^{V12} induces senescence and increases ROS levels (Lee et al 1999). Interestingly, *Seladin-1*, which encodes an oxidoreductase enzyme involved in cholesterol synthesis (Waterham et al 2001) and protection of neurons from oxidative stress in

Alzheimer's disease (Greeve et al 2000) has been identified as a crucial mediator of H-RAS^{V12} induced senescence and has been linked to RAS-induced reactive oxygen species signalling (Wu et al 2004). Moreover, the p53 transcriptional target p21^{WAF1}, when ectopically expressed induces the hallmarks of senescence with an accompanying rise in intracellular ROS (Macip et al 2002). Treatment with antioxidant NAC (N-acetyl cysteine) has been shown to prevent both RAS-induced senescence and p21-induced senescence (Lee at 1999; Macip et al 2002). Recently, Takahashi and coworkers have demonstrated that p16^{INK4a}/pRb pathway can also induce a rise in intracellular ROS levels through activation of PKCδ (Protein Kinase C δ), which, in turn seems to lead to further production of ROS by activating NADPH oxidase, thus establishing a self-sustained positive feedback loop. In addition, the activation of PKCδ results in dramatic depletion of WARTS protein (WTS/large tumour-suppressor 1 mitotic kinase) expression, the kinase essential in cytokinesis, and G2M cell cycle arrest which act as a second barrier ensuring irreversibility of senescence (Takahashi et al 2006).

1.10.3 p38 Mitogen-acivated protein kinase represents a common senescence pathway

The p38 kinase belongs to the family of mitogen-activated protein kinases (together with extracellular regulated kinase, ERK and c-Jun N-terminal kinase, JNK) and is also known as stress-activated protein kinase (SAPK). The mammalian genome encodes four isoforms of p38 (α, ß, γ, δ). P38 plays a crucial role in various processes such as inflammation, cellular responses to micro-organisms and other environmental stresses (Bulavin and Fornace 2004; Nebreda and Porras 2000) and has aslo been also been strongly linked to cellular senescence in mouse and human cells. It has emerged as a common signalling pathway that is required by various stimuli to cause senescence including replicative stress, oncogene overexpression, hydrogen peroxide and culture shock (Iwasa et al 2003; Trost et al 2005; Wang et al 2002). The mitogen-activated protein kinase (MAPK) signalling cascade is the principal Ras-effector pathway responsible for premature senescence (Lin et al 1998). Remarkably, this is the same pathway whereby Ras induces mitogenesis in immortal cells suggesting the existence within the RAS signalling cascade of a signalling branch that mediates premature senescence and therefore limits transformation. It has

been shown that activation of MEK-ERK pathway by RAS in primary fibroblasts leads to activation of p38 MAPK, which in turn induces accumulation of cell cycle inhibitors and senescence. RAS-induced p38 activation is achieved by its upstream kinases MKK3 and MKK6 (Wang et al 2002). Constitutive activation of p38 signalling by overexpression of active mutants of MKK3 or MKK6 results in premature senescence. Conversly, suppression of p38 by the inhibitor SB203580 or by dominant negative mutants of MKK3/MKK6, substantially rescues senescence induced by RAS (Wang et al 2002; Iwasa et al 2003). In addition, expression of Wip1 (a p38 phosphatase) which inactivates p38, renders primary human fibroblasts refractory to RAS induced senescence (Bulavin et al 2002), whereas inactivation of Wip1 causes p38 activation and premature senescence in MEFs (Bulavin et al 2004). Furthermore, MEFs that are deficient in Gadd45a, a DNA damage and stress-induced protein that binds and activates p38, are unable to undergo senescence induced by RAS (Bulavin et al 2003). Interestingly, expression of RAS oncogene in human osteosarcoma U2OS results in a $p16^{INK4a}$/ARF independent senescence-like growth arrest that can be rescued by the inhibition of p38 MAPK (Bihani et al 2004). Another oncogene, erbB2, the tyrosine kinase receptor that is frequently overexpressed in breast carcinomas and other human cancers induces premature senescence that requires intact p38 MAPK (Trost et al 2005). These studies strongly implicate p38 MAPK in oncogene-induced senescence. Currently, it remains largely unknown what are the downstream effectors of p38 in the context of senescence. However, the $p16^{INK4a}$ and p53 are believed to be two major downstream targets of p38 in RAS induced senescence. It has been suggested that p38 activation stabilises $p16^{INK4a}$ and p53 mRNA by as yet elusive mechanisms (Wang et al 2002). Other studies identified PRAK (p38-regulated/activated protein kinase), a downstream regulator of p38 MAPK to be essential for RAS induced transcriptional activity of p53. PRAK directly phosphorylates p53 at Ser37, a residue required for p53 to drive RAS induced senescence. In addition to PRAK, p38 directly phosphorylates p53 at Ser33 and Ser46 during RAS-induced senescence (Sun et al 2007). It is also not very clear what is the mechanism by which MKK3/6-p38 is activated since there is a profound delay in the transduction of signal from MEK-ERK to MKK3/6 and p38, indicating that it occurs via an indirect and slow route (Wang et al 2002). Reactive oxygen species emerged as a potential missing link given that they are

induced by RAS and mediate both p38 activation and oncogene-induced senescence (Colavitti and Finkel 2005); Iwasa et al 2003; Lee et al 1999). In support of this hypothesis, recent studies demonstrated that MINK kinase is activated by RAS induced ROS and subsequent activation of p38 by MINK (a Ste20/germinal center kinase family MAP kinase kinase kinase) results in premature senescence (Nicke et al 2005). Moreover, p38 itself has also been shown to restrict RAS-induced tumourigenesis by acting as a sensor of ROS (Dolado et al 2007).

1.11 Oncogene induced senescence as a cancer fail-safe mechanism

In principle, cellular senescence is thought to be an important, evolutionary conserved fail-safe mechanism, a natural barrier that cells must overcome in order to become immortal and induce tumourigenesis. Apoptosis has been a well established mechanism of tumour suppression for a long time (Brown and Attardi 2005; Kim et al 2006) but to what extent the observed cellular senescence *in vitro* reflects a relevant anti-cancer mechanism *in vivo* has been controversial. It was important to address this issue especially in view of some studies showing that not all primary fibroblasts undergo H-Ras induced senescence. Galloway and collegues reported that ectopic expression of Ras in human foreskin fibroblasts (HFFs) freshly established from the primary tissue does not result in premature senescence but instead causes mild transformation of these cells (Benanti and Galloway 2004). Interestingly freshly established HFFs were found to differ from routinely used strain of IMR90 fibroblasts in the basal levels of p16 (undetectable in HFFs, detectable in IMR90s) and the relative extent of p16 upregulation by H-Ras. The authors suggested that passaging of cells leads to culture-imposed stress causing accumulation of p16 allowing for Ras-induced arrest. Hence HFFs used directly after isolation from the tissue had been exposed to considerably less environmental stress, did not express any detectable p16 and were resistant to senescence. In support of this hypothesis it has been demonstrated that extended passaging of HFFs may render them sensitive to H-Ras induced senescence. Several recent studies, however, have reported that oncogene-induced senescence can occur *in vivo* in human tumours and mouse cancer

models, and indeed provides a vital mechanism that constrains neoplastic transformation (Figure 1.11). Abnormal activation of oncogenic Ras, BRAF, E2F or loss of PTEN tumour suppressor can promote aberrant cell proliferation, which eventually provokes activation of a cellular senescence programme *in vivo*. If the programme remains intact, the neoplastic growth may remain benign for many years. However, mutations that disrupt p53, $p16^{INK4a}$ or Suv39H1 which are sustaining cellular senescence cooperate with tumour progression (Braig et al 2005; Chen et al 2005; Collado et al 2005; Lazzerini et al 2005; Michaloglou et al 2005). Probably the most spectacular example of oncogene-induced senescence *in vivo* is the appearance of naevi or moles on human skin, which are benign tumours of cutaneous melanocytes containing senescent cells (Michaloglou et al 2005). In addition several studies have demonstrated that re-expression of endogenous p53 rapidly induces senescence and curtails oncogenesis in genetically engineered mouse models of sarcoma and hepatocellular carcinoma (Ventura et al 2007; Xue et al 2007). Xue and coworkers showed that even brief reactivation of p53 in p53-deficient tumours can result in complete tumour regression. This response also triggered an innate immune response that was associated with tumour clearance (Xue et al 2007). Importantly cellular senescence has also been found to be involved in the tumour regression related to the inactivation of the c-Myc oncogene in diverse tumour types including lymphoma, osteosarcoma, hepatocellular carcinoma (Wu et al 2007).

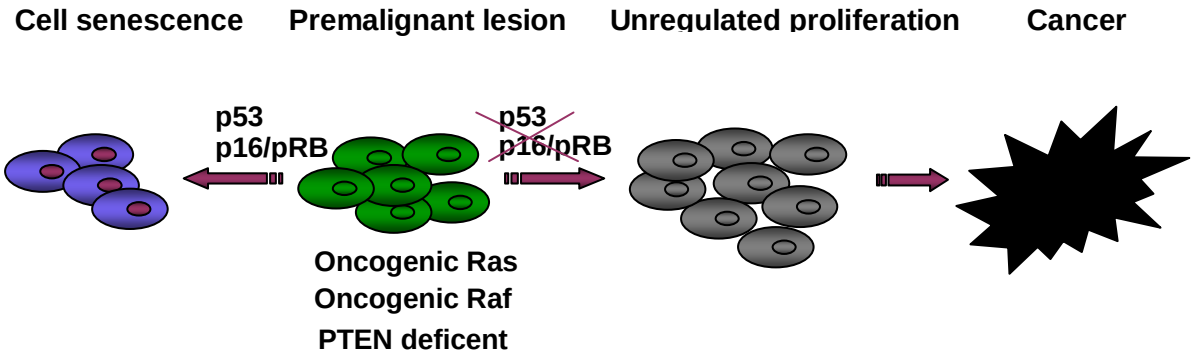

Figure 1.11 Oncogene induced senescence as an anti-cancer fail-safe mechanism

Activating mutations of RAS or BRAF or inactivation of PTEN resulting in hypermitogenic signalling produce premalignant lesions. Disruption of tumour suppressors p53 and p16/pRb allows escape from senescence and progression to malignant tumours

1.12 RUNX genes and senescence

It has been reported by our laboratory that all three RUNX proteins are capable of inducing senescence-like growth arrest in primary MEFs (Kilbey et al 2007; Wotton et al 2004). RUNX1 induced senescence in MEFs was found to be p53 dependent and pro-oncogenic activity of RUNX1 could be revealed in p53 null MEFs (Wotton et al 2004). RUNX expressing MEFs were found to undergo profound growth arrest without the initial burst of proliferation which characterizes oncogenic RAS induced senescence (Kilbey et al 2007, Wotton et al 2004). However, issues such as whether RUNX1 can also induce senescence in primary human fibroblasts or which structural domains of RUNX1 are required for the senescence induction have not been previously investigated. Furthermore the mechanism by which RUNX1 expressing cells acquire a senescent phenotype and the potential of RUNX1 fusion oncoproteins to cause senescence had not been addressed at the outset of my studies.

1.13 Aims of the project

1. To investigate the mechanism and structural requirements for senescence-like growth arrest induced by RUNX1.

2. To test the effect of ectopic RUNX1 expression in human primary fibroblasts as well as characterise a system to study oncogene-induced senescence.

3. To compare the effects of RUNX1 and its derivatives to Ras^{V12}, a prototypic inducer of oncogene-induced senescence in human fibroblasts.

Chapter 2

2 Materials and methods

2.1 Materials

2.1.1 Antibodies

Antibodies were used for Western blotting or immunolocalisation in microscopy. The dilution used for each antibody is provided in brackets.

Active Motif Europe (Belgium)

Anti-AML1/Runx1 (39000), (1:1000)

Cell Signalling Technology (New England Biolabs, UK)

Anti-p38 (9212), (1:1000)

Anti-phospho-p38 (9211), (1:1000)

DAKO Ltd, UK

Polyclonal rabbit Anti-mouse immunoglobulins/HRP, (1:1000)

Polyclonal swine Anti-rabbit immunoglobulins/HRP, (1:3000)

Polyclonal rabbit Anti-goat immunoglobulins/HRP, (1:2000)

Dr. Nancy Speck (Department of Biochemistry, Dartmouth Medical School, Hanover, USA)

Monoclonal supernatant recognising CBFβ (peptide 42-214 amino acids)

Dr. Scott Hiebert (Vanderbilt Cancer Center, USA)

Anti-Runx1-ETO polyclonal rabbit antibody that recognising ETO zinc finger motif was a kind gift from Dr. Scott Hiebert, (1:500)

Dr. Tina Rich (University of Glasgow, UK)

Anti-PML (N19, Santa Cruz) (1:200) and Alexa Fluor-conjugated secondary antibody (Molecular Probes) (1:100)

Jackson Immuno Reasearch Laboratories, Inc (Stratech Scientific Ltd., UK)

Fluorescein (FITC)-conjugated Affinity Purified Sheep Anti-Mouse IgG, (1:100)

Medical and Biological Laboratories Co., Ltd (MBL) (Stratech Scientific Ltd, UK)

Anti-Runx (D207-3), (1:1000)

NeoMarkers (Lab Vision Products Thermo Fisher Scientific, UK)

Anti-p14ARF (Ab-2), (1:500)

Positive control for anti-p14 (MS-850-PCL)

Oncogene Research Products (Merck, UK)

Anti-H-ras (Ab-1), (1:200)

Roche Diagnostics Ltd, UK (In situ Cell Proliferation Kit, FLUOS)

Monoclonal anti-BrdU conjugated with fluorescein

Santa Cruz Biotechnology Inc (Insight Biotechnology, UK)

Anti-p16 (sc-468), (1:1000)

Anti-p21 (sc-397), (1:250)

Anti-p53 (sc 126), (1:1000)

Anti-actin (sc-1616), (1:1000)

Upstate Cell Signalling Solutions (Millipore, UK)

Anti-phospho-Histone-H2A.X (Ser139) (05-636), (1:200)

2.1.2 Cell culture

2.1.2.1 Cell lines

Wild type and p53$^{-/-}$ mouse embryo fibroblasts (MEFs) were prepared from E13.5 day embryos of wild-type (C57B16/CBA) and p53 null mice as described before (Wotton et al 2004). Briefly, the head and red organs were removed and the body minced and treated with 0.5% trypsin for 15 min to disperse the cells. The cells were expanded in culture and frozen at passage two in 60% FCS, 10% DMSO

Hs68 strain of human neonatal foreskin fibroblasts (passage 30; ATCC: CRL 1635). These were rendered sensitive to ecotropic retroviruses by expression of murine leukaemia virus receptor have been previously described (Brookes et al 2004) and kindly provided by Prof. Gordon Peters (CR-UK, London).

Leiden cells (passage 29). These are a p16^{INK4a} deficient human diploid fibroblasts that were originally isolated from a male patient who from the age of 6 developed multiple prominent naevi which by puberty had become atypical. Dermal fibroblasts were isolated from a region of normal epidermis adjacent to one of the dysplastic naevi removed when the patient was 24 years of age. Leiden cells expressing mouse ecotropic receptor were kindly provided by Prof. Gordon Peters (CR-UK, London) (Brookes et al 2002)

Phoenix ecotropic packaging cell line is a second-generation retrovirus producer lines for the generation of helper free ecotropic retroviruses. The line is based on the 293T cell line (a human embryonic kidney line transformed with adenovirus E1a and carrying a temperature sensitive T antigen co-selected with neomycin). The unique feature of this cell line is that it is highly transfectable with either calcium phosphate mediated transfection or lipid-based transfection protocols. The lines were created by placing into 293T cells constructs capable of producing gag-pol, and envelope protein for ecotropic and amphotropic

viruses. Phoenix cell line was obtained from G. Nolan, Stanford University, Palto Alto, CA, USA.

2.1.2.2 Media and supplements

All supplements and media for cell culture were supplied by Invitrogen Life Technologies

Media

The media was delivered as sterile 1x solution and stored at 4°C.

Dulbecco's Minimum Essential Medium (DMEM) with 4500 mg/L glucose, L-Glutamine and pyruvate.

Supplements

Foetal Bovine Serum (FBS), HyClone, Perbio: virus and mycoplasma screened. FBS was heat inactivated at 56 °C for 30 minutes by the supplier and routinely used at a concentration of 10%.

L-glutamine: supplied as a 200 mM (100x) stock solution. This was routinely added to culture media prior to use to a final concentration of 2mM.

Penicillin/streptomycin (P/S): supplied as a 100x stock solution of 10,000 units penicillin and 10,000 units streptomycin per millilitre. This was used to supplement media to a final concentration of 100 units penicillin/100 units of streptomycin.

2.1.2.3 Solutions, reagents and antibiotics

Antibiotics

Puromycin (Sigma), solid was dissolved in water, aliquotted and stored as 5mg/ml stock solution in –20 °C

Transfection Reagent

Superfect transfection Reagent (Qiagen) stored in –4 °C

SA-ß-galactosidase staining

25% glutaraldehyde stock solution stored in –4 °C (5% PBS pH 7.2) solution freshly prepared prior to use)

0.12 M stock solution of $K_3Fe[CN]_6$ and $K_4[Fe]CN_6$ stored in –4 °C

1M stock solution of $MgCl_2$ stored in –4 °C

Ultra pure™ X-Gal (Invitrogen) stored as solid in –4 °C

Fresh SA-ß-gal staining solution in PBS (pH 6) prepared immediately prior to use consisted of: X-gal (1mg/ml), 0.12 mM $K_3Fe[CN]_6$ and $K_4[Fe]CN_6$ and 1mM $MgCl_2$

Inhibitors

SB203580, a highly specific p38 kinase inhibitor (Calbiochem) was dissolved in DMSO, aliquoted and stored in –20 °C as 8mM stock solutions

Other

Trypsin-EDTA (Invitrogen): supplied as 0.5% 1x liquid, stored at –20 °C

DCF (2', 7'-dichlorofluorescein diacetate, Calbiochem), cell-permeable fluorogenic probe that is used for the detection of reactive oxygen species was stored in –20 °C as a powder and diluted in DMSO prior to use

2.1.2.4 Plasticware

Tissue culture flasks, pipettes (5, 10, and 25 ml), 100 mm cell culture dish, 12 well plates were supplied by Costar (Corning Incorporated, Netherlands)

Cryotubes 1.8 ml were supplied by Nunc (DK 400, Roskilde, Denmark)

Falcon conical centrifuge tubes (15 and 50 ml) were supplied by Becton Dickinson Labware Europe

Syringe filters (0.2 µm and 0.45 µm) were supplied by Sartorius (Hannover, Germany); used for sterilising of filtering small volumes of solutions

Syringes (2, 5, 10, 20, 50) ml were supplied by Becton Dickinson

Chamber Slide System-2 well glass slide was supplied by Lab-Tek (Nalge Nunc International, Rochester, New York). Chamber slides were coated with poly-L-lysine (13.3 µg/ml) prior to use

2.1.3 Bacteriology

2.1.3.1 Bacterial strain

***E. coli* One shot ® TOP10**: One Shot Chemically Competent *E.coli* cells (~1 x 10^9 colony forming units/µg) (Invitrogen). Genotype: F^- *mcr*A Δ(*mrr-hsd*RMS-*mcr*BC)Φ80 *lac*ZΔM15 Δ*lac*X74 *deo*R *rec*A1 *ara*D139 Δ(*ara-leu*)7697 *gal*U *gal*K *rps*L (Str^R) *end*A1 *nup*G.

2.1.3.2 Antibiotics

Ampicillin (Sigma): 100 mg/ml in ddH_2O. Filtered through a 0.22 µm filter, aliquotted and stored at –20°C until use

2.1.3.3 Bacteriological media

Media were sterilised by autoclaving at 121 °C for 15 minutes, unless otherwise stated.

LB (Luria Bertani) medium: 1% (w/v) Tryptone, 0.5% (w/v) Yeast extract, 1% (w/v) NaCl in dH_20. pH then adjusted to 7.0 with NaOH.

LB-agar: as for LB medium but also containing 1.5% (w/v) agar.

SOC medium: 2% Tryptone, 0.5% Yeast extract, 10 mM NaCl, 2.5 mM KCl, 10 mM $MgCl_2$, 10 mM $MgSO_4$, and 20 mM Glucose. (Invitrogen, UK).

2.1.3.4 LB agar plates supplemented with ampicillin

Plates were prepared (Sterilin, Staffordshire, UK) with LB agar which was supplemented with 100 µg/ml ampicillin. Plates were stored in -4°C for no more than two weeks.

2.1.4 Complete kits

Big Dye® Terminator Version 1.1 Cycle Sequencing Kit (Applied Biosystems)

ECL™ Western Blotting Detection Reagents (Amersham Biosciences)

EndoFree® Plasmid Maxi Kit (Qiagen)

QIAquick® PCR Purification Kit (Qiagen)

QIAquick® Gel Extraction Kit (Qiagen)

Klenow Fill-In Kit (Stratagene)

Quick Ligation™ Kit (New England Biolabs)

In Situ Cell Proliferation Kit, FLUOS (Roche)

2.1.5 DNA

Plasmid, molecular weight markers and oligonucleotide DNAs were stored at -20 °C.

2.1.5.1 Retroviral vectors

pBabe puro

The pBabe puro retroviral vector facilitates the transmission of inserted genes at high viral titres and their expression them from the Long Terminal Repeat (LTR) of the Moloney murine leukaemia virus (Mo MuLV). This vector includes a dominantly acting selectable marker, conferring resistance to puromycin to infected mammalian cells during selection with puromycin (Figure 2.1) (Morgenstern and Land 1990). pBabe puro also contains an ORI origin of replication and the AmpR gene for propagation and antibiotic selection in bacteria.

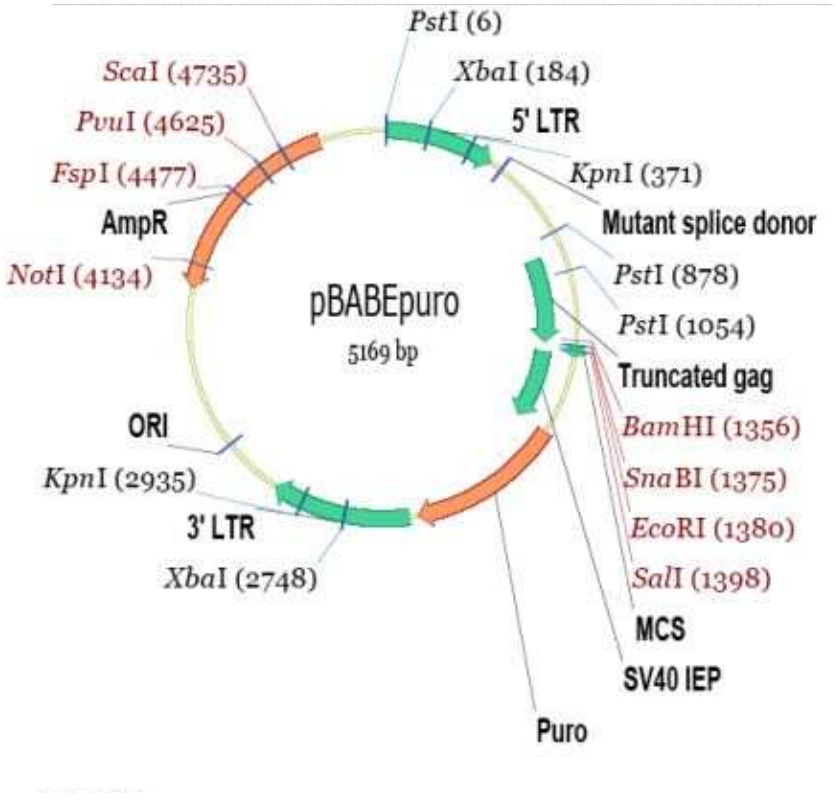

Figure 2.1 Structure of pBabe puro retroviral vector

LTR-long terminal repeats; MCS-multiple cloning sites; SV40-simian virus promoter; Puro-puromycin resistance gene; ORI-origin of replication; ; AmpR-ampicillin resistance gene

pBabe puro plasmids containing human RUNX1 P1, RUNX1-ETO and RUNX1-ETOΔ469 were kindly provided by Dr. Scott Hiebert (USA) (Linggi et al 2002). The pBabe puro plasmids containing H-RAS^{V12} was a kind gift from Dr. Scott Lowe (USA) and the plasmid encoding p53 was supplied by Prof. Gordon Peters (London). The other pBabe puro vectors including AML1a and TEL-RUNX1 or RUNX1 mutants: K83N and T161A were constructed as described in Section 2.2.2.7. All of the constructs were sequenced as described in Section 2.2.3.

pLXSN

pLXSN contains elements derived from Moloney murine leukaemia virus (MoMuLV) and Moloney murine sarcoma virus (MoMuSV) and is designed for retroviral gene delivery and expression. Upon transfection into packaging cell line, pLXSN can transiently express or integrate and stably express the gene of interest. The 5' viral LTR in this vector contains promoter/enhancer sequences that control expression of the gene in the multiple cloning site. The SV40 early promoter (P_{SV40}) controls expression of the neomycin resistance gene which allows antibiotic selection in eukaryotic cells. pLXSN also includes the ColE1 origin of replication and Amp^r gene for propagation and antibiotic selection in bacteria (Figure 2.2).

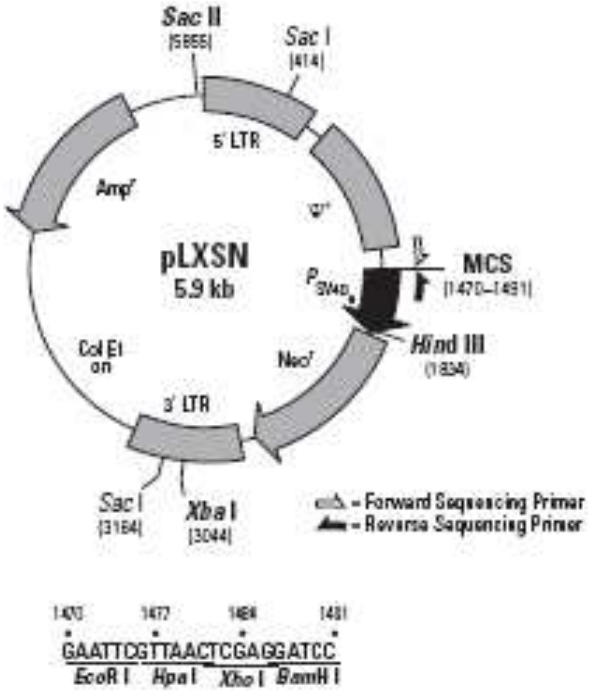

Figure 2.2 Structure of pLXSN retroviral vector

LTR-long terminal repeats; MCS-multiple cloning sites; P_{SV40}-simian virus promoter; Neo-puromycin resistance gene; ColE1-origin of replication; Amp-ampicilllin resistance gene

Empty vector (pLXSN) and vector containing Human papilloma virus 16 E6 oncoprotein (pLXNS-E6) were kindly provided by Prof. Saveria Campo (University of Glasgow)

2.1.5.2 Molecular size standards

Molecular size standards used include ϕX174 RF DNA/HaeIII fragments (size range 72 bp to 1,353 bp), λ DNA/HindIII fragments (size range 125 bp to 23,130 bp), and Low DNA Mass™ Ladder (size range: 100-2000 bp) all supplied by Invitrogen Life Technologies.

2.1.5.3 Oligonucleotide primers

Oligonucleotides for sequencing were synthesised by MWG Biotech, and delivered as high purity salt free lyophilised DNA. Primers were reconstituted at 100 pmol/µl in distilled water (dH_20) and stored at –20 °C.

2.1.6 Enzymes

All enzymes were stored at –20 °C and were removed from storage immediately before use.

2.1.6.1 Restriction enzymes

All enzymes and their associated buffers were supplied by Invitrogen Life Technologies (UK) except for SnaBI which was supplied by Promega (UK).

Details of restriction enzymes, their restriction sites and reaction conditions are shown in Table 2.1.

Table 2.1 Restriction enzymes.

Restriction enzyme	Restriction site	Buffer	Temperature of incubation (°C)
EcoR I	[5´-G↓AATTC-3´]	REACT® 3	37
Sna BI	[5´-TAC↓GTA-3´]	Buffer B	37
Not I	[5´-GC↓GGCCGC-3´]	REACT® 3	37
Hind III	[5'-A^A G C T T-3']	REACT® 3	37
Sal I	[5´-G↓TCGAC-3´]	REACT® 10	37

2.1.6.2 Antarctic phosphatase

Recombinant Antarctic phosphatase (New England Biolabs) supplied with 10x buffer

2.1.7 Protein SDS-PAGE standards

Prestained SDS-PAGE (Sodium Dodecyl Sulphate - Polyacrylamide Gel Electrophoresis) standard was the Precision Plus Protein™ Standards, supplied by Biorad. This standard contains ten highly purified recombinant proteins ranging from 10 kDa to 250 kDa. The stock was aliquoted and stored at –20 °C. Each aliquot was heated to 95 °C for 3 minutes prior to use to dissolve any precipitated solids.

2.1.8 General chemicals

Chemicals used were of analytic, ultrapure or molecular grade quality and were supplied by Sigma Aldrich, Fisher Scientific UK Limited, Invitrogen Life Technologies, unless stated otherwise.

Acetic acid sodium salt (Sodium acetate)

Agarose

Albumin from bovine serum (BSA)

Butanol

β-Mercaptoethanol

Crude ethanol (University of Glasgow Stores)

Crystal Violet

Dimethyl sulfoxide (DMSO)

D-(+)-Glucose

Ethanol

Ethidium Bromide

Ethylene diamine tetra acetate (EDTA) disodium salt

Glycerol

Glycine

Hi-Di™ Formamide (Applied Biosystems)

4-(2-Hydroxyethyl) piperazine-1-ethanesulfonic acid (HEPES)

Hydrochloric acid

Magnesium Chloride

Methanol

Nonident P-40 (NP40)

16% paraformaldehyde (Science Services Ltd)

Propan-2-ol (Isopropanol) Molecular Biology Grade

Potassium Chloride

Potassium hexacyanoferrate(III) ($K_3Fe[CN]_6$)

Potassium hexacyanoferrate(IV) ($K_4[Fe]CN_6$)

Sodium Acetate

Sodium Chloride

Sodium dodecyl sulphate (SDS)

3′,5′,5″-Tetrabromophenolsulfophethalein (Bromphenol Blue)

Tris Base (2-Amino-2-(hydroxymethyl)-1, 3-propanediol)

Triton X-100

Tween 20 (Polyoxethylene sorbitan nonolaurate)

2.1.9 Equipment

2.1.9.1 Major Equipment

Automated Processor: SRX-101A Compact X4 (Xograph Imaging Systems, Gloucestershire, UK)

Automatic Sequencing Apparatus: ABI Prism 3100 Genetic Analyzer (Applied Biosystems, Foster City, USA)

Benchtop centrifuge: Legend™ Sorvall (Kendro Laboratory Products, Germany), Avanti® J-E Centrifuge (Beckman Coulter, USA), Centrifuge 5810, 5810R (Eppendorf, Cambridge, UK), EBA-12R (Hettich Zentrifugen, Tuttlingen, Germany), Biofuge 13 (Heraeus, Germany)

Bench-top microprocessor pH meter: pH 213 Microprocessor pH Meter (Hanna Instruments, Sarmeola di Rubano, Italy)

Biological safety cabinet: Fume Cupboard (Premier Laboratory Systems, Scotland), and TriMAT^2, Class II Microbiological Safety Cabinet (Medical Air Technology Ltd, Oldham, UK)

Flow cytometer: Coulter Epics XL MCL (Beckman Coulter Company, Florida, USA)

Gel cast: AE-6210 Slab Gel Cast (Atto Incorporation, Japan); casting stand and casting frames from Mini-Protean 3 Cell and Systems, and gel caster from Sub-Cell Systems (Bio-Rad Hertfordshire, UK)

Gel electrophoresis systems: Biomax QS710 Horizontal Unit (Scientific Imaging Systems – Eastman Kodak Company, New York, USA); Sub-Cell GT Submerged Horizontal Agarose Gel Electrophoresis System, and MiniProteanII™ (Bio-Rad,

Hertfordshire, UK); AE-6200 Slab EP Chamber, and AE-6220 Slab EP Chamber, for two gels (Atto Incorporation, Japan)

Hemocytometer (Bright Line Sigma), cell counting chamber

Horizontal orbital shaker: Orbital Incubator (Gallenkamp, Leicester, UK)

Incubator: MIR-262 (Sanyo Electric Biomedical Co. Ltd., Japan)

Incubators for tissue culture: Hera cell 150 (Heraeus, Surrey, UK)

Microcentrifuges: Minispin (Eppendorf, Cambridge UK), Mikroliter (Hettich Zentrifugen, Tuttlingen, Germany)

Microscopes: Laser Confocal Scanning Microscope (Leica DM IRE2), Inverted Microscope (Leica DM IL)

Microwave Micro chef St44 (Proline, UK)

Oven Maxi 14 (Hybaid Limited, Middlesex, UK)

PCR Machine: PTC-220 DNA Engine Dyad® Cycler (MJ Research Incorporated, Massachusetts, USA)

PCR workstation: PCR 6 Vertical Laminar Airflow Cabinet with UV Sterilisation (Labcaire Systems Ltd, North Somerset, UK)

Pipettes: Pipetman (P10, P20, P200, and P1000) supplied by Gilson Medical Electronics (Villiers-le-Bel, France)

Power packs: Electrophoresis Power Supply EPS 500/400 (Pharmacia Fine Chemicals, Uppsala, Sweden), and Power PAC 300 (Bio-Rad, Hertfordshire, UK)

Rotator: Spiramix 5 (Denley Instruments Ltd, England)

Semi-dry electrophoretic transfer: Trans-blot® SD Semi-Dry Transfer Cell (Bio-Rad Hertfordshire, UK)

Shaker: Model R100 Rotatest Shaker (Luckham, England), Stuart SSL1 Orbital Shaker (Bibby Sterilin Ltd, Staffordshire, UK), and Orbital Shaker (Bellco Biotechnology, New Jersey, USA)

Spectrophotometer: DU® 640 Spectrophotometer (Beckman, California, USA), Agilent 2100 Bioanalyzer (Agilent Technologies, Germany)

Stirrer: Magnetic Stirrer Hotplate B212 (J. Bibby Science Products Limited, Staffordshire, England), and Stir SB161 (Stuart Scientific Laboratory, Surrey, UK)

Thermo Block: Dri-block® DB-2A (Techne, Cambridge, UK)

Ultraviolet trans-illuminator: High Performance Ultraviolet Transluminator (UVP-Ultra Violet Products, San Gabriel, CA), and Geneflash Syngene Bio Imaging (Fisher Scientific- Synoptics Ltd, UK)

Vortex: WhirliMixer™ (Fisons Scientific Equipment, Leicestershire, UK)

Water baths: Grant, SBB6, and Y14 (Grant Instruments Ltd, Cambridge, England)

2.1.9.2 Consumables

Caterers foil (Morrisons, Anniesland, Glasgow)

Eppendorf tubes: Flip-top 0.5 ml and 1.5 ml, and screw-top 1.5 ml (Elbkay Laboratory Products, Hampshire, UK), and Rnase-free Microfuge Tubes (Ambion, Cambridgeshire, UK)

Filter paper: Qualitative Circles 185 mm Ø (Whatman®, Kent, England)

Filter tip pipette tips: A range of capacities (10, 20, 200, 1000) µl supplied by Rainin Instrument Co (Woburn, MA); for use in setting up PCR reactions

Fine Tip Pastette Sterile were supplied by Alpha Laboratories (Hampshire, UK)

Hybond^{TM}-ECL nitrocellulose membrane (Amersham Biosciences, Buckingshamshire, UK)

Hyperfilm ECL (Amersham Biosciences, Buckingshamshire, UK)

Marvel Dried Skimmed Milk (Premier Beverages, Stafford, UK)

Parafilm was supplied by Pechiney Plastic Packaging (Menasha WI)

Petri dishes were supplied by Sterilin (Staffordshire, UK)

Pipette tips were supplied by Sarstedt (Nümbrecht, Germany)

Pipette tips RNAse free: 1000 µl and 200 µl supplied by Starlab (Ahrensburg, Germany), and 1 µl to 20 µl supplied by Elkay Laboratory Products Ltd (Hampshire, England)

Saran barrier food wrap (Morrisons, Anniesland, Glasgow)

Scalpel blades: Sterile disposable scalpels (Schwann-Morton , Sheffield, UK)

Spreaders, L shaped were supplied by VWR International (Lutterworth, UK)

Sterile plastic containers: Bijoux and Universals (Greiner Bio-One, Gloucestershire, UK)

Syringes (2, 5, 10, 20, 50) ml were supplied by Becton Dickinson

Syringe filters (0.2 µm and 0.45 µm) were supplied by Sartorius (Hannover, Germany); used for sterilising of filtering small volumes of solutions

Vectashield Mounting Medium with DAPI (Vector Laboratories, Ltd)

2.1.10 Buffers and solutions

Water

Diethylpyrocarbonate (DEPC) treated RNAse free water was supplied by Ambion, Cambridgeshire, UK. Tissue culture grade distilled water was supplied by Invitrogen Life Technologies. Ultrapure water (for procedures involving recombinant DNA, PCR etc.) was provided by a Milli Q® ultrapure water purification system (Millipore Ltd., Watford, UK). An Elix® purification system (Millipore Ltd., Watford, UK) was used to supply water for preparation of general solutions and media.

Buffers and solutions

10x Dry Blot Buffer: 0.5 M Tris base, 0.4 M Glycine, 12.8 mM Sodium Dodecyl Sulfate (SDS). Working stock was prepared prior to use at a 1:10 dilution with 20% (v/v) Methanol.

10x SDS-PAGE Running Buffer: 0.25 M Tris base, 1.92 M Glycine, 34.7 mM SDS

10x TBE (Tris-borate-EDTA) Buffer Solution: 0.9 M Tris base, 0.9 M Boric acid, 23 mM Na_2EDTA. pH 8.2/8.3. Stored at room temperature.

10x TBST (Tris-buffered-saline-tween) Buffer Solution: 0.1 M Tris base, 1.5 M NaCl, 0.5% Tween-20, adjusted to pH 8.0.

10x Tris-glycine buffer for electrotransfer of proteins onto membranes (transfer buffer): 0.25 M Tris base, 1.92 M Glycine. Working stock was prepared prior to use at a 1:10 dilution with 15% (v/v) Methanol.

1M Tris HCl: 121 g Tris base, 800 ml dH_2O. Adjusted to desired pH with concentrated HCl and made up to 1 L.

1x Phosphate buffered saline (PBS): 140 mM NaCl, 2.7 mM KCl, 10 mM Na_2HPO4, 1.8 mM KH_2PO_4 (pH 7.3)

20x Propidium iodide (PI) stock solution: made to a working solution of 1 mg/ml with ddH_2O in a fume cupboard. This was filtered through a 0.22 μm syringe filter, and stored at 4 °C in the dark.

50x TAE (Tris-acetate-EDTA) Buffer Solution: 2 M Tris base, 50 mM Na_2EDTA, 1 M glacial acetic acid.

Ammonium persulphate: 10% (w/v) stock solution in ddH_2O, freshly made.

Ethidium bromide: made to a working solution of 3 mg/ml with ddH_2O in a fume cupboard. Stored at room temperature in the dark.

Gel loading buffers:

1. DNA- 30% Glycerol, 0.25% (w/v) Bromophenol blue, 0.25% (w/v) Xylene cyanol, in ddH_2O. Stored at room temperature and used at a 1:5 dilution.

2. Protein- SDS-PAGE Protein 2x Sample Loading Buffer: 120 mM Tris-HCl, pH 6.8, 20% (v/v) Glycerol, 5% SDS, 7.4% β-mercaptoethanol, 0.5% (w/v) Bromophenol blue in ddH_2O. Stored in aliquots at –20 °C. Sample diluted at least 1:2 with buffer and heated at 100 °C for 5 minutes prior to loading gel.

PI Staining solution: 50 μg/ml 20x PI stock solution, 100 U/ml Rnase A in sample buffer (1 g/l Glucose in PBS. This was filtered through a 0.22 μm syringe filter, and stored at 4 °C)

TE Buffer: 10 mM Tris-HCl, 1 mM Na_2EDTA adjusted to pH 8.0. Autoclaved and stored at room temperature.

Whole Cell Lysis Buffer (Marais et al 1993): 20 mM Hepes pH 7.0, 5 mM EDTA, 10 mM EGTA, 5 mM NaF, 1 mM DTT, 0.4 M KCl, 0.4% (v/v) Triton X-100, 10% (v/v) Glycerol. Stored in aliquots at –20 °C. Working Whole Cell Extract buffer was prepared prior to use by addition of 0.1 μg/ml Okadaic acid, and protease inhibitors as follows: 5 μg/ml Aprotinin, 5 μg/ml Leupeptin, 5 μg/ml Pepstatin A, 1 mM Benzamidine, 50 μg/ml PMSF.

Mild stripping solution: prepared fresh by adding 20 ml 2M glycine pH 2.5, 20 ml 10% SDS to 160 ml dH_20

Sringent sripping solution: 100mM 2-Mercaptoethanol, 2% SDS, and 62.5mM Tris-HCl pH 6.7

3.7% paraformaldehyde in PBS: prepared fresh from 16% solution obtained from Science Services Ltd)

0.1 % Triton X-100 in PBS

10% FBS (Fetal Bovine Serum), 0.5% BSA(Bovine Serum Albumin/) in PBS

2.2 Methods

Many of the methods described here are based on standard protocols, which are found in several laboratory manuals (Sambrook et al 1989).

2.2.1 Growth, manipulation of mammalian cells and cell assays

All procedures involving mammalian cells were carried out in a laminar flow hood using standard aseptic procedures.

2.2.1.1 Cryopreservation of cells

Stocks of cells for long-term storage were preserved over liquid nitrogen. Cells to be frozen were grown to confluence and removed into a sterile 50 ml centrifuge tube (using 1x trypsin-EDTA solution). Cells were centrifuged at 1000 rpm for 5 minutes and the supernatant discarded. The cells were then re-suspended in freezing medium at a concentration of 2-4 x 10^6 cells/ml. Freezing medium consisted of the DMEM culture medium supplemented with FBS to 50% for MEFs, 20% for Hs68 cells and Leiden cells and 10% dimethylsulphoxide (DMSO, Sigma Aldrich) as a cryoprotectant. Phoenix cell were frozen down as advised in 90% FBS and 10% DMSO. The cell suspension was transferred in one millilitre aliquots, to labelled cryovials (Nunc cryotubes) and brought to –70 °C at a controlled rate of –1 °C per minute using a NALGENE™ Cryo 1 °C Freezing container (NALGENE, USA). The vials were transferred to a liquid nitrogen freezer for long-term storage after 24hs. Cell stocks were revived by rapid thawing in a 37 °C water bath and maintained following standard techniques (described below).

2.2.1.2 Cell counting

Cells were counted in a haemocytometer (Bright-Line Hemacytometer, Sigma) as follows. Cell pellets were suspended in an appropriate volume of media to allow ease of counting in the haemocytometer chamber. A 10 µl volume of the cell suspension was then diluted 1:1 in trypan blue stain 0.4% (Invitrogen Life Technologies) and incubated at room temperature for 1 minute. The suspension was then introduced to the haemocytometer chamber and cell counts made

using an inverted microscope with a 4x or 10x objective. Cells lying on the top and right hand perimeter of each large square (1 mm) were included; those on the bottom or left hand perimeters were excluded. Cell concentrations (cells/ml) were calculated by multiplying the mean numbers of cells per large marked square by 2 x 10^4 to account for the volume of the haemocytometer chamber and to correct for the dilution factor. Dead cells were differentiated by uptake of the trypan blue stain.

2.2.1.3 Maintenance of mammalian adherent cell lines

All cell lines (MEF, Hs68, Leiden, Phoenix) form adherent monolayers in culture, and were cultured in 75 cm^2, 162 cm^2 tissue culture flasks or 100mm cell culture dishes kept at 37 °C in a humidified incubator containing 5% (v/v) CO_2. Cells were cultured in 20 ml, 50 ml or 10 ml DMEM (Section 2.1.2.2) supplemented with 10% FBS, 100 international units (IU)/ml penicillin, 100 µg/ml streptomycin, and 2 mM glutamine. Cultures were passaged, every 3-4 days, when they have reached approximately 80% of confluence. To split cultures the medium was decanted from the cell monolayer and cells washed with 10 ml of warm PBS. Then, 3 ml to 5 ml of 1x trypsin-EDTA solution was added, cells were incubated at 37 °C for 5 to 15 minutes and observed by microscopy to ensure cell layer dispersal. The detached cells were then washed in fresh medium, pelleted by centrifugation at 1000 rpm for 5 minutes, prior to resuspending in fresh medium and seeding new tissue culture flasks.

2.2.1.4 Retroviral transduction

Phoenix cells were plated at 5 x 10^6 in 10 cm dishes and incubated overnight at 37°C. Transfections of Phoenix cells with relevant retroviral plasmids were performed using Superfect Transfection Reagent (Qiagen) according to the manufacturer's protocol for transient transfection of adherent cells. Viral supernatants were harvested after 48 h incubation at 37°C and filtered through 0.45 µm filters (Sartorius). The media was replaced and the cells incubated for a further 24 h before retrieval of a second viral supernatant. Each 10 ml of supernatant was supplemented with 4µg/ml polybrene and split between two 10 mm plates of target cells plated at 8 x 10^5 per dish 24 h earlier. Cells were incubated with the appropriate first harvested supernatant overnight and with

the second harvested supernatant during the day for 8 h. Infected cells were then incubated overnight in normal growth medium after which selection was applied using puromycin (Sigma) at 2ug/ml for 4 days. The efficacy of the selection protocol was confirmed using untransduced cells which all died under these selection conditions. Following selection (designated day 0), transduced cells were replated for experimental purposes. Puromycin selection was maintained throughout.

2.2.1.5 Growth curves

MEFs were plated at day 0 (day following 4 days of puromycin selection) at 2.5 x 10^4/well in 12 well plates in selection DMEM medium containing 2μg/ml puromycin (2ml/well). Live cell counts were carried out in triplicate using a haemocytometer and trypan blue exclusion to assess viability. Media changes were carried out every 3-4 days. Graphs were plotted using Sigma plot and significance values determined by Student's *t*-test. Error bars relate to standard deviations.

2.2.1.6 Senescence-Associated-β-galactosidase

SA-ß-gal activity was detected as previously described (Serrano et al., 1997). Cells were washed once with PBS (pH 7.2), fixed with 0.5% glutaraldehyde (PBS pH 7.2) and washed in PBS (pH 7.2) supplemented with 1mM $MgCl_2$. Cells were stained in X-Gal solution (1mg/ml [Invitrogen], 0.12 mM $K_3Fe[CN]_6$ and $K_4[Fe]CN_6$ and 1mM $MgCl_2$ in PBS at ph 6.0) overnight at 37°C.

2.2.1.7 Cell cycle analysis

Hs68s plated at 1 x 10^6 cells/10cm dish were sampled for flow cytometry on day 7 post-selection. The protocol for cell cycle analysis has been described previously (Blyth et al 2006). For simultaneous labelling with bromodeoxyuridine (BrdUrd), cells were incubated at 37°C for 3-hours with 10μM BrdUrd (Sigma) then rinsed three times in warmed PBS. After harvesting, cells (10^6) were washed in 2ml cold PBS, resuspended in 0.2ml cold PBS and fixed for at least 30 minutes in 2mls 70% ethanol at 4°C. BrdUrd incorporation was identified using FITC-conjugated anti-BrdUrd antibody (In situ Cell Proliferation Kit, Roche) according to manufacturers' instructions. Samples were resuspended in PBS

containing 10µg/ml PI and analysed on a Beckman Coulter Epics XL. The analysis was performed using EXPO32 software

2.2.1.8 Analysis of intracellular ROS

To assess the generation of intracellular ROS levels at day 7 of cell culture period, cells were incubated for 20 min in the dark at 37°C with 15µm DCF-DA (Calbiochem). Then cells were washed in PBS, trypsinised and DCF fluorescence was measured using a flow cytometer (Beckman Coulter Epics XL) with excitation at 488 nm and emission at 530 nm

2.2.1.9 Visulisation of ROS by confocal laser microscopy

Cell were grown on plated on poly-L-lysine-coated glass chamber slides (Section 2.1.2.4) and at day 7 of cell culture period were incubated for 20 min in the dark at 37°C with 15µm DCF-DA (Calbiochem). Then cell were washed in PBS and fixed with freshly prepared 4% paraformaldehyde (in PBS) for 10 minutes and subsequently coverslips were mounted in glycerol mixed with water (1:1). DCF fluorescence was detected using a FITC filter and fluorescent images were captured using a confocal microscope (Leica DM IRE2) (Section 2.1.9.1)

2.2.2 Recombinant DNA techniques

2.2.2.1 Storage and growth of bacteria

Plasmid DNA was maintained and stored in the *E.coli* strain One Shot Chemically Competent cells®. Glycerol stocks were prepared from transformed bacteria and their long-term storage as outlined below.

The desired bacterial culture was streaked onto a LB agar plate (Section 2.1.3.4) as the plasmid conferred ampicillin resistance the medium was supplemented with 100 µg/ml ampicillin. The plate was then incubated overnight at 37 °C and the following day single colonies were picked using a sterile pipette tip into a sterile universal containing 5 ml LB medium supplemented with 100 µg/ml ampicillin. Cultures were incubated at 37 °C overnight in a horizontal orbital incubator at 220 rpm. Confirmation that overnight cultures were derived from bacteria containing the correct plasmid was achieved by DNA isolation and

restriction digestion. Glycerol stocks were prepared by addition of 150 µl of glycerol to 850 µl of culture broth to produce a 15% glycerol mixture. Glycerol stocks were then stored at –70 °C. Bacterial stocks were revived for subsequent work by using a sterile platinum loop dipped into the glycerol stock and streaked onto an agar plate as outlined above.

2.2.2.2 Extraction and purification of plasmid DNA

Small scale plasmid preparation

Plasmid DNA was isolated using a modification of the alkaline lysis technique described by Birnboim and Doly (Birnboim and Doly 1979).

Large-scale plasmid preparation

Large quantities of highly pure, endotoxin free plasmid were prepared using the EndoFree® Plasmid Maxi Kit (Qiagen,UK). 50 µl of glycerol stock from the desired transformant was used to seed an overnight multiplier culture in 100 ml of LB medium incubated at 37°C with shaking at 220 rpm. These exponentially growing bacteria were harvested by centrifugation of the culture in 50 ml sterile centrifuge tubes at 4000 g for 20 minutes at 4°C. The remainder of the protocol was performed according to the manufacturers instructions. DNA was stored at –20°C.

2.2.2.3 Determination of nucleic acid concentration and quality

Determination by spectrophotometry

Nucleic acid samples were diluted either at 1:20 by addition of 25 µl of resuspended nucleic acid in 475 µl of dH_2O, or 1:100 by addition of 5 µl of the resuspended nucleic acid in 495 µl of dH_2O. Optical density readings were taken at 260 nm and 280 nm, using dH_2O as a blank. An optical density reading of 1.0 at 260 nm corresponds to an approximate nucleic acid concentration of 50 µg/ml for double stranded (ds) DNA and 40 µg/ml for single stranded (ss) RNA. The ratio of the readings taken at 260 nm and 280 nm (OD_{260}/OD_{280}) was used to give

an estimate of the purity of the nucleic acid. Pure preparations of DNA and RNA have an OD_{260}/OD_{280} of 1.8 and 2.0 respectively; a lower value suggests contamination, typically with protein or phenol.

Estimation of double stranded DNA concentration and quality by agarose gel electrophoresis.

This method was used when there were insufficient amounts of dsDNA for spectrophotometry, or when purity of a particular DNA fragment needed to be investigated. The concentration of dsDNA was determined by running the sample on an agarose gel electrophoresis (Section 2.2.3.5), and the intensity of the fluorescence of the unknown DNA was compared to that of a known quantity of the appropriate size marker (ϕX174 RF DNA/HaeIII fragments or Low DNA Mass™ Ladder) following staining with ethidium bromide and visualisation by UV transillumination. Smearing of a DNA band indicated degradation of the sample and resulted in exclusion of that DNA from further analysis.

2.2.2.4 Restriction endonuclease digestion

Typically, 1 μg of DNA was digested in a 20 μl reaction mix containing the appropriate buffer for the restriction endonuclease(s) and 10 units of the desired restriction enzyme. The reactions were incubated at 37 °C for a minimum of 1 hour. Where the isolation of restriction fragments was required, larger quantities of DNA, generally 10 μg, were digested with 50 units of enzyme, and the reaction volume and others components increased proportionally. In this case, reactions were incubated at 37 °C overnight.

2.2.2.5 Electrophoresis of DNA

Agarose gel electrophoresis

DNA fragments of 1.0 kb to 10 kb were separated by agarose gel electrophoresis using a Biomax QS710 Horizontal Unit (Scientific Imaging Systems – Eastman Kodak Company, New York, USA) or Sub-Cell GT Submerged Horizontal Agarose Gel Electrophoresis Systems (Bio-Rad, Hertfordshire, UK). Typically, 0.6 g to 0.9 g or 2 g to 3 g agarose was added to 60ml or 200ml 1x TAE buffer, respectively;

melted in a microwave for 1 minute to 2 minutes and mixed to produce a 1% to 1.5% gel (w/v). Once the gel mix had cooled to 55 °C, the gel was poured into a 100 mm x 65 mm or 150 mm x 200 mm gel support in its casting tray and an appropriate gel comb (eight, twelve or twenty well) inserted. The gel was allowed to solidify before transferring to an electrophoresis tank; the gel was immersed in 1x TBE or 1x TAE buffer and the comb carefully removed. Gel loading buffer (Section 2.1.1) was added to DNA samples and samples loaded into the wells using a micropipette. Known concentrations of DNA size markers were prepared similarly and run alongside the samples in order to gauge both product size and yield. Gels were run at 100 volts for 60 to 120 minutes, then removed from the gel apparatus and stained in buffer solution containing 0.5 μg/ml ethidium bromide for 20 minutes. Following destaining for 20 minutes in dH_2O, gels were visualised on a medium wave UV transilluminator (UVP Inc. and Geneflash Syngene Bio Imaging) and photographed using black and white Video Graphic Printer Sony UP-895MD (Fisher Scientific- Synoptics Ltd, UK).

2.2.2.6 Purification of restriction enzyme fragments

Purification of the DNA fragments required for construction of recombinant plasmids was purified from agarose gels using the QIAquick® Gel Extraction Kit (Qiagen). The DNA fragments of interest were cut from an agarose gel using a clean scalpel blade and extracted according to the manufacturers instructions.

2.2.2.7 Subcloning the cDNAs of RUNX1 mutants (K83N, T161A), TEL-RUNX1 and AML1a

Preperation of relevant inserts

Inserts containing cDNAs of RUNX1 mutants (K83N and T161A) were excised from the pGFP retroviral vectors (kind gift from Dr. Carol Stocking, Hamburg) by digestion with NotI. After fragment separation and purification by electrophoresis on 1% Agarose TBE gel, the NotI restriction fragments were extracted using the QIAquick Gel Extraction Kit (Qiagen) (Section 1.2.2.6) and suspended in 30μl of TE buffer. The overhanging 5' ends (NotI) of the obtained fragments were blunt ended using a Klenow Fill-in Kit (Klenow) according to manufacturers protocol.

The cDNA insert of TEL-RUNX1 was excised from pcDNA3 vector (kindly provided by Dr. Olivier Bernard, Paris), by digestion with EcoRI. After fragment separation and purification by electrophoresis on 1% Agarose TBE gel, the EcoRI restriction fragments were extracted using the QIAquick Gel Extraction Kit (Qiagen) (Section 1.2.2.6) and suspended in 30µl of TE buffer

The cDNA insert of AML1a was excised from pCR®II-TOPO® by digestion with EcoRI (The AML1a DNA had been previously PCR amplified from thymus and cloned into EcoRI site using Invitrogen TOPO TA Cloning® kit by Dr. Monica Stewart from this laboratory). After fragment separation and purification by electrophoresis on 1% Agarose TBE gel, the EcoRI restriction fragments were extracted using the QIAquick Gel Extraction Kit (Qiagen) (2.1.4) and suspended in 30µl of TE buffer

Ligation of vector and insert DNA

The quantity of vector and insert DNA used in ligations was calculated to produce a molar ratio between 1:3 using the equation:

$$\frac{\text{X ng of vector x Y kb of insert}}{\text{Z kb of vector}} \times \text{insert : vector ratio} = \text{ng of insert required}$$

Vector DNA (pBabe puro) was linearised using appropriate restriction enzyme(s). For the blunt-end cloning of K83N and T161A RUNX1 mutants pBabe puro was cut with SnaBI whereas for cloning of AML1a and TEL-RUNX1 pBabe puro was cut with EcoRI. To prevent re-circularisation of the vector DNA following digestion with a single enzyme, both 5'-phosphate groups were dephosporylated with 5 units of antarctic phosphatase according to the manufacturer protocol (New England Biolabs) at 37 °C for 15 minutes. Generally, 50 ng of vector DNA and a three fold molar excess of insert DNA were ligated, using Quick Ligation™ Kit (New England Biolabs) according to manufacturer protocol. A control ligation, omitting insert DNA was set up in parallel to the above, in order to check for 'background' when performing subsequent bacterial transformations.

Transformation of bacteria with plasmid DNA

All transformations included a positive control using supercoiled plasmid DNA (eg pUC19 10 pg/ml) to monitor the efficiency of the transforming bacteria and a ligation control (vector DNA, no insert) to monitor the background rate of transformation due to recircularisation of vector DNA.

2 µl of a 1:5 dilution of ligation mix, 2 µl of neat ligation mix or 2 µl of TA ligation mix were added to 50 µl of One Shot®TOP10 Chemically Competent *E. coli* cells (Invitrogen). Cells and DNA were mixed by gentle tapping to avoid damage to the bacterial cells. In all cases the reactions were then incubated on ice for 30 minutes. Cells transformed with ligation mix were subsequently heat shocked at 42 °C for exactly 40 seconds and 30 seconds respectively, and then returned to ice. 250 µl of SOC medium (Invitrogen) was then added and incubated at 37 °C for 1 hour with shaking at 220 rpm. Cells (50 µl and 200 µl) were plated onto LB plates containing 100 µg/ml ampicillin. Plates were incubated overnight at 37 °C.

Screening for transformants with the right orientation of insert

All plasmid strains used in this project conferred ampicillin resistance, allowing selection and maintenance of transformed bacteria with ampicillin supplemented media.

The DNA from 10-20 clones was prepared and used for restriction fragment length polymorphism analysis to find clones with the appropriate orientation of insert. SalI restriction analysis were performed for K83N and T161A mutants of RUNX1 and HindIII restriction analysis for TEL-RUNX1 and AML1a.

2.2.3 DNA sequence analysis (automated sequencing)

2.2.3.1 Sample preparation

DNA sequencing was carried out using the Big Dye® Terminator Version 1.1 Cycle Sequencing Kit (Applied Biosystems). Generally, 200 ng to 500 ng of highly purified DNA template was added into the cycle sequencing reaction containing

3.2 pmol of sequencing primers (Table 2), 0.5x sequencing buffer (80 mM Tris-HCl, 2 mM $MgCl_2$) and 4 µl of cycle sequencing mix (Big Dye® Terminator Version 1.1 Cycle Sequencing Kit, Applied Biosystems). Samples were prepared in the PTC-220 DNA Engine Dyad® Cycler (MJ Research Incorporated) employing 25 cycles of amplification, each cycle consisting of a denaturing step at 96 °C for 30 seconds followed by an annealing step at 50 °C for 15 seconds, and an elongation phase at 60 °C for 4 minutes. Sequencing products were purified by precipitation using ethanol (80%) at room temperature for 15 minutes. Pelleted DNA (14000 rpm for 20 minutes) was washed in ethanol (70%) and repelleted (14000 rpm for 10 minutes). After all the ethanol was removed, the pellet was dried at 90 °C for 1 minute, and was subsequently resuspended in 25 µl of Hi-Di Formamide (Applied Biosystems).

2.2.3.2 Sample sequencing and evaluation

Samples were loaded into 96 well plates and run on the ABI PRISM® 3100 Genetic Analyzer (PE Applied Biosystems, UK) under standard sequencing conditions for generation of automated sequence data. Electrophoresis on the ABI PRISM® 3100 Genetic Analyzer was performed using 36 cm and 80 cm capillaries which read up to 500 nucleotides and 950 nucleotides respectively, with a 98.5% base calling accuracy and less than 2% ambiguity. A computational software ClustalW was used for sequence alignments (http://www.ncbi.nlm.nih.gov/)

Table 2. Sequencing primers.

Primer name	Primer sequence	Description
pBabe 5'	5'd[CTTTATCCAGCCCTCAC]3'	Forward sequencing primer from pBabe puro vector
pBabe 3'	5'd[ACCCTAACTGACACACATTCC]3'	Reverse sequencing primer from pBabe puro vector
Runx1 xd5	5'd[GCAGAAACTAGATGATCAGACC]3'	Forward sequencing primer from exon 5 of Runx1
Runx1 xd3	5'd[CCTCAAAGTCAGATGCAG]3'	Reverse sequencing primer from exon 5 of Runx1

2.2.4 Protein analysis

2.2.4.1 Protein extraction

Whole cell extracts, from cells grown in tissue culture were prepared for western blot analysis according to the method of Marais et al (Marais et al 1993). All procedures were performed at 4 °C. Typically, cells were washed twice with ice-cold PBS, drained thoroughly, lysed in 100 µl working whole cell lysis buffer (Section 2.1.10) per 10^6 cells or 60 mm dish and rotated for 10 minutes. The crude extract was cleared in a bench top centrifuge at 14000 rpm for 30 minutes and the supernatant transferred to a fresh pre-cooled eppendorf. Extracts were quantitated as described below, and stored at –70 °C.

2.2.4.2 Estimation of protein concentration

In order to estimate protein yields, a Bio-Rad Protein Assay (Bio-Rad), based on the method of Bradford was used, in which a differential colour change of a dye occurs in response to various concentrations of protein (Bradford 1976).

A protein standard (bovine serum albumin, BSA) was diluted with dH_2O to concentrations ranging from 0.025 to 0.8 mg/ml to allow the production of a standard curve each time the assay was performed. Aliquots of protein for quantification were diluted in order to give a concentration in the above range. The dye reagent was prepared by addition of 4 volumes of ddH_2O to 1 volume of Dye Reagent Concentrate (Bio-Rad) and filtration through a Whatman #1 to remove particulates. Samples were diluted 1/500 in diluted dye reagent, and incubated in sterile polystyrene cuvettes at room temperature for 5 minutes to 1 hour. OD_{595} was determined against the reagent blank. The absorbance of the protein standards was used to construct a standard curve from which an approximate concentration of the unknown samples could be read.

2.2.4.3 SDS - PAGE of proteins

The separation and analysis of proteins was facilitated by one dimensional denaturing discontinuous gel electrophoresis, as originally described by Laemmli (Laemmli, 1970).

Standard SDS-PAGE gels (13.8 cm x 13 cm) were formed and run using the AE-6200 Slab EP Chamber, and AE-6220 Slab EP Chamber, for two gels (Atto Incorporation). The separating gel was poured to a depth of approximately 10 cm; consisting of 16.7 ml 30%: 0.8% w/v acrylamide/bisacrylamide (giving a 10% gel), 13.4 ml dH_2O, 18.75 ml 1 M Tris-HCl (pH 8.8), 500 µl 10% SDS, 375 µl 10% APS and 20 µl TEMED. This was overlain with ddH_2O-saturated butanol and allowed to polymerise. The butanol was then poured off and the surface of the separating gel rinsed with ddH_2O. Excess water was removed with a sheet of 3mm Whatman filter paper, and the stacking gel poured; consisting of 3.4 ml 30%: 0.8% w/v acrylamide/bisacrylamide, 13.6 ml dH_2O, 2.5 ml 1 M Tris-HCl (pH 6.8), 200 µl 10% SDS, 200 µl 10% APS and 20 µl TEMED. A 14 well comb was inserted and the gel allowed polymerising. Gels were run in 1x running buffer,

and samples were treated as for mini SDS-PAGE gels (see above). Moreover, 14 µl of a protein molecular weight standard (Precision Plus Protein™ Standards, Bio-Rad) was loaded in one or both outer wells to allow estimation of the size of sample proteins.

Standard SDS-PAGE gels were electrophoresed 230 volts to 250 volts for 2-3 hours until the bromophenol blue dye reached the bottom of the separating gel. The gel was then removed from the glass plates, the stacking gel discarded, and the protein bands detected by immunodetection (Section 2.2.4.5).

2.2.4.4 Electroblotting

After polyacrylamide resolving gel electrophoresis proteins were transferred to a nitrocellulose membrane by electroblotting:

Standard SDS-PAGE gels were removed from the glass plates, and the resolving gel equilibrated in 1x dry blot buffer with 20% methanol (Section 2.1.10) for 15 minutes at room temperature. The gel was covered in pre-wetted nitrocellulose membrane (1x dry blot buffer) and sandwiched between 12 pieces of Whatman 3MM rinsed in 1x dry blot buffer. The sandwich was turned over and placed on the semi dry blotter (Trans-blot® SD Semi-Dry Transfer Cell, Bio-Rad). Air bubbles were removed and transfer effected at 20 volts for 2 hours. Molecular weight marker positions were highlighted and the membrane stored at 4 °C.

2.2.4.5 ECL detection

The detection of proteins by immunoblotting (Western Blotting) is a rapid and sensitive technique that exploits the inherent specificity of antigen recognition by antibodies (Towbin et al 1979):

Hybond-ECL nitrocellulose membrane (Amersham Biosciences) was immersed in 1x TBST buffer (Section 2.1.10) containing 5% low fat dried milk (Marvel - Premier Beverages, Stafford, UK) and left overnight at 4 °C, to block non-specific binding sites. The membrane was rinsed briefly with 1x TBST buffer, washed once for 15 minutes, and then twice for 10 minutes, with shaking at room temperature in 1x TBST buffer. It was then incubated with the primary

antibody, at a pre-determined dilution in blocking buffer (either 5% low fat dried milk TBST or, 5%BSA TBST), with shaking. This was followed by washing three times in 1x TBST buffer for 10 minutes, with shaking at room temperature, prior to incubating with secondary antibody (HRP labelled), appropriately diluted in 5% low fat dried milk TBST, for 1 hour, at room temperature, with shaking. The membrane was washed as above before detection using the ECL™ Western Blotting Detection Reagents (Amersham Biosciences). The Enhanced Chemiluminescence system (ECL) is a light-emitting-non-radioactive method for detecting immobilized specific primary antibodies using secondary antibodies conjugated with horseradish peroxidase (HPR-linked secondary antibodies). Light emission is generated by the HPR/hydrogen peroxide catalysis of luminal to an excited oxidated state, and it is dramatically enhanced in the ECL system by chemical enhancers such as phenol (Durrant et al 1990). Briefly, an equal volume of detection reagent A was mixed with reagent B (typically 4 ml each). Excess buffer was drained from the membrane and the detection solution was pipetted onto the surface of the membrane to which the protein are bound. After 2-5 minutes incubation at room temperature, excess reagent was drained from the membrane, which was then wrapped in plastic film. The membrane was exposed to blue-light sensitive autoradiography film (Hyperfilm ECL, Amersham Biosciences) for seconds or minutes, before developing the film in an automated processor (SRX-101A Compact X4, Xograph Imaging Systems).

2.2.4.6 Stripping membranes

Antibodies and substrate complexes could be removed from the membranes allowing for reprobing of the same blot with different antibodies. The membranes were stripped by submerging in either mild stripping buffer or stringent stripping buffer (Section 2.1.10), and incubating at room temperature for 1h or at 50˚C for 30 minutes with agitation. Following this incubation the membranes were washed three times for 10 minutes with PBS at room temperature, and blocked overnight in 5% milk TBST, before adding the desired antibody

2.2.5 Confocal laser scanning microscopy

Cells were plated on poly-L-lysine-coated glass chamber slides (Section 2.1.2.4) and fixed for 15 min with freshly prepared 4% paraformaldehyde (in PBS). After washing with PBS, cells were permeabilized for 15 min with PBST (PBS with 0.1% Triton X-100). The specimens were blocked with 10% FCS, 0.5% BSA in PBS for 30 min and incubated overnight in 4°C with a relevant primary antibody diluted in blocking buffer. After washing x3 in 10% FCS, 0.5% BSA in PBS, cells were stained with FITC-conjugated secondary antibody (1:100, Jackson Immuno Research Laboratories) (Section 2.1.1) for 45 min at room temperature. Finally, cells were washed 3x in PBS and coverslips were mounted in VectaShield containing DAPI (4', 6'-diamidino-2-phenylindole) (Vector Laboratories) (Section 2.1.9.2). Fluorescent images were captured using a confocal microscope (Leica DM IRE2) (Section 2.1.9.1)

2.2.6 Statistical significance

Statistical significance for the data presented in this thesis was typically calculated using a Students-T-test to give a significance value (p). This was carried out using Sigma Plot Software (T-test function). The cut off for all experiments was taken as 0.05, therefore if two sets of data return a p value of <0.05 there is a less than 5% chance that the result observed is due to chance, and the two groups are therefore statistically significantly different

Chapter 3

3 Structural requirements for RUNX1 induced senescence

3.1 Introduction

Previous work in this laboratory established that RUNX1 induces senescence in primary murine embryonic fibroblasts (MEFs) (Wotton et al 2004), but the structural components of RUNX1 necessary to effect this cellular response have not been examined. To investigate this question various mutated or deleted forms of RUNX1 were used to dissect out which functional domains were required for the induction of premature senescence by RUNX1. It was also important to investigate whether RUNX1 retains potential to induce premature senescence in human primary fibroblasts and hence if it can be regarded as a universal phenomenon caused by ectopic expression of RUNX1.

3.2 RUNX1 requires DNA binding and CBFβ interaction to induce senescence in murine embryonic fibroblasts

To test whether RUNX1 binding to DNA and heterodimerisation with CBFβ are required for the induction of premature senescence, two mutated forms of RUNX1 were used in the MEF system. The DNA-binding mutant of RUNX1 (K83N), which was identified in a retrospective genetic study of patients with myeloblastic leukaemias (Matheny et al 2007; Osato et al 1999) and another point mutant, T161A, which was reported to be defective in heterodimerization with CBFβ (Matheny et al 2007; Zhang et al 2003b), MEFs were transduced with these mutants of RUNX1 (K83N and T161A), wild type RUNX1 or the empty vector (here also referred to as pBabe) via retroviral mediated gene transfer. Following infection, cells were kept under puromycin selection for 4 days from which point (day 0) monitoring of their proliferative properties using viable cell counts was started. All the proteins were expressed at similar levels as determined by Western blot (Figure 3.1a). As previously reported MEFs expressing RUNX1 displayed obvious growth suppression immediately after selection (pBabe vs RUNX1 day 10 $p \leq 0.00005$) (Figure 3.1b). RUNX1 mediated growth arrest was

accompanied by morphological alterations indicative of cellular senescence whereby most cells carrying RUNX1 became flat and enlarged between day 2 and 4 of the culture period. Senescence associated-β-galactosidase (SA-β-Gal) was detected at day 7 in virtually every cell (Figure 3.1c). By contrast, cells expressing the mutants of RUNX1 continued to proliferate although not as rapidly as empty vector control cells (K83N vs RUNX1 day 10 $p \leq 0.00005$; T161A vs RUNX1 day 10 $p \leq 0.005$) (Figure 3.1b). Furthermore, they displayed no morphological changes and expressed no SA-β-Gal (Figure 3.1c). The puro-controls and cultures expressing the mutants of RUNX1 reached high cell densities and showed some background SA-β-Gal staining but this was not associated with single cells and was not as intense as the specific intracellular staining seen in large, flattened senescent cells. Indeed it has been previously reported that cellular stress, unrelated to senescence such as high levels of confluency in culture can cause positive SA-β-Gal reaction (Severino et al 2000).

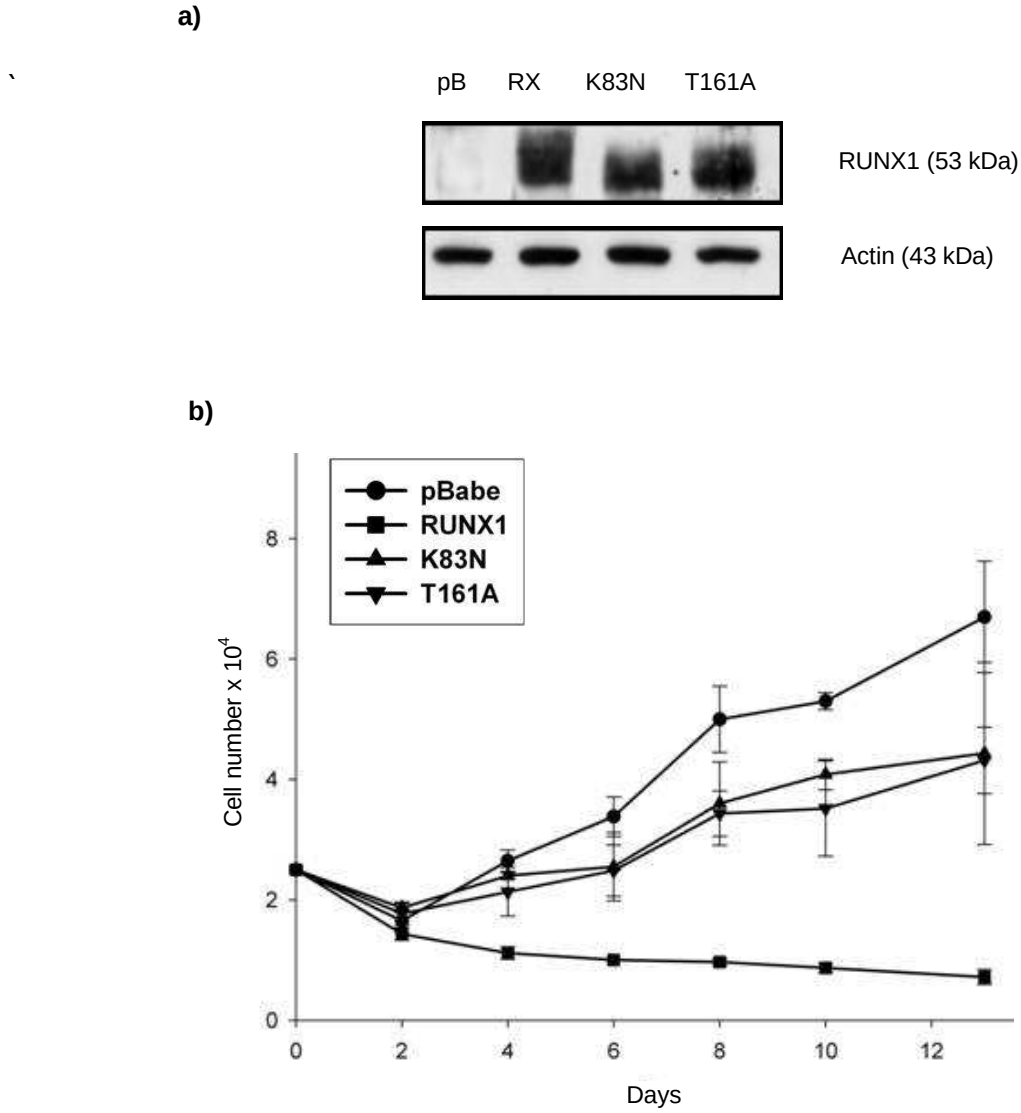

Figure 3.1 DNA (K83N) and CBFβ (T161A) binding mutants of RUNX1 fail to induce senescence-like growth arrest in murine embryonic fibroblasts

Cells were transduced with retroviral vectors expressing RUNX1, K83N, T161A or control vector (pBabe) and selected for 4 days in puromycin. (a) The expression of RUNX1 was measured by immunoblotting lysates from MEFs containing an empty vector (pB), RUNX1 (RX) or RUNX1 mutants (K83N and T161A) on day 7 post-selection using anti-AML1/Runx1 (3900, Active Motif) (b) Representative growth curves showing viable cell numbers corresponding to cell populations containing control vector (pBabe), RUNX1, K83N or T161A. Each experiment was performed three times and each time point was determined in triplicate

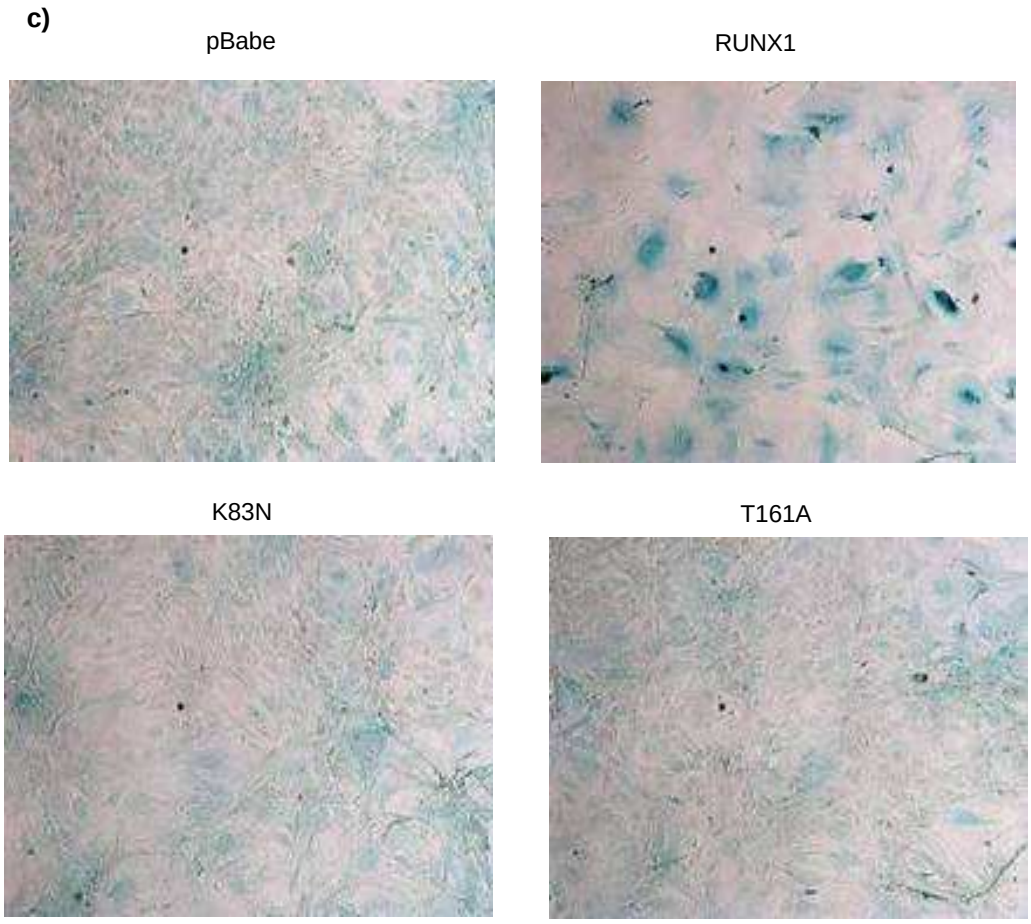

Figure 3.1 continued

(c) SA-β-Gal staining of cells containing control vector (pBabe), RUNX1, K83N or T161A (day 7 post-selection)

3.3 RUNX1 requires DNA binding and CBFβ interaction to induce senescence in human primary fibroblasts

Fundamental differences in the requirements for the senescence phenotype in mouse and human cells have been reported (Itahana et al 2004; Campisi, 2005), therefore it was important to address the question of whether the ability of RUNX1 to induce premature senescence could be recapitulated in human cells, indicating a general feature of RUNX1 overexpression. To address this issue, Hs68 human neonatal foreskin fibroblasts expressing the ecotropic murine leukaemia virus receptor were employed (Brookes et al 2002). This enabled the same retroviral system as for murine cells to be used. Hs68 cells were infected with retroviruses containing RUNX1, the mutants (K83N and T161A) or control vector (pBabe) and selected with puromycin. Western blotting confirmed that all the introduced constructs were expressed at similar levels (Figure 3.2a). Interestingly, it also revealed that the endogenous RUNX1 levels in these cells were quite high and could be readily detected in control vector expressing cells (Figure 3.2a). Ectopic expression of RUNX1 in human neonatal foreskin fibroblasts resulted in a growth arrest as determined by analysis of growth curve data (pBabe vs RUNX1 day 9 $p \leq 0.0001$) (Figure 3.2b) and SA-β-Gal staining was detected by day 7 (Figure 3.2c). These cells were enlarged and flattened, although not to the same extent as was observed in murine cells. The two mutants of RUNX1 failed to cause a proliferative arrest (K83N vs RUNX1 day 9 $p \leq 0.0005$; T161A vs RUNX1 day 9 $p \leq 0.005$) (Figure 2b) and did not induce SA-β-Gal activity nor any change to the enlarged and flattened cellular morphology characteristic of senescence (Figure 3.2c). These results indicate that high affinity binding to DNA is absolutely critical for RUNX1 to elicit the senescence response in human cells. However unlike in the primary mouse cells, Hs68 expressing T161A mutant did not proliferate as well as K83N mutant (K83N vs T161A day 9 $p \leq 0.005$) (Figure 3.2b) despite similar levels of expression (Figure 3.2a)

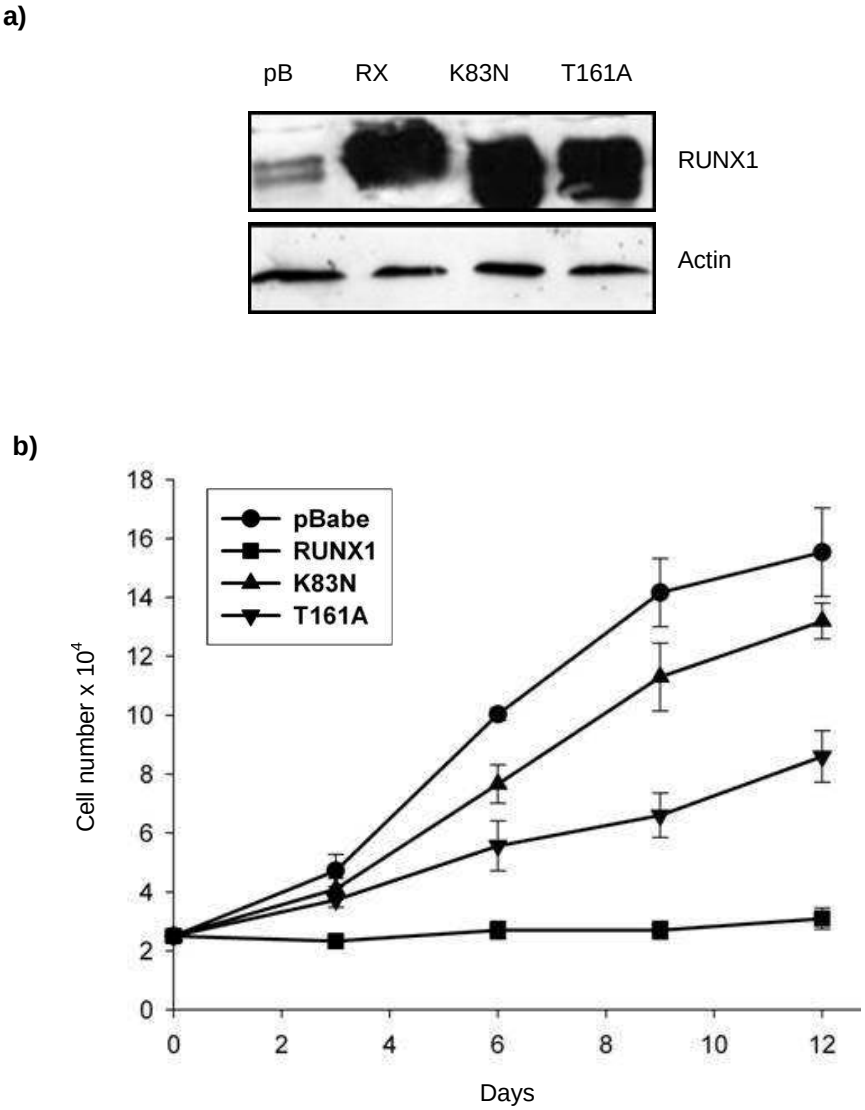

Figure 3.2 The ability of RUNX1 to induce senescence-like growth arrest in human neonatal foreskin fibroblasts is impaired in K83N and T161A mutants

Cells were transduced with retroviral vectors expressing RUNX1, K83N, T161A or control vector (pBabe) and selected for 4 days in puromycin. (a) The expression of RUNX1 was measured by immunoblotting lysates from Hs68 cells containing empty vector (pB), RUNX1 (RX) or RUNX1 mutants (K83N and T161A) on day 7 post-selection using anti-AML1/Runx1 (3900, Active Motif) (b) Representative growth curves showing viable cell numbers corresponding to cell populations containing control vector (pBabe), RUNX1, K83N or T161A. Each experiment was performed three times and each time point was determined in triplicate

c)

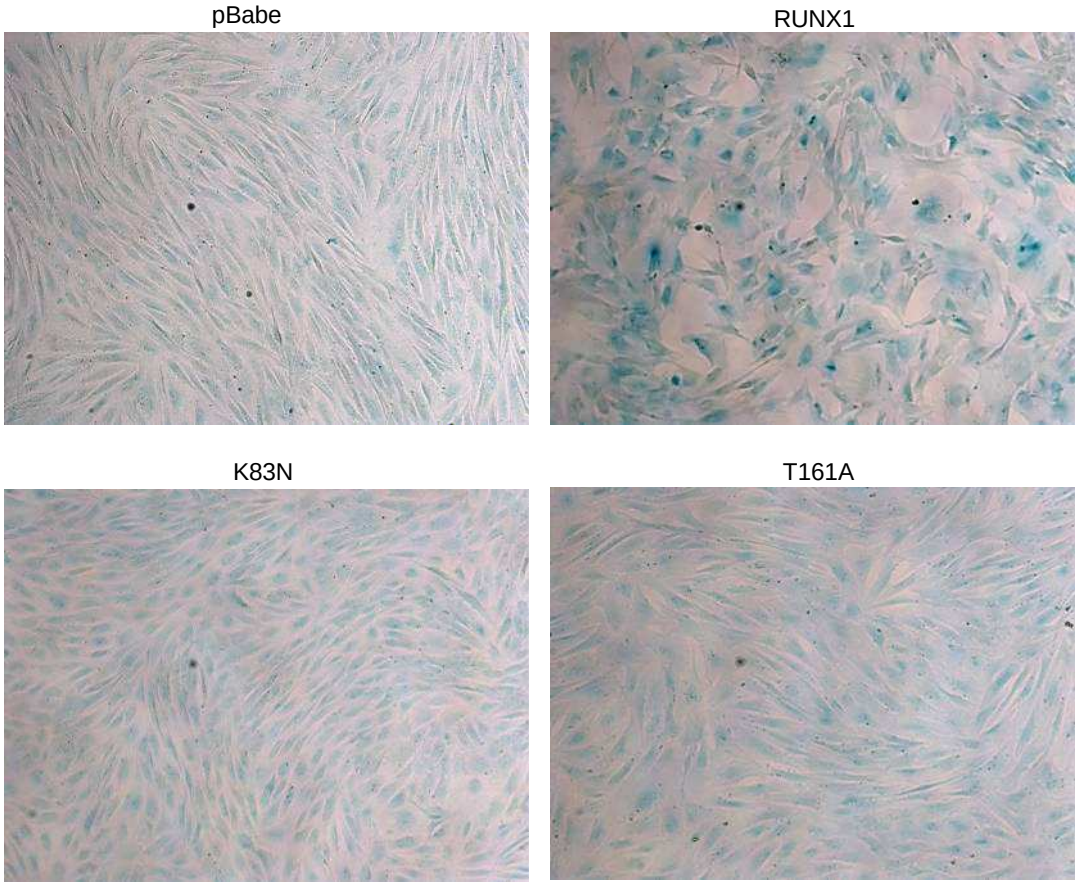

Figure 3.2 continued

(c) SA-β-Gal staining of cells containing control vector (pBabe), RUNX1, K83N or T161A (day 7 post-selection)

3.4 The C-terminal transcriptional activation/repression domain of RUNX1 is essential for induction of senescence in human primary fibroblasts

AML1a is a short isoform of RUNX1 (250 amino acids), with a large deletion that includes the C-terminal transactivation domain (Miyoshi et al 1991, Miyoshi et al 1995). It has been shown to antagonise wt RUNX1 *in vitro* and may be important for leukaemogenesis and/or myeloid cell differentiation (Tanaka et al 1995). AML1a has no transactivational function by itself, but inhibits the transcriptional activity of wt RUNX1 by competing for the DNA sequence of target genes with a higher affinity (Tanaka et al 1995). Overexpression of AML1a inhibits the myeloid terminal differentiation of the myeloid precursor lineage 32Dcl3 induced by granulocyte-colony stimulating factor (G-CSF) and importantly levels of AML1a are commonly elevated in AML patients (Tanaka et al 1995).

The RUNX1 protein has a number of transcriptional activation and repression domains in the C-terminal region (Aronson et al 1997; Kanno et al1998a). The effect of overexpressing the C-terminal truncation isoform, AML1a, in human fibroblasts was examined. Retroviral mediated gene transfer was employed to introduce control vector (pBabe) or AML1a into Hs68 cells. The AML1a expressing cells proliferated almost as well as control cells (pBabe vs AML1a day 6 $p \geq 0.05$) and displayed no features of senescence as determined by lack of staining for SA-β-Gal and lack of characteristic alterations to the cellular morphology (Figure 3.3). These data demonstrate the requirement for C-terminal transactivation and/ or repressor domains in senescence induction by RUNX1 in Hs68 cells.

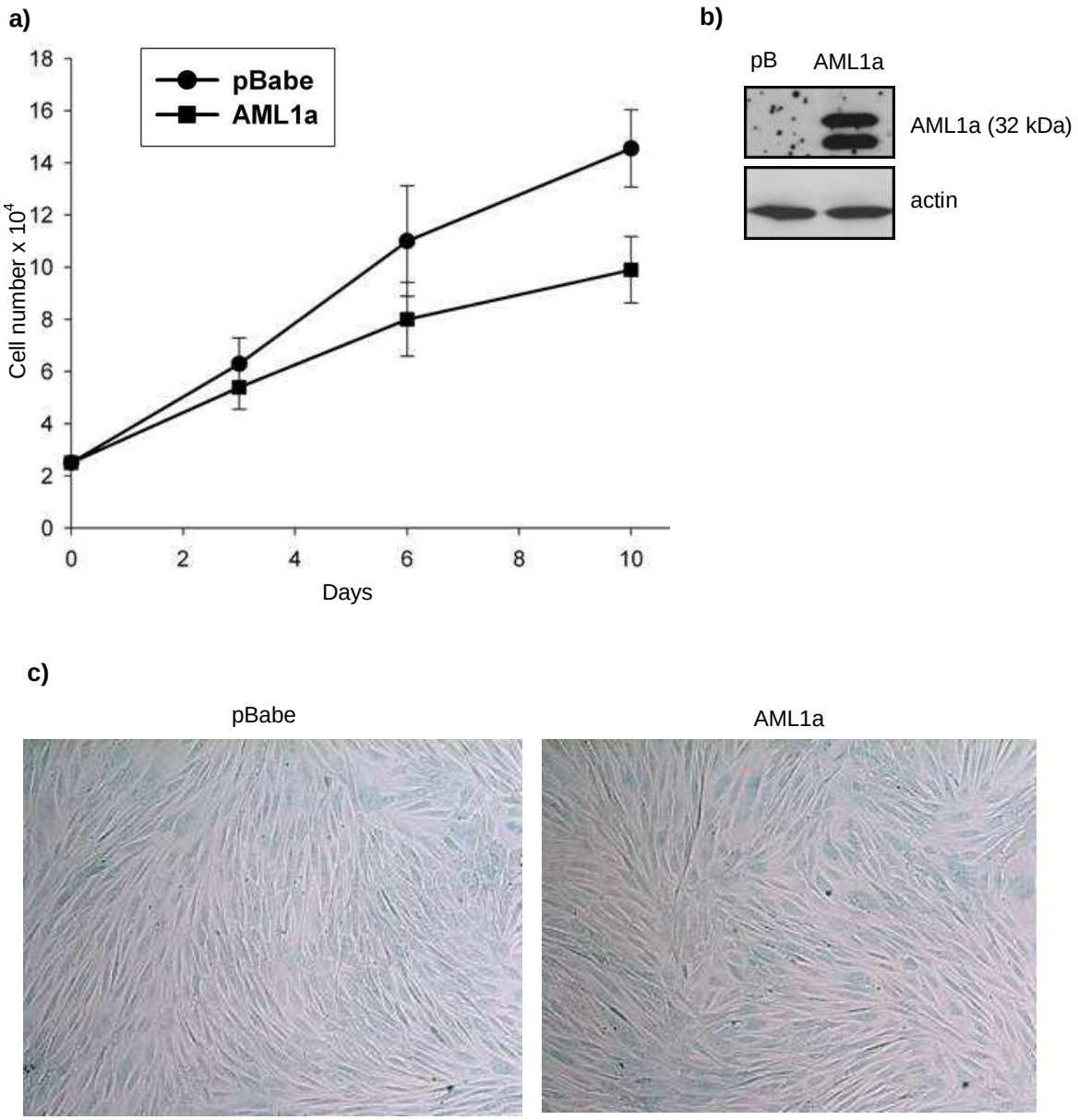

Figure 3.3 C-terminal transactivation/repression domain of RUNX1 is required to induce senescence in Hs68 cells

Cells were transduced with retroviral vectors expressing AML1a or control vector (pBabe) and selected for 4 days in puromycin. (a) Representative growth curves showing viable cell numbers corresponding to cell populations containing control vector (pBabe) or AML1a. Each experiment was performed three times and each time point was determined in triplicate. (b) The expression of AML1a was measured by immunoblotting lysates from Hs68 cells containing empty vector (pB) or AML1a on day 7 post-selection using anti-Runx (D207-3, MBL) (c) Lack of SA-β-Gal staining of cells containing control vector (pBabe), or AML1a (day 7 post-selection)

3.5 Discussion

In this study RUNX1 was clearly demonstrated to require both intact DNA binding activity and CBFβ interaction, allowing high affinity binding to the target DNA sequences to drive premature senescence. Moreover the ability of RUNX1 to induce senescence seems to be a general feature as it is observed in both human primary fibroblasts and murine primary fibroblasts. Furthermore, neither the K83N DNA binding mutant nor the T161A CBFβ interaction mutant was able to induce senescence in Hs68 cells or MEFs, although in the higher proliferating human cells, the T161A CBFβ mutant produced more dramatic reduction in the rate of proliferation than in the MEFs. Could this represent a difference between the human and mouse system? Does this demonstrate a greater dependence on CBFβ heterodimerisation to drive senescence by RUNX1 in the murine cells? Perhaps this observation reflects higher affinity of CBFβ for binding to RUNX1 in MEFs compared to Hs68 fibroblasts or relative abundance of CBFβ in murine cells compared to human cells. This could be addressed by performing electrophoretic mobility shift assays and examining endogenous levels of CBFβ in murine and human fibroblasts. Importantly, the AML1a isoform of RUNX1 has been found to fail to induce senescence in Hs68 cells indicating that the C-terminal transactivation/repression portion of RUNX1 is critical in this response. These results are consistent with the well established role of AML1a as an antagonist of wild type RUNX1 in the context of myeloid and erythroid cell culture models of differentiation (Tanaka et al 1995; Nitsu et al 1997) and with the report that overexpression of RUNX1 but not AML1a can transform NIH3T3 cells (Kurokawa et al 1996) suggesting that AML1a does not act as an oncogene *per se*. Given that senescence is recognised as an anti-cancer barrier in primary cells it is perhaps not surprising that AML1a did not trigger senescence in Hs68 cells. Taken together, these data confirm that RUNX1 transcriptional regulatory activity is required to drive premature senescence in primary fibroblasts of murine and human origin.

Chapter 4

4 Induction of premature cellular senescence by RUNX1 fusion oncoproteins

4.1 Introduction

The existence of naturally occurring RUNX1 fusion oncoproteins associated with various leukaemias not only makes the investigation into RUNX1 function clinically relevant but provides useful tools to carry out that investigation. The accepted hypothesis has been that these oncoproteins interfere with RUNX1 function by acting in a dominant negative fashion or acting as a constitutive repressors of RUNX1 target genes. Hence it was of considerable interest to address the question as to whether leukaemia-related fusion oncoproteins would antagonise senescence induction.

4.2 RUNX1-ETO is a potent inducer of senescence in murine embryonic fibroblasts

The RUNX1-ETO fusion oncoprotein arises as a consequence of the t(8;21) chromosomal translocation and is a frequent feature of acute myeloid leukaemia (AML). RUNX1-ETO is a chimeric protein that lacks the transactivation domain of RUNX1 but is fused to a putative transcriptional repressor, ETO, and likewise AML1a has been shown to have dominant negative activity with respect to wild type RUNX1. RUNX1-ETO blocks transactivation of the GM-CSF promoter and the T cell receptor beta enhancer by RUNX1 (Frank et al 1995; Meyers et al 1995). Consistent with a negative effect on RUNX1 function, RUNX1-ETO has been shown to inhibit differentiation of myeloid progenitor cells (Kitabayashi et al 1998; Westendorf at al 1998). RUNX1-ETO was found to repress $p19^{ARF}$, the upstream effector of p53 which is required for RUNX1 induced senescence in murine embryonic fibroblasts (Linggi et al 2002) and was also reported to transform NIH3T3 cells (Frank et al 1999).

It was therefore of particular interest to test the effects of ectopically expressing RUNX1-ETO in primary murine embryonic fibroblasts. To this end

RUNX1-ETO and RUNX1 were overexpressed in MEFs (Figure 4.1a) and cell growth assayed and SA-ß-Gal staining carried out to test for senescence, as described in Chapter 2 and 3. Again, RUNX1 proved to be an inducer of senescence as these cells ceased proliferation (pBabe vs RUNX1 day 9 $p \leq 0.005$) (Figure 4.1b) and approximately 70% of total cell population were stained for SA-β-Gal (Figure 4.1c). A more unexpected finding was that the fusion derivative seemed to be at least as potent inducer of senescence as RUNX1 itself. The population of RUNX1-ETO expressing cells underwent a profound proliferative block (pBabe vs RUNX1-ETO day 9 $p \leq 0.005$) (Figure 4.1b) and approximately 80% of the total cell population displayed more intense staining for SA-β-Gal activity compared to RUNX1 expressing cells (Figure 4.1c,d).

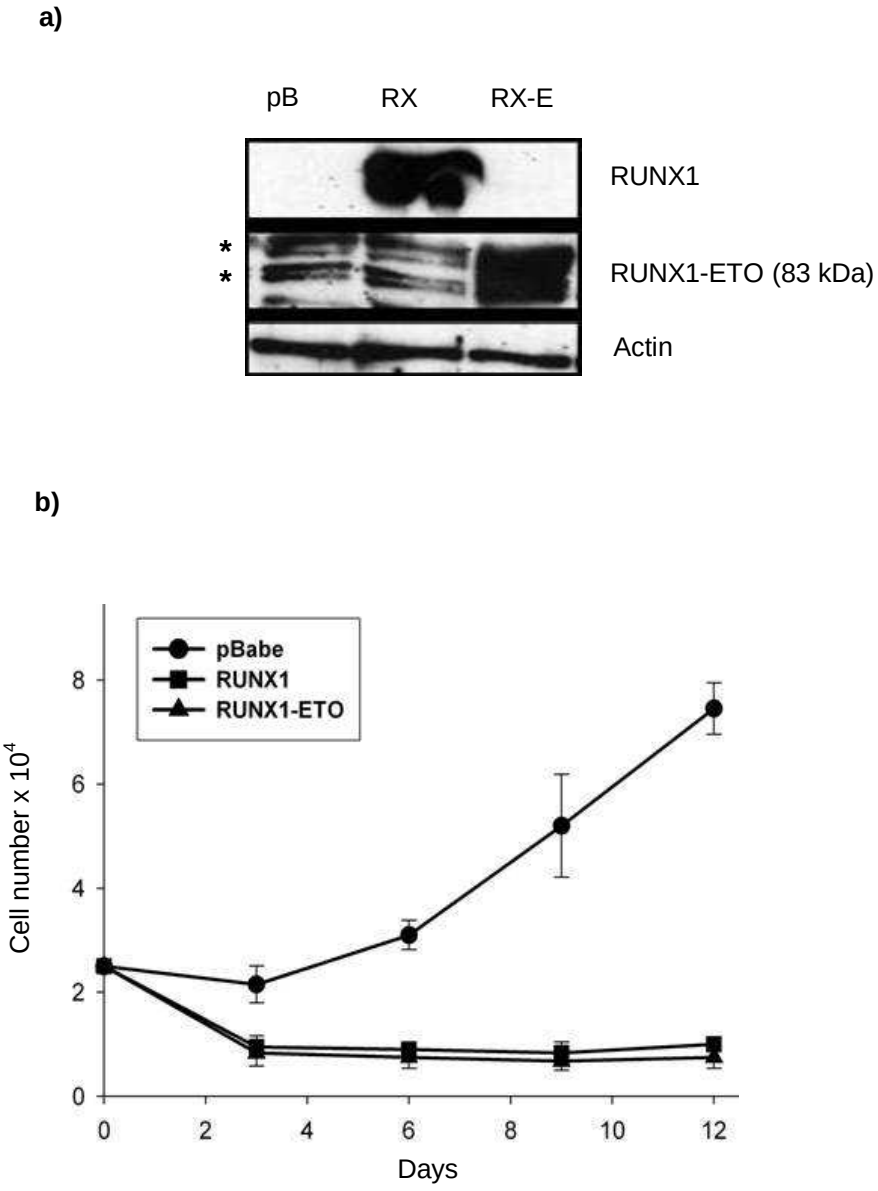

Figure 4.1 RUNX1-ETO induces senescence-like growth arrest in MEFs

Cells were transduced with retroviral vectors expressing RUNX1, RUNX1-ETO or control vector (pBabe) and selected for 4 days in puromycin. (a) Western Blot analysis of RUNX1 (using anti-AML1/Runx1, 3900, Active Motif) and RUNX1-ETO (using anti-RUNX1-ETO from Dr. Scott Hiebert) expression in cells containing empty vector (pB), RUNX1 (RX) or RUNX1-ETO (RX-E) on day 7 post-selection; * indicates non-specific bands (b) Representative growth curves of cells containing control vector (pBabe), RUNX1 or RUNX1-ETO. Each experiment was performed three times and each time point was determined in triplicate

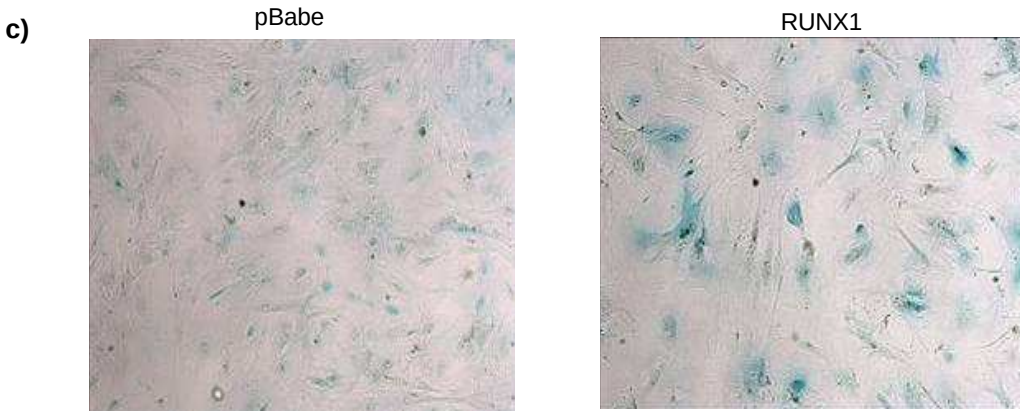

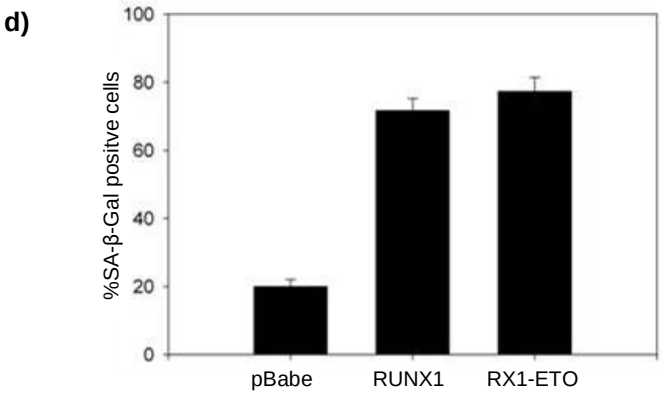

Figure 4.1 continued

(c) SA-β-Gal staining of cells containing control vector (pBabe), RUNX1 or RUNX1-ETO (day 7 post-selection) (d) Quantitation of data in (c), showing the percentage of SA-β-Gal positive cells. The data represent the mean of three independent counts of 200 cells (error bars relate to standard deviation)

4.3 RUNX1-ETO induces profound premature senescence-like growth arrest in human primary fibroblasts

Again the question arose as to whether RUNX1-ETO retains the capacity to induce senescence in human cells and if so whether the phenomenon is as potent as in murine cells. Human neonatal foreskin fibroblasts were transduced with retroviral constructs encoding RUNX1-ETO, RUNX1, H-RAS^{V12} or control vector (pBabe) and following puromycin selection were analysed as previously described for proliferative properties and SA-ß-Gal activity. In this experiment the prototypic inducer of premature senescence, oncogenic H-RAS^{V12} (Lin and Lowe, 2001; Serrano et al 1997), was also expressed to compare the senescent phenotypes of RUNX1, H-RAS^{V12} and potentially RUNX1-ETO. All the introduced constructs were expressed at readily detectable levels (Figure 4.2a). Interestingly, it was noticeable that H-RAS^{V12} clearly downregulated endogenous RUNX1 (Figure 4.2a). Ectopic expression of both RUNX1 and RUNX1-ETO resulted in a growth arrest that was more pronounced than that of the H-RAS^{V12} expressing cells (RUNX1 vs H-RAS^{V12} day 9 $p \leq 0.05$; RUNX1-ETO vs H-RAS^{V12} day 9 $p \leq 0.005$) (Figure 4.2a) with RUNX1-ETO expressing cells showing an even more profound proliferative arrest than RUNX1 (RUNX1-ETO vs RUNX1 day 9 $p \leq 0.05$). In addition, in contrast to H-RAS^{V12}, which initially stimulated growth as previously reported by others (Kilbey et al 2007; Lin et al 1998), RUNX1 and especially RUNX1-ETO were potent growth suppressors immediately after puromycin selection. This was reflected in the growth rates over first 3 days during which period H-RAS^{V12} was not significantly different from the puro control (day 3 $p \geq 0.1$) (Figure 4.2b). Interestingly, RUNX1-ETO expressing cells displayed more profound morphological changes (very flat and enlarged) than RUNX1 expressing cells and stained more intensly for SA-β-Gal (Figure 4.2c). This more pronounced senescent phenotype of RUNX1-ETO expressing cells was also reflected by significant quantitative changes in SA-β-Gal staining where as many as 80% of RUNX1-ETO cells were positively stained compared to 40% of the RUNX1 expressing cells (RUNX1-ETO vs RUNX1 $p=0.01$) (Figure 4.2d). Therefore it

appears that RUNX1-ETO can induce an even stronger senescence response than RUNX1 or even H-RAS^{V12} in human cells.

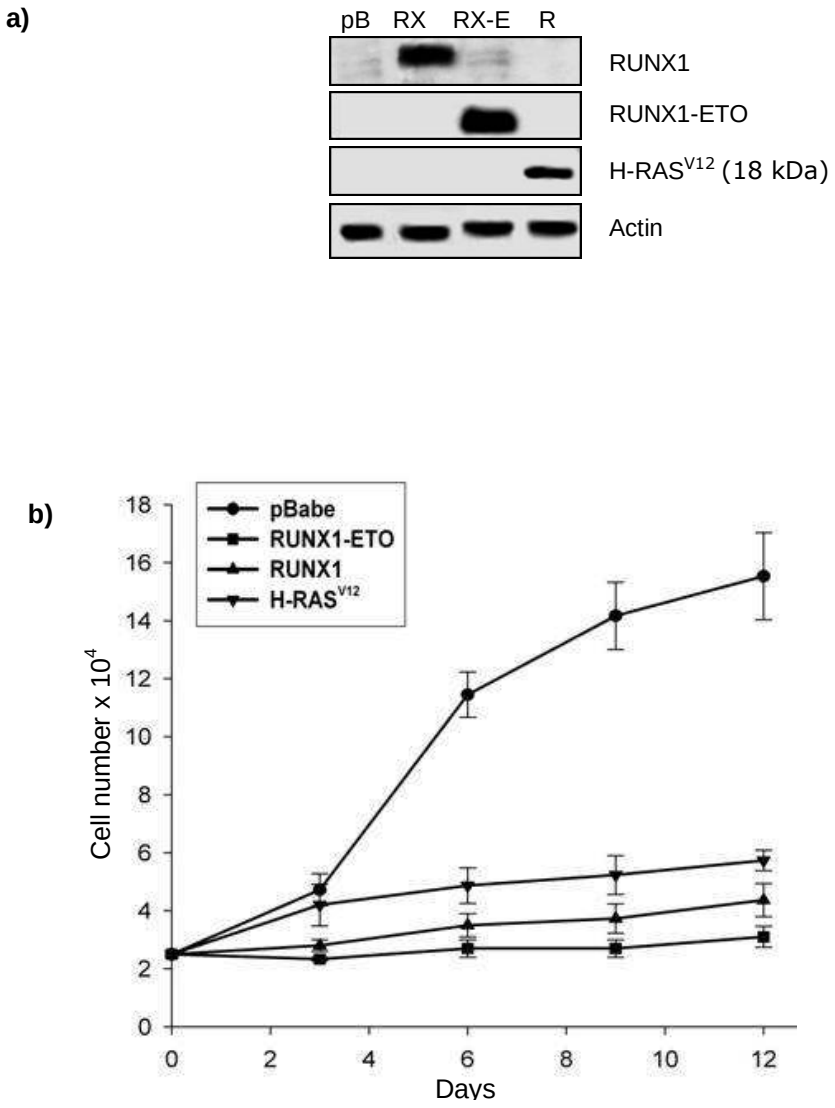

Figure 4.2 RUNX1-ETO induces more profound senescence than RUNX1 in human neonatal foreskin fibroblasts

Cells were transduced with retroviral vectors expressing RUNX1-ETO, RUNX1, H-RAS^{V12} or control vector (pBabe) and selected for 4 days in puromycin. (a) Western Blot analysis of RUNX1-ETO (anti-RUNX1-ETO from Dr. Scott.Hiebert), RUNX1 (anti-AML1/Runx1, 3900, Active Motif) and H-RAS^{V12} (Anti-H-ras, Ab-1, Oncogene Research) expression in cells containing empty vector (pB), RUNX1 (RX), RUNX1-ETO (RX-E) or H-RAS^{V12} (R) on day 7 post-selection (b) Representative growth curves of cells containing control vector (pBabe), RUNX1-ETO, RUNX1 or H-RAS^{V12}. Each experiment was performed three times and each time point was determined in triplicate

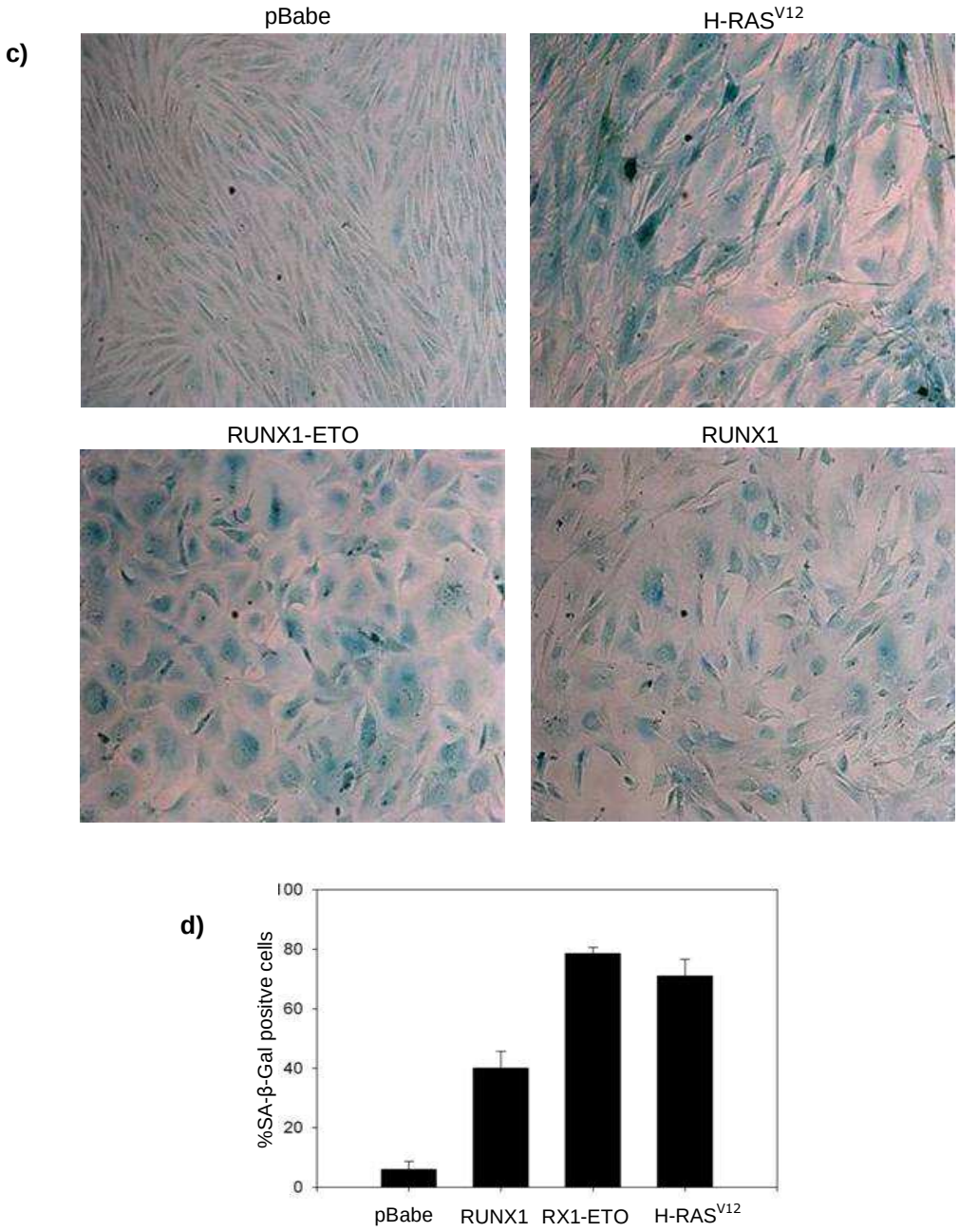

Figure 4.2 continued

(c) SA-β-Gal staining of cells containing control vector (pBabe), RUNX1 or RUNX1-ETO (day 7 post-selection) (d) Quantitation of data in (c) showing the percentage of SA-β-Gal positive cells. The data represent the mean of three independent counts of 200 cells (error bars relate to standard deviation)

4.4 RUNX1-ETO requires transcriptional repressor activity to drive senescence in human primary fibroblasts

To gain more insight into the premature senescence triggered by RUNX1-ETO the ability to induce senescence by RUNX1-ETO mutant (RUNX1-ETOΔ469) was examined. In contrast to RUNX1-ETO this mutant lacks corepressor binding sites and fails to repress transactivation of RUNX1 target genes (Lenny et al 1995). In addition RUNX1-ETOΔ469, as opposed to full length RUNX1-ETO, was reported to be unable to transform NIH3T3 (Frank et al 1999). Retroviral mediated gene transfer was employed to overexpress mutant RUNX1-ETOΔ469 and RUNX1-ETO in human neonatal foreskin fibroblasts. In contrast to RUNX1-ETO cells, RUNX1-ETOΔ469 expressing cells continued to proliferate after puromycin selection (RUNX1-ETOΔ469 vs RUNX1-ETO day 10, $p \leq 0.05$), although growth rates were reduced compared to empty vector control cells (Figure 4.3a). The RUNX1-ETOΔ469 protein was expressed at an equivalent level to that of RUNX1-ETO (Figure 4.3b). Furthermore, RUNX1-ETOΔ469 expressing cells did not stain with SA-β-Gal, nor did they display the characteristic senescence-associated morphology (Figure 4.3c) indicating that RUNX1-ETOΔ469 does not induce premature senescence in Hs68 cells. These data identify the importance of repressor domains of ETO fusion partner in RUNX1-ETO induced senescence in Hs68 cells.

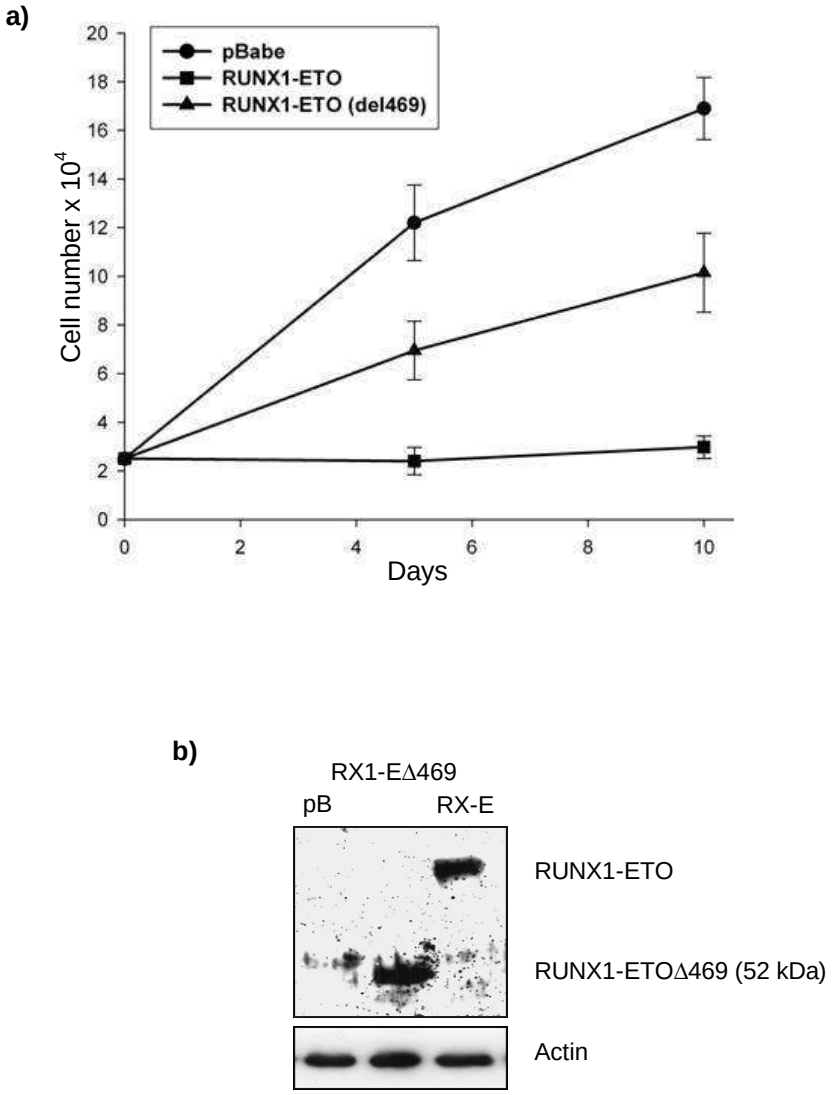

Figure 4.3 RUNX1-ETO requires ETO transcriptional repressor domains to induce senescence in human neonatal foreskin fibroblasts

Cells were transduced with retroviral vectors expressing RUNX1-ETOΔ469, RUNX1-ETO or control vector (pBabe) and selected for 4 days in puromycin. (a) Representative growth curves showing viable cell numbers corresponding to cell populations containing control vector (pBabe), RUNX1-ETOΔ469 or RUNX1-ETO. Each experiment was performed three times and each time point was determined in triplicate. (b) Western Blot analysis of RUNX1-ETOΔ469 and RUNX1-ETO expression in cells containing empty vector (pB), RUNX1-ETOΔ469 (RX1-EΔ469) or RUNX1-ETO (RX-E) on day 7 post-selection using Anti-Runx (D207-3, MBL)

c)

pBabe

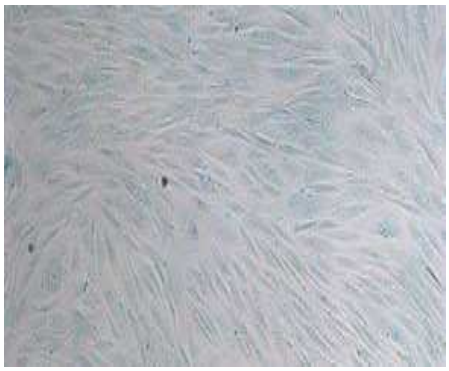

RUNX1-ETOΔ469

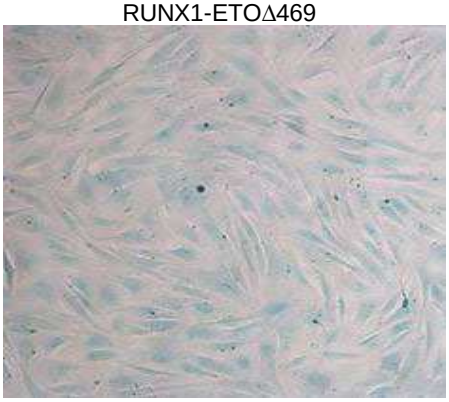

RUNX1-ETO

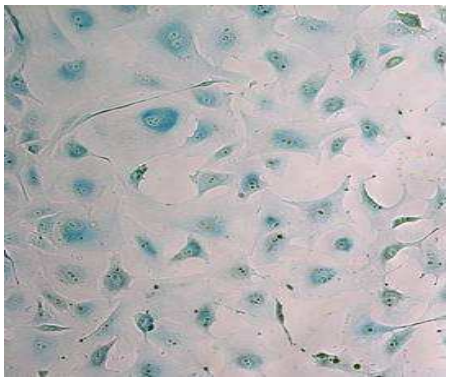

Figure 4.3 continued

(c) SA-β-Gal staining of cells containing control vector (pBabe), RUNX1-ETOΔ469 or RUNX1-ETO (day 7 post-selection)

4.5 CBFβ-MYH11 oncoprotein but not TEL-RUNX1 induces a moderate senescence-like growth arrest in human primary fibroblasts

Since RUNX1-ETO proved to be a very potent inducer of premature senescence it was tempting to speculate that other fusion oncoproteins e.g. TEL-RUNX1 or CBFβ-MYH11 which target RUNX1 and CBFβ, respectively, and would share the same property of being able to execute a senescence programme in human primary fibroblasts. TEL-RUNX1 is generated through the t(12;21) chromosomal translocation, which occurs in approximately 25% cases of B-cell origin pediatric acute lymphoblastic leukaemias. CBFβ-MYH11, is a consequence of a common chromosomal inversion event (INV16) which occurs in myelomonocytic leukaemias and results in fusion of the *CBFβ* gene with a smooth-muscle myosin-heavy-chain gene (*MYH11*). Both are thought to act as dominant negative regulators of RUNX1 function (Speck and Gilliland 2002). To investigate the effects of TEL-RUNX1 and CBFβ-MYH11 overexpression, Hs68 cells were transduced with either construct and monitored for their growth characteristics, morphological changes and SA-β-Gal staining. Interestingly, western blot analysis of expression of transgenes revealed that whereas CBFβ-MYH11 seemed to be stably expressed over the course of time, TEL-RUNX1 protein levels gradually declined over the same period (Figure 4.4a). Intriguingly, overexpression of CBFβ-MYH11 fusion protein but not TEL-RUNX1 partially repressed cell growth (Figure 4.4b). The proportion of CBFβ-MYH11 expressing cells which acquired flat and enlarged morphology and displayed positive staining for SA-β-Gal (Figure 4.4b) was significantly higher than TEL-RUNX1 or vector control cells and accounted for approximately 25% of the total cell population (CBFβ-MYH11 vs pBabe, $p \leq 0.05$; CBFβ-MYH11 vs TEL-RUNX1, $p \leq 0.05$) (Figure 4.4c) indicating that CBFβ-MYH11 unlike TEL-RUNX1 can induce senescence-like growth arrest.

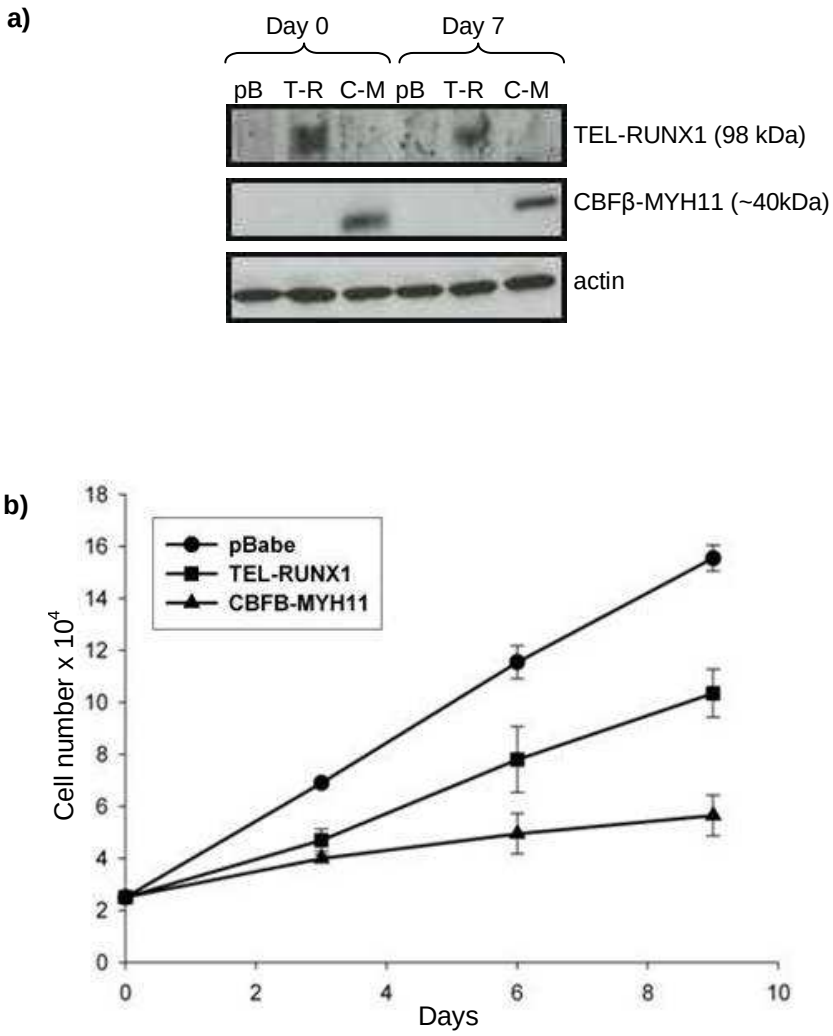

Figure 4.4 CBFβ-MYH11 but not TEL-RUNX1 induces a moderate senescence-like growth arrest in human neonatal foreskin fibroblasts

Cells were transduced with retroviral vectors expressing TEL-RUNX1, CBFβ-MYH11 or control vector (pBabe) and selected for 4 days in puromycin. (a) Western Blot analysis of TEL-RUNX1 (Anti-Runx, D207-3, MBL) and CBFβ-MYH11 (anti-CBFβ from Dr. Nancy Speck) expression in cells containing empty vector (pB), TEL-RUNX1 (T-R), CBFβ-MYH11 (C-M) on day 0 and day 7 post-selection (b) Representative growth curves showing viable cell numbers corresponding to cell populations containing control vector (pBabe), TEL-RUNX1 or CBFβ-MYH11. Each experiment was performed three times and each time point was determined in triplicate

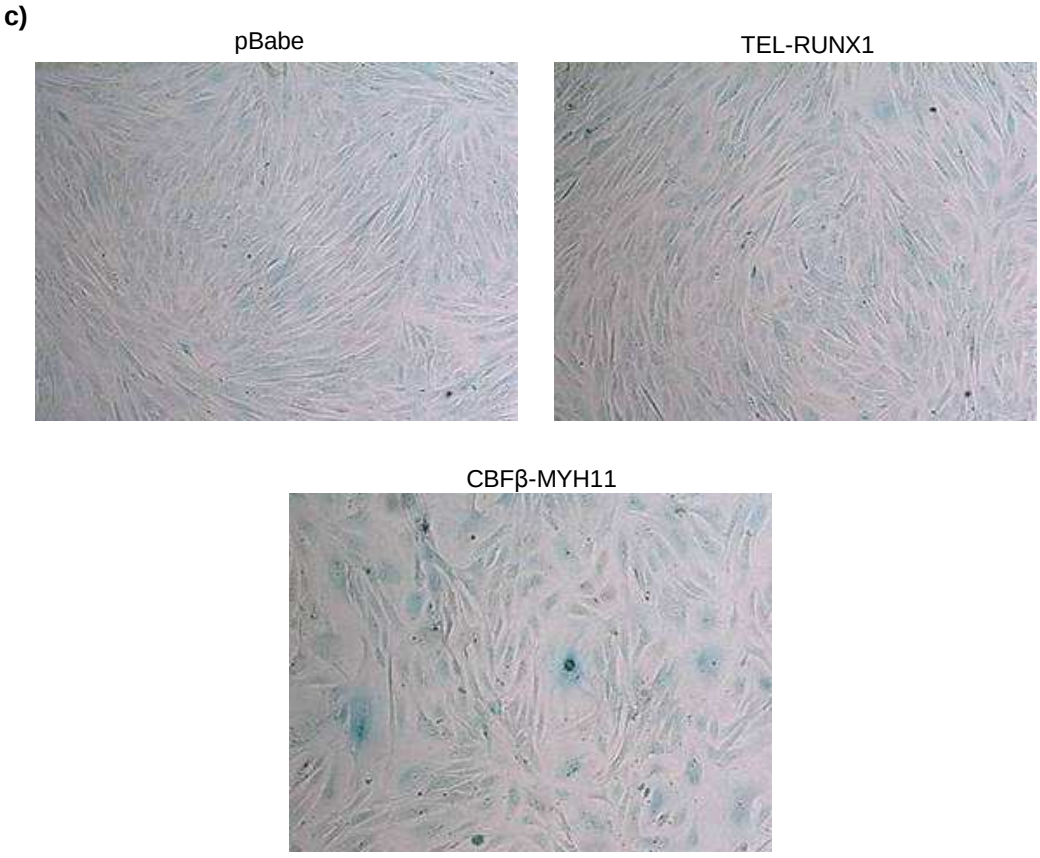

Figure 4.4 continued

(c) SA-β-Gal staining of cells containing control vector (pBabe), TEL-RUNX1 or CBFβ-MYH11 (day 7 post-selection) (d) Quantitation of data in (c) showing the percentage of SA-β-Gal positive cells. The data represent the mean of three independent counts of 200 cells (error bars relate to standard deviation)

4.6 Discussion

The discovery that the RUNX1-ETO oncoprotein is capable of inducing profound senescence-like growth arrest both in MEFs and Hs68 cells more dramatically than the archetypal RAS inuced senescence was both novel and surprising. Its established role as a dominant negative inhibitor of RUNX1 would lead to the prediction that, contrary to the senescence phenotype resulting from RUNX1 expression, RUNX1-ETO would fail to induce senescence, although this assumes that RUNX1 induces senescence via its gene activation potential. However, unlike AML1a which also lacks the C-terminal domain of wild type RUNX1, RUNX1-ETO proved to drive premature senescence, that was even more pronounced that of RUNX1 itself. This suggests that it has unique features independent of RUNX1 function that are likely to be conferred by its fusion partner protein, ETO. Indeed, ETO itself is known to be a strong transcriptional repressor (Lutterbach et al 1998; Wang et al 1998) and and the results reported here show that the mutant of RUNX1-ETO containing the deletion of corepressor binding sites of ETO (RUNX1-ETOΔ469) is unable to promote senescence. Therefore it is likely that RUNX1-ETO mediated senescence engages a repression of important target genes whereas it is not clear from the data presented here whether RUNX1 induced senescence relies on transcriptional activation and/or repression, although previous work in our laboratory showed a requirement for p53 while Linggi et al reported that $p19^{ARF}$ was required and induced by RUNX1 but repressed by RUNX1-ETO (Linggi et al 2002). This may imply that RUNX1-ETO induced senescence occurs independently of $p19^{ARF}$ in MEFs and it is possible that RUNX1 and RUNX1-ETO employ distinct signalling pathways for the induction of premature senescence or that both can induce a senescence response based on gene repression. Given that RUNX1-ETO has oncogenic properties, the senescence response may act as an initial barrier that restricts a full blown transformation by RUNX1-ETO.

Interestingly, overexpression of two other leukaemia related oncoproteins TEL-AML and CBFβ-MYH11 that target RUNX1 or CBFβ, respectively, revealed that only the latter displayed a limited activity to induce premature senescence in Hs68 human fibroblasts. Only 25% CBFβ-MYH11 expressing cells displayed

hallmarks of senescence (compare with approximately 40% for RUNX1, 80% for RUNX1-ETO or 75% for RAS as shown in Figure 2d of this chapter). It could be possible that CBFB-MYH11 requires more time for manisfestation of the complete senescent phenotype and therefore by day 7, when the analysis was performed, only 25% of cells displayed SA-ß-gal activity. The other explanation could be that CBFB-MYH11 requires endogenous RUNX, which would be rate limiting, for induction of senescence. TEL-RUNX1 failed to induce senescence at all but western blot analysis revealed that whereas CBFβ-MYH11 was stably expressed over the course of time, TEL-RUNX1 protein levels rapidly declined making interpretation of this result difficult. It is possible that TEL-RUNX1 fails to induce senescence due to relatively low levels of expression and that a threshold of signal potency may be required to elicit a senescence response that could not be achieved by TEL-RUNX1. It is also possible that cells with low expression may have a selective advantage in the population if the cells were unable to tolerate high levels of TEL-RUNX1 expression. Alternatively since some level of TEL-RUNX1 did remain throughout the time course the result may be a true reflection of TEL-RUNX1 expression conferring a specific advantage to this oncoprotein in its target cell and may suggest that TEL-RUNX1 exerts its effect by a different mechanism to the other fusion oncoproteins used.

Chapter 5

5 Characterisation of RUNX1 and RUNX1-ETO induced senescence in human primary fibroblasts

5.1 Introduction

The exciting finding that RUNX1-ETO induces a more profound senescent phenotype than H-RAS^{V12} in human fibroblasts clearly warranted further investigation. The pathways underlying H-RAS^{V12} induced senescence have been largely elucidated, hence I decided to examine RUNX1-ETO and RUNX1 induced senescent phenotypes by comparing and contrasting them with H-RAS^{V12}. Human primary fibroblasts overexpressing H-RAS^{V12} are predominantly arrested in G1 phase of the cell cycle (Serrano et al 1997). This senescence-like growth arrest induced by H-RAS^{V12} is associated with accumulation of growth inhibitors such as p21^{WAF1}, p53 and p16^{INK4a} (Serrano et al 1997). Oncogenic RAS induced senescence is also characterised by accumulation of PML nuclear bodies (Ferbeyre et al., 2000), high levels of reactive oxygen species (ROS) (Lee at al 1999) and activation of p38 MAPK (Wang et al 2002). Furthermore, formation of specific chromatin condensations described as senescence-associated heterochromatin foci (SAHF) has been linked recently to H-RAS^{V12} induced senescence (Narita et al 2003). Ras also triggers the accumulation of DNA double strand breaks (DSBs) following a pre-eliminary burst of proliferation (DiMicco et al 2006).

5.2 RUNX1 and RUNX1-ETO cell cycle arrest

Since both RUNX1 and RUNX1-ETO have been found to cause growth arrest in human neonatal foreskin fibroblasts it was important to define where in the cell cycle RUNX1 and RUNX1-ETO expressing cells are arrested. The cell cycle profile of RUNX1 and RUNX1-ETO expressing Hs68 cells was analysed at day 7 of growth curve, by employing bromodeoxyuridine (BrdU) incorporation combined with propidium iodide staining (PI) followed by flow cytometry analysis. H-RAS^{V12} expressing cells were used as a positive control. In accord with previously

published data (Serrano et al 1997, Ferbeyre et al 2000), oncogenic RAS expressing cells were arrested in G1 and G2M with a preference to accumulate in G1. RUNX1 and RUNX1-ETO expressing cells had slightly different cell-cycle profiles to that of H-RAS^{V12} with a prominent G1/G2M arrest and loss of S phase DNA content, an effect that was more pronounced in RUNX1-ETO cells (Figure 5.1 and Table 5.1). RUNX1-ETO containing cells in particular displayed a skew towards the G2M phase of the cell cycle (Table 5.1) (pBabe vs RUNX1-ETO, p=0.01). In this respect it was interesting to note that this finding corresponded to a relatively high proportion of binucleate and multinucleate RUNX1-ETO expressing cells observed under the light microscope (Figure 5.2) suggesting a defect in cytokinesis. It may also be the case that the arrested cells are G1 tetraploid binucleates and further analysis of cell cycle arrest will be useful.

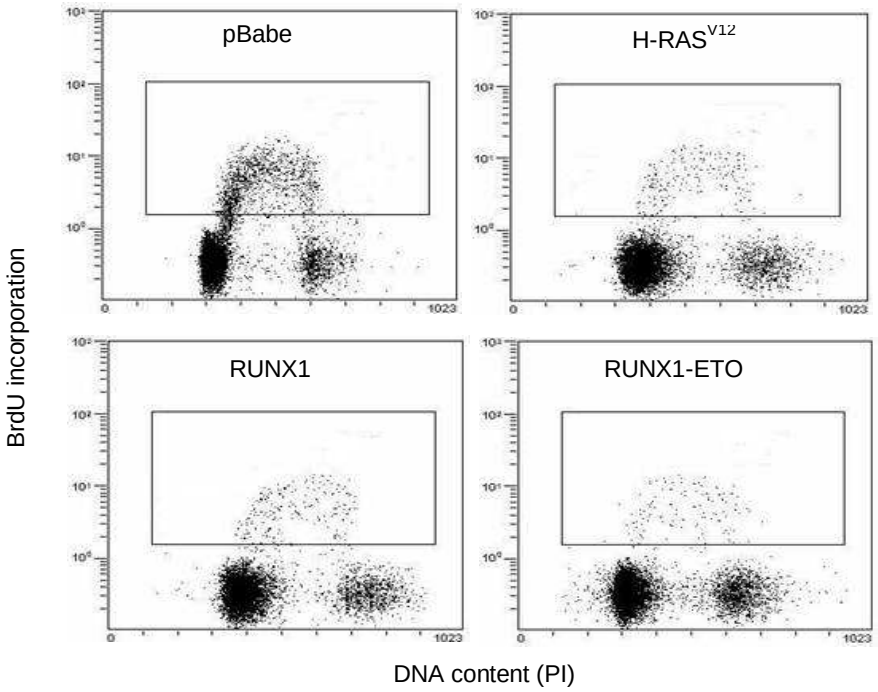

Figure 5.1 RUNX1 and RUNX1-ETO causes G1/G2M arrest in Hs68 cells

Representative cell cycle profiles of cells transduced with retroviral vectors expressing RUNX1-ETO, RUNX1, H-RAS^{V12} or control vector (pBabe). The cells at day 7 post-selection were pulsed with BrdU for 3 hours and analyzed for BrdU uptake and DNA content by two-colour flow cytometry using a FITC-conjugated anti-BrdU antibody and propidium iodide. The experiment was performed twice and yielded similar results

	pBabe	RX	RUNX1-ETO	H-RAS^{V12}
S	14.4%	2.7%	1.4%	2.8%
G1	76.7%	86.3%	83.5%	87.6%
G2/M	8.9%	11%	15.1%	9.6%

Table 5.1 RUNX1-ETO growth arrested Hs68 cells display a greater tendency to accumulate in the G2/M phase of the cell cycle

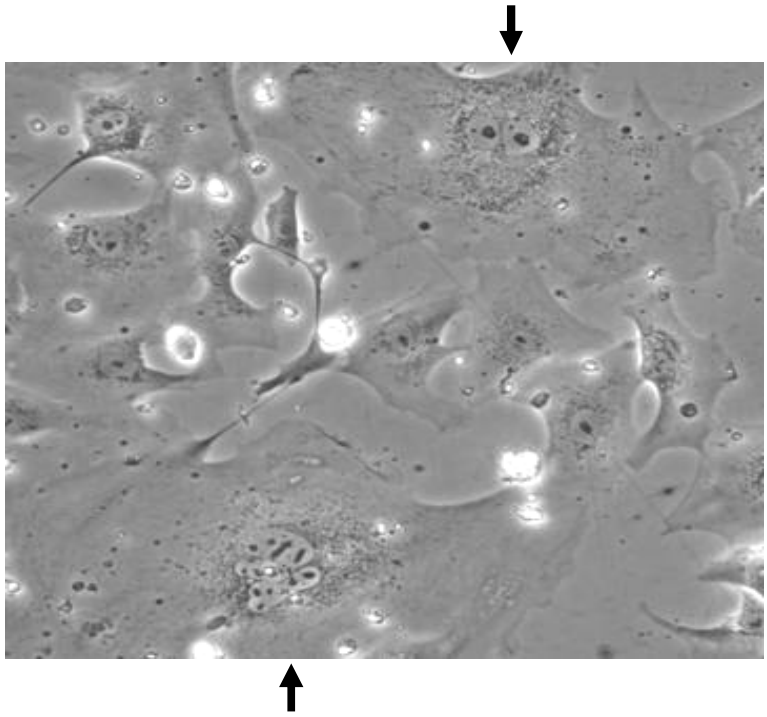

Figure 5.2 Phase-contrast photomicrograph illustrating binucleate (right upper corner) and multinucleate (left bottom corner) RUNX1-ETO expressing Hs68 cells (day 8 post-selection)

5.3 RUNX1-ETO and RUNX1 induced senescence display distinct pattern of induction of $p16^{INK4a}$, $p21^{WAF1}$ and p53

$P16^{INK4a}$, $p14^{ARF}$, $p21^{WAF1}$ and p53 are well established negative growth regulators that are upregulated in senescent cells (Collado and Serrano 2006). $P16^{INK4a}$ and $p21^{WAF1}$ act as inhibitors of cyclin-dependent kinases (CDK) and interfere with G1 to S progression during the cell cycle. $P21^{WAF1}$ is induced by p53 and inhibits CDK2/Cyclin E activity whereas $p16^{INK4a}$ inhibits CDK4 and CDK6 activity (Sherr 2000). This in turn results in hypophosphorylation of pRb and cell cycle arrest during senescence. $P14^{ARF}$ has been shown to neutralise the ability of Mdm2 to promote p53 degradation leading to the stabilisation and accumulation of p53 (Weber et al 1999; Zhang et al 1998). Overexpression of $p16^{INK4a}$, $p14^{ARF}$ and $p21^{WAF1}$ in human primary fibroblasts induces the hallmarks of premature senescence (Dimri et al 2000; McConnell et al 1998; Wei et al 2001).

To further explore the nature of the senescence programmes elicited by RUNX1 and RUNX1-ETO in human primary fibroblasts the levels of expression of $p16^{INK4a}$, $p14^{ARF}$, $p21^{WAF1}$ and p53 were analysed in Hs68 cells. The $H\text{-}RAS^{V12}$ oncogene has been reported to upregulate all of these effectors except for $p14^{ARF}$ (Serrano et al 1997; Wei at al 2001]. In the work reported here a similar pattern of regulation was seen in human neonatal foreskin fibroblasts expressing $H\text{-}RAS^{V12}$ (Figure 5.3a). It was of particular interest to determine whether $p14^{ARF}$ status is affected either by RUNX1 or RUNX1-ETO expression in Hs68 cells since RUNX1 and RUNX1-ETO have been reported to have opposing effects on this gene locus (Linggi et al 2002). Analysis of d7 post selection Hs68 fibroblasts gave contrasting results with levels of $p14^{ARF}$ appearing refractory to RUNX1 or RUNX1-ETO status (Figure 5.3b). Further western blot analysis revealed interesting differences in $p16^{INK4a}$, $p21^{WAF1}$ and p53 expression between RUNX1 and RUNX1-ETO expressing cells suggestive of distinct senescence execution pathways. Notably RUNX1-ETO and RUNX1 induced p53, with RUNX1-ETO the more potent agonist (Figure 5.3a). Intriguingly, the levels of p53 did not correlate with the potency of induction of $p21^{WAF1}$, the downstream target of p53 (Figure 5.3b). In this respect $p21^{WAF1}$

expression levels were dramatically induced by RUNX1 but not by RUNX1-ETO suggesting possible opposing transcriptional effects on the $p21^{WAF1}$ promoter. Even more surprisingly, especially in comparison to $H\text{-}RAS^{V12}$, RUNX1 but not RUNX1-ETO upregulated $p16^{INK4a}$ (Figure 5.3a).

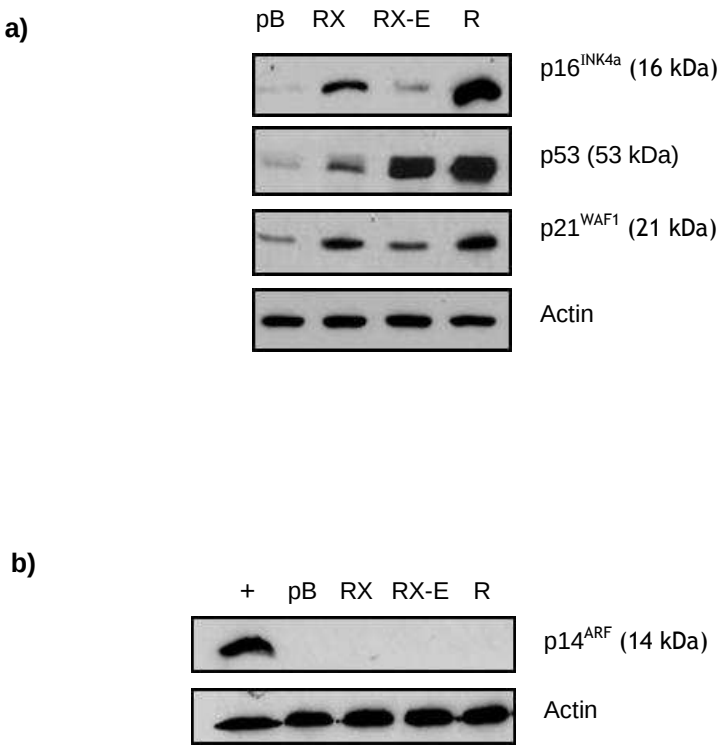

Figure 5.3 RUNX1-ETO and RUNX1 induced senescence display distinct patterns of induction of $p16^{INK4a}$, $p21^{WAF1}$ and p53 in Hs68 cells

(a) Western blot analysis of expression of $p16^{INK4a}$ (anti-p16, sc-468, Santa Cruz) $p21^{WAF1}$ (anti-p21, sc-397, Santa Cruz) and p53 (anti-p53, sc-126, Santa Cruz) in cells containing control vector (pB), RUNX1 (RX), RUNX1-ETO (RX-E) and or H-RasV12 (R) (day 7 post-selection) (b) Western blot analysis of expression of $p14^{ARF}$ (anti-p14ARF, Ab-2, Neomarkers) in Hs68 cells containing control vector (pB), RUNX1 (RX), RUNX1-ETO (RX1-E) or $H\text{-}Ras^{V12}$ (R) (day 7 post-selection). Human cells-13 lysate (MS-850-PCL, neomarkers) was used as a positive control (+)

5.4 Activation of p38 MAPK in RUNX1 and RUNX1-ETO induced senescence

The p38 MAPK pathway mediates responses to environmental stresses, including DNA-damaging agents such as UV and γ-irradiation [Bulavin and Fornance, 2004]. Interestingly, the mitogen-activated protein kinase p38 plays a pivotal role in mediating cellular senescence caused by a broad spectrum of stimuli, including oxidative stress, dysfunctional telomeres, culture shock and the proto-oncogene erbB2 (Iwasa et al 2003, Trost et al 2005]. Therefore it has been suggested that p38 kinase links pro-oncogenic signals to tumour suppressors. P38 MAPK has been also implicated in H-RAS^{V12} induced senescence where p38 is phosphorylated by two upstream kinases, MKK3 and MKK6 (Wang et al 2002) and was shown to be responsible for H-RAS^{V12} induced transcriptional activity of p53 (Sun et al 2007) and to contribute to the upregulation of p16^{INK4a} and p53 (Wang et al 2002).

Therefore, I considered that the p38 MAPK pathway may also mediate RUNX1 and RUNX1-ETO induced senescence. To investigate this hypothesis, the abilities of RUNX1 and RUNX1-ETO to activate p38 MAPK were examined using a specific antibody that recognises two phosphorylation sites responsible for p38 MAPK activation (Thr180 and Tyr182) (Wang et al 2002). Indeed, western blot analysis on day 7 of culture period revealed that both RUNX1 and RUNX1-ETO elevated levels of phospho-p38 while RUNX1-ETO was more potent agonist and induced phospho-p38 to a similar degree as H-RAS^{V12} (Figure 5.4). Notably, the levels of total p38 MAPK remained unaffected (Figure 5.4). These results suggest that the p38 MAPK is involved in RUNX1 and RUNX1-ETO induced senescence. Furthermore, the upregulation of phospho-p38 by RUNX1 and RUNX1-ETO reflected the p53 levels (Section 5.3, Chapter 5) suggestive of a common signalling pathway.

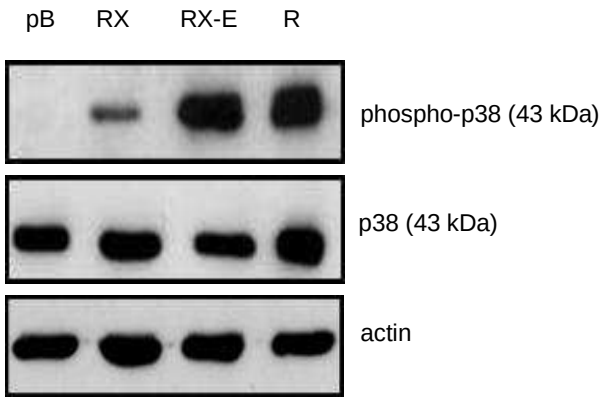

Figure 5.4 RUNX1-ETO and RUNX1 induce phospho-p38 with differing potencies in Hs68 cells

Western blot analysis of phospho-p38 (anti-phospho-p38, 9211, Cell signalling) and p38 (anti-p38, 9212, Cell signalling) expression in cells containing control vector (pB), RUNX1 (RX), RUNX1-ETO (RX-E) or H-RasV12 (R) (day 8 post-selection).

5.5 Activation of p38 MAPK correlates with induction of intracellular reactive oxygen species

There is a significant body of experimental evidence supporting the idea that a rise in intracellular reactive oxygen species (ROS) contributes to cellular senescence (Colavitti and Finkel, 2005; Passos and Zglinicki, 2006). Various extrinsic or intrinsic manipulations changing the intracellular antioxidant status, raising the ambient oxygen concentration, direct exposure of cells to hydrogen peroxide or the expression of certain oncogenes like H-RAS^{V12}, all appear to produce a rise in intracellular ROS levels (Lee et al 1999; Chen et al 1998; Frippiat et al 2000). This rise in ROS within cells accompanies and potentially triggers senescence entry (Passos and Zglinicki, 2006). It has been reported that ROS induction leads to activation of p38 kinase (Iwasa et al 2003; Guyton et al 1996) and upregulation of a subset of p38 target genes (Zdanov et al 2006) in cells treated with hydrogen peroxide. It was also demonstrated that MINK kinase is activated by RAS induced ROS and subsequent activation of p38 by MINK results in premature senescence (Nicke et al 2005).

To investigate whether ROS levels are altered in prematurely senescent cells expressing RUNX1 and RUNX1-ETO and could therefore cause the activation of p38 MAPK in these cells, the levels of ROS in human neonatal foreskin fibroblasts were examined at day 7 post-selection by using FACS based detection of fluorescence emitted by the peroxide-sensitive fluorophore DCF. As expected H-RAS^{V12} cells displayed high levels of intracellular ROS consistent with published data (H-RASV12 vs pBabe, $p \leq 0.005$) (Figure 5.5a, b) (Lee et al 1999). Interestingly, both RUNX1 and RUNX1-ETO expressing cells were found to have elevated intracellular ROS levels compared to empty vector control cells (RUNX1 vs pBabe, $p \leq 0.05$; RUNX1-ETO vs pBabe, $p \leq 0.0001$) (Figure 5.5a, b) but only RUNX1-ETO expressing cells showed as profound or even greater induction than H-RAS^{V12} expressing cells (Figure 5.5a, b). Furthermore, the intracellular ROS levels appeared to correlate well with the degree of phospho-p38 activation by RUNX1 and RUNX1-ETO as found in previous experiments. The DCF fluorescence was also imaged with a laser scanning confocal microscope visually confirming the quantitative analysis of ROS levels (Figure 5.5c)

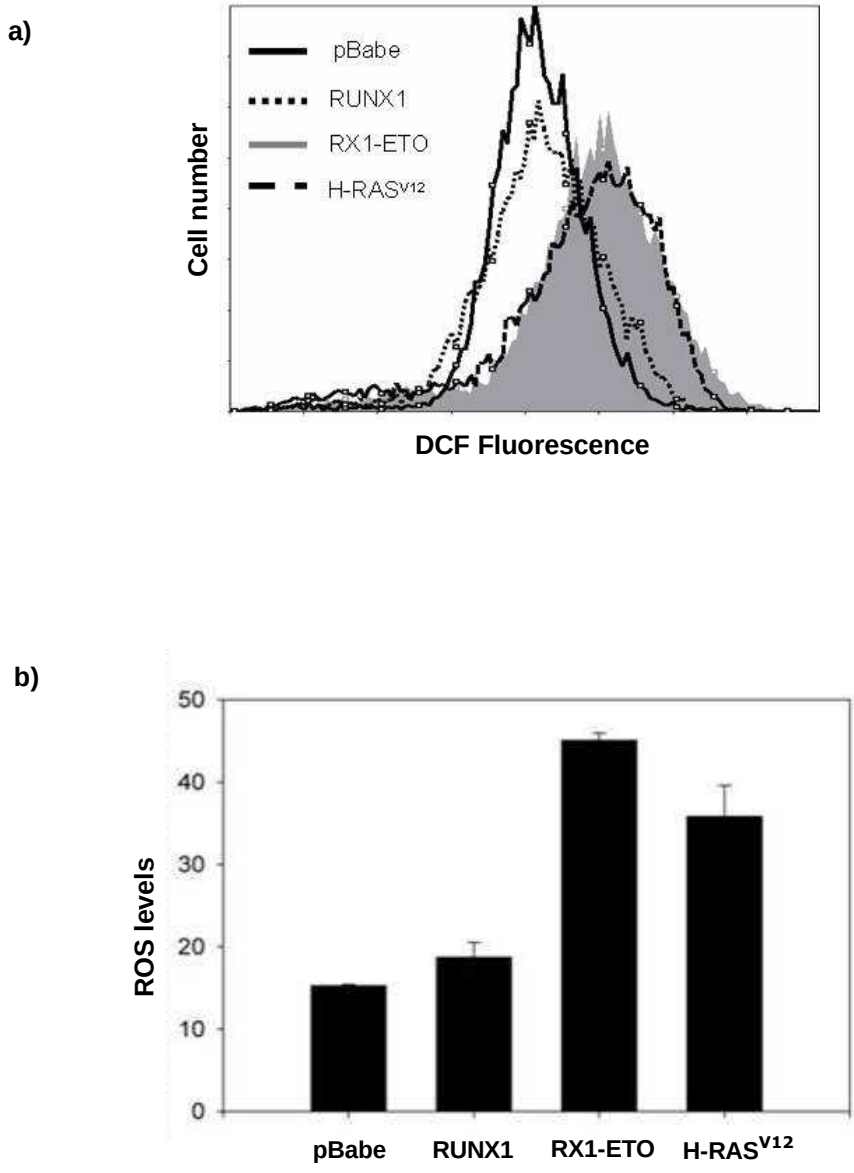

Figure 5.5 Activation of p38 MAPK correlates with induction of intracellular ROS in Hs68 cells

Cells were infected with retrovirus encoding RUNX1, RUNX1-ETO, H-RAS^{V12} or control retrovirus (pBabe) and analysed with DCF for intracellular ROS levels 7 days after puromycin selection (a) Intracellular ROS was monitored by FACS analysis of DCF fluorescence (b) Quantitation of DCF fluorescence

c)

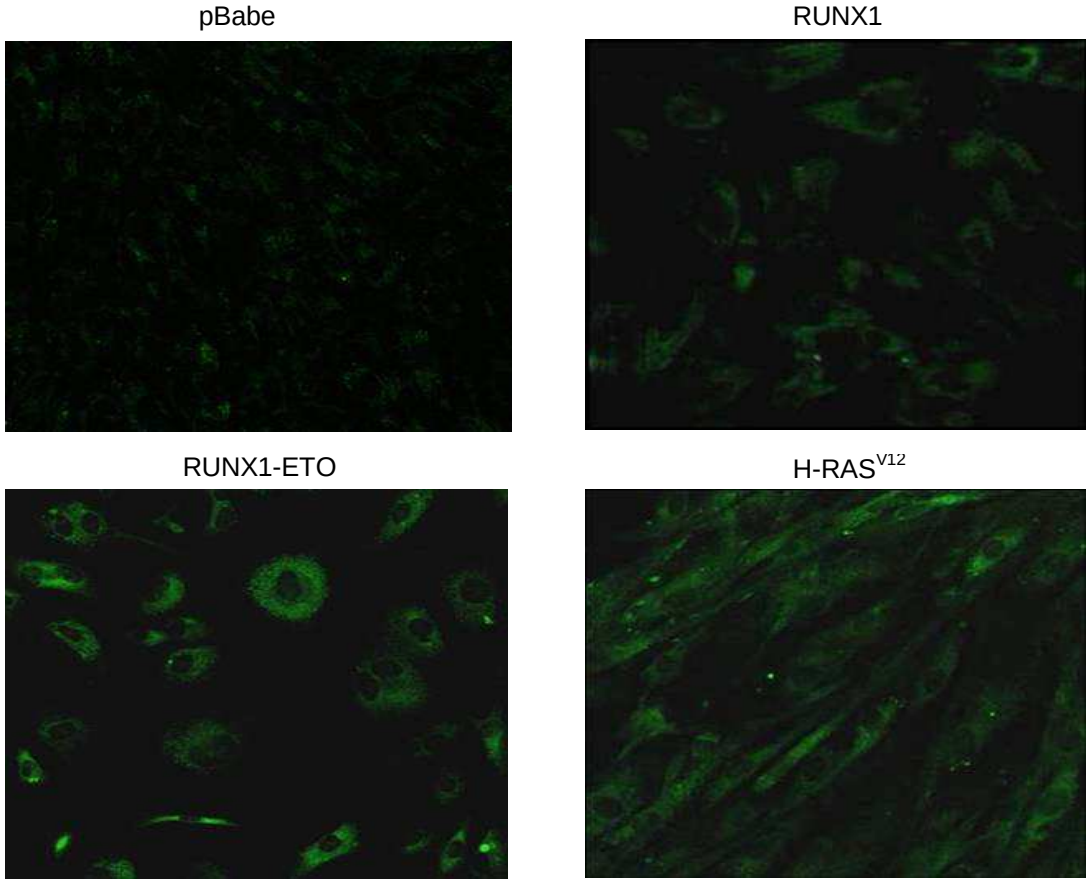

Figure 5.5 continued

(c) Visualisation of DCF fluorescence by confocal laser scanning microscopy (day 7 post-selection)

5.6 DNA damage and senescence associated heterochromatin foci in RUNX1 and RUNX1-ETO induced senescence

Severe DNA damage, especially damage that involves DNA double-strand breaks, (DSBs) causes many cell types to undergo senescence (DiLeonardo et al 1994). Critically short, dysfunctional telomeres can also trigger a classical DNA damage response (DDR) (Herbig et al., 2004). Moreover, oncogenic RAS induced senescence has been linked to the accumulation of DNA damage. It has been suggested that DNA damage is caused by oncogene-driven increases in cellular levels of reactive oxygen species which can result in DNA single and double-strand breaks (Lee et al 1999). Other possible mechanisms have been proposed whereby oncogenes such as H-RAS^{V12} induce a robust DDR owing to prematurely terminated DNA replication forks and DSBs that are caused by DNA hyper-replication stress (DiMicco et al 2006; Bartkova et al 2006).

To determine whether DNA damage signalling is associated with RUNX1 and RUNX1-ETO induced senescence in Hs68 cells, confocal laser scanning immunofluorescence microscopy was performed on Hs68 fibroblasts on day 7 post selection following retroviral transduction with RUNX1, RUNX1-ETO and H-RAS^{V12}. The cells were fixed and dual labelled with a monoclonal antibody that recognises phosphorylated histone H2AX (γ-H2AX), a marker of DNA double-strand breaks and DAPI to visualise nuclear DNA. As shown in Figure 5.6, overexpression of H-RAS^{V12} resulted in accumulation of multiple γ-H2AX positive nuclear foci on day 7 of culture. These correspond to DSBs and have previously been reported in H-RAS^{V12} induced senescence. In contrast, RUNX1 and RUNX1-ETO expressing populations of cells exhibited only one or two fluorescent dots and more closely resembled vector control cells than H-RAS^{V12} expressing ones (Figure 5.6) DAPI staining of the nuclear content revealed that RUNX1 and RUNX1-ETO, in contrast to oncogenic RAS, did not cause specific chromatin condensations or senescence associated heterochromatin foci (SAHF) that have previously been observed during cellular senescence (Figure 5.6).

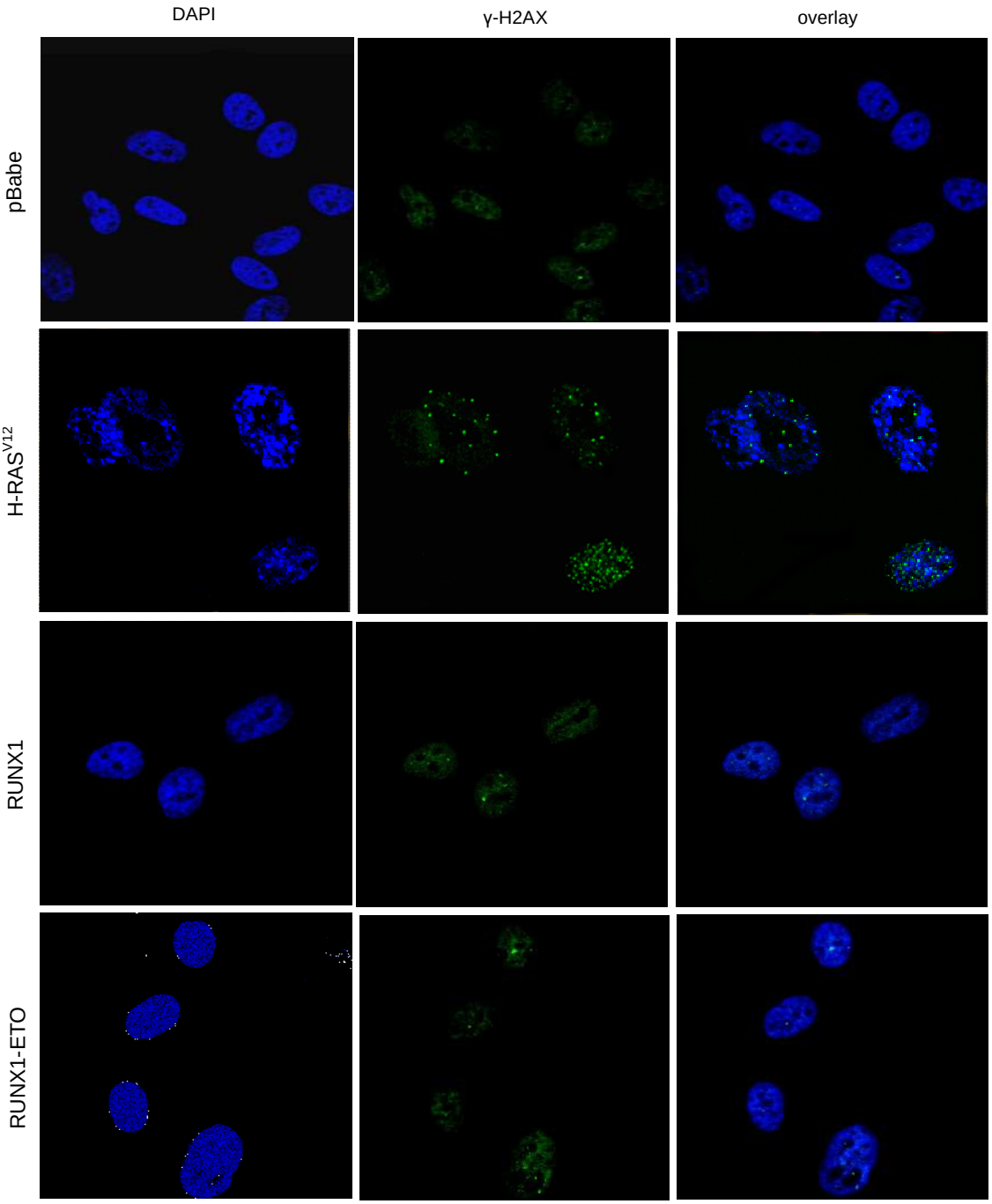

Figure 5.6 Ras but not RUNX1 or RUNX1-ETO induces DNA damage foci and SAHF in Hs68 human fibroblasts

Indirect immunofluorescence for γH2AX foci (using anti-H2AX, 05-636, Upstate) in Hs68 cells expressing control vector (pBabe), RUNX1, RUNX1-ETO or H-RAS^{V12} (day 7 post-selection). DAPI was used to stain the nuclear DNA

5.7 Accumulation of PML nuclear bodies in RUNX1 and RUNX1-ETO induced senescence

PML has recently been described as a senescence regulatory protein. PML is upregulated during cellular senescence, and induces premature senescence in response to oncogenic H-RAS (Ferbeyre et al 2000). Interestingly, PML has been shown to regulate the p53 response to oncogenic signals by binding MDM2 and sequestering it into the nucleus, thus protecting p53 from proteosome-mediated degradation (Bernardi et al 2004), as well as specifically acetylating p53 (Pearson et al 2000). Both of these processes stabilize the p53 protein. Interestingly PML is also a direct p53 target that modulates p53 functions indicating the existence of a regulatory feedback loop between these tumour suppressors (de Stanchina et al 2004).

As shown in section 5.3 of this chapter, RUNX1 and RUNX1-ETO expressing cells displayed substantial differences in the levels of expression of p53 protein with only RUNX1-ETO inducing p53 as profoundly as H-RAS^{V12}. It was therefore interesting to establish the status of PML in RUNX1-ETO or RUNX1 senescent cells and to determine whether PML could play a role in the differential upregulation of p53 in these cells. Hs68 cells were transduced with retroviral vectors expressing RUNX1, RUNX1-ETO and H-RAS^{V12}, and double stained using a specific antibody recognising PML with DAPI as a nuclear DNA marker at day 7 post-selection. Visualisation of PML nuclear bodies by laser scanning confocal microscopy revealed increased PML bodies in H-RAS^{V12} expressing cells, and RUNX1-ETO cells but not in RUNX1 cells (Figure 5.7). Again, unlike H-RAS^{V12}, RUNX1 and RUNX1-ETO expressing cells did not exhibit SAHF. This result suggests that PML may be involved in the stabilisation and increased p53 expression in RUNX1-ETO expressing cells.

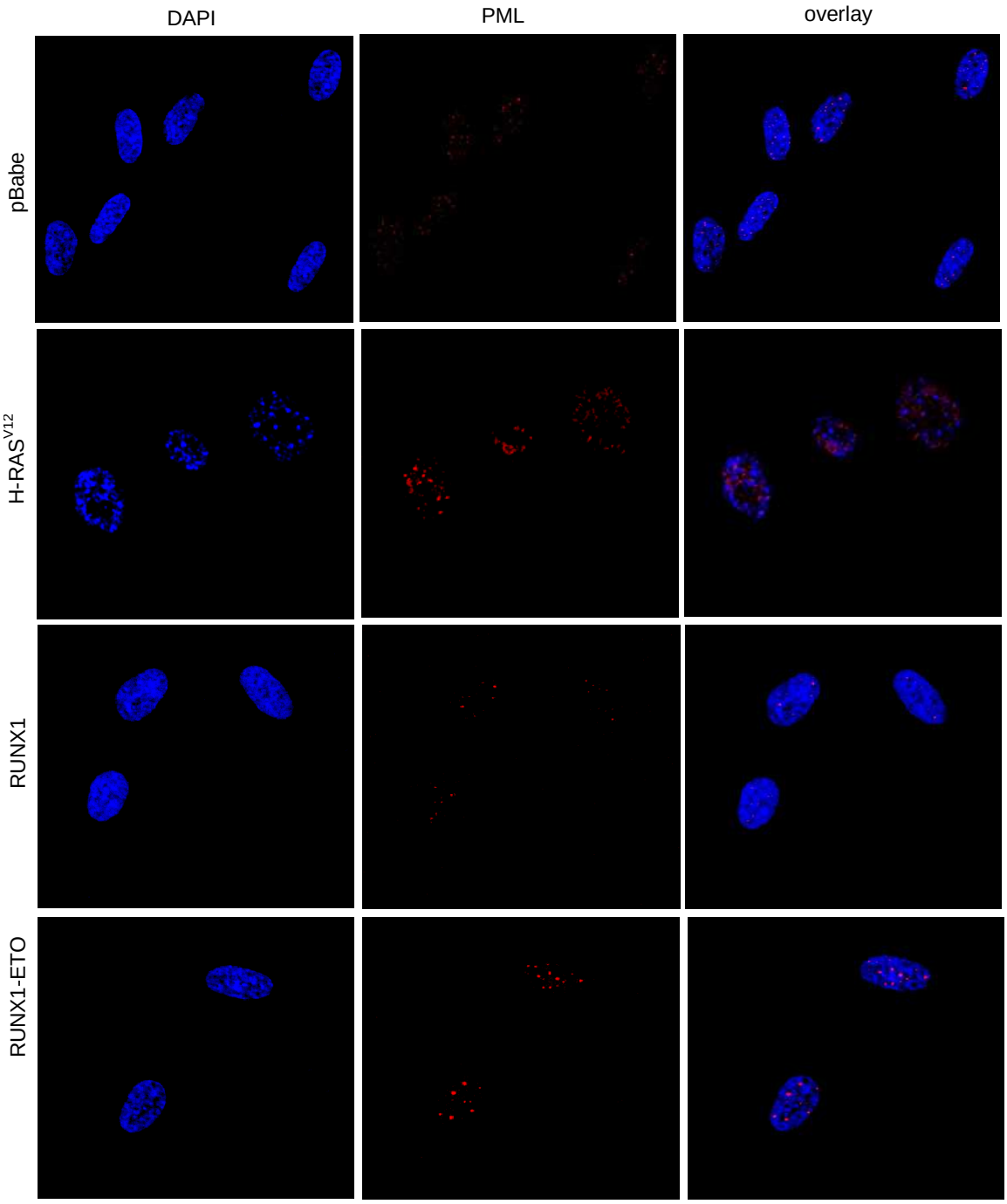

Figure 5.7 PML accumulation is induced by RUNX1-ETO but not RUNX1 in human fibroblasts Hs68

Indirect immunofluorescence for PML (anti-PML, N19, Santa Cruz) in Hs68 cells expressing control vector (pBabe), RUNX1, RUNX1-ETO or H-RAS^{V12} (day 7 post-selection). DAPI was used to stain the nuclear DNA

5.8 Partial recapitulation of RUNX1-ETO induced senescence by ectopic expression of p53

RUNX1-ETO profoundly elevates levels of p53 expression but importantly while RUNX1-ETO induces p53 it simultaneously attenuates downstream upregulation of $p21^{WAF1}$ expression in Hs68 cells. It was therefore particularly interesting to address the question of whether the ectopic expression of p53 alone drives premature senescence in Hs68 fibroblasts and if so, how does the phenotype of p53 expressing cells compares to that of RUNX1-ETO.

Hs68 cells were infected with retroviruses containing p53 and RUNX1-ETO or control vector. Ectopic expression of RUNX1-ETO resulted in a substantial growth arrest (RUNX1-ETO vs pBabe, day 8 $p=0.01$) (Figure 5.8a) and characteristic senescence-related alterations to cellular morphology and positive staining of RUNX1-ETO expressing cells for SA-ß-Gal activity (Figure 5.8b). Overexpression of p53 also caused significant growth arrest (p53 vs pBabe, day 8 $p \leq 0.01$) (Figure 5.8a), however p53 expressing cells were not as flat and enlarged as RUNX1-ETO expressing cells and the intensity of SA-β-Gal staining was not as pronounced (Figure 5.8b). As before (Section 5.3, Chapter 5), RUNX1-ETO expressing Hs68 fibroblasts, in contrast to p53 expressing cells, were found to be refractory to the induction of $p21^{WAF1}$ despite the upregulation of p53 (Figure 5.8c). Interestingly, overexpression of p53 did not cause the accumulation of γ-H2AX DNA damage foci or senescence associated heterochromatin foci in Hs68 cells as visualised by laser scanning confocal microscopy using anti-γ-H2AX and DAPI staining (Figure 5.8d). These data show that ectopic expression of p53 in Hs68 cells induces senescence-like growth arrest that partially recapitulates that of RUNX1-ETO expressing cells clearly indicating that RUNX1-ETO induces senescence via p53 yet apparently modulates its signalling pathway.

a)

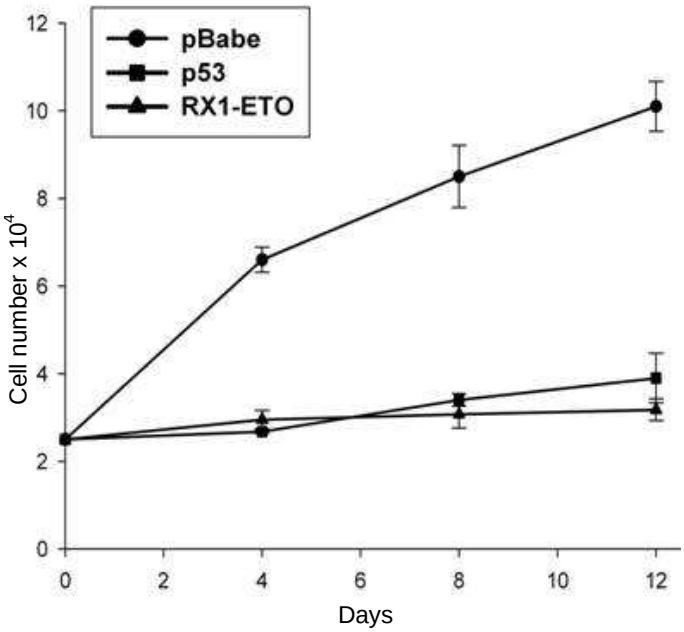

b)

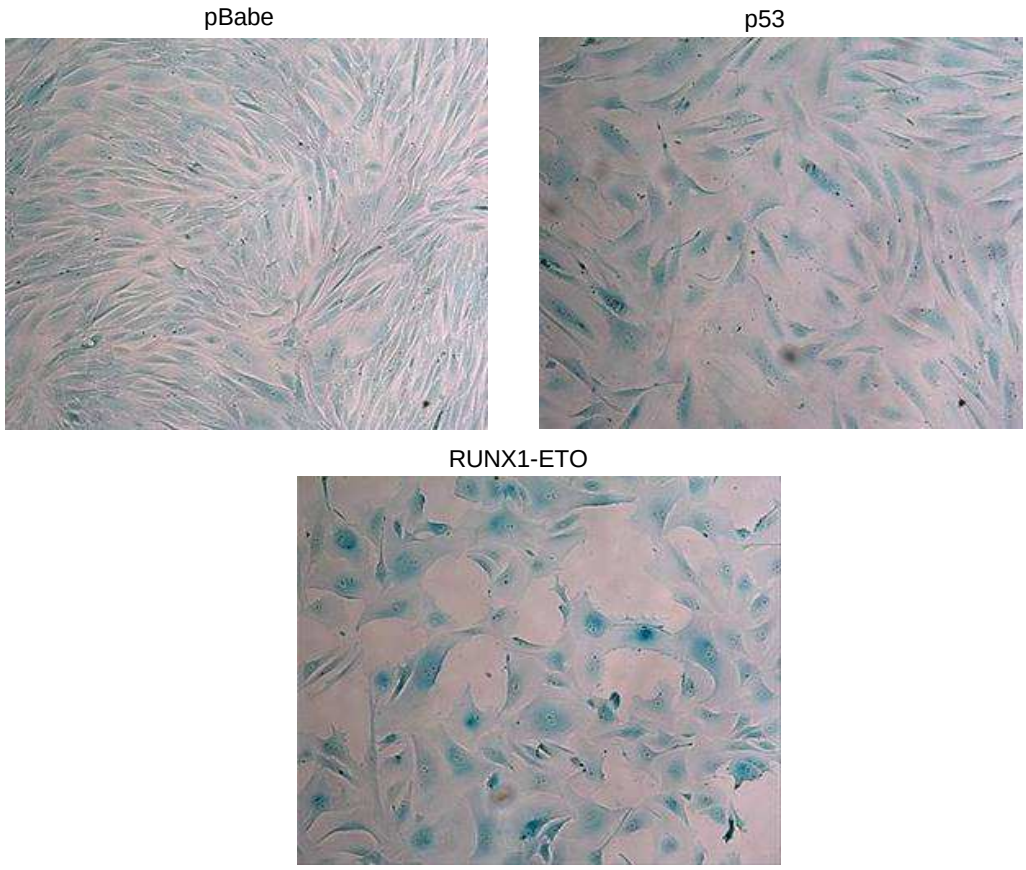

Figure 5.8 Ectopic expression of p53 partially recapitulates RUNX1-ETO induced senescence in Hs68 cells

(a) Representative growth curves of Hs68 cells transduced with control vector (pBabe), RUNX1-ETO or p53 (c) SA-β-Gal staining of cells expressing p53 or RUNX1-ETO (day 7 post-selection)

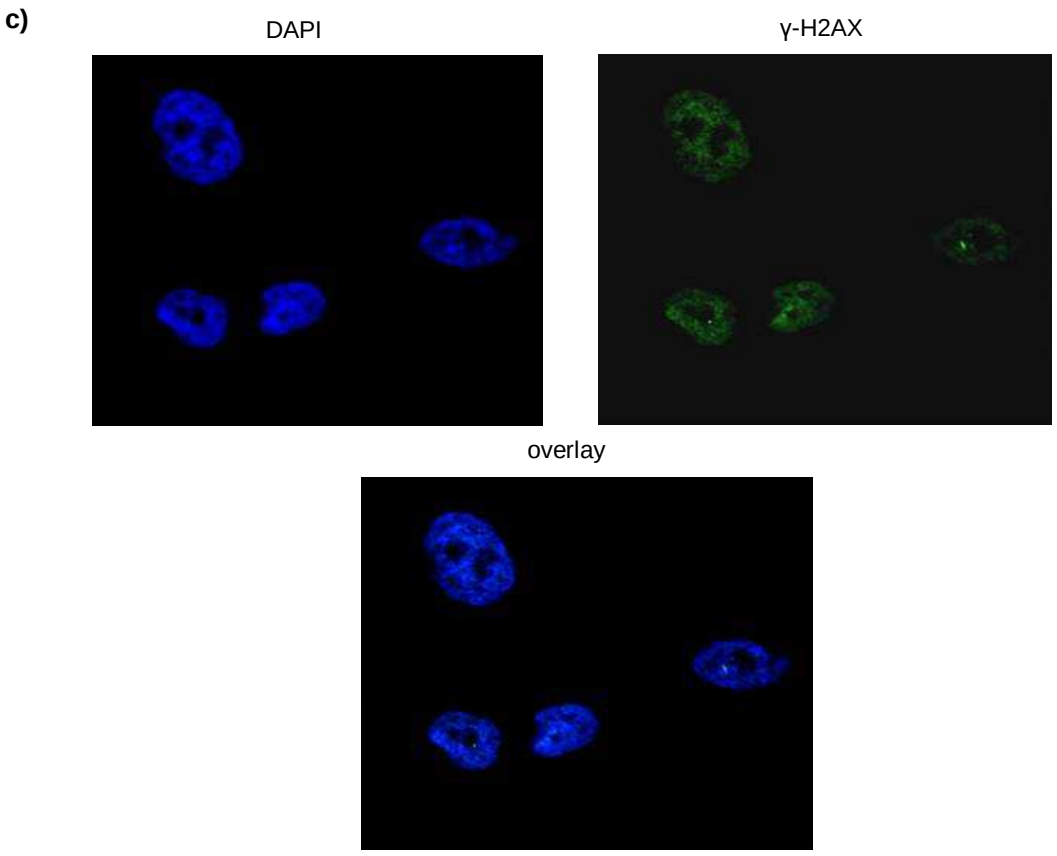

Figure 5.8 continued

(c) Indirect immunofluorescence for γ-H2AX foci in cells expressing p53 and visualisation of SAHF by staining with DAPI (day 7 post-selection) (d) Western blot analysis of p53 (anti-p53, sc-126, Santa Cruz) and $p21^{WAF1}$ (anti-p21, sc-397, Santa Cruz) in lysates from cells containing empty vector (pB), p53 (p53) or RUNX1-ETO (RX-E) (day 7 post-selection)

5.9 Discussion

Further characterisation of RUNX1 and RUNX1-ETO induced senescence revealed interesting differences and common features in their respective phenotypes and also highlighted some similarities and differences to H-RAS^{V12} induced senescence. Analysis of the cell cycle showed that whereas H-RAS^{V12} or RUNX1 expressing cells arrest in G1 phase, the RUNX1-ETO cell cycle arrest was skewed towards G2M phase and these cells showed an increase in the proportion of bi- and multi-nucleate cells suggesting some defects in cytokinesis. The expression levels of well established biomarkers of senescence involved in the execution of growth arrest were then examined, clearly identifying substantial differences between RUNX1, RUNX1-ETO and H-RAS^{V12} induced senescent phenotypes in Hs68 cells. In contrast to previous reports where RUNX1 has been reported to stimulate p19^{ARF} while RUNX1-ETO to have the opposite effect (Linggi et al 2002), p14^{ARF} status in Hs68 human fibroblasts was unaffected by either RUNX1 or RUNX1-ETO, consistent with the notion that the ARF locus is not a major regulator of cellular senescence in human cells (Wei et al 2001, Brookes at al 2002). Interestingly, expression levels of the downstream target of p14^{ARF}, p53, were profoundly upregulated by RUNX1-ETO and to a much lesser extent by RUNX1. Because PML has been shown to be involved in the regulation of p53 in senescence (Ferbeyre et al 2000; Langley et al 2002; Pearson et al 2000), theoretically it could be responsible for these differences. Indeed, fluorescent confocal scanning microscopy revealed increased PML nuclear bodies in RUNX1-ETO and H-RAS^{V12} expressing cells but not in RUNX1 expressing cells suggesting a direct link between PML and p53 status in these cells. Furthermore, although p53 was highly elevated by RUNX1-ETO, the expression levels of the downstream effector of p53, p21^{WAF1}, were dramatically induced by RUNX1 but not by RUNX1-ETO. Given that the p21^{WAF1} promoter contains RUNX1 DNA-binding sites it is conceivable that RUNX1 and RUNX1-ETO exert direct and opposing transcriptional effects on p21^{WAF1} promoter in Hs68 human fibroblasts. The antagonistic activities of RUNX1 and RUNX1-ETO were also apparent with regard to the p16^{INK4a} locus where only RUNX1 induced p16^{INK4a} expression to a substantial level although not as strongly as H-RAS^{V12}. p38 MAPK has been recently identified as a major regulator of cellular senescence caused by a

diverse spectrum of signals (Iwasa et al., 2003) and it has been proposed to be involved in the downstream activation of negative regulators of the cell cycle such as $p16^{INK4A}$ and p53 during H-RAS^{V12} induced senescence (Iwasa et al 2003; Wang et al 2002; Sun et al 2007). Western blot analysis revealed profound induction of the activated form of p38 MAPK, phospho-p38, in RUNX1-ETO expressing cells and a much weaker induction in RUNX1 expressing cells. Notably, the degree of activation of p38 in these cells appeared to correlate with the potency of p53 upregulation suggesting the existence of a common regulatory signalling pathway whereby p38 may regulate p53 expression and vice versa. Interestingly, increased p38 activation in RUNX1-ETO expressing cells did not have an effect on $p16^{INK4a}$, in contrast to H-RAS^{V12}, where p38 MAPK has been demonstrated to stabilise $p16^{INK4a}$ mRNA levels (Wang et al 2002). The next question that arose was related to the upstream signals activating p38. In H-RAS^{V12} induced senescence increased ROS levels have been linked to the activation of p38 MAPK (Nicke et al 2002; Sun et al 2007). Both RUNX1 and RUNX1-ETO expressing cells were found to have elevated levels of ROS which paralleled the induction of p38 phosphorylation suggesting that ROS may play a role in the activation of p38 in RUNX1 and RUNX1-ETO expressing Hs68 human fibroblasts. The generation of high ROS levels has been postulated to be one of the potential causes of DNA double strand break accumulation and DNA damage responses in senescent cells (Lee et al 1999). Interestingly, despite increases in ROS levels induced by RUNX1 and RUNX1-ETO, convincing DSBs as visualised by γ-H2AX foci were not observed. It is possible that the activity of ROS could be modulated by RUNX1 and RUNX1-ETO due to their action as second messengers in signal transduction pathways. The accumulation of γ-H2AX foci associated with oncogene-induced senescence has also been associated with 'replicative stress' occurring due to a strong proliferative burst preceding growth arrest (DiMicco et al 2006). Neither RUNX1 nor RUNX1-ETO showed any hyper-proliferation but instead displayed strong growth suppression immediately after viral transductions which may partially explain lack of γ-H2AX foci in these cells. Another interesting finding was that both RUNX1 and RUNX1-ETO induced senescent cells, in contrast to H-RAS^{V12} expressing cells, exhibited lack of SAHF. The $p16^{INK4a}$/pRb pathway has been shown to be involved in SAHF formation (Narita et al 2003), therefore it is possible that RUNX1-ETO expressing cells did

not show SAHF because $p16^{INK4a}$ was not upregulated in these cells. In support of this, STAT5a induced senescence in human primary fibroblasts also does not involve induction of $p16^{INK4a}$ or SAHF formation (Hemann and Narita, 2008), but unusually despite $p16^{INK4a}$ upregulation in RUNX1 induced senescent cells, SAHF are not present. Since the induction of $p16^{INK4a}$ by RUNX1 was not as potent as that of $H\text{-}RAS^{V12}$ it is plausible that a certain threshold level of $p16^{INK4a}$ expression needs to be achieved in order to initiate the process of SAHF formation. Also the mechanism of SAHF formation relies not only p16/pRb but also on many other components such as HIRA/ASF1a and PML that are required to interact in a specific spatio-temporal manner (Adams 2007). RUNX1 may interfere with these processes especially since it fails to induce PML bodies. These results identify RUNX1, RUNX1-ETO and $H\text{-}RAS^{V12}$ induced senescence as distinct programmes engaging diverse signalling pathways, however the biological relevance of these findings remains to be investigated further.

Chapter 6

6 Dissecting functional requirements of the host cell for RUNX1 and RUNX1-ETO induced senescence

6.1 Introduction

Characterisation of RUNX1 and RUNX1-ETO induced senescence has revealed a number of interesting differences from the pathways previously reported to execute this cellular programme. Of particular importance was the finding that overexpression of RUNX1 or RUNX1-ETO led to differing levels of $p16^{INK4a}$, p53 and p38 MAPK induction. Hence it was important to examine the functional requirements for these mediators in RUNX1 and RUNX1-ETO induced senescence in primary fibroblasts. In human cells, as opposed to murine cells, Ras has been reported to drive premature senescence by a p53 independent mechanism despite strong induction of p53 (Wei et al 2001; Bischof et al 2005). It relies, however, on intact $p16^{INK4a}$ and p38 MAPK for senescence induction (Wang et al 2002; Brookes et al 2002).

6.2 The requirement for p38 MAPK in RUNX1 and RUNX1-ETO induced senescence in Hs68 cells

Inactivation of p38 MAPK by the inhibitor SB203580 or dominant-negative mutants of MKK3 and MKK6 at least partially rescues senescence induced by $H\text{-}RAS^{V12}$ or replicative and oxidative stress-induced senescence (Wang et al 2002, Iwasa et al 2003). RUNX1-ETO and to a lesser extent RUNX1 activates p38 (Section 5.4, Chapter 5). Requirement for p38 in RUNX1 and RUNX1-ETO induced senescence was investigated using the p38 inhibitor (SB203580) to pharmacologically abrogate p38 function. If p38 activation is an important mediator of RUNX1 and or RUNX1-ETO induced senescence, its inhibition should prevent or delay onset of the phenotype.

RUNX1, RUNX1-ETO and H-RAS^{V12} were introduced to human neonatal foreskin fibroblasts via retroviral gene transfer and after puromycin selection cells were cultured in the presence or absence of 8μM SB203580. Cells containing the empty vector grew well in both the presence and absence of SB203580. By day 7 there was a substantial fraction of cells positive for SA-β-Gal in the RUNX1, RUNX1-ETO and H-RAS^{V12} expressing cells (Figure 6.1a). However, in the presence of the p38 MAPK inhibitor there was a significant increase in the growth rate of RUNX1-ETO expressing cells (RUNX1-ETO(SB) vs RUNX1-ETO(DMSO), day12 $p \leq 0.005$) (Figure 6.1a), and fewer cells had a flattened morphology or SA-β-Gal activity (Figure 1b). A similar effect was observed for H-RAS^{V12} expressing cells (RAS(SB) vs RAS(DMSO), day12 $p=0.01$) (Figure 6.1a) consistent with previous reports (Wang et al., 2002). Treatment of RUNX1 expressing cells with SB203580 also resulted in a partial rescue of the growth arrest (Figure 6.1a) (RUNX1(SB) vs RUNX1(DMSO), day 12 $p \leq 0.05$) and reduced senescence associated characteristics (flat, enlarged cells with SA-β-Gal activity) (Figure 6.1b), however the effect was clearly less pronounced relative to RUNX1-ETO expressing cells. These results indicate that RUNX1-ETO and RUNX1 are dependent at least to some extent on p38 MAPK to induce senescence in Hs68 fibroblasts. However, the growth rates of RUNX1-ETO, RUNX1 or H-RAS^{V12} in the presence of inhibitor were still lower than that of the control cells (Figure 6.1a).

a)

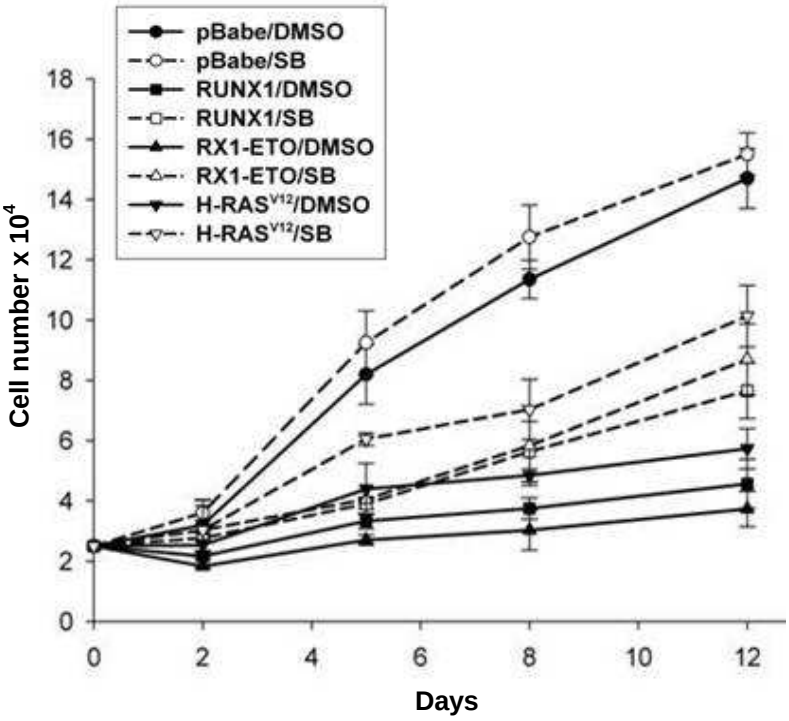

Figure 6.1 Inhibition of p38MAPK rescues RUNX1-ETO and RUNX1 induced senescence in Hs68 cells

Cells were transduced with retroviral vectors expressing RUNX1, RUNX1-ETO, H-Ras^{V12} or control vector (pBabe), selected in puromycin and then fed daily with fresh medium containing 8μM SB203580 (SB) or vehicle alone (DMSO) (a) Representative growth curves illustrating the effects of p38MAPK inhibitor (SB203580) on proliferation of RUNX1-ETO, RUNX1 or H-Ras^{V12} cells

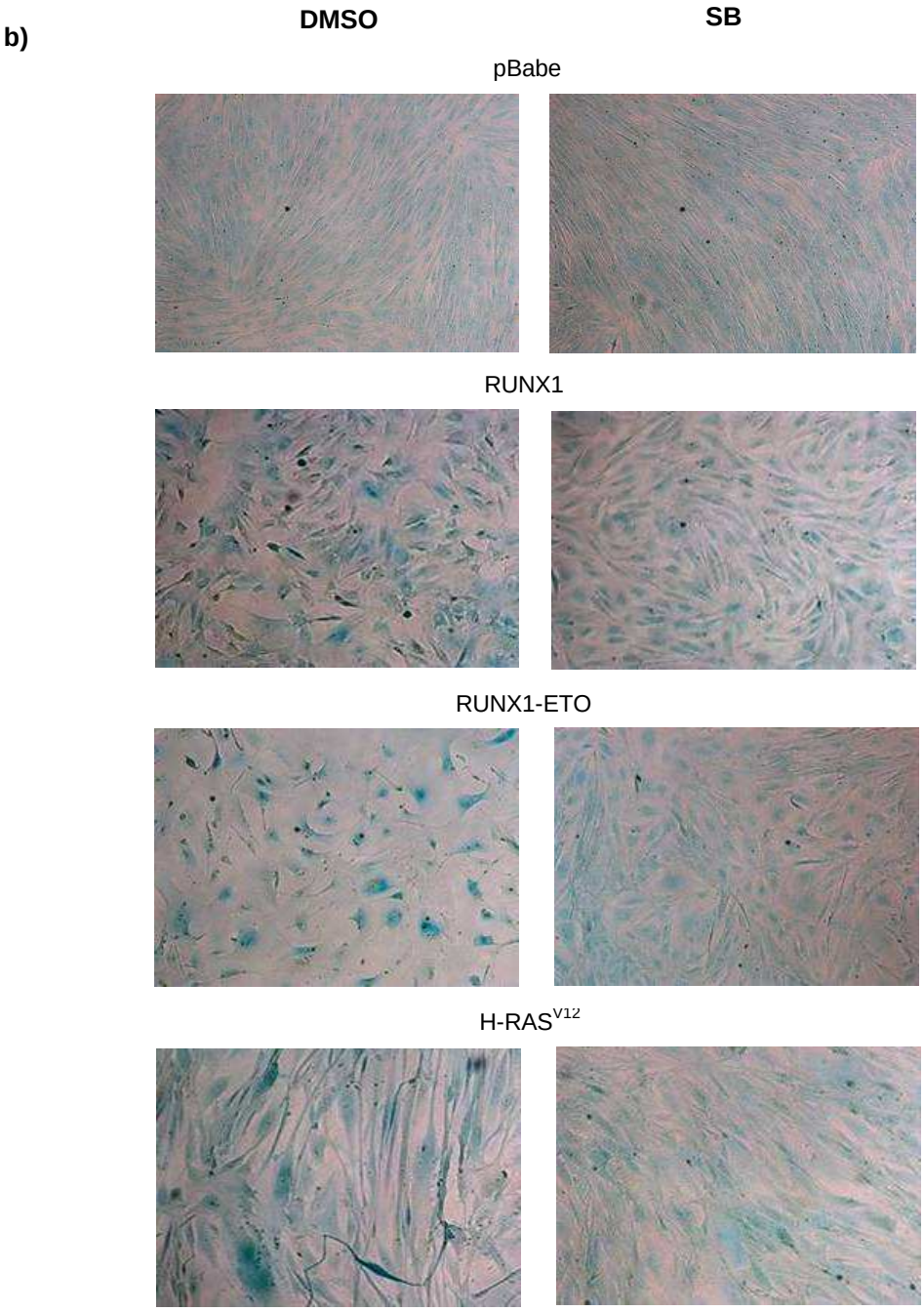

Figure 6.1 continued

(b) SA-β-Gal staining of SB203580-treated (SB) cells and mock-treated Hs68 cells (DMSO) containing control vector (pBabe), RUNX1, RUNX1-ETO or H-RAS^{V12} (H-RAS^{V12}) on day 9 post-selection

6.3 RUNX1 and RUNX1-ETO differ in their requirement for $p16^{INK4a}$ to induce senescence

Elevated $p16^{INK4a}$ levels are usually seen in human cells that have undergone either replicative senescence or H-RAS^{V12} induced senescence (Brookes et al 2004; Serrano et al 1997). While increased $p16^{INK4a}$ was found in cells transduced with RUNX1, no such effect was found in RUNX1-ETO induced senescence in Hs68 cells suggesting that a different mechanism may be involved. Therefore it was important to determine whether $p16^{INK4a}$ was required for RUNX1-ETO induced senescence. Leiden human diploid fibroblasts were originally isolated from a rare individual homozygous for an intragenic 19bp deletion in the second exon of CDKN2A, and therefore lacking functional $p16^{INK4a}$ but retaining $p14^{ARF}$ activity. It has been reported previously that Leiden cells are resistant to H-RAS^{V12} mediated senescence-like growth arrest (Brookes at al 2002) indicating that $p16^{INK4a}$ is absolutely required by oncogenic RAS.

To this end Leiden cells previously engineered to express an ecotropic virus receptor were transduced either with control vector (pBabe), RUNX1, RUNX1-ETO or H-RAS^{V12}. Interestingly, these p16-deficient cells underwent profound premature senescence when RUNX1-ETO was overexpressed. The senescent phenotype was confirmed by a cessation of proliferation (RUNX1 vs pBabe, day8, $p \leq 0.001$) (Figure 6.2a) morphologic alterations (increased cell volume, gross flattening) and SA-β-Gal staining (Figure 6.2b, c). Initially, RUNX1 and H-RAS^{V12} caused a moderate growth suppression but despite this, these cells continued to increase their numbers exponentially from day 6 onwards (RUNX1 vs RUNX1-ETO, day 9, $p=0.01$; H-RAS^{V12} vs RUNX1-ETO, day 9, $p \leq 0.005$) (Figure 6.2a) and displayed no SA-β-Gal activity at day 8 (Figure 6.2b). All the ectopic proteins were readily expressed as determined by western blot analysis (Figure 6.2c). It seems that RUNX1 and H-RAS^{V12} induced senescence share a requirement for $p16^{INK4a}$ but RUNX1-ETO can induce senescence even in the absence of $p16^{INK4a}$.

a)

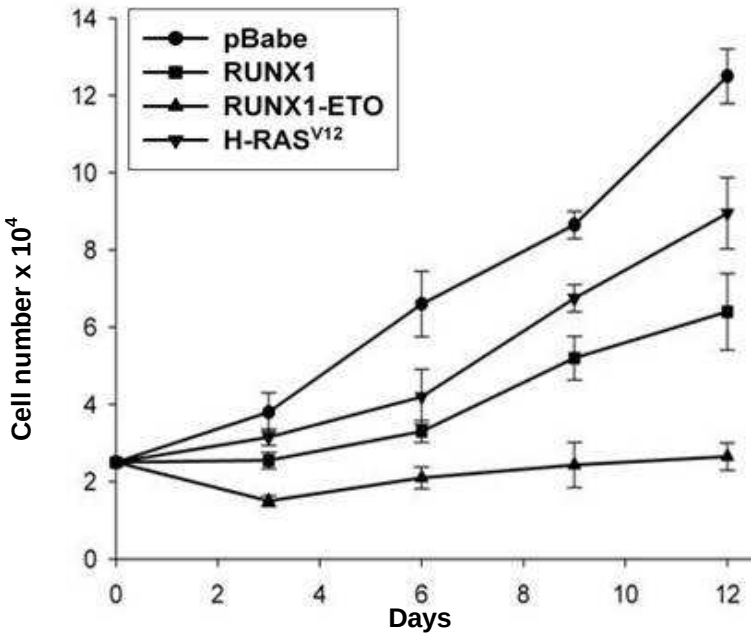

Figure 6.2 RUNX1-ETO does not require p16 to induce senescence in contrast with RUNX1

Leiden cells were transduced with retroviral vectors expressing RUNX1, RUNX1-ETO, H-Ras^{V12} or control vector (pBabe) and selected for 4 days in puromycin (a) Representative growth curves of cells containing control vector (pBabe), RUNX1, RUNX1-ETO or H-Ras^{V12}. Similar results were observed in three independent experiments and each time point was determined in triplicate

b)

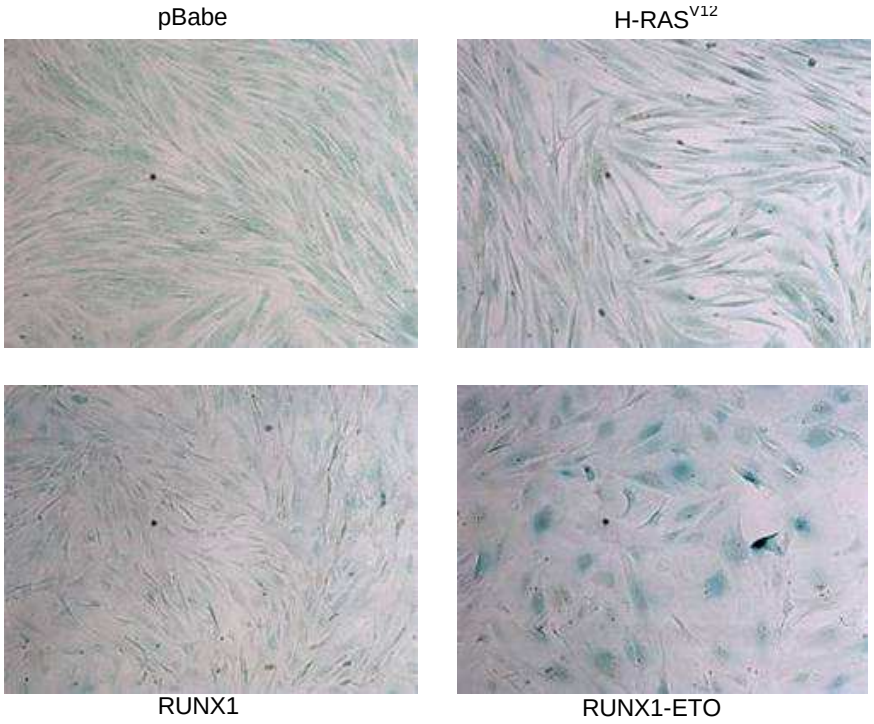

c)

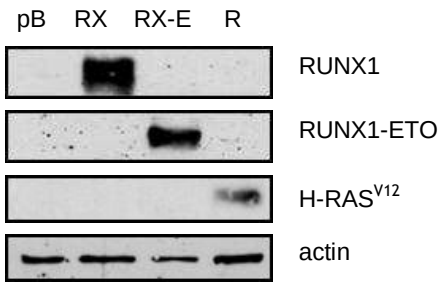

Figure 6.2 continued

(b) SA-β-Gal staining of Leiden cells containing control vector (pBabe), RUNX1, RUNX1-ETO or H-Ras^{V12} (day 8 post-selection)

(c) Western blot analysis of RUNX1 (anti-AML1/Runx1, 3900, Active Motif), RUNX1-ETO (anti-RUNX1-ETO from Dr. Scott Hiebert) or H-Ras^{V12} (anti-H-ras, Ab-1, Oncogene Research) expression in Leiden cells containing control vector (pB), RUNX1 (RX), RUNX1-ETO (RX-E) or H-Ras^{V12} (R) (day 7 post-selection)

6.4 The requirement for p53 in RUNX1 and RUNX1-ETO induced senescence in human primary fibroblasts

Given that $p16^{INK4a}$ was not required to mediate senescence-like growth arrest in response to RUNX1-ETO but p53 expression was profoundly upregulated under the same conditions it was of interest to determine the functional role of p53 during RUNX1-ETO induced senescence in human fibroblasts. To this end Hs68 cell were transduced with HPV16 E6 oncoprotein (E6), which acts to downregulate p53, or empty vector (LXSN). It was not possible to select these cells on the basis of neomycin resistance as this was already a property conferred on the cells through neomycin selection for the ecotropic virus receptor. However, cultures transduced with HPV16 E6 showed an obvious growth advantage over cultures transduced with the empty vector (E6 vs LXSN, day 7, $p \leq 0.05$) (Figure 6.3a). After 4 days neomycin pseudo-selection, these cells were subsequently infected with retroviruses encoding RUNX1, RUNX1-ETO, H-RAS^{V12} or control vector (pBabe) and selected with puromycin. The capability of HPV16 E6 to downregulate p53 was confirmed by western blot analysis (Figure 6.3b). Consistent with previous reports [Wei et al., 2001; Bischof et al., 2005], H-RAS^{V12} did not require p53 to induce senescence in human primary fibroblasts as shown by growth curves (H-RAS^{V12} (E6) vs H-RAS^{V12} (LXSN), day 7, $p=0.5$) (Figure 6.3a) and SA-β-Gal staining (Figure 6.3b). RUNX1 induced a growth arrest that was partially rescued by E6 but only at day 10 was this statistically significant (RUNX1(E6) vs RUNX1(LXSN), day 10, $p=0.05$) (Figure 6.3a) and some flat and enlarged cells remained that exhibited the SA-β-Gal marker (Figure 6.3c). In contrast, proliferation of RUNX1-ETO expressing cells was substantially rescued by E6 (RUNX1-ETO(E6) vs RUNX1-ETO(LXSN), day 7, $p \leq 0.01$) (Figure 6.3a) and SA-β-Gal staining as well as the characteristic flattened cell morphology were dramatically reduced (Figure 6.3c). These data suggest that RUNX1-ETO induced senescence has a greater dependence on p53 than RUNX1.

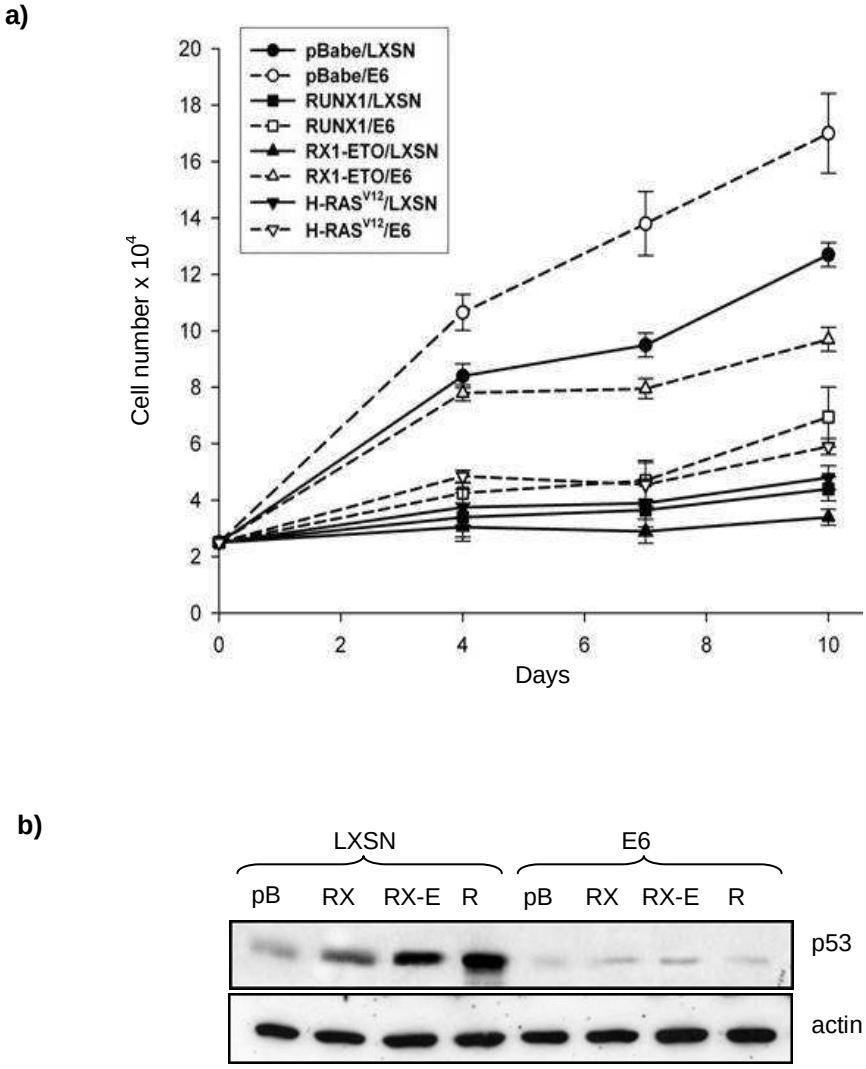

Figure 6.3 HPV16 E6 abrogates RUNX1-ETO induced senescence but only partially abrogates RUNX1 senescence in Hs68 cells

Hs68 cells containing HPV16 E6 (E6) or control vector (LXSN) were cotransduced with retroviral vectors expressing RUNX1, RUNX1-ETO, H-RasV12 or control vector (pBabe). (a) Representative growth curves of cells containing HPV16 E6 (E6) or control vector (LXSN) cotransduced with RUNX1, RUNX1-ETO or H-RAS^{V12}. Similar results were observed in three independent experiments and each time point was determined in triplicate. (b) Western Blot analysis of p53 expression (anti-p53, sc-126, Santa Cruz) in the indicated populations of cells containing control vector (pB), RUNX1 (RX), RUNX1-ETO (RX-E) or H-RAS^{V12} (R) on day 7 post-selection

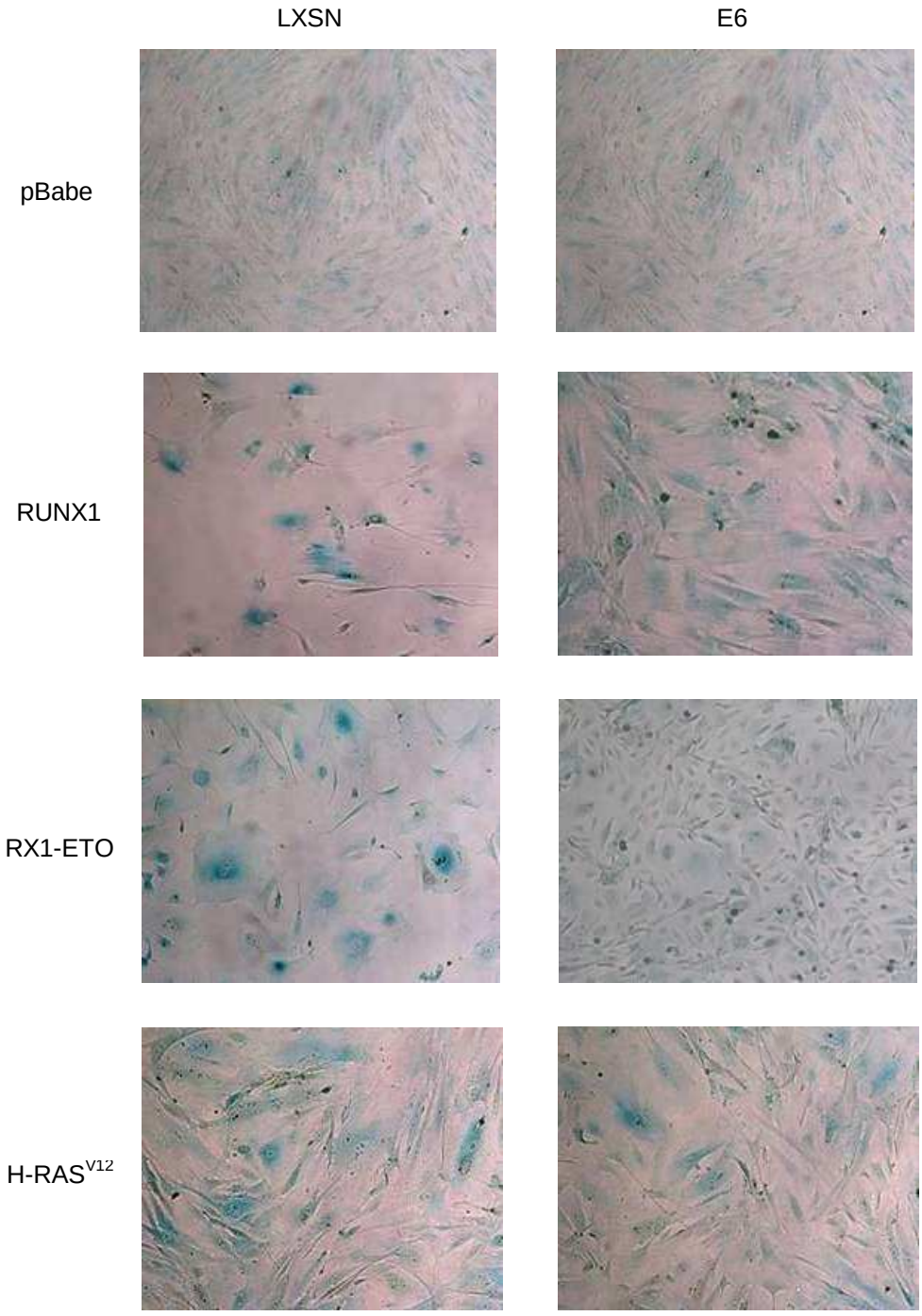

Figure 6.3 continued

(c) SA-β-Gal staining of cells containing HPV16 E6 (E6) or control vector (LXSN) cotransduced with RUNX1, RUNX1-ETO, H-RAS^{V12} or control vector (pBabe) (day 8 post-selection)

6.5 RUNX1-ETO fails to induce senescence in p53 deficient murine embryonic fibroblasts

It has been shown in this laboratory previously that p53 is a critical regulator of RUNX1 induced senescence in MEFs since RUNX1 pro-oncogenic potential can be revealed on p53 null genetic background (Wotton et al 2004). Unlike RUNX1, RUNX1-ETO displayed obvious p53 dependence in human fibroblasts Hs68, hence it was interesting to see if the p53 pathway is also relevant in murine cell.

To determine whether p53 is required for RUNX1-ETO induced senescence in murine primary cells, $p53^{-/-}$ MEFs were infected with retroviruses containing RUNX1-ETO, RUNX1 or empty vector (pBabe). RUNX1 and RUNX1-ETO transduced cells expressed detectable levels of transgene (Figure 6.4a), accumulated exponentially and had comparable growth rates, although RUNX1 expressing cells grew slightly better (RUNX1 vs RUNX1-ETO, day 9, $p \leq 0.05$) (Figure 6.4b). The populations of RUNX1-ETO and RUNX1 cells were quite heterogeneous but no flattened and enlarged cells indicative of senescence were observed. As reported previously (Wotton et al 2004), RUNX1 expressing p53 null MEFs can show two distinct morphological phenomena i) a shift to an epithelial-like morphology (Figure 6.4c) and ii) the sporadic appearance of transformation foci (Figure 6.4d). Similar changes were not observed in RUNX1-ETO expressing or empty vector control cells (Figure 6.4c, d). Interestingly, p53 null primary MEFs expressing RUNX1-ETO morphologically resembled immortalised 3T3 cells and were quite distinct from either RUNX1 expressing or control cell populations (Figure 6.4c, d). These results show that RUNX1-ETO requires p53 in MEFs and highlights the importance of p53 in RUNX1-ETO induced senescence.

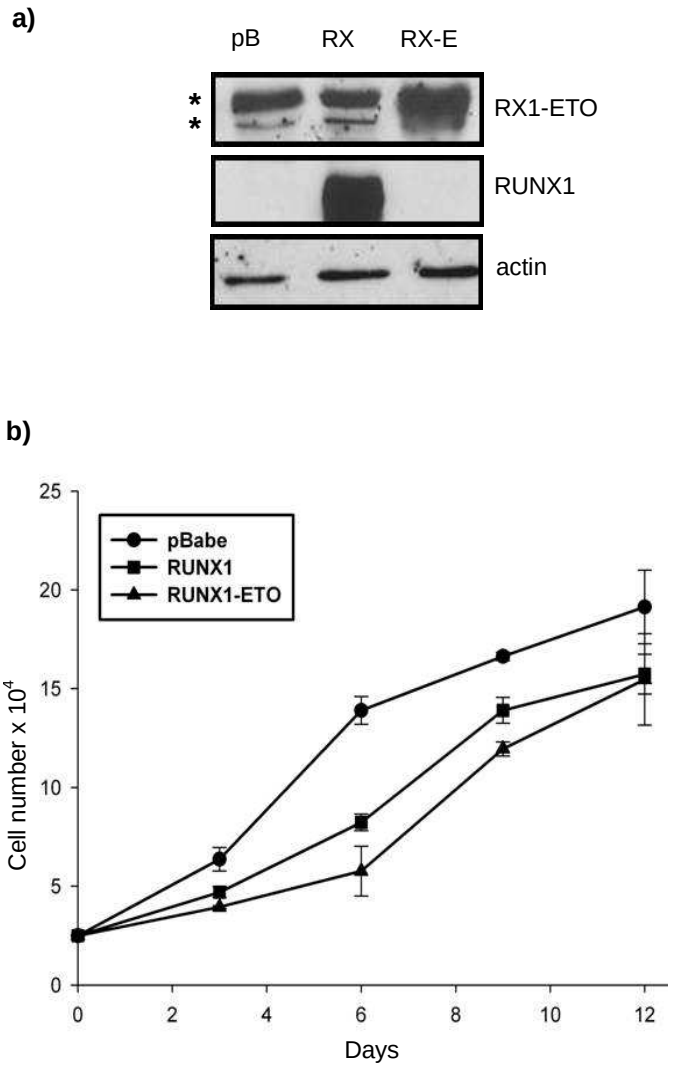

Figure 6.4 p53null MEFs are resistant to RUNX1-ETO induced senescence

$p53^{-/-}$ MEFs were transduced with retroviral vectors expressing RUNX1, RUNX1-ETO, H-Ras^{V12} or control vector (pBabe) and selected for 4 days in puromycin (a) Western blot analysis of RUNX1 (anti-AML1/Runx1, 3900, Active Motif), RUNX1-ETO (anti-RUNX1-ETO from Dr. Scott Hiebert) expression in $p53^{-/-}$ MEFs containing control vector (pB), RUNX1 (RX) or RUNX1-ETO (RX-E) (day 7 post-selection); * - non-specific bands (b) Representative growth curves of cells containing control vector (pBabe), RUNX1, RUNX1-ETO or H-Ras^{V12}. Similar results were observed in three independent experiments and each time point was determined in triplicate

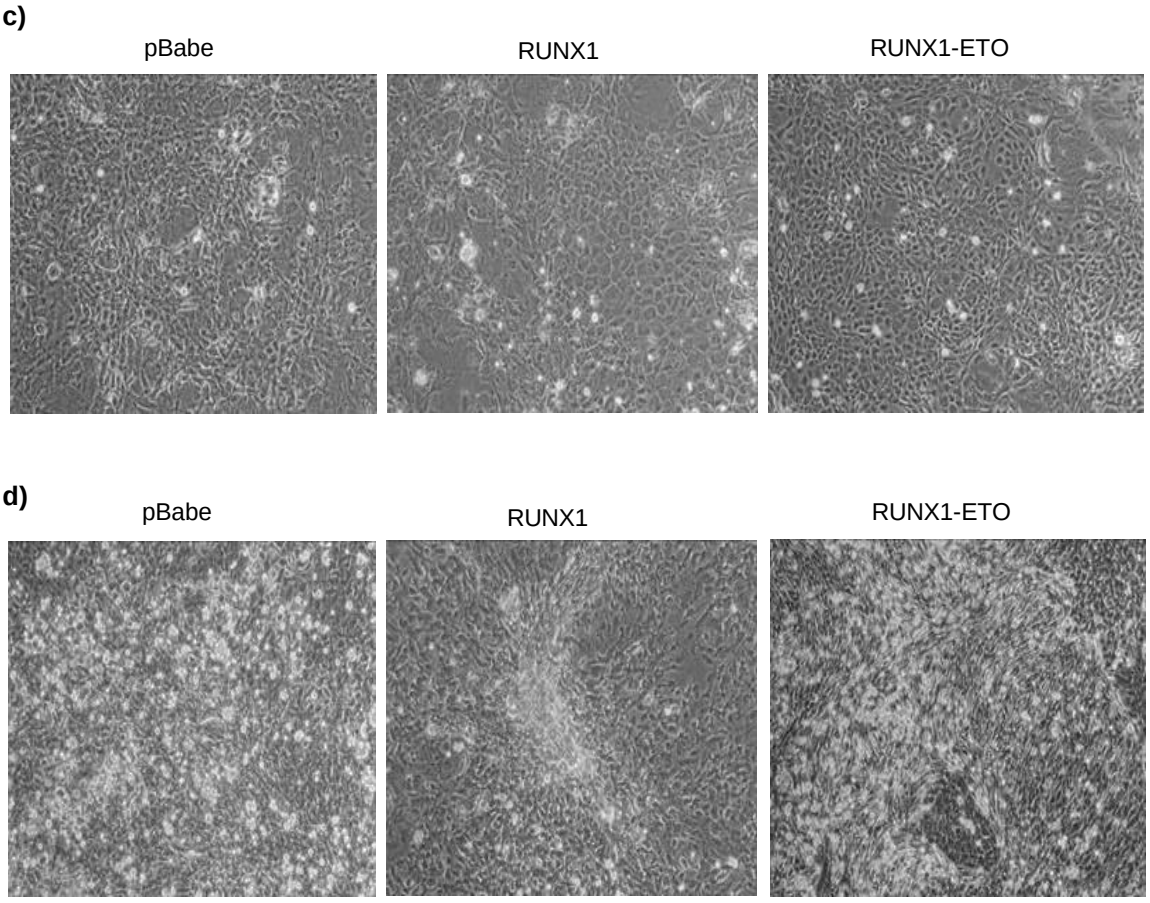

Figure 6.4 continued

(c) Phase-contrast photomicrographs of $p53^{-/-}$ MEFs containing empty vector (pBabe), RUNX1 or RUNX1-ETO taken on day 7 post-selection (d) Microscopic photographs of $p53^{-/-}$ MEFs containing empty vector (pBabe), RUNX1 or RUNX1-ETO taken on day 20 post-selection

6.6 Discussion

These investigations into the requirement for $p16^{INK4a}$, p53 and p38 kinase in RUNX1 and RUNX1-ETO induced senescence have revealed significant differences in the pathways executing these cellular programmes in primary fibroblasts. The exciting finding was that RUNX1-ETO, in contrast to RUNX1 and $H\text{-}RAS^{V12}$ could drive premature senescence in the absence of $p16^{INK4a}$. Very few oncogenes bypass $p16^{INK4a}$ signalling in primary human cells to provoke a senescence response. One example is RAF in human mammary epithelial cells (Olsen et al 2002). Further analysis identified p53 and p38 MAPK as important signal transducers in RUNX1-ETO induced senescence since their inactivation either by HPV16 E6 (p53) or the selective inhibitor of p38 MAPK SB203580, substantially rescued the senescent phenotype. In both cases, however, it was not a complete effect and rescued RUNX1-ETO expressing cells did not proliferate as well as control cells. Given that HPV16 E6 profoundly downregulated p53 as determined by western blot it seems unlikely that it was due to incomplete p53 ablation and it is possible that there are other cooperating factors that regulate growth arrest during RUNX1-ETO induced senescence. The evidence supporting an important role for p53 in RUNX1-ETO induced senescence was provided by the lack of premature senescence in p53 null primary MEFs. In this system, RUNX1-ETO expressing cells proliferated slower than control cells and in contrast to RUNX1 expressing cells displayed no signs of foci formation, indicating that RUNX1-ETO requires additional events to become oncogenic. Notably, while substantial proportion of RUNX1 expressing p53 null MEFs aquired epitheloid morphology, RUNX1-ETO cells remained fibroblastic. As far as p38 MAPK is concerned it should be stressed that the inhibitor used in this study inhibits only the α and β isoforms of p38, therefore the two other isoforms γ and δ may account for the partial complementary effect. Also, because the inhibitor was added to cultures 4 days after the actual viral transduction, irreversible changes refractory to the effects of the inhibitor might have occurred by this time. In contrast to RUNX1-ETO, RUNX1 was found to require $p16^{INK4a}$ since it failed to drive premature senescence in p16 deficient Leiden human fibroblasts and showed a lesser response to p53 inactivation in Hs68 fibroblasts. Interestingly, RUNX1 induced senescence also relies on p38 MAPK since its inhibition with SB203580 partially

rescues senescence-like growth arrest. Taken together these data identify p38 MAPK as a common signalling pathway in RUNX1 and RUNX1-ETO induced senescence in human fibroblasts consistent with its universal role in various types of senescence. On the other hand differential requirements for $p16^{INK4a}$ and p53 by RUNX and RUNX1-ETO have been identified. Unlike RUNX1-ETO induced senescence which is p53 dependent, RUNX1 induced senescence predominantly requires $p16^{INK4a}$.

Chapter 7

7 General discussion and future directions

Currently cellular senescence is regarded as an important anti-cancer mechanism that restricts uncontrolled proliferation of cells and prevents neoplastic transformation *in vitro* and *in vivo* and is recognised as a tumour suppressor mechanism that is equally important as apoptosis and governed by the p53 and pRb pathways. While its importance is beyond doubt, there are many key questions yet to be answered:

- Why certain oncogenes induce senescence while others induce apoptosis, is this due to the strength and/or duration of a signal or perhaps to the cell type and specificity of oncogenic signal or both?

- How homogeneous is this response in different cellular contexts?

- Which features of senescent phenotype are of fundamental importance?

- How universal is DNA damage signalling or chromatin remodelling in the context of senescence and do they represent cause or effect?

- What are the fundamental mechanisms leading to senescence and why do they appear to differ in mouse and human cells?

In this study I have demonstrated for the first time that RUNX1 induces senescence in human primary fibroblasts and that RUNX1/CBFβ derived oncogenic fusion proteins associated with human leukaemias such as: RUNX1-ETO and CBFβ -MYH11 also retain the potential to drive premature senescence. Further characterisation of RUNX1 and RUNX1-ETO induced senescence has not only revealed interesting similarities and differences with regard to the signalling pathways underlying these senescence programmes, but also provided evidence that these senescent phenotypes are distinct from classical oncogene induced senescence as exemplified by RAS. This study has shed new light on central aspects of cellular senescence and demonstrates how complex and heterogeneous this important biological programme can be.

Previous studies in this laboratory showed that inducible RUNX1-ER (RUNX1 fused to oestrogen receptor) is a potent inducer of premature senescence in MEFs (Wotton et al 2004). The disruption of p53 allowed bypass of senescence and promoted increased survival and partial transformation (Wotton et al 2004). Interestingly, the promotion of senescence by RUNX1 was seen in the presence and absence of inducer (tamoxifen) and some RUNX1-ER protein was present in the nucleus even without treatment with tamoxifen suggesting that the senescence response was either mediated by protein-protein interactions or that there was a leakiness in the system sufficient to induce the phenotype (Wotton et al 2004). Therefore it was important to dissect RUNX1 functional requirements for induction of premature senescence. I addressed this issue by testing the ability of DNA and CBFß binding mutants of RUNX1 to induce senescence. Unlike RUNX1, ectopic expression of these constructs failed to trigger a senescence response, providing evidence that RUNX1 absolutely requires both intact DNA and CBFß binding activity and indicating that high affinity binding to the target DNA sequences in the nucleus is probably critical. Importantly, I have found that the ability of RUNX1 to induce senescence seems to be a universal feature of RUNX1 overexpression since RUNX1 also induces senescence in human primary fibroblasts Hs68. As found in MEFs, neither the DNA binding mutant nor the CBFß interaction mutant was able to induce senescence in human cells. Further investigations into functional domains of RUNX1, revealed that RUNX1 relies on its C-terminal domain to induce senescence in Hs68 fibroblasts as shown by comparison with AML1a, a truncated isoform of RUNX1. Given that the C-terminal portion of RUNX1 contains both a transactivation domain and a repression domain it remains unclear which mode of action is more important once RUNX1 has bound to the DNA target sequences. This could be examined by testing the ability of RUNX1 fused to constitutive transactivation domain such as VP16 to induce senescence in primary cells (Cao et al 1998). Conversely, it was also of particular interest to examine effects of RUNX1-ETO overexpression since RUNX1-ETO, like AML1a, not only lacks the RUNX1 C-terminal domain but is also thought to act as a constitutive repressor of wild type RUNX1.

The finding that RUNX1-ETO induced senescence in murine and human primary fibroblasts more potently than RUNX1 itself was exciting and surprising since it is reported to repress the ARF promoter (Linggi et al 2002). This not only suggests that, in contrast to RUNX1, ARF is dispensable for RUNX1-ETO induced senescence in MEFs, but also indicated that RUNX1-ETO oncoprotein may have additional functions independent of RUNX1 that may be attributed to its fusion partner protein, ETO. Indeed, overexpression of the mutant of RUNX1-ETO containing the deletion of ETO corepressor binding sites (RUNX1-ETOΔ469) failed to induce senescence, suggesting that RUNX1-ETO mediated senescence results from repression of important target genes whereas it is not clear whether RUNX1 induced senescence relies on transcriptional activation and/or repression. One explanation may be that RUNX1 functions as a repressor whereas RUNX1-ETO acts as a super-repressor and therefore induces a more profound senescent phenotype. If this was true the signalling pathways underlying RUNX1 and RUNX1-ETO induced senescence would be commonly engaged.

The discovery that the RUNX1-ETO oncoprotein drives premature senescence in murine and human fibroblasts may have more general clinical implications. The relevance of senescence in haematopoietic tissues and cancer is an area of growing interest (Braig et al 2005; Wu et al 2007). Given that the RUNX1-ETO fusion protein, a product of t(8;21) translocation in AML, is not sufficient to cause leukaemia alone in various experimental models (Yuan et al 2001; Higuchi et al., 2002, Peterson et al., 2007), one possibility is that it initially triggers cellular senescence, a cancer fail-safe mechanism which needs to be overcome to induce full blown malignancy. Interestingly, a truncated form of RUNX1-ETO (552 amino acids) with a deleted C-terminal NcoR/SMRT-interacting region [Yan et al 2004] as well as an alternatively spliced AML-ETO9a isoform (572 amino acids) that has been recently identified in AML patients (Yan et al 2006) both strongly induce leukaemogenesis in mice. These two leukaemogenic forms of RUNX1-ETO show remarkable similarity to RUNX1-ETOΔ469 which, in contrast to RUNX1-ETO, failed to induce senescence in Hs68 cells. Hence, it is tempting to speculate that these two RUNX1-ETO isoforms are highly leukaemogenic because

they are intrinsically capable of overcoming senescence. In view of these observations, it was interesting to discover that another leukaemia-related fusion oncoprotein CBFß-MYH11 also induced senescence in human primary cells, although less potently than RUNX1-ETO. Importantly, recent studies show collaboration between RUNX1-ETO and CBFß-MYH11 oncoproteins and genetic inactivation of senescence mediators such as $p19^{ARF}$, $p16^{INK4a}$ and $p21^{WAF1}$ in murine *in vivo* models of leukaemogenesis (Peterson et al 2007; Moreno-Miralles et al 2005; Yang et al 2002). However, the TEL-RUNX1 oncoprotein which is associated with B-ALL, did not induce senescence in Hs68 cells suggesting that TEL-RUNX1 functions differently from RUNX1-ETO and CBFß-MYH1 and/or it requires higher levels of expression to trigger cellular senescence in this system. This may also suggest an important loss-of-function event of TEL-RUNX1, intracellular misdirection or steric hindrance at crucial target gene promoters. It will be important to explore these hypotheses by analysis of deletion mutants of TEL-RUNX1 lacking domains of TEL to look for rescue of the ability to induce senescence.

The comparative characterisation of RUNX1, RUNX1-ETO and $H\text{-}RAS^{V12}$ induced senescence in human primary fibroblasts revealed interesting differences and similarities in the phenotypes and pathways regulating these cellular programmes (Table 7.1). From the analysis of the expression of growth inhibitory proteins it became apparent that RUNX1 but not RUNX1-ETO expressing cells had elevated levels of $p16^{INK4a}$ (Chapter 5, Section 5.3). The requirement for $p16^{INK4a}$ was confirmed by the lack of senescence induction by RUNX1 in p16null Leiden human fibroblasts.

	pBABE	RUNX1	RUNX1-ETO	RAS
P16	-	++	+	+++
P53	+/-	+	+++	+++
P21	+/-	++	+	+++
P14	-	-	-	-
Phospho-p38	-	+	+++	+++
Cell cycle arrest	-	G1>G2M	G1<G2/M	G1≥G2M
ROS	-	+	+++	+++
Hyper-proliferation	-	-	-	+
γ-H2AX foci	-	-	-	+
SAHF	-	-	-	+
PML bodies accumulation	-	-	+	+
Senescence - asscociated ß-gal	-	+	+	+

Table 7.1 Comparison of known hallmarks of senescence

However, RUNX1-ETO, unlike RUNX1 or H-RAS^{V12}, was able to drive profound premature senescence even in the absence of p16^{INK4a} indicating that different pathways are required by RUNX1 and RUNX1-ETO (Chapter 6, Section 6.3). Interestingly, it has been recently reported that p16^{INK4a} deficiency does not promote RUNX1-ETO associated leukaemia in mice (Ko et al 2008). In contrast to RUNX1, RUNX1-ETO strongly upregulated p53 and inactivation of p53 by HPV16 E6 substantially supressed RUNX1-ETO but not the RUNX1 senescent phenotype, re-emphasising the fact that RUNX1 and RUNX1-ETO operate via distinct routes (Chapter 5, Section 5.3 and Chapter 6, section 6.4). RUNX1-ETO also induces a p53-dependent senescence in primary MEFs (Chapter 6, Section 6.5). This suggests that p53 may play an important role in RUNX1-ETO driven tumourigenesis. While p53 is central to the process *in vitro*, the mechanism by which senescence pathways are overcome in leukaemias is as yet unknown. The mutations of tumour suppressor genes are common events in human haematological malignancies. Mutations of p53 have been found in haematological malignant diseases, but the frequency of theses alterations is much lower than in solid tumours (14% vs >50%) (Krug et al 2002). The p53 gene is not commonly mutated in primary t(8;21) AML (Imamura et al 1994; Krug et al 2002) but is frequently lost, mutated or modulated in t(8;21) cell lines such as Kasumi-1 and SKNO (Banker et al 1998a; Banker et al 1998b) and mutations of p53 are commonly associated with therapy related AML/MDS (Christiansen et al 2001; Fenaux et al 1992; Horiike et al 1999; Jonveaux et al 1991; Lai et al 1995). Loss of p53 function has been also linked to drug resistance and correlates with poor prognosis in AML patients (Melo et al 2002; Nakano et al 2000). Paradoxically, the expression of p21^{WAF1}, the downstream effector of p53 was dramatically increased in RUNX1 but not RUNX1-ETO expressing Hs68 fibroblasts (Chapter 5, Section 5.3). Given that p21^{WAF} is a well known direct target of RUNX1 (Lutterbach et al 2000) it is possible that RUNX1 and RUNX1-ETO exert opposing direct effects on the p21^{WAF1} promoter in this cell system and it will be important to investigate the requirement for p21^{WAF1} further. Given that p21^{WAF1} was not completely downregulated in RUNX1-ETO expressing cells and that the p21^{WAF1} pathway has been demonstrated to be involved in blocking leukaemogenesis induced by RUNX1-ETO in mice (Paterson et al 2007) it would be interesting to evaluate the role of p21^{WAF1} in senescence either by knocking-

down its expression by shRNA or employing $p21^{-/-}$ MEFs (Pantoja et al 1999) or $p21^{-/-}$ human fibroblasts (Wei et al 2001). Consistent with a dominant role of p53 in RUNX1-ETO induced senescence, the ectopic expression of p53 alone partially recapitulates the senescent phenotype in Hs68 cells, causing a profound growth arrest, although with less pronounced alterations to cellular morphology and weaker SA-β-Gal staining compared to RUNX1-ETO (Chapter 5, Section 5.8), indicating that RUNX1-ETO induces senescence via p53 yet apparently modulates its signalling pathway. Therefore, it was important to find out how p53 is upregulated. ARF-MDM2-p53 is a well established regulatory pathway whereby ARF is thought to antagonise MDM2-mediated ubiquitination of p53 through translocation of MDM2 to the nucleolus, thereby stabilising p53 (Lowe and Sherr, 2003). It was of particular interest to determine whether $p14^{ARF}$ is affected either by RUNX1 or RUNX1-ETO expression in Hs68 cells since RUNX1 and RUNX1-ETO have been reported to have opposing effects on this gene locus in primary MEFs (Linggi et al 2002). Intriguingly $p14^{ARF}$ was not upregulated neither by RUNX1-ETO nor RUNX1 (Chapter 5, Section 5.3). This observation supports the notion that $p14^{ARF}$ is not strongly implicated in cellular senescence in human cells, except for its crucial role in E2F induced senescence (Dimri et al 2000). Another molecule that could potentially stabilise p53 is PML. PML is an important component of senescence pathways and has been demonstrated to regulate p53 via several post-translational modifications (Bischof et al 2002; Ferbeyre et al 2000, Pearson et al 2000). It has been also reported to stabilize p53 by sequestering MDM2 to the nucleolus (Bernardi et al 2004). Fluorescence microscopy has revealed increased size of PML bodies (also known as PODs for PML oncogenic domains) in RUNX1-ETO but not RUNX1 expressing cells suggesting that PML may indeed be at least partially responsible for increased p53 expression and vice versa consistent with the notion that PML is a downstream target of p53 (DeStanchina et al 2004) (Chapter 5, Section 5.6). It will be important to validate this finding by overexpressing RUNX1-ETO in human diploid fibroblasts containing shRNA for PML. Another growing body of evidence suggests that p38 MAPK can contribute to p53 regulation (Bulavin et al., 1999; (Huang et al 1999); Wang et al 2002, Sun et al 2007). Indeed, levels of the activated form of p38, phospho-p38, were significantly elevated in RUNX1-ETO or $H\text{-}RAS^{V12}$ expressing cells (Chapter 5, Section 5.4) as previously reported (Wang et al

2002) and correlated well with the induction of p53. Furthermore, pharmacological inhibition of the p38 MAPK pathway rescued the senescent phenotype induced by RUNX1-ETO and therefore implicated p38 as a critical mediator of RUNX1-ETO induced senescence in Hs68 cells (Chapter 6, Section 6.3). It will be important to see whether inhibition of p38 MAPK itself would prevent p53 accumulation, confirming the sequential mode of action. The involvement of p38 MAPK in t(8;21) associated AML has not been investigated but it seems possible that the disruption of p38 could explain the lack of p53 mutations in primary t(8;21) AML, assuming that the p38-p53 activating pathway is operative in myeloid cells. A weak upregulation of p38 kinase has also been identified in RUNX1 expressing cells and its inhibition partially rescued the senescence-like growth arrest suggesting that p38 MAPK is commonly engaged by RUNX1 and RUNX1-ETO consistent with its established role in various types of senescence (Ischikawa et al 2003; Wang et al 2002). Given that p38 has been also reported to regulate expression of $p16^{INK4a}$ during senescence through stabilisation of its mRNA (Wang et al 2002) it is possible that it may contribute to the increase in $p16^{INK4a}$ in RUNX1 induced senescent cells. However, other not necessarily mutually exclusive mechanisms may be responsible for $p16^{INK4a}$ upregulation by RUNX1. It will be interesting to see if regulators of $p16^{INK4a}$ such as ETS, ID (Itahana et al 2001) or polycomb INK4a repressors e.g. BMI1 or CBX7 (Alani et al 2001; Bracken et al 2007; Gil et al 2003; Ohtani et al 2001) are affected in RUNX1 induced senescence. Importantly inactivation of p16 and p15 is common in human leukaemias. P15 and p16 loci are frequently found to be deleted in acute lymphoblastic leukaemia (>30%), whereas hypermethylation of the promoter region of p16 and p15 is particularly prevalent in acute myeloid leukaemia (40-80%) (Drexler 1998)

A further consideration given the involvement of p38 MAPK is the question of how RUNX1 and in particular RUNX1-ETO achieve the activation of p38 MAPK? Gadd45α which contains *bona fide* RUNX DNA binding sites adjacent to p53 sites in intron 3 is a potential link as it has been demonstrated to be required for p38 activation in the presence of $H\text{-}RAS^{V12}$ (Bulavin et al 2003). It is possible that

RUNX1-ETO which has been previously reported to activate some genes such as bcl-2 (Klampfer et al 1996) may stimulate the expression of Gadd45α more effectively than RUNX1 which would result in profound p38 activation. While the role of Gadd45α remains to be investigated, increased ROS levels were found in RUNX1 and RUNX1-ETO expressing cells (Chapter 5, section 5.5) which could also be responsible for p38 activation.

Reactive oxygen species have not only been shown to be critical mediators of H-RAS^{V12} induced senescence (Lee et al 1999) but have also been tightly linked to the activation of p38 MAPK (Dolado et al 2007; Iwasa et al 2003; Nicke et al 2005; Zdanov et al 2006). The induction of ROS by RUNX1 was much weaker compared to RUNX1-ETO and, importantly, ROS levels seem to parallel the levels of phospho-p38 in the senescent human fibroblasts Hs68 (Chapter 5, Section 5.4 and 5.5). Therefore, one can speculate that ROS may play an important role especially in RUNX1-ETO induced senescence where the levels of ROS were even higher than these observed in H-RAS^{V12} expressing cells. This, however, would need to be tested directly either by culturing cells in low oxygen tension or in the presence of antioxidant such as NAC (N-acetyl cystein). Recently, it has been shown that increased levels of ROS are associated with the formation of the activated, catalytic fragment PKCδ (protein kinase C δ), which, in turn, seems to lead to further production of ROS and irreversible senescence (Takahashi et al 2006). Activation of PKCδ causes profound reduction of WARTS (WTS/large tumour-suppressor 1 mitotic kinase) kinase which is required for cytokinesis and subsequent G2M arrest (Takahashi et al 2006). The role of PKCδ and WARTS in RUNX1-ETO induced senescence is of particular interest given that overexpression of RUNX1-ETO causes cell cycle arrest with a strong G2M component and is associated with high ROS levels. Reactive oxygen species have been also demonstrated to oxidise and inactivate Cdc25 phosphatases and therefore may control the cell cycle directly (Nilsson and Hoffmann 2000). Cdc25 phosphatases are responsible for dephosphorylation of pThr14 and pTyr15 and thereby trigger the activation of the Cdk/cyclin complexes which are required for the progression of cell cycle, however high ROS levels interfere with the

function of Cdc25 phosphatases and may cause growth arrest (Nilsson and Hoffmann 2000). Cdc25A controls G1/S transition by its activity on the Cdk2/cyclin E and Cdk2/cyclin A complexes, whereas Cdc25B and Cdc25C are primarly required for entry into mitosis (Boutros et al 2007). Interestingly, a contrasting result with respect to ROS has been recently reported, where overexpression of RUNX1-ETO in $CD34^{+}$ umbilical blood early progenitor cells did not cause the accumulation of ROS (Krejci et al 2008). This may, of course, reflect cell-type specific differences, however there was a major difference in that the ROS levels in senescent fibroblasts were measured on day 11 after transduction (Chapter 5, Section 5.5) whereas Krejci at al measured ROS five weeks after transduction. Thus it is conceivable that ROS induction by RUNX1-ETO is an early event. If ROS is demonstrated to be an absolute requirement for RUNX1-ETO or RUNX1 induced senescence the question arises as to how ROS are generated. Notably, none of the studies published so far has clearly defined the origin of ROS generation in senescence or why it is generated in the first place. It is still not known if this response is a mitochondrial specific ROS production or whether ROS are generated by, for instance, NADPH oxidase. It is clear that ROS generation is intimately associated with the senescent phenotype, however the details of this association still need to be unravelled. Due to its unspecific nature it is unlikely that ROS could have evolved as a specific signalling pathway in senescence. In RAS induced senescence, one potential candidate responsible for high ROS levels is 5-lipoxygenase (5LO). This enzyme generates ROS in the process of its enzymatic conversion of arachidonic acid to leukotrienes. In primary cells overexpressing RAS, 5LO activity increases (Catalano et al 2005) and ectopic expression of 5LO promotes senescence in a redox dependent, p53/p21 mediated fashion (Catalano et al 2005). The involvement of this enzyme in other routes to senescence seems worthy of further investigation.

DNA damage signalling has been recently proposed to be an important mechanism by which senescence occurs. Oncogenes such as $H\text{-}RAS^{V12}$ have been shown to trigger a classical DNA damage response mediated by the ATM/ATR and Chk1/Chk2 proteins which cause the post-translational stabilisation of p53

through phosphorylation (DiMicco et al 2006; Barkova et al 2006). RUNX1-ETO was found to induce p53-dependent senescence (Chapter 6, Section 5.4 and 5.5), accompanied by high ROS accumulation (Chapter 5, Section 5.5) therefore it seemed possible that DNA damage signalling may also underlie RUNX1-ETO induced senescence. However, fluorescent confocal microscopy revealed no convincing γ-H2AX foci, a marker of DSB, in either RUNX1-ETO or RUNX1 expressing human fibroblasts (Chapter 5, Section 5.6), although they were readily detected in H-RAS^{V12} expressing cells as previously reported (DiMicco et al 2006). This result was not surprising for RUNX1, given that it primarly involves p16^{INK4a} and does not generate large amounts of ROS. However, the result was unexpected in the case of RUNX1-ETO induced senescence. Nevertheless, there are some possible explanations. Firstly, ROS could be modulated by an as yet unknown mechanism such that it mainly acts as a signalling molecule more than as DNA damaging agent. Secondly, neither RUNX1 nor RUNX1-ETO induced senescence involves a preliminary hyper-proliferative burst (Chapter 4, Section 4.3) which has been linked to DNA damage signalling caused by H-RAS^{V12} due to 'replicative stress'-related DSB formation (DiMicco et al 2006; Bartkova et al 2006). Thirdly, lack of γ-H2AX foci may not necessarily mean that DNA damage response is not involved in senescence as it has been demonstrated recently that activation of ATR by TopBP1 induces premature senescence in the absence of DNA double strand breaks (Toledo et al 2008). Further investigations are required to see if ATM/ATR and/or Chk1/Chk2 are affected by RUNX1 and RUNX1-ETO. Finally, RUNX1 and RUNX1-ETO could exert their effects downstream of DNA damage signalling pathways. Interestingly, it has been reported recently that overexpression of RUNX1-ETO in human CD34^{+} cells drives DNA damage and p53 dependent apoptosis (Krejci et al 2008). There is however, one caveat in this study, which is that γ-H2AX foci were detected five weeks after transduction. It is quite likely that by this time the secondary changes may occur, including accumulation of DNA damage. It was also reported that DNA repair enzymes were downregulated in these CD34^{+} cells which may suggest that these cell were actually survivors that escape apoptosis or growth arrest. It is also important to remember that this observation may also reflect intrinsic cell type differences in the propensity to accumulate DSBs (fibroblasts vs haematopoetic progenitors).

Another interesting finding that distinguishes RUNX1 and RUNX1-ETO from H-RAS^{V12} induced senescence is the lack of chromatin condensation. Senescence-associated heterochromatin foci (SAHF) were not observed in either RUNX1 or RUNX1-ETO expressing cells as visualised by staining with DAPI (Chapter 5, Section 5.6). SAHF formation is a multi-step process involving cooperation between p16-pRb and HIRA/ASF1 pathways. PML bodies play an important role in this process as they serve as a molecular integrating platform for assembly and modification of HIRA-containing complexes, prior to export of these complexes to sites of nascent SAHF. Also it has been suggested that senescent cells may maintain their irreversible growth arrested state, at least in part, by stably forming heterochromatin and epigenetically silencing proliferation-promoting gene loci, which are resistant to E2F-mediated transcriptional activation (Narita et al., 2003). If this is the case, why then do RUNX1 and RUNX1-ETO not induce SAHF and what does this tell us? Perhaps SAHF are not present in RUNX1-ETO induced senescent cells because this from of senescence is primarly driven via the p53 pathway. RUNX1-ETO has also been demonstrated to constitutively activate the Wnt pathway (Muller-Tidow et al 2004; Simon et al 2005) whereas the downregulation of Wnt signalling is absolutely required for formation of SAHF (Ye et al 2007). The lack of SAHF in RUNX1 expressing cells could also be related to a certain threshold level of p16^{INK4a} that RUNX1 fails to achieve and/or it could be due to the inability of RUNX1 to induce PML bodies. Alternatively, RUNX1 and RUNX1-ETO induced senescence may represent a form of senescence which is reversible upon inactivation of the p53 and/or the p16-pRb pathways and therefore SAHF are not apparent. This could be addressed by co-transducing cells with RUNX1 or RUNX1-ETO and inducible large T antigen which could be switched on when cells enter senescence or by infecting senescent cells with a lentiviral vector encoding SV40 large T antigen to abrogate p53 and pRb function. Another possibility could be that DNA damage and SAHF accumulation are somehow mechanistically linked to each other. It is possible that DNA damage foci might trigger SAHF formation cooperatively with p16^{INK4a}, HIRA/ASF1 and PML bodies and there may be a threshold level of DNA damage above which formation of SAHF appears. For example, it has been demonstrated that CHK1

can modify chromatin and trancriptionally repress some genes (Shimada et al 2008). In addition, at sites of DNA damage a number of chromatin modifications occur, most of which, however, lead to chromatin relaxation (Murr et al 2006; Ziv et al 2006). It could be speculated that SAHF formation is a consequence of cellular attempts to counteract DNA damage-induced chromatin relaxation and DNA damage responses. Further detailed analysis of kinetics of the formation of DNA damage foci and SAHF as well as spatial comparison between those structures would help to address the issue of whether DNA damage foci play a causative role in SAHF formation.

The RUNX genes share an intriguing and paradoxical dualistic nature. This means that depending on the context they can act as oncogenes or tumour suppressors (Blyth et al 2005). Given that both RUNX1 and RUNX1-ETO senescent phenotypes differ significantly from classical oncogene-induced senescence it is reasonable to postulate that RUNX1 and RUNX1-ETO induced senescence reflect failsafe rather than oncogenic functions. This hypothesis is supported by the fact that RUNX1 and RUNX1-ETO expressing cells undergo growth arrest without a preliminary phase of hyper-replication and do not trigger a DNA damage response. In this respect they resemble p53 induced senescence where ectopic expression of p53 did not result in γ-H2AX foci or SAHF formation (Chapter 5, Section 5.8) suggesting that the appearance of SAHF and γ-H2AX foci may distinguish oncogene from tumour suppressor induced senescence. It has been demonstrated in our laboratory that other RUNX genes when ectopically expressed in primary murine embryonic fibroblasts (MEFs) also induce premature senescence without an initial hyper-replicative phase (Kilbey et al 2007; Wotton et al 2004) suggesting that ectopic RUNX may be activating a downstream execution phase of oncogene-induced senescence. This may indicate that, in the context of senescence, the RUNX genes act as tumour suppressors rather than oncogenes. In support of this hypothesis, primary fibroblasts lacking RUNX2 fail to undergo senescence and are instead transformed by oncogenic H-RAS^{V12} pointing to an intrinsic role of RUNX genes in this process (Kilbey et al 2007). The requirement for RUNX2 may reflect relative abundance of its expression

compared to other family members in MEFs rather than a unique RUNX2-specific function. Consistent with this idea, it has been shown that RUNX1 is required for growth arrest in response to N-RAS in haematopoietic progenitor cells (Motoda et al 2007). Taken together, this may indicate that different RUNX proteins play similar non-redundant roles in cellular senescence. Interestingly, loss of RUNX2 has been recently implicated in the bypass of senescence in primary osteoblasts and their immortalisation, underpinning the role of RUNX2 as a tumour suppressor (Zaidi et al 2007). Furthermore, a RUNX1 tumour suppressive function has been recently linked to a number of types of solid cancers. For example, RUNX1 has been found to be downregulated in the early stages of hepatocellular carcinoma (Miyagawa et al 2006) and gastric cancer (Sakakura et al 2005). Interestingly, a novel splice variant of RUNX1 which confers loss of wild-type tumour suppressive functions has been identified in ovarian cancer patients (Nanjundan et al 2007).

From the observations made in this study a scenario emerges whereby RUNX1 and RUNX1-ETO induce senescence by different yet to some extent overlapping pathways (Figure 7.1). While it is clear that RUNX1 requires p53 in MEFs to induce senescence (Wotton et al 2004), p53 has not been found to be essential for senescence in human cells where $p16^{INK4a}$ appeared to be more important. The role of $p21^{WAF1}$ in RUNX1 induced senescence requires further investigation since it is dramatically induced in human fibroblasts possibly due to direct activation of the promoter. It is plausible that both $p16^{INK4a}$ and $p21^{WAF1}$ cooperate to achieve pRb activation and establish growth arrest. RUNX1 induced senescence partially relies on p38 MAPK signalling and p38 could contribute to $p16^{INK4a}$ upregulation in these cells, although there are other mediators also likely to be involved in $p16^{INK4a}$ regulation. Slightly elevated ROS levels in RUNX1 expressing cells could be responsible for the activation of p38 MAPK given that these two events correlated well with each other, however other molecules such as Gadd45a must also be considered as potential candidates. Finally, the finding that RUNX1 induced senescence does not entail DNA damage foci and SAHF formation leads to the hypothesis that RUNX1 act as a tumour suppressor rather

than an oncogene in the context of senescence. Interestingly several genes belonging to the ceramide pathway have been shown to be up- or down-regulated by RUNX1 in microarray experiment which has been recently performed in our laboratory (Wotton et al 2008). Ceramide has been implicated in cellular senescence (Mouton and Venable 2000; Venable et al 1995) and even RAS induces senescence via ceramide accumulation (Castro et al 2008). It may represent another signalling pathway or another interacting factor involved in RUNX1 mediated senescence and may warrant further investigation in the future.

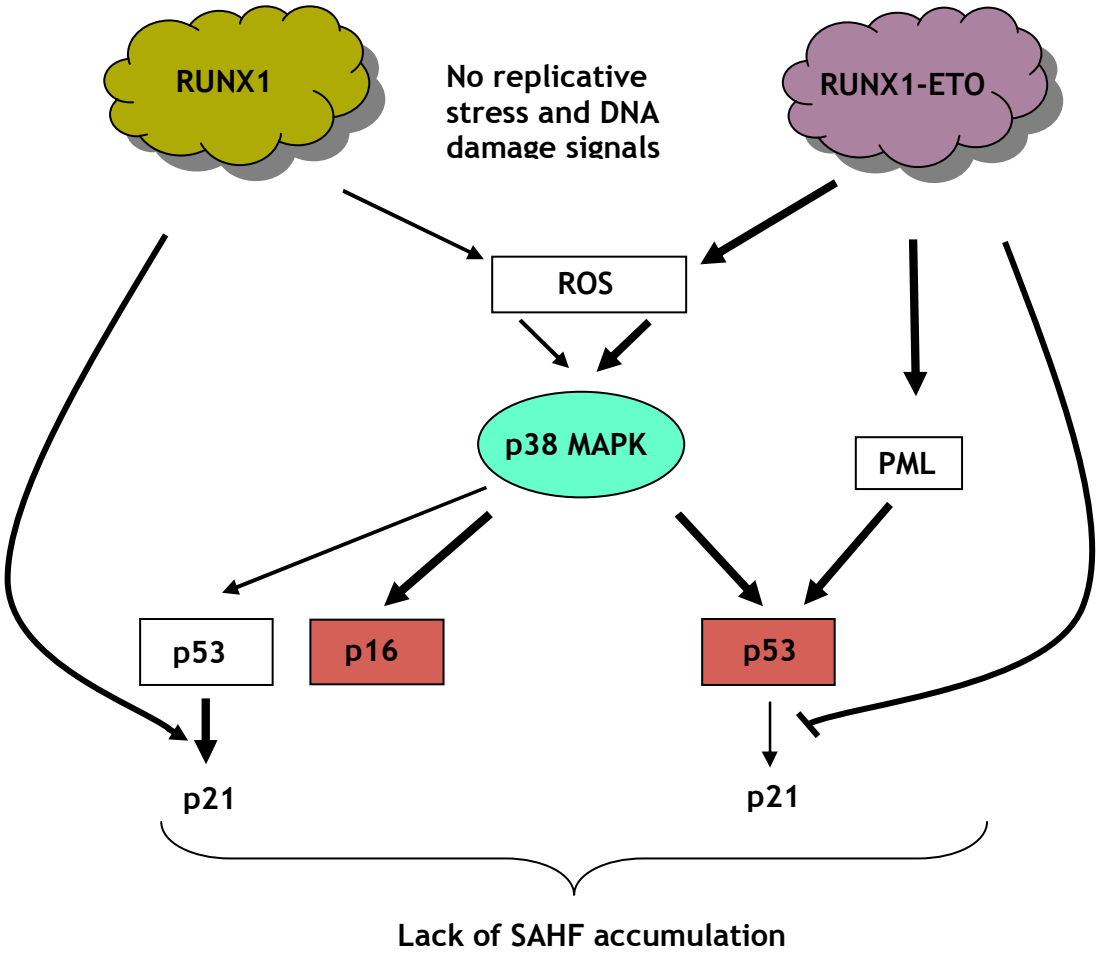

Figure 7.1 Diagram illustrating the potential mechanism of RUNX1 and RUNX1-ETO induced senescence

Increases in ROS levels activate p38 MAPK which in turn regulates the expression of p53 and p16. RUNX1 induces p16-dependent senescence whereas RUNX1-ETO

induces p53-dependent senescence. RUNX1 and RUNX1-ETO differentially induce p21, possibly due to exerting direct opposing effects on the p21 promoter. PML may play a role in p53 stabilisation in RUNX1-ETO induced senescence. The thickness of the arrows reflect the level of upregulation of relevant mediators of senescence by RUNX1 or RUNX1-ETO

Physical and functional interactions between STAT5 and RUNX1 have been revealed recently (Ogawa et al 2008). This is particularly interesting given that STAT5 is also capable of inducing premature senescence when overexpressed in primary human fibroblasts and, like RUNX1, does not involve SAHF formation (Hemann and Narita 2008) suggesting that they may share some common pathway to senescence. On the other hand RUNX1-ETO, in contrast to RUNX1, induces p16-independent but p53-dependent senescence. RUNX1-ETO potently induces reactive oxygen species and ROS may be responsible for the accumulation of phosphorylated p38 MAPK, which is required for the development of the senescent phenotype. It seems that p38 MAPK, in turn, activates p53, which is also likely to be stabilised by PML. Given that RUNX1-ETO seems to have a suppressive effect on $p21^{WAF1}$, it will be important to see if p21 is indeed dispensable for RUNX1-ETO to induce senescence. If this proves to be the case it will be important to identify the downstream effectors of p53 that establish G2/M arrest in RUNX1-ETO expressing cells. The mechanism by which p53 regulates the G2/M transition involves regulation of the cyclin dependent kinase Cdc2 which is essential for entry into mitosis (Nurse 1990; Taylor and Stark 2001b). Binding to cyclin B and phosphorylation by CDK-activating kinase (CAK) are required to activate Cdc2 (Pines 1995; Taylor and Stark 2001a). Gadd45α and/or 14-3-3 sigma emerge as interesting effectors of p53 that may play a role in RUNX1-ETO induced senescence. Both Gadd45α and 14-3-3 sigma are direct targets of p53 and are known to inhibit Cdc2 activity. The protein 14-3-3 sigma binds to Cdc2-Cyclin B complex and sequesters it in the cytoplasm (Chan et al 1999; Hermeking et al 1997) whereas Gadd45α inhibits Cdc2 by blocking its binding to cyclin B (Jin et al 2000; Zhan et al 1999). Thus, it could be that RUNX1-ETO causes G2/M arrest due to p53-dependent activation of

Gadd45α and/or 14-3-3 sigma. Given that Gadd45α has been shown to be involved in p38 activation in H-RAS^{V12} induced senescence (Bulavin et al 2003) it is tempting to speculate that the same p53-Gadd45α -p38 positive feedback loop is operative in RUNX1-ETO induced senescence.

In conclusion, I have reported that RUNX1 and the RUNX1/CBFβ oncogenic fusion derivatives: RUNX1-ETO and CBFβ-MYH11 induce premature senescence when ectopically expressed in primary cells revealing a central role for Runx-regulated pathways in this tumour suppressive response. While the nature of CBFβ-MYH11 induced senescence remains to be investigated I have demonstrated that RUNX1 and RUNX1-ETO induce senescence by distinctive yet partially overlapping cellular mechanisms. I have also identified DNA binding and the C-terminal domain as an absolute requirement to induce senescence by RUNX1. In addition I have found that RUNX1-ETO C-terminal domain containing corepressor binding sites of ETO protein is critical for RUNX1-ETO induced senescence. Importantly, I have shown that both RUNX1 and RUNX1-ETO induced senescence differ from prototypical H-RAS^{V12} induced senescence. This study emphasises the fact that cellular senescence represents a heterogeneous process driven by diverse pathways depending on the stimuli and the cell type.

References

References

Adams,P.D., 2007. Remodeling of chromatin structure in senescent cells and its potential impact on tumor suppression and aging. Gene 397, 84-93.

Adya,N., Stacy,T., Speck,N.A., Liu,P.P., 1998. The leukemic protein core binding factor beta (CBFbeta)-smooth-muscle myosin heavy chain sequesters CBFalpha2 into cytoskeletal filaments and aggregates. Mol. Cell Biol. 18, 7432-7443.

Alani,R.M., Young,A.Z., Shifflett,C.B., 2001. Id1 regulation of cellular senescence through transcriptional repression of p16/Ink4a. Proc. Natl. Acad. Sci. U. S. A 98, 7812-7816.

Alcorta,D.A., Xiong,Y., Phelps,D., Hannon,G., Beach,D., Barrett,J.C., 1996. Involvement of the cyclin-dependent kinase inhibitor p16 (INK4a) in replicative senescence of normal human fibroblasts. Proc. Natl. Acad. Sci. U. S. A 93, 13742-13747.

Andreasson,P., Schwaller,J., Anastasiadou,E., Aster,J., Gilliland,D.G., 2001. The expression of ETV6/CBFA2 (TEL/AML1) is not sufficient for the transformation of hematopoietic cell lines in vitro or the induction of hematologic disease in vivo. Cancer Genet. Cytogenet. 130, 93-104.

Aronson,B.D., Fisher,A.L., Blechman,K., Caudy,M., Gergen,J.P., 1997. Groucho-dependent and -independent repression activities of Runt domain proteins. Mol. Cell Biol. 17, 5581-5587.

Artandi,S.E., DePinho,R.A., 2000. Mice without telomerase: what can they teach us about human cancer? Nat. Med. 6, 852-855.

Avraham,K.B., Levanon,D., Negreanu,V., Bernstein,Y., Groner,Y., Copeland,N.G., Jenkins,N.A., 1995. Mapping of the mouse homolog of the human runt domain gene, AML2, to the distal region of mouse chromosome 4. Genomics 25, 603-605.

Bae,S.C., Ogawa,E., Maruyama,M., Oka,H., Satake,M., Shigesada,K., Jenkins,N.A., Gilbert,D.J., Copeland,N.G., Ito,Y., 1994. PEBP2 alpha B/mouse AML1 consists of multiple isoforms that possess differential transactivation potentials. Mol. Cell Biol. 14, 3242-3252.

Banker,D.E., Groudine,M., Willman,C.L., Norwood,T., Appelbaum,F.R., 1998a. Cell cycle perturbations in acute myeloid leukemia samples following in vitro exposures to therapeutic agents. Leuk. Res. 22, 221-239.

Banker,D.E., Radich,J., Becker,A., Kerkof,K., Norwood,T., Willman,C., Appelbaum,F.R., 1998b. The t(8;21) translocation is not consistently associated with high Bcl-2 expression in de novo acute myeloid leukemias of adults. Clin. Cancer Res. 4, 3051-3062.

Bartkova,J., Rezaei,N., Liontos,M., Karakaidos,P., Kletsas,D., Issaeva,N., Vassiliou,L.V., Kolettas,E., Niforou,K., Zoumpourlis,V.C., Takaoka,M., Nakagawa,H., Tort,F., Fugger,K., Johansson,F., Sehested,M., Andersen,C.L., Dyrskjot,L., Orntoft,T., Lukas,J., Kittas,C., Helleday,T., Halazonetis,T.D., Bartek,J., Gorgoulis,V.G., 2006. Oncogene-induced senescence is part of the tumorigenesis barrier imposed by DNA damage checkpoints. Nature 444, 633-637.

Beausejour,C.M., Krtolica,A., Galimi,F., Narita,M., Lowe,S.W., Yaswen,P., Campisi,J., 2003. Reversal of human cellular senescence: roles of the p53 and p16 pathways. EMBO J. 22, 4212-4222.

Berardi,M.J., Sun,C., Zehr,M., Abildgaard,F., Peng,J., Speck,N.A., Bushweller,J.H., 1999. The Ig fold of the core binding factor alpha Runt domain is a member of a family of structurally and functionally related Ig-fold DNA-binding domains. Structure. 7, 1247-1256.

Bernardi,R., Scaglioni,P.P., Bergmann,S., Horn,H.F., Vousden,K.H., Pandolfi,P.P., 2004. PML regulates p53 stability by sequestering Mdm2 to the nucleolus. Nat. Cell Biol. 6, 665-672.

Bernardin,F., Yang,Y., Civin,C.I., Friedman,A.D., 2002a. c-Myc overcomes cell cycle inhibition by CBFbeta-SMMHC, a myeloid leukemia oncoprotein. Cancer Biol. Ther. 1, 492-496.

Bernardin,F., Yang,Y., Cleaves,R., Zahurak,M., Cheng,L., Civin,C.I., Friedman,A.D., 2002b. TEL-AML1, expressed from t(12;21) in human acute lymphocytic leukemia, induces acute leukemia in mice. Cancer Res. 62, 3904-3908.

Bernardin-Fried,F., Kummalue,T., Leijen,S., Collector,M.I., Ravid,K., Friedman,A.D., 2004. AML1/RUNX1 increases during G1 to S cell cycle progression independent of cytokine-dependent phosphorylation and induces cyclin D3 gene expression. J. Biol. Chem. 279, 15678-15687.

Bihani,T., Mason,D.X., Jackson,T.J., Chen,S.C., Boettner,B., Lin,A.W., 2004. Differential oncogenic Ras signaling and senescence in tumor cells. Cell Cycle 3, 1201-1207.

Birnboim,H.C., Doly,J., 1979. A rapid alkaline extraction procedure for screening recombinant plasmid DNA. Nucleic Acids Res. 7, 1513-1523.

Blander,G., de Oliveira,R.M., Conboy,C.M., Haigis,M., Guarente,L., 2003. Superoxide dismutase 1 knock-down induces senescence in human fibroblasts. J. Biol. Chem. 278, 38966-38969.

Blyth,K., Cameron,E.R., Neil,J.C., 2005. The RUNX genes: gain or loss of function in cancer. Nat. Rev. Cancer 5, 376-387.

Blyth,K., Terry,A., Mackay,N., Vaillant,F., Bell,M., Cameron,E.R., Neil,J.C., Stewart,M., 2001. Runx2: a novel oncogenic effector revealed by in vivo complementation and retroviral tagging. Oncogene 20, 295-302.

Boutros,R., Lobjois,V., Ducommun,B., 2007. CDC25 phosphatases in cancer cells: key players? Good targets? Nat. Rev. Cancer 7, 495-507.

Bracken,A.P., Kleine-Kohlbrecher,D., Dietrich,N., Pasini,D., Gargiulo,G., Beekman,C., Theilgaard-Monch,K., Minucci,S., Porse,B.T., Marine,J.C., Hansen,K.H., Helin,K., 2007. The Polycomb group proteins bind throughout the INK4A-ARF locus and are disassociated in senescent cells. Genes Dev. 21, 525-530.

Bradford,M.M., 1976. A rapid and sensitive method for the quantitation of microgram quantities of protein utilizing the principle of protein-dye binding. Anal. Biochem. 72, 248-254.

Braig,M., Lee,S., Loddenkemper,C., Rudolph,C., Peters,A.H., Schlegelberger,B., Stein,H., Dorken,B., Jenuwein,T., Schmitt,C.A., 2005. Oncogene-induced senescence as an initial barrier in lymphoma development. Nature 436, 660-665.

Bringold,F., Serrano,M., 2000. Tumor suppressors and oncogenes in cellular senescence. Exp. Gerontol. 35, 317-329.

Britos-Bray,M., Friedman,A.D., 1997. Core binding factor cannot synergistically activate the myeloperoxidase proximal enhancer in immature myeloid cells without c-Myb. Mol. Cell Biol. 17, 5127-5135.

Brookes,S., Rowe,J., Gutierrez,D.A., Bond,J., Peters,G., 2004. Contribution of p16(INK4a) to replicative senescence of human fibroblasts. Exp. Cell Res. 298, 549-559.

Brookes,S., Rowe,J., Ruas,M., Llanos,S., Clark,P.A., Lomax,M., James,M.C., Vatcheva,R., Bates,S., Vousden,K.H., Parry,D., Gruis,N., Smit,N., Bergman,W., Peters,G., 2002. INK4a-deficient human diploid fibroblasts are resistant to RAS-induced senescence. EMBO J. 21, 2936-2945.

Brown,J.M., Attardi,L.D., 2005. The role of apoptosis in cancer development and treatment response. Nat. Rev. Cancer 5, 231-237.

Brown,J.P., Wei,W., Sedivy,J.M., 1997. Bypass of senescence after disruption of p21CIP1/WAF1 gene in normal diploid human fibroblasts. Science 277, 831-834.

Bruhn,L., Munnerlyn,A., Grosschedl,R., 1997. ALY, a context-dependent coactivator of LEF-1 and AML-1, is required for TCRalpha enhancer function. Genes Dev. 11, 640-653.

Bulavin,D.V., Demidov,O.N., Saito,S., Kauraniemi,P., Phillips,C., Amundson,S.A., Ambrosino,C., Sauter,G., Nebreda,A.R., Anderson,C.W., Kallioniemi,A., Fornace,A.J., Jr., Appella,E., 2002. Amplification of

PPM1D in human tumors abrogates p53 tumor-suppressor activity. Nat. Genet. 31, 210-215.

Bulavin,D.V., Fornace,A.J., Jr., 2004. p38 MAP kinase's emerging role as a tumor suppressor. Adv. Cancer Res. 92, 95-118.

Bulavin,D.V., Kovalsky,O., Hollander,M.C., Fornace,A.J., Jr., 2003. Loss of oncogenic H-ras-induced cell cycle arrest and p38 mitogen-activated protein kinase activation by disruption of Gadd45a. Mol. Cell Biol. 23, 3859-3871.

Bulavin,D.V., Phillips,C., Nannenga,B., Timofeev,O., Donehower,L.A., Anderson,C.W., Appella,E., Fornace,A.J., Jr., 2004. Inactivation of the Wip1 phosphatase inhibits mammary tumorigenesis through p38 MAPK-mediated activation of the p16(Ink4a)-p19(Arf) pathway. Nat. Genet. 36, 343-350.

Burel,S.A., Harakawa,N., Zhou,L., Pabst,T., Tenen,D.G., Zhang,D.E., 2001. Dichotomy of AML1-ETO functions: growth arrest versus block of differentiation. Mol. Cell Biol. 21, 5577-5590.

Busuttil,R.A., Rubio,M., Dolle,M.E., Campisi,J., Vijg,J., 2003. Oxygen accelerates the accumulation of mutations during the senescence and immortalization of murine cells in culture. Aging Cell 2, 287-294.

Cai,Z., de Bruijn,M., Ma,X., Dortland,B., Luteijn,T., Downing,R.J., Dzierzak,E., 2000. Haploinsufficiency of AML1 affects the temporal and spatial generation of hematopoietic stem cells in the mouse embryo. Immunity. 13, 423-431.

Calabi,F., Rhodes,M., Williamson,P., Boyd,Y., 1995. Identification and chromosomal mapping of a third mouse runt-like locus. Genomics 26, 607-610.

Campisi,J., 2001. Cellular senescence as a tumor-suppressor mechanism. Trends Cell Biol. 11, S27-S31.

Campisi,J., 2005. Senescent cells, tumor suppression, and organismal aging: good citizens, bad neighbors. Cell 120, 513-522.

Cao,W., Adya,N., Britos-Bray,M., Liu,P.P., Friedman,A.D., 1998. The core binding factor (CBF) alpha interaction domain and the smooth muscle myosin heavy chain (SMMHC) segment of CBFbeta-SMMHC are both required to slow cell proliferation. J. Biol. Chem. 273, 31534-31540.

Castilla,L.H., Garrett,L., Adya,N., Orlic,D., Dutra,A., Anderson,S., Owens,J., Eckhaus,M., Bodine,D., Liu,P.P., 1999. The fusion gene Cbfb-MYH11 blocks myeloid differentiation and predisposes mice to acute myelomonocytic leukaemia. Nat. Genet. 23, 144-146.

Castilla,L.H., Perrat,P., Martinez,N.J., Landrette,S.F., Keys,R., Oikemus,S., Flanegan,J., Heilman,S., Garrett,L., Dutra,A., Anderson,S., Pihan,G.A., Wolff,L., Liu,P.P., 2004. Identification of genes that synergize with Cbfb-MYH11 in the pathogenesis of acute myeloid leukemia. Proc. Natl. Acad. Sci. U. S. A 101, 4924-4929.

Castilla,L.H., Wijmenga,C., Wang,Q., Stacy,T., Speck,N.A., Eckhaus,M., Marin-Padilla,M., Collins,F.S., Wynshaw-Boris,A., Liu,P.P., 1996. Failure of embryonic hematopoiesis and lethal hemorrhages in mouse embryos

heterozygous for a knocked-in leukemia gene CBFB-MYH11. Cell 87, 687-696.

Castro,M.E., Ferrer,I., Cascon,A., Guijarro,M.V., Lleonart,M., Cajal,S., Leal,J.F., Robledo,M., Carnero,A., 2008. PPP1CA contributes to the senescence program induced by oncogenic Ras. Carcinogenesis 29, 491-499.

Catalano,A., Rodilossi,S., Caprari,P., Coppola,V., Procopio,A., 2005. 5-Lipoxygenase regulates senescence-like growth arrest by promoting ROS-dependent p53 activation. EMBO J. 24, 170-179.

Chakraborty,S., Sinha,K.K., Senyuk,V., Nucifora,G., 2003. SUV39H1 interacts with AML1 and abrogates AML1 transactivity. AML1 is methylated in vivo. Oncogene 22, 5229-5237.

Chan,T.A., Hermeking,H., Lengauer,C., Kinzler,K.W., Vogelstein,B., 1999. 14-3-3Sigma is required to prevent mitotic catastrophe after DNA damage. Nature 401, 616-620.

Chang,B.D., Swift,M.E., Shen,M., Fang,J., Broude,E.V., Roninson,I.B., 2002. Molecular determinants of terminal growth arrest induced in tumor cells by a chemotherapeutic agent. Proc. Natl. Acad. Sci. U. S. A 99, 389-394.

Chen,Q., Ames,B.N., 1994. Senescence-like growth arrest induced by hydrogen peroxide in human diploid fibroblast F65 cells. Proc. Natl. Acad. Sci. U. S. A 91, 4130-4134.

Chen,Q., Fischer,A., Reagan,J.D., Yan,L.J., Ames,B.N., 1995. Oxidative DNA damage and senescence of human diploid fibroblast cells. Proc. Natl. Acad. Sci. U. S. A 92, 4337-4341.

Chen,Q.M., Bartholomew,J.C., Campisi,J., Acosta,M., Reagan,J.D., Ames,B.N., 1998. Molecular analysis of H2O2-induced senescent-like growth arrest in normal human fibroblasts: p53 and Rb control G1 arrest but not cell replication. Biochem. J. 332 (Pt 1), 43-50.

Chen,Z., Trotman,L.C., Shaffer,D., Lin,H.K., Dotan,Z.A., Niki,M., Koutcher,J.A., Scher,H.I., Ludwig,T., Gerald,W., Cordon-Cardo,C., Pandolfi,P.P., 2005. Crucial role of p53-dependent cellular senescence in suppression of Pten-deficient tumorigenesis. Nature 436, 725-730.

Christiansen,D.H., Andersen,M.K., Desta,F., Pedersen-Bjergaard,J., 2005. Mutations of genes in the receptor tyrosine kinase (RTK)/RAS-BRAF signal transduction pathway in therapy-related myelodysplasia and acute myeloid leukemia. Leukemia 19, 2232-2240.

Christiansen,D.H., Andersen,M.K., Pedersen-Bjergaard,J., 2001. Mutations with loss of heterozygosity of p53 are common in therapy-related myelodysplasia and acute myeloid leukemia after exposure to alkylating agents and significantly associated with deletion or loss of 5q, a complex karyotype, and a poor prognosis. J. Clin. Oncol. 19, 1405-1413.

Colavitti,R., Finkel,T., 2005. Reactive oxygen species as mediators of cellular senescence. IUBMB. Life 57, 277-281.

Collado,M., Gil,J., Efeyan,A., Guerra,C., Schuhmacher,A.J., Barradas,M., Benguria,A., Zaballos,A., Flores,J.M., Barbacid,M., Beach,D., Serrano,M., 2005. Tumour biology: senescence in premalignant tumours. Nature 436, 642.

Collado,M., Serrano,M., 2006. The power and the promise of oncogene-induced senescence markers. Nat. Rev. Cancer 6, 472-476.

Cosme-Blanco,W., Shen,M.F., Lazar,A.J., Pathak,S., Lozano,G., Multani,A.S., Chang,S., 2007. Telomere dysfunction suppresses spontaneous tumorigenesis in vivo by initiating p53-dependent cellular senescence. EMBO Rep. 8, 497-503.

Crute,B.E., Lewis,A.F., Wu,Z., Bushweller,J.H., Speck,N.A., 1996. Biochemical and biophysical properties of the core-binding factor alpha2 (AML1) DNA-binding domain. J. Biol. Chem. 271, 26251-26260.

d'Adda,d.F., Reaper,P.M., Clay-Farrace,L., Fiegler,H., Carr,P., von Zglinicki,T., Saretzki,G., Carter,N.P., Jackson,S.P., 2003. A DNA damage checkpoint response in telomere-initiated senescence. Nature 426, 194-198.

Dannenberg,J.H., van Rossum,A., Schuijff,L., te,R.H., 2000. Ablation of the retinoblastoma gene family deregulates G(1) control causing immortalization and increased cell turnover under growth-restricting conditions. Genes Dev. 14, 3051-3064.

de Guzman,C.G., Warren,A.J., Zhang,Z., Gartland,L., Erickson,P., Drabkin,H., Hiebert,S.W., Klug,C.A., 2002. Hematopoietic stem cell expansion and distinct myeloid developmental abnormalities in a murine model of the AML1-ETO translocation. Mol. Cell Biol. 22, 5506-5517.

de Stanchina,E., McCurrach,M.E., Zindy,F., Shieh,S.Y., Ferbeyre,G., Samuelson,A.V., Prives,C., Roussel,M.F., Sherr,C.J., Lowe,S.W., 1998. E1A signaling to p53 involves the p19(ARF) tumor suppressor. Genes Dev. 12, 2434-2442.

de Stanchina,E., Querido,E., Narita,M., Davuluri,R.V., Pandolfi,P.P., Ferbeyre,G., Lowe,S.W., 2004. PML is a direct p53 target that modulates p53 effector functions. Mol. Cell 13, 523-535.

Di Leonardo,A., Linke,S.P., Clarkin,K., Wahl,G.M., 1994. DNA damage triggers a prolonged p53-dependent G1 arrest and long-term induction of Cip1 in normal human fibroblasts. Genes Dev. 8, 2540-2551.

Di Micco,R., Fumagalli,M., Cicalese,A., Piccinin,S., Gasparini,P., Luise,C., Schurra,C., Garre',M., Nuciforo,P.G., Bensimon,A., Maestro,R., Pelicci,P.G., d'Adda,d.F., 2006. Oncogene-induced senescence is a DNA damage response triggered by DNA hyper-replication. Nature 444, 638-642.

Dimri,G.P., 2005. What has senescence got to do with cancer? Cancer Cell 7, 505-512.

Dimri,G.P., Itahana,K., Acosta,M., Campisi,J., 2000. Regulation of a senescence checkpoint response by the E2F1 transcription factor and p14(ARF) tumor suppressor. Mol. Cell Biol. 20, 273-285.

Dimri,G.P., Lee,X., Basile,G., Acosta,M., Scott,G., Roskelley,C., Medrano,E.E., Linskens,M., Rubelj,I., Pereira-Smith,O., ., 1995. A biomarker that identifies senescent human cells in culture and in aging skin in vivo. Proc. Natl. Acad. Sci. U. S. A 92, 9363-9367.

Dirac,A.M., Bernards,R., 2003. Reversal of senescence in mouse fibroblasts through lentiviral suppression of p53. J. Biol. Chem. 278, 11731-11734.

Dolado,I., Swat,A., Ajenjo,N., De Vita,G., Cuadrado,A., Nebreda,A.R., 2007. p38alpha MAP kinase as a sensor of reactive oxygen species in tumorigenesis. Cancer Cell 11, 191-205.

Drayton,S., Peters,G., 2002. Immortalisation and transformation revisited. Curr. Opin. Genet. Dev. 12, 98-104.

Duffy,J.B., Gergen,J.P., 1991. The Drosophila segmentation gene runt acts as a position-specific numerator element necessary for the uniform expression of the sex-determining gene Sex-lethal. Genes Dev. 5, 2176-2187.

Duffy,J.B., Kania,M.A., Gergen,J.P., 1991. Expression and function of the Drosophila gene runt in early stages of neural development. Development 113, 1223-1230.

Durrant,I., Benge,L.C., Sturrock,C., Devenish,A.T., Howe,R., Roe,S., Moore,M., Scozzafava,G., Proudfoot,L.M., Richardson,T.C., ., 1990. The application of enhanced chemiluminescence to membrane-based nucleic acid detection. Biotechniques 8, 564-570.

Durst,K.L., Hiebert,S.W., 2004. Role of RUNX family members in transcriptional repression and gene silencing. Oncogene 23, 4220-4224.

Eggers,J.H., Stock,M., Fliegauf,M., Vonderstrass,B., Otto,F., 2002. Genomic characterization of the RUNX2 gene of Fugu rubripes. Gene 291, 159-167.

Elsasser,A., Franzen,M., Kohlmann,A., Weisser,M., Schnittger,S., Schoch,C., Reddy,V.A., Burel,S., Zhang,D.E., Ueffing,M., Tenen,D.G., Hiddemann,W., Behre,G., 2003. The fusion protein AML1-ETO in acute myeloid leukemia with translocation t(8;21) induces c-jun protein

expression via the proximal AP-1 site of the c-jun promoter in an indirect, JNK-dependent manner. Oncogene 22, 5646-5657.

Erickson,P., Gao,J., Chang,K.S., Look,T., Whisenant,E., Raimondi,S., Lasher,R., Trujillo,J., Rowley,J., Drabkin,H., 1992. Identification of breakpoints in t(8;21) acute myelogenous leukemia and isolation of a fusion transcript, AML1/ETO, with similarity to Drosophila segmentation gene, runt. Blood 80, 1825-1831.

Erman,B., Cortes,M., Nikolajczyk,B.S., Speck,N.A., Sen,R., 1998. ETS-core binding factor: a common composite motif in antigen receptor gene enhancers. Mol. Cell Biol. 18, 1322-1330.

Fears,S., Gavin,M., Zhang,D.E., Hetherington,C., Ben David,Y., Rowley,J.D., Nucifora,G., 1997. Functional characterization of ETV6 and ETV6/CBFA2 in the regulation of the MCSFR proximal promoter. Proc. Natl. Acad. Sci. U. S. A 94, 1949-1954.

Feldser,D.M., Greider,C.W., 2007. Short telomeres limit tumor progression in vivo by inducing senescence. Cancer Cell 11, 461-469.

Fenaux,P., Preudhomme,C., Quiquandon,I., Jonveaux,P., Lai,J.L., Vanrumbeke,M., Loucheux-Lefebvre,M.H., Bauters,F., Berger,R., Kerckaert,J.P., 1992. Mutations of the P53 gene in acute myeloid leukaemia. Br. J. Haematol. 80, 178-183.

Fenrick,R., Amann,J.M., Lutterbach,B., Wang,L., Westendorf,J.J., Downing,J.R., Hiebert,S.W., 1999. Both TEL and AML-1 contribute repression domains to the t(12;21) fusion protein. Mol. Cell Biol. 19, 6566-6574.

Fenske,T.S., Pengue,G., Mathews,V., Hanson,P.T., Hamm,S.E., Riaz,N., Graubert,T.A., 2004. Stem cell expression of the AML1/ETO fusion protein induces a myeloproliferative disorder in mice. Proc. Natl. Acad. Sci. U. S. A 101, 15184-15189.

Ferbeyre,G., de Stanchina,E., Querido,E., Baptiste,N., Prives,C., Lowe,S.W., 2000. PML is induced by oncogenic ras and promotes premature senescence. Genes Dev. 14, 2015-2027.

Frank,K.M., Sharpless,N.E., Gao,Y., Sekiguchi,J.M., Ferguson,D.O., Zhu,C., Manis,J.P., Horner,J., DePinho,R.A., Alt,F.W., 2000. DNA ligase IV deficiency in mice leads to defective neurogenesis and embryonic lethality via the p53 pathway. Mol. Cell 5, 993-1002.

Frank,R., Zhang,J., Uchida,H., Meyers,S., Hiebert,S.W., Nimer,S.D., 1995. The AML1/ETO fusion protein blocks transactivation of the GM-CSF promoter by AML1B. Oncogene 11, 2667-2674.

Frank,R.C., Sun,X., Berguido,F.J., Jakubowiak,A., Nimer,S.D., 1999. The t(8;21) fusion protein, AML1/ETO, transforms NIH3T3 cells and activates AP-1. Oncogene 18, 1701-1710.

Frippiat,C., Dewelle,J., Remacle,J., Toussaint,O., 2002. Signal transduction in H2O2-induced senescence-like phenotype in human diploid fibroblasts. Free Radic. Biol. Med. 33, 1334-1346.

Funayama,R., Saito,M., Tanobe,H., Ishikawa,F., 2006. Loss of linker histone H1 in cellular senescence. J. Cell Biol. 175, 869-880.

Gao,Y., Ferguson,D.O., Xie,W., Manis,J.P., Sekiguchi,J., Frank,K.M., Chaudhuri,J., Horner,J., DePinho,R.A., Alt,F.W., 2000. Interplay of p53

and DNA-repair protein XRCC4 in tumorigenesis, genomic stability and development. Nature 404, 897-900.

Geiger,H., Van Zant,G., 2002. The aging of lympho-hematopoietic stem cells. Nat. Immunol. 3, 329-333.

Gelmetti,V., Zhang,J., Fanelli,M., Minucci,S., Pelicci,P.G., Lazar,M.A., 1998. Aberrant recruitment of the nuclear receptor corepressor-histone deacetylase complex by the acute myeloid leukemia fusion partner ETO. Mol. Cell Biol. 18, 7185-7191.

Gergen,J.P., Butler,B.A., 1988. Isolation of the Drosophila segmentation gene runt and analysis of its expression during embryogenesis. Genes Dev. 2, 1179-1193.

Gil,J., Bernard,D., Martinez,D., Beach,D., 2004. Polycomb CBX7 has a unifying role in cellular lifespan. Nat. Cell Biol. 6, 67-72.

Gil,J., Peters,G., 2006. Regulation of the INK4b-ARF-INK4a tumour suppressor locus: all for one or one for all. Nat. Rev. Mol. Cell Biol. 7, 667-677.

Gire,V., Roux,P., Wynford-Thomas,D., Brondello,J.M., Dulic,V., 2004. DNA damage checkpoint kinase Chk2 triggers replicative senescence. EMBO J. 23, 2554-2563.

Goemans,B.F., Zwaan,C.M., Miller,M., Zimmermann,M., Harlow,A., Meshinchi,S., Loonen,A.H., Hahlen,K., Reinhardt,D., Creutzig,U., Kaspers,G.J., Heinrich,M.C., 2005. Mutations in KIT and RAS are frequent events in pediatric core-binding factor acute myeloid leukemia. Leukemia 19, 1536-1542.

Golub,T.R., Barker,G.F., Bohlander,S.K., Hiebert,S.W., Ward,D.C., Bray-Ward,P., Morgan,E., Raimondi,S.C., Rowley,J.D., Gilliland,D.G., 1995. Fusion of the TEL gene on 12p13 to the AML1 gene on 21q22 in acute lymphoblastic leukemia. Proc. Natl. Acad. Sci. U. S. A 92, 4917-4921.

Greeve,I., Hermans-Borgmeyer,I., Brellinger,C., Kasper,D., Gomez-Isla,T., Behl,C., Levkau,B., Nitsch,R.M., 2000. The human DIMINUTO/DWARF1 homolog seladin-1 confers resistance to Alzheimer's disease-associated neurodegeneration and oxidative stress. J. Neurosci. 20, 7345-7352.

Guidez,F., Petrie,K., Ford,A.M., Lu,H., Bennett,C.A., MacGregor,A., Hannemann,J., Ito,Y., Ghysdael,J., Greaves,M., Wiedemann,L.M., Zelent,A., 2000. Recruitment of the nuclear receptor corepressor N-CoR by the TEL moiety of the childhood leukemia-associated TEL-AML1 oncoprotein. Blood 96, 2557-2561.

Gunji,H., Waga,K., Nakamura,F., Maki,K., Sasaki,K., Nakamura,Y., Mitani,K., 2004. TEL/AML1 shows dominant-negative effects over TEL as well as AML1. Biochem. Biophys. Res. Commun. 322, 623-630.

Halliwell,B., 2007. Oxidative stress and cancer: have we moved forward? Biochem. J. 401, 1-11.

Hampel,B., Malisan,F., Niederegger,H., Testi,R., Jansen-Durr,P., 2004. Differential regulation of apoptotic cell death in senescent human cells. Exp. Gerontol. 39, 1713-1721.

Hayashi,K., Abe,N., Watanabe,T., Obinata,M., Ito,M., Sato,T., Habu,S., Satake,M., 2001. Overexpression of AML1 transcription factor drives

thymocytes into the CD8 single-positive lineage. J. Immunol. 167, 4957-4965.

Hayashi,K., Natsume,W., Watanabe,T., Abe,N., Iwai,N., Okada,H., Ito,Y., Asano,M., Iwakura,Y., Habu,S., Takahama,Y., Satake,M., 2000. Diminution of the AML1 transcription factor function causes differential effects on the fates of CD4 and CD8 single-positive T cells. J. Immunol. 165, 6816-6824.

Hayflick,L., 1965. THE LIMITED IN VITRO LIFETIME OF HUMAN DIPLOID CELL STRAINS. Exp. Cell Res. 37, 614-636.

Hemann,M.T., Narita,M., 2007. Oncogenes and senescence: breaking down in the fast lane. Genes Dev. 21, 1-5.

Herbig,U., Jobling,W.A., Chen,B.P., Chen,D.J., Sedivy,J.M., 2004. Telomere shortening triggers senescence of human cells through a pathway involving ATM, p53, and p21(CIP1), but not p16(INK4a). Mol. Cell 14, 501-513.

Hermeking,H., Lengauer,C., Polyak,K., He,T.C., Zhang,L., Thiagalingam,S., Kinzler,K.W., Vogelstein,B., 1997. 14-3-3 sigma is a p53-regulated inhibitor of G2/M progression. Mol. Cell 1, 3-11.

Hernandez-Munain,C., Krangel,M.S., 1994. Regulation of the T-cell receptor delta enhancer by functional cooperation between c-Myb and core-binding factors. Mol. Cell Biol. 14, 473-483.

Hiebert,S.W., Sun,W., Davis,J.N., Golub,T., Shurtleff,S., Buijs,A., Downing,J.R., Grosveld,G., Roussell,M.F., Gilliland,D.G., Lenny,N., Meyers,S., 1996. The t(12;21) translocation converts AML-1B from an activator to a repressor of transcription. Mol. Cell Biol. 16, 1349-1355.

Higuchi,M., O'Brien,D., Kumaravelu,P., Lenny,N., Yeoh,E.J., Downing,J.R., 2002. Expression of a conditional AML1-ETO oncogene bypasses embryonic lethality and establishes a murine model of human t(8;21) acute myeloid leukemia. Cancer Cell 1, 63-74.

Hohaus,S., Petrovick,M.S., Voso,M.T., Sun,Z., Zhang,D.E., Tenen,D.G., 1995. PU.1 (Spi-1) and C/EBP alpha regulate expression of the granulocyte-macrophage colony-stimulating factor receptor alpha gene. Mol. Cell Biol. 15, 5830-5845.

Horiike,S., Misawa,S., Kaneko,H., Sasai,Y., Kobayashi,M., Fujii,H., Tanaka,S., Yagita,M., Abe,T., Kashima,K., Taniwaki,M., 1999. Distinct genetic involvement of the TP53 gene in therapy-related leukemia and myelodysplasia with chromosomal losses of Nos 5 and/or 7 and its possible relationship to replication error phenotype. Leukemia 13, 1235-1242.

Huang,C., Ma,W.Y., Maxiner,A., Sun,Y., Dong,Z., 1999. p38 kinase mediates UV-induced phosphorylation of p53 protein at serine 389. J. Biol. Chem. 274, 12229-12235.

Ichikawa,M., Asai,T., Saito,T., Seo,S., Yamazaki,I., Yamagata,T., Mitani,K., Chiba,S., Ogawa,S., Kurokawa,M., Hirai,H., 2004. AML-1 is required for megakaryocytic maturation and lymphocytic differentiation, but not for maintenance of hematopoietic stem cells in adult hematopoiesis. Nat. Med. 10, 299-304.

Imamura,J., Miyoshi,I., Koeffler,H.P., 1994. p53 in hematologic malignancies. Blood 84, 2412-2421.

Inoue,K., Ozaki,S., Ito,K., Iseda,T., Kawaguchi,S., Ogawa,M., Bae,S.C., Yamashita,N., Itohara,S., Kudo,N., Ito,Y., 2003. Runx3 is essential for the target-specific axon pathfinding of trkc-expressing dorsal root ganglion neurons. Blood Cells Mol. Dis. 30, 157-160.

Inoue,K., Wen,R., Rehg,J.E., Adachi,M., Cleveland,J.L., Roussel,M.F., Sherr,C.J., 2000. Disruption of the ARF transcriptional activator DMP1 facilitates cell immortalization, Ras transformation, and tumorigenesis. Genes Dev. 14, 1797-1809.

Itahana,K., Campisi,J., Dimri,G.P., 2004. Mechanisms of cellular senescence in human and mouse cells. Biogerontology. 5, 1-10.

Itahana,K., Dimri,G., Campisi,J., 2001. Regulation of cellular senescence by p53. Eur. J. Biochem. 268, 2784-2791.

Itahana,K., Zou,Y., Itahana,Y., Martinez,J.L., Beausejour,C., Jacobs,J.J., Van Lohuizen,M., Band,V., Campisi,J., Dimri,G.P., 2003. Control of the replicative life span of human fibroblasts by p16 and the polycomb protein Bmi-1. Mol. Cell Biol. 23, 389-401.

Ito,Y., 2004. Oncogenic potential of the RUNX gene family: 'overview'. Oncogene 23, 4198-4208.

Iwasa,H., Han,J., Ishikawa,F., 2003. Mitogen-activated protein kinase p38 defines the common senescence-signalling pathway. Genes Cells 8, 131-144.

Jacobs,J.J., Keblusek,P., Robanus-Maandag,E., Kristel,P., Lingbeek,M., Nederlof,P.M., van Welsem,T., van de Vijver,M.J., Koh,E.Y., Daley,G.Q., Van Lohuizen,M., 2000. Senescence bypass screen identifies TBX2, which

represses Cdkn2a (p19(ARF)) and is amplified in a subset of human breast cancers. Nat. Genet. 26, 291-299.

Jiang,H., Zhang,F., Kurosu,T., Peterlin,B.M., 2005. Runx1 binds positive transcription elongation factor b and represses transcriptional elongation by RNA polymerase II: possible mechanism of CD4 silencing. Mol. Cell Biol. 25, 10675-10683.

Jin,S., Antinore,M.J., Lung,F.D., Dong,X., Zhao,H., Fan,F., Colchagie,A.B., Blanck,P., Roller,P.P., Fornace,A.J., Jr., Zhan,Q., 2000. The GADD45 inhibition of Cdc2 kinase correlates with GADD45-mediated growth suppression. J. Biol. Chem. 275, 16602-16608.

Jones,C.J., Kipling,D., Morris,M., Hepburn,P., Skinner,J., Bounacer,A., Wyllie,F.S., Ivan,M., Bartek,J., Wynford-Thomas,D., Bond,J.A., 2000. Evidence for a telomere-independent "clock" limiting RAS oncogene-driven proliferation of human thyroid epithelial cells. Mol. Cell Biol. 20, 5690-5699.

Jonveaux,P., Fenaux,P., Quiquandon,I., Pignon,J.M., Lai,J.L., Loucheux-Lefebvre,M.H., Goossens,M., Bauters,F., Berger,R., 1991. Mutations in the p53 gene in myelodysplastic syndromes. Oncogene 6, 2243-2247.

Kagoshima,H., Shigesada,K., Satake,M., Ito,Y., Miyoshi,H., Ohki,M., Pepling,M., Gergen,P., 1993. The Runt domain identifies a new family of heteromeric transcriptional regulators. Trends Genet. 9, 338-341.

Kamachi,Y., Ogawa,E., Asano,M., Ishida,S., Murakami,Y., Satake,M., Ito,Y., Shigesada,K., 1990. Purification of a mouse nuclear factor that binds to

both the A and B cores of the polyomavirus enhancer. J. Virol. 64, 4808-4819.

Kamijo,T., Bodner,S., van de,K.E., Randle,D.H., Sherr,C.J., 1999. Tumor spectrum in ARF-deficient mice. Cancer Res. 59, 2217-2222.

Kamijo,T., Zindy,F., Roussel,M.F., Quelle,D.E., Downing,J.R., Ashmun,R.A., Grosveld,G., Sherr,C.J., 1997. Tumor suppression at the mouse INK4a locus mediated by the alternative reading frame product p19ARF. Cell 91, 649-659.

Kanno,T., Kanno,Y., Chen,L.F., Ogawa,E., Kim,W.Y., Ito,Y., 1998a. Intrinsic transcriptional activation-inhibition domains of the polyomavirus enhancer binding protein 2/core binding factor alpha subunit revealed in the presence of the beta subunit. Mol. Cell Biol. 18, 2444-2454.

Kanno,Y., Kanno,T., Sakakura,C., Bae,S.C., Ito,Y., 1998b. Cytoplasmic sequestration of the polyomavirus enhancer binding protein 2 (PEBP2)/core binding factor alpha (CBFalpha) subunit by the leukemia-related PEBP2/CBFbeta-SMMHC fusion protein inhibits PEBP2/CBF-mediated transactivation. Mol. Cell Biol. 18, 4252-4261.

Katakura,Y., Nakata,E., Miura,T., Shirahata,S., 1999. Transforming growth factor beta triggers two independent-senescence programs in cancer cells. Biochem. Biophys. Res. Commun. 255, 110-115.

Kilbey,A., Blyth,K., Wotton,S., Terry,A., Jenkins,A., Bell,M., Hanlon,L., Cameron,E.R., Neil,J.C., 2007. Runx2 disruption promotes immortalization and confers resistance to oncogene-induced senescence in primary murine fibroblasts. Cancer Res. 67, 11263-11271.

Kim,R., Emi,M., Tanabe,K., Uchida,Y., Arihiro,K., 2006. The role of apoptotic or nonapoptotic cell death in determining cellular response to anticancer treatment. Eur. J. Surg. Oncol. 32, 269-277.

Kitabayashi,I., Yokoyama,A., Shimizu,K., Ohki,M., 1998. Interaction and functional cooperation of the leukemia-associated factors AML1 and p300 in myeloid cell differentiation. EMBO J. 17, 2994-3004.

Klampfer,L., Zhang,J., Zelenetz,A.O., Uchida,H., Nimer,S.D., 1996. The AML1/ETO fusion protein activates transcription of BCL-2. Proc. Natl. Acad. Sci. U. S. A 93, 14059-14064.

Ko,R.M., Kim,H.G., Wolff,L., Klug,C.A., 2008. Roles of p15Ink4b and p16Ink4a in myeloid differentiation and RUNX1-ETO-associated acute myeloid leukemia. Leuk. Res. 32, 1101-1111.

Kogan,S.C., Lagasse,E., Atwater,S., Bae,S.C., Weissman,I., Ito,Y., Bishop,J.M., 1998. The PEBP2betaMYH11 fusion created by Inv(16)(p13;q22) in myeloid leukemia impairs neutrophil maturation and contributes to granulocytic dysplasia. Proc. Natl. Acad. Sci. U. S. A 95, 11863-11868.

Komori,T., Yagi,H., Nomura,S., Yamaguchi,A., Sasaki,K., Deguchi,K., Shimizu,Y., Bronson,R.T., Gao,Y.H., Inada,M., Sato,M., Okamoto,R., Kitamura,Y., Yoshiki,S., Kishimoto,T., 1997. Targeted disruption of Cbfa1 results in a complete lack of bone formation owing to maturational arrest of osteoblasts. Cell 89, 755-764.

Krejci,O., Wunderlich,M., Geiger,H., Chou,F.S., Schleimer,D., Jansen,M., Andreassen,P.R., Mulloy,J.C., 2008. p53 signaling in response to increased

DNA damage sensitizes AML1-ETO cells to stress-induced death. Blood 111, 2190-2199.

Krimpenfort,P., Quon,K.C., Mooi,W.J., Loonstra,A., Berns,A., 2001. Loss of p16Ink4a confers susceptibility to metastatic melanoma in mice. Nature 413, 83-86.

Krtolica,A., Parrinello,S., Lockett,S., Desprez,P.Y., Campisi,J., 2001. Senescent fibroblasts promote epithelial cell growth and tumorigenesis: a link between cancer and aging. Proc. Natl. Acad. Sci. U. S. A 98, 12072-12077.

Krug,U., Ganser,A., Koeffler,H.P., 2002. Tumor suppressor genes in normal and malignant hematopoiesis. Oncogene 21, 3475-3495.

Kuilman,T., Michaloglou,C., Vredeveld,L.C., Douma,S., van Doorn,R., Desmet,C.J., Aarden,L.A., Mooi,W.J., Peeper,D.S., 2008. Oncogene-induced senescence relayed by an interleukin-dependent inflammatory network. Cell 133, 1019-1031.

Kurokawa,M., Tanaka,T., Tanaka,K., Ogawa,S., Mitani,K., Yazaki,Y., Hirai,H., 1996. Overexpression of the AML1 proto-oncoprotein in NIH3T3 cells leads to neoplastic transformation depending on the DNA-binding and transactivational potencies. Oncogene 12, 883-892.

Kurz,D.J., Decary,S., Hong,Y., Erusalimsky,J.D., 2000. Senescence-associated (beta)-galactosidase reflects an increase in lysosomal mass during replicative ageing of human endothelial cells. J. Cell Sci. 113 (Pt 20), 3613-3622.

Lai,J.L., Preudhomme,C., Zandecki,M., Flactif,M., Vanrumbeke,M., Lepelley,P., Wattel,E., Fenaux,P., 1995. Myelodysplastic syndromes and acute myeloid

leukemia with 17p deletion. An entity characterized by specific dysgranulopoiesis and a high incidence of P53 mutations. Leukemia 9, 370-381.

Langley,E., Pearson,M., Faretta,M., Bauer,U.M., Frye,R.A., Minucci,S., Pelicci,P.G., Kouzarides,T., 2002. Human SIR2 deacetylates p53 and antagonizes PML/p53-induced cellular senescence. EMBO J. 21, 2383-2396.

Lazzerini,D.E., Attwooll,C., Pasini,D., Helin,K., 2005. Deregulated E2F activity induces hyperplasia and senescence-like features in the mouse pituitary gland. Mol. Cell Biol. 25, 2660-2672.

Lee,A.C., Fenster,B.E., Ito,H., Takeda,K., Bae,N.S., Hirai,T., Yu,Z.X., Ferrans,V.J., Howard,B.H., Finkel,T., 1999. Ras proteins induce senescence by altering the intracellular levels of reactive oxygen species. J. Biol. Chem. 274, 7936-7940.

Lee,B.Y., Han,J.A., Im,J.S., Morrone,A., Johung,K., Goodwin,E.C., Kleijer,W.J., DiMaio,D., Hwang,E.S., 2006. Senescence-associated beta-galactosidase is lysosomal beta-galactosidase. Aging Cell 5, 187-195.

Lenny,N., Meyers,S., Hiebert,S.W., 1995. Functional domains of the t(8;21) fusion protein, AML-1/ETO. Oncogene 11, 1761-1769.

Levanon,D., Bettoun,D., Harris-Cerruti,C., Woolf,E., Negreanu,V., Eilam,R., Bernstein,Y., Goldenberg,D., Xiao,C., Fliegauf,M., Kremer,E., Otto,F., Brenner,O., Lev-Tov,A., Groner,Y., 2002. The Runx3 transcription factor regulates development and survival of TrkC dorsal root ganglia neurons. EMBO J. 21, 3454-3463.

Levanon,D., Brenner,O., Otto,F., Groner,Y., 2003a. Runx3 knockouts and stomach cancer. EMBO Rep. 4, 560-564.

Levanon,D., Glusman,G., Bangsow,T., Ben Asher,E., Male,D.A., Avidan,N., Bangsow,C., Hattori,M., Taylor,T.D., Taudien,S., Blechschmidt,K., Shimizu,N., Rosenthal,A., Sakaki,Y., Lancet,D., Groner,Y., 2001. Architecture and anatomy of the genomic locus encoding the human leukemia-associated transcription factor RUNX1/AML1. Gene 262, 23-33.

Levanon,D., Glusman,G., Bettoun,D., Ben Asher,E., Negreanu,V., Bernstein,Y., Harris-Cerruti,C., Brenner,O., Eilam,R., Lotem,J., Fainaru,O., Goldenberg,D., Pozner,A., Woolf,E., Xiao,C., Yarmus,M., Groner,Y., 2003b. Phylogenesis and regulated expression of the RUNT domain transcription factors RUNX1 and RUNX3. Blood Cells Mol. Dis. 30, 161-163.

Levanon,D., Groner,Y., 2004. Structure and regulated expression of mammalian RUNX genes. Oncogene 23, 4211-4219.

Levanon,D., Negreanu,V., Bernstein,Y., Bar-Am,I., Avivi,L., Groner,Y., 1994. AML1, AML2, and AML3, the human members of the runt domain gene-family: cDNA structure, expression, and chromosomal localization. Genomics 23, 425-432.

Li,Q.L., Ito,K., Sakakura,C., Fukamachi,H., Inoue,K., Chi,X.Z., Lee,K.Y., Nomura,S., Lee,C.W., Han,S.B., Kim,H.M., Kim,W.J., Yamamoto,H., Yamashita,N., Yano,T., Ikeda,T., Itohara,S., Inazawa,J., Abe,T., Hagiwara,A., Yamagishi,H., Ooe,A., Kaneda,A., Sugimura,T., Ushijima,T., Bae,S.C., Ito,Y., 2002. Causal relationship between the loss of RUNX3 expression and gastric cancer. Cell 109, 113-124.

Lin,A.W., Barradas,M., Stone,J.C., van Aelst,L., Serrano,M., Lowe,S.W., 1998. Premature senescence involving p53 and p16 is activated in response to constitutive MEK/MAPK mitogenic signaling. Genes Dev. 12, 3008-3019.

Lin,A.W., Lowe,S.W., 2001. Oncogenic ras activates the ARF-p53 pathway to suppress epithelial cell transformation. Proc. Natl. Acad. Sci. U. S. A 98, 5025-5030.

Linggi,B., Muller-Tidow,C., van de,L.L., Hu,M., Nip,J., Serve,H., Berdel,W.E., van der,R.B., Quelle,D.E., Rowley,J.D., Cleveland,J., Jansen,J.H., Pandolfi,P.P., Hiebert,S.W., 2002. The t(8;21) fusion protein, AML1 ETO, specifically represses the transcription of the p14(ARF) tumor suppressor in acute myeloid leukemia. Nat. Med. 8, 743-750.

Lou,J., Cao,W., Bernardin,F., Ayyanathan,K., RauscherIII,F.J., Friedman,A.D., 2000. Exogenous cdk4 overcomes reduced cdk4 RNA and inhibition of G1 progression in hematopoietic cells expressing a dominant-negative. Oncogene 19, 2695-2703.

Lutterbach,B., Hou,Y., Durst,K.L., Hiebert,S.W., 1999. The inv(16) encodes an acute myeloid leukemia 1 transcriptional corepressor. Proc. Natl. Acad. Sci. U. S. A 96, 12822-12827.

Lutterbach,B., Westendorf,J.J., Linggi,B., Isaac,S., Seto,E., Hiebert,S.W., 2000. A mechanism of repression by acute myeloid leukemia-1, the target of multiple chromosomal translocations in acute leukemia. J. Biol. Chem. 275, 651-656.

Lutterbach,B., Westendorf,J.J., Linggi,B., Patten,A., Moniwa,M., Davie,J.R., Huynh,K.D., Bardwell,V.J., Lavinsky,R.M., Rosenfeld,M.G., Glass,C.,

Seto,E., Hiebert,S.W., 1998. ETO, a target of t(8;21) in acute leukemia, interacts with the N-CoR and mSin3 corepressors. Mol. Cell Biol. 18, 7176-7184.

Macip,S., Igarashi,M., Fang,L., Chen,A., Pan,Z.Q., Lee,S.W., Aaronson,S.A., 2002. Inhibition of p21-mediated ROS accumulation can rescue p21-induced senescence. EMBO J. 21, 2180-2188.

Maeda,T., Hobbs,R.M., Merghoub,T., Guernah,I., Zelent,A., Cordon-Cardo,C., Teruya-Feldstein,J., Pandolfi,P.P., 2005. Role of the proto-oncogene Pokemon in cellular transformation and ARF repression. Nature 433, 278-285.

Mallette,F.A., Gaumont-Leclerc,M.F., Ferbeyre,G., 2007. The DNA damage signaling pathway is a critical mediator of oncogene-induced senescence. Genes Dev. 21, 43-48.

Mao,S., Frank,R.C., Zhang,J., Miyazaki,Y., Nimer,S.D., 1999. Functional and physical interactions between AML1 proteins and an ETS protein, MEF: implications for the pathogenesis of t(8;21)-positive leukemias. Mol. Cell Biol. 19, 3635-3644.

Mason,D.X., Jackson,T.J., Lin,A.W., 2004. Molecular signature of oncogenic ras-induced senescence. Oncogene 23, 9238-9246.

Matheny,C.J., Speck,M.E., Cushing,P.R., Zhou,Y., Corpora,T., Regan,M., Newman,M., Roudaia,L., Speck,C.L., Gu,T.L., Griffey,S.M., Bushweller,J.H., Speck,N.A., 2007. Disease mutations in RUNX1 and RUNX2 create nonfunctional, dominant-negative, or hypomorphic alleles. EMBO J. 26, 1163-1175.

McConnell,B.B., Starborg,M., Brookes,S., Peters,G., 1998. Inhibitors of cyclin-dependent kinases induce features of replicative senescence in early passage human diploid fibroblasts. Curr. Biol. 8, 351-354.

Melo,M.B., Ahmad,N.N., Lima,C.S., Pagnano,K.B., Bordin,S., Lorand-Metze,I., SaAd,S.T., Costa,F.F., 2002. Mutations in the p53 gene in acute myeloid leukemia patients correlate with poor prognosis. Hematology. 7, 13-19.

Meyers,S., Downing,J.R., Hiebert,S.W., 1993. Identification of AML-1 and the (8;21) translocation protein (AML-1/ETO) as sequence-specific DNA-binding proteins: the runt homology domain is required for DNA binding and protein-protein interactions. Mol. Cell Biol. 13, 6336-6345.

Meyers,S., Lenny,N., Hiebert,S.W., 1995. The t(8;21) fusion protein interferes with AML-1B-dependent transcriptional activation. Mol. Cell Biol. 15, 1974-1982.

Michaloglou,C., Vredeveld,L.C., Soengas,M.S., Denoyelle,C., Kuilman,T., van der Horst,C.M., Majoor,D.M., Shay,J.W., Mooi,W.J., Peeper,D.S., 2005. BRAFE600-associated senescence-like cell cycle arrest of human naevi. Nature 436, 720-724.

Miyagawa,K., Sakakura,C., Nakashima,S., Yoshikawa,T., Kin,S., Nakase,Y., Ito,K., Yamagishi,H., Ida,H., Yazumi,S., Chiba,T., Ito,Y., Hagiwara,A., 2006. Down-regulation of RUNX1, RUNX3 and CBFbeta in hepatocellular carcinomas in an early stage of hepatocarcinogenesis. Anticancer Res. 26, 3633-3643.

Miyoshi,H., Ohira,M., Shimizu,K., Mitani,K., Hirai,H., Imai,T., Yokoyama,K., Soeda,E., Ohki,M., 1995. Alternative splicing and genomic structure of the

AML1 gene involved in acute myeloid leukemia. Nucleic Acids Res. 23, 2762-2769.

Miyoshi,H., Shimizu,K., Kozu,T., Maseki,N., Kaneko,Y., Ohki,M., 1991. t(8;21) breakpoints on chromosome 21 in acute myeloid leukemia are clustered within a limited region of a single gene, AML1. Proc. Natl. Acad. Sci. U. S. A 88, 10431-10434.

Moiseeva,O., Mallette,F.A., Mukhopadhyay,U.K., Moores,A., Ferbeyre,G., 2006. DNA damage signaling and p53-dependent senescence after prolonged beta-interferon stimulation. Mol. Biol. Cell 17, 1583-1592.

Moreno-Miralles,I., Pan,L., Keates-Baleeiro,J., Durst-Goodwin,K., Yang,C., Kim,H.G., Thompson,M.A., Klug,C.A., Cleveland,J.L., Hiebert,S.W., 2005. The inv(16) cooperates with ARF haploinsufficiency to induce acute myeloid leukemia. J. Biol. Chem. 280, 40097-40103.

Morgenstern,J.P., Land,H., 1990. Advanced mammalian gene transfer: high titre retroviral vectors with multiple drug selection markers and a complementary helper-free packaging cell line. Nucleic Acids Res. 18, 3587-3596.

Morrow,M., Horton,S., Kioussis,D., Brady,H.J., Williams,O., 2004. TEL-AML1 promotes development of specific hematopoietic lineages consistent with preleukemic activity. Blood 103, 3890-3896.

Motoda,L., Osato,M., Yamashita,N., Jacob,B., Chen,L.Q., Yanagida,M., Ida,H., Wee,H.J., Sun,A.X., Taniuchi,I., Littman,D., Ito,Y., 2007. Runx1 protects hematopoietic stem/progenitor cells from oncogenic insult. Stem Cells 25, 2976-2986.

Mouton,R.E., Venable,M.E., 2000. Ceramide induces expression of the senescence histochemical marker, beta-galactosidase, in human fibroblasts. Mech. Ageing Dev. 113, 169-181.

Muller-Tidow,C., Steffen,B., Cauvet,T., Tickenbrock,L., Ji,P., Diederichs,S., Sargin,B., Kohler,G., Stelljes,M., Puccetti,E., Ruthardt,M., deVos,S., Hiebert,S.W., Koeffler,H.P., Berdel,W.E., Serve,H., 2004. Translocation products in acute myeloid leukemia activate the Wnt signaling pathway in hematopoietic cells. Mol. Cell Biol. 24, 2890-2904.

Munro,J., Barr,N.I., Ireland,H., Morrison,V., Parkinson,E.K., 2004. Histone deacetylase inhibitors induce a senescence-like state in human cells by a p16-dependent mechanism that is independent of a mitotic clock. Exp. Cell Res. 295, 525-538.

Murr,R., Loizou,J.I., Yang,Y.G., Cuenin,C., Li,H., Wang,Z.Q., Herceg,Z., 2006. Histone acetylation by Trrap-Tip60 modulates loading of repair proteins and repair of DNA double-strand breaks. Nat. Cell Biol. 8, 91-99.

Nagata,T., Gupta,V., Sorce,D., Kim,W.Y., Sali,A., Chait,B.T., Shigesada,K., Ito,Y., Werner,M.H., 1999. Immunoglobulin motif DNA recognition and heterodimerization of the PEBP2/CBF Runt domain. Nat. Struct. Biol. 6, 615-619.

Nakano,Y., Naoe,T., Kiyoi,H., Kitamura,K., Minami,S., Miyawaki,S., Asou,N., Kuriyama,K., Kusumoto,S., Shimazaki,C., Akiyama,H., Saito,K., Nishimura,M., Motoji,T., Shinagawa,K., Saito,H., Ohno,R., 2000. Prognostic value of p53 gene mutations and the product expression in de novo acute myeloid leukemia. Eur. J. Haematol. 65, 23-31.

Nam,S., Jin,Y.H., Li,Q.L., Lee,K.Y., Jeong,G.B., Ito,Y., Lee,J., Bae,S.C., 2002. Expression pattern, regulation, and biological role of runt domain transcription factor, run, in Caenorhabditis elegans. Mol. Cell Biol. 22, 547-554.

Nanjundan,M., Zhang,F., Schmandt,R., Smith-McCune,K., Mills,G.B., 2007. Identification of a novel splice variant of AML1b in ovarian cancer patients conferring loss of wild-type tumor suppressive functions. Oncogene 26, 2574-2584.

Narita,M., Narita,M., Krizhanovsky,V., Nunez,S., Chicas,A., Hearn,S.A., Myers,M.P., Lowe,S.W., 2006. A novel role for high-mobility group a proteins in cellular senescence and heterochromatin formation. Cell 126, 503-514.

Narita,M., Nunez,S., Heard,E., Narita,M., Lin,A.W., Hearn,S.A., Spector,D.L., Hannon,G.J., Lowe,S.W., 2003. Rb-mediated heterochromatin formation and silencing of E2F target genes during cellular senescence. Cell 113, 703-716.

Nebreda,A.R., Porras,A., 2000. p38 MAP kinases: beyond the stress response. Trends Biochem. Sci. 25, 257-260.

Neumeister,P., Albanese,C., Balent,B., Greally,J., Pestell,R.G., 2002. Senescence and epigenetic dysregulation in cancer. Int. J. Biochem. Cell Biol. 34, 1475-1490.

Nicke,B., Bastien,J., Khanna,S.J., Warne,P.H., Cowling,V., Cook,S.J., Peters,G., Delpuech,O., Schulze,A., Berns,K., Mullenders,J., Beijersbergen,R.L., Bernards,R., Ganesan,T.S., Downward,J., Hancock,D.C., 2005.

Involvement of MINK, a Ste20 family kinase, in Ras oncogene-induced growth arrest in human ovarian surface epithelial cells. Mol. Cell 20, 673-685.

Niitsu,N., Yamamoto-Yamaguchi,Y., Miyoshi,H., Shimizu,K., Ohki,M., Umeda,M., Honma,Y., 1997. AML1a but not AML1b inhibits erythroid differentiation induced by sodium butyrate and enhances the megakaryocytic differentiation of K562 leukemia cells. Cell Growth Differ. 8, 319-326.

Niki,M., Okada,H., Takano,H., Kuno,J., Tani,K., Hibino,H., Asano,S., Ito,Y., Satake,M., Noda,T., 1997. Hematopoiesis in the fetal liver is impaired by targeted mutagenesis of a gene encoding a non-DNA binding subunit of the transcription factor, polyomavirus enhancer binding protein 2/core binding factor. Proc. Natl. Acad. Sci. U. S. A 94, 5697-5702.

Nilsson,I., Hoffmann,I., 2000. Cell cycle regulation by the Cdc25 phosphatase family. Prog. Cell Cycle Res. 4, 107-114.

Nisson,P.E., Watkins,P.C., Sacchi,N., 1992. Transcriptionally active chimeric gene derived from the fusion of the AML1 gene and a novel gene on chromosome 8 in t(8;21) leukemic cells. Cancer Genet. Cytogenet. 63, 81-88.

Nuchprayoon,I., Meyers,S., Scott,L.M., Suzow,J., Hiebert,S., Friedman,A.D., 1994. PEBP2/CBF, the murine homolog of the human myeloid AML1 and PEBP2 beta/CBF beta proto-oncoproteins, regulates the murine myeloperoxidase and neutrophil elastase genes in immature myeloid cells. Mol. Cell Biol. 14, 5558-5568.

Nurse,P., 1990. Universal control mechanism regulating onset of M-phase. Nature 344, 503-508.

Ogawa,E., Inuzuka,M., Maruyama,M., Satake,M., Naito-Fujimoto,M., Ito,Y., Shigesada,K., 1993a. Molecular cloning and characterization of PEBP2 beta, the heterodimeric partner of a novel Drosophila runt-related DNA binding protein PEBP2 alpha. Virology 194, 314-331.

Ogawa,E., Maruyama,M., Kagoshima,H., Inuzuka,M., Lu,J., Satake,M., Shigesada,K., Ito,Y., 1993b. PEBP2/PEA2 represents a family of transcription factors homologous to the products of the Drosophila runt gene and the human AML1 gene. Proc. Natl. Acad. Sci. U. S. A 90, 6859-6863.

Ogawa,S., Satake,M., Ikuta,K., 2008. Physical and functional interactions between STAT5 and Runx transcription factors. J. Biochem. 143, 695-709.

Ogryzko,V.V., Hirai,T.H., Russanova,V.R., Barbie,D.A., Howard,B.H., 1996. Human fibroblast commitment to a senescence-like state in response to histone deacetylase inhibitors is cell cycle dependent. Mol. Cell Biol. 16, 5210-5218.

Ohtani,N., Zebedee,Z., Huot,T.J., Stinson,J.A., Sugimoto,M., Ohashi,Y., Sharrocks,A.D., Peters,G., Hara,E., 2001. Opposing effects of Ets and Id proteins on p16INK4a expression during cellular senescence. Nature 409, 1067-1070.

Okuda,T., Cai,Z., Yang,S., Lenny,N., Lyu,C.J., van Deursen,J.M., Harada,H., Downing,J.R., 1998. Expression of a knocked-in AML1-ETO leukemia gene

inhibits the establishment of normal definitive hematopoiesis and directly generates dysplastic hematopoietic progenitors. Blood 91, 3134-3143.

Okuda,T., van Deursen,J., Hiebert,S.W., Grosveld,G., Downing,J.R., 1996. AML1, the target of multiple chromosomal translocations in human leukemia, is essential for normal fetal liver hematopoiesis. Cell 84, 321-330.

Olsen,C.L., Gardie,B., Yaswen,P., Stampfer,M.R., 2002. Raf-1-induced growth arrest in human mammary epithelial cells is p16-independent and is overcome in immortal cells during conversion. Oncogene 21, 6328-6339.

Ongusaha,P.P., Ouchi,T., Kim,K.T., Nytko,E., Kwak,J.C., Duda,R.B., Deng,C.X., Lee,S.W., 2003. BRCA1 shifts p53-mediated cellular outcomes towards irreversible growth arrest. Oncogene 22, 3749-3758.

Osato,M., 2004. Point mutations in the RUNX1/AML1 gene: another actor in RUNX leukemia. Oncogene 23, 4284-4296.

Osato,M., Asou,N., Abdalla,E., Hoshino,K., Yamasaki,H., Okubo,T., Suzushima,H., Takatsuki,K., Kanno,T., Shigesada,K., Ito,Y., 1999. Biallelic and heterozygous point mutations in the runt domain of the AML1/PEBP2alphaB gene associated with myeloblastic leukemias. Blood 93, 1817-1824.

Osato,M., Ito,Y., 2005. Increased dosage of the RUNX1/AML1 gene: a third mode of RUNX leukemia? Crit Rev. Eukaryot. Gene Expr. 15, 217-228.

Otto,F., Kanegane,H., Mundlos,S., 2002. Mutations in the RUNX2 gene in patients with cleidocranial dysplasia. Hum. Mutat. 19, 209-216.

Otto,F., Lubbert,M., Stock,M., 2003. Upstream and downstream targets of RUNX proteins. J. Cell Biochem. 89, 9-18.

Palmer,T.D., Schwartz,P.H., Taupin,P., Kaspar,B., Stein,S.A., Gage,F.H., 2001. Cell culture. Progenitor cells from human brain after death. Nature 411, 42-43.

Palmero,I., Pantoja,C., Serrano,M., 1998. p19ARF links the tumour suppressor p53 to Ras. Nature 395, 125-126.

Pang,J.H., Chen,K.Y., 1994. Global change of gene expression at late G1/S boundary may occur in human IMR-90 diploid fibroblasts during senescence. J. Cell Physiol 160, 531-538.

Pantoja,C., Serrano,M., 1999. Murine fibroblasts lacking p21 undergo senescence and are resistant to transformation by oncogenic Ras. Oncogene 18, 4974-4982.

Parrinello,S., Samper,E., Krtolica,A., Goldstein,J., Melov,S., Campisi,J., 2003. Oxygen sensitivity severely limits the replicative lifespan of murine fibroblasts. Nat. Cell Biol. 5, 741-747.

Passegue,E., Wagner,E.F., 2000. JunB suppresses cell proliferation by transcriptional activation of p16(INK4a) expression. EMBO J. 19, 2969-2979.

Pearson,M., Carbone,R., Sebastiani,C., Cioce,M., Fagioli,M., Saito,S., Higashimoto,Y., Appella,E., Minucci,S., Pandolfi,P.P., Pelicci,P.G., 2000. PML regulates p53 acetylation and premature senescence induced by oncogenic Ras. Nature 406, 207-210.

Peterson,L.F., Yan,M., Zhang,D.E., 2007. The p21Waf1 pathway is involved in blocking leukemogenesis by the t(8;21) fusion protein AML1-ETO. Blood 109, 4392-4398.

Petrovick,M.S., Hiebert,S.W., Friedman,A.D., Hetherington,C.J., Tenen,D.G., Zhang,D.E., 1998. Multiple functional domains of AML1: PU.1 and C/EBPalpha synergize with different regions of AML1. Mol. Cell Biol. 18, 3915-3925.

Pines,J., 1995. Cyclins and cyclin-dependent kinases: a biochemical view. Biochem. J. 308 (Pt 3), 697-711.

Preudhomme,C., Warot-Loze,D., Roumier,C., Grardel-Duflos,N., Garand,R., Lai,J.L., Dastugue,N., MacIntyre,E., Denis,C., Bauters,F., Kerckaert,J.P., Cosson,A., Fenaux,P., 2000. High incidence of biallelic point mutations in the Runt domain of the AML1/PEBP2 alpha B gene in Mo acute myeloid leukemia and in myeloid malignancies with acquired trisomy 21. Blood 96, 2862-2869.

Prosser,H.M., Wotton,D., Gegonne,A., Ghysdael,J., Wang,S., Speck,N.A., Owen,M.J., 1992. A phorbol ester response element within the human T-cell receptor beta-chain enhancer. Proc. Natl. Acad. Sci. U. S. A 89, 9934-9938.

Ramirez,R.D., Morales,C.P., Herbert,B.S., Rohde,J.M., Passons,C., Shay,J.W., Wright,W.E., 2001. Putative telomere-independent mechanisms of replicative aging reflect inadequate growth conditions. Genes Dev. 15, 398-403.

Redondo,J.M., Pfohl,J.L., Hernandez-Munain,C., Wang,S., Speck,N.A., Krangel,M.S., 1992. Indistinguishable nuclear factor binding to functional core sites of the T-cell receptor delta and murine leukemia virus enhancers. Mol. Cell Biol. 12, 4817-4823.

Reed-Inderbitzin,E., Moreno-Miralles,I., Vanden Eynden,S.K., Xie,J., Lutterbach,B., Durst-Goodwin,K.L., Luce,K.S., Irvin,B.J., Cleary,M.L., Brandt,S.J., Hiebert,S.W., 2006. RUNX1 associates with histone deacetylases and SUV39H1 to repress transcription. Oncogene 25, 5777-5786.

Rennert,J., Coffman,J.A., Mushegian,A.R., Robertson,A.J., 2003. The evolution of Runx genes I. A comparative study of sequences from phylogenetically diverse model organisms. BMC. Evol. Biol. 3, 4.

Rhoades,K.L., Hetherington,C.J., Harakawa,N., Yergeau,D.A., Zhou,L., Liu,L.Q., Little,M.T., Tenen,D.G., Zhang,D.E., 2000. Analysis of the role of AML1-ETO in leukemogenesis, using an inducible transgenic mouse model. Blood 96, 2108-2115.

Roberson,R.S., Kussick,S.J., Vallieres,E., Chen,S.Y., Wu,D.Y., 2005. Escape from therapy-induced accelerated cellular senescence in p53-null lung cancer cells and in human lung cancers. Cancer Res. 65, 2795-2803.

Robertson,A.J., Dickey,C.E., McCarthy,J.J., Coffman,J.A., 2002. The expression of SpRunt during sea urchin embryogenesis. Mech. Dev. 117, 327-330.

Robles,S.J., Adami,G.R., 1998. Agents that cause DNA double strand breaks lead to p16INK4a enrichment and the premature senescence of normal fibroblasts. Oncogene 16, 1113-1123.

Romana,S.P., Mauchauffe,M., Le Coniat,M., Chumakov,I., Le Paslier,D., Berger,R., Bernard,O.A., 1995. The t(12;21) of acute lymphoblastic leukemia results in a tel-AML1 gene fusion. Blood 85, 3662-3670.

Roninson,I.B., 2003. Tumor cell senescence in cancer treatment. Cancer Res. 63, 2705-2715.

Sage,J., Mulligan,G.J., Attardi,L.D., Miller,A., Chen,S., Williams,B., Theodorou,E., Jacks,T., 2000. Targeted disruption of the three Rb-related genes leads to loss of G(1) control and immortalization. Genes Dev. 14, 3037-3050.

Sakakura,C., Hagiwara,A., Miyagawa,K., Nakashima,S., Yoshikawa,T., Kin,S., Nakase,Y., Ito,K., Yamagishi,H., Yazumi,S., Chiba,T., Ito,Y., 2005. Frequent downregulation of the runt domain transcription factors RUNX1, RUNX3 and their cofactor CBFB in gastric cancer. Int. J. Cancer 113, 221-228.

Sasaki,K., Yagi,H., Bronson,R.T., Tominaga,K., Matsunashi,T., Deguchi,K., Tani,Y., Kishimoto,T., Komori,T., 1996. Absence of fetal liver hematopoiesis in mice deficient in transcriptional coactivator core binding factor beta. Proc. Natl. Acad. Sci. U. S. A 93, 12359-12363.

Schmitt,C.A., Fridman,J.S., Yang,M., Lee,S., Baranov,E., Hoffman,R.M., Lowe,S.W., 2002. A senescence program controlled by p53 and p16INK4a contributes to the outcome of cancer therapy. Cell 109, 335-346.

Serrano,M., Lin,A.W., McCurrach,M.E., Beach,D., Lowe,S.W., 1997. Oncogenic ras provokes premature cell senescence associated with accumulation of p53 and p16INK4a. Cell 88, 593-602.

Seshadri,T., Campisi,J., 1990. Repression of c-fos transcription and an altered genetic program in senescent human fibroblasts. Science 247, 205-209.

Severino,J., Allen,R.G., Balin,S., Balin,A., Cristofalo,V.J., 2000. Is beta-galactosidase staining a marker of senescence in vitro and in vivo? Exp. Cell Res. 257, 162-171.

Sharpless,N.E., Bardeesy,N., Lee,K.H., Carrasco,D., Castrillon,D.H., Aguirre,A.J., Wu,E.A., Horner,J.W., DePinho,R.A., 2001. Loss of p16Ink4a with retention of p19Arf predisposes mice to tumorigenesis. Nature 413, 86-91.

Sharpless,N.E., Ramsey,M.R., Balasubramanian,P., Castrillon,D.H., DePinho,R.A., 2004. The differential impact of p16(INK4a) or p19(ARF) deficiency on cell growth and tumorigenesis. Oncogene 23, 379-385.

Shay,J.W., Pereira-Smith,O.M., Wright,W.E., 1991. A role for both RB and p53 in the regulation of human cellular senescence. Exp. Cell Res. 196, 33-39.

Shay,J.W., Roninson,I.B., 2004. Hallmarks of senescence in carcinogenesis and cancer therapy. Oncogene 23, 2919-2933.

Shelton,D.N., Chang,E., Whittier,P.S., Choi,D., Funk,W.D., 1999. Microarray analysis of replicative senescence. Curr. Biol. 9, 939-945.

Sherr,C.J., 2000. The Pezcoller lecture: cancer cell cycles revisited. Cancer Res. 60, 3689-3695.

Sherr,C.J., DePinho,R.A., 2000. Cellular senescence: mitotic clock or culture shock? Cell 102, 407-410.

Sherr,C.J., McCormick,F., 2002. The RB and p53 pathways in cancer. Cancer Cell 2, 103-112.

Shimada,M., Niida,H., Zineldeen,D.H., Tagami,H., Tanaka,M., Saito,H., Nakanishi,M., 2008. Chk1 is a histone H3 threonine 11 kinase that regulates DNA damage-induced transcriptional repression. Cell 132, 221-232.

Shimizu,K., Kitabayashi,I., Kamada,N., Abe,T., Maseki,N., Suzukawa,K., Ohki,M., 2000. AML1-MTG8 leukemic protein induces the expression of granulocyte colony-stimulating factor (G-CSF) receptor through the up-regulation of CCAAT/enhancer binding protein epsilon. Blood 96, 288-296.

Simon,M., Grandage,V.L., Linch,D.C., Khwaja,A., 2005. Constitutive activation of the Wnt/beta-catenin signalling pathway in acute myeloid leukaemia. Oncogene 24, 2410-2420.

Smogorzewska,A., de Lange,T., 2002. Different telomere damage signaling pathways in human and mouse cells. EMBO J. 21, 4338-4348.

Song,W.J., Sullivan,M.G., Legare,R.D., Hutchings,S., Tan,X., Kufrin,D., Ratajczak,J., Resende,I.C., Haworth,C., Hock,R., Loh,M., Felix,C., Roy,D.C., Busque,L., Kurnit,D., Willman,C., Gewirtz,A.M., Speck,N.A., Bushweller,J.H., Li,F.P., Gardiner,K., Poncz,M., Maris,J.M., Gilliland,D.G., 1999. Haploinsufficiency of CBFA2 causes familial thrombocytopenia with propensity to develop acute myelogenous leukaemia. Nat. Genet. 23, 166-175.

Speck,N.A., Gilliland,D.G., 2002. Core-binding factors in haematopoiesis and leukaemia. Nat. Rev. Cancer 2, 502-513.

Sreeramaneni,R., Chaudhry,A., McMahon,M., Sherr,C.J., Inoue,K., 2005. Ras-Raf-Arf signaling critically depends on the Dmp1 transcription factor. Mol. Cell Biol. 25, 220-232.

Stein,G.H., Drullinger,L.F., Soulard,A., Dulic,V., 1999. Differential roles for cyclin-dependent kinase inhibitors p21 and p16 in the mechanisms of senescence and differentiation in human fibroblasts. Mol. Cell Biol. 19, 2109-2117.

Stewart,M., Mackay,N., Cameron,E.R., Neil,J.C., 2002. The common retroviral insertion locus Dsi1 maps 30 kilobases upstream of the P1 promoter of the murine Runx3/Cbfa3/Aml2 gene. J. Virol. 76, 4364-4369.

Stewart,M., Terry,A., Hu,M., O'Hara,M., Blyth,K., Baxter,E., Cameron,E., Onions,D.E., Neil,J.C., 1997. Proviral insertions induce the expression of bone-specific isoforms of PEBP2alphaA (CBFA1): evidence for a new myc collaborating oncogene. Proc. Natl. Acad. Sci. U. S. A 94, 8646-8651.

Stewart,M., Terry,A., O'Hara,M., Cameron,E., Onions,D., Neil,J.C., 1996. til-1: a novel proviral insertion locus for Moloney murine leukaemia virus in lymphomas of CD2-myc transgenic mice. J. Gen. Virol. 77 (Pt 3), 443-446.

Sun,P., Yoshizuka,N., New,L., Moser,B.A., Li,Y., Liao,R., Xie,C., Chen,J., Deng,Q., Yamout,M., Dong,M.Q., Frangou,C.G., Yates,J.R., III, Wright,P.E., Han,J., 2007. PRAK is essential for ras-induced senescence and tumor suppression. Cell 128, 295-308.

Sun,W., Graves,B.J., Speck,N.A., 1995. Transactivation of the Moloney murine leukemia virus and T-cell receptor beta-chain enhancers by cbf and ets requires intact binding sites for both proteins. J. Virol. 69, 4941-4949.

Takahashi,A., Ohtani,N., Yamakoshi,K., Iida,S., Tahara,H., Nakayama,K., Nakayama,K.I., Ide,T., Saya,H., Hara,E., 2006. Mitogenic signalling and the p16INK4a-Rb pathway cooperate to enforce irreversible cellular senescence. Nat. Cell Biol. 8, 1291-1297.

Takahashi,A., Satake,M., Yamaguchi-Iwai,Y., Bae,S.C., Lu,J., Maruyama,M., Zhang,Y.W., Oka,H., Arai,N., Arai,K., ., 1995. Positive and negative regulation of granulocyte-macrophage colony-stimulating factor promoter activity by AML1-related transcription factor, PEBP2. Blood 86, 607-616.

Tanaka,K., Tanaka,T., Kurokawa,M., Imai,Y., Ogawa,S., Mitani,K., Yazaki,Y., Hirai,H., 1998. The AML1/ETO(MTG8) and AML1/Evi-1 leukemia-associated chimeric oncoproteins accumulate PEBP2beta(CBFbeta) in the nucleus more efficiently than wild-type AML1. Blood 91, 1688-1699.

Tanaka,T., Kurokawa,M., Ueki,K., Tanaka,K., Imai,Y., Mitani,K., Okazaki,K., Sagata,N., Yazaki,Y., Shibata,Y., Kadowaki,T., Hirai,H., 1996. The extracellular signal-regulated kinase pathway phosphorylates AML1, an acute myeloid leukemia gene product, and potentially regulates its transactivation ability. Mol. Cell Biol. 16, 3967-3979.

Tanaka,T., Tanaka,K., Ogawa,S., Kurokawa,M., Mitani,K., Nishida,J., Shibata,Y., Yazaki,Y., Hirai,H., 1995. An acute myeloid leukemia gene, AML1, regulates hemopoietic myeloid cell differentiation and transcriptional activation antagonistically by two alternative spliced forms. EMBO J. 14, 341-350.

Taniuchi,I., Osato,M., Egawa,T., Sunshine,M.J., Bae,S.C., Komori,T., Ito,Y., Littman,D.R., 2002. Differential requirements for Runx proteins in CD4

repression and epigenetic silencing during T lymphocyte development. Cell 111, 621-633.

Taylor,W.R., Stark,G.R., 2001b. Regulation of the G2/M transition by p53. Oncogene 20, 1803-1815.

Taylor,W.R., Stark,G.R., 2001a. Regulation of the G2/M transition by p53. Oncogene 20, 1803-1815.

Te Poele,R.H., Okorokov,A.L., Jardine,L., Cummings,J., Joel,S.P., 2002. DNA damage is able to induce senescence in tumor cells in vitro and in vivo. Cancer Res. 62, 1876-1883.

Toledo,L.I., Murga,M., Gutierrez-Martinez,P., Soria,R., Fernandez-Capetillo,O., 2008. ATR signaling can drive cells into senescence in the absence of DNA breaks. Genes Dev. 22, 297-302.

Towbin,H., Staehelin,T., Gordon,J., 1979. Electrophoretic transfer of proteins from polyacrylamide gels to nitrocellulose sheets: procedure and some applications. Proc. Natl. Acad. Sci. U. S. A 76, 4350-4354.

Trost,T.M., Lausch,E.U., Fees,S.A., Schmitt,S., Enklaar,T., Reutzel,D., Brixel,L.R., Schmidtke,P., Maringer,M., Schiffer,I.B., Heimerdinger,C.K., Hengstler,J.G., Fritz,G., Bockamp,E.O., Prawitt,D., Zabel,B.U., Spangenberg,C., 2005. Premature senescence is a primary fail-safe mechanism of ERBB2-driven tumorigenesis in breast carcinoma cells. Cancer Res. 65, 840-849.

Trougakos,I.P., Saridaki,A., Panayotou,G., Gonos,E.S., 2006. Identification of differentially expressed proteins in senescent human embryonic fibroblasts. Mech. Ageing Dev. 127, 88-92.

Tsuzuki,S., Seto,M., Greaves,M., Enver,T., 2004. Modeling first-hit functions of the t(12;21) TEL-AML1 translocation in mice. Proc. Natl. Acad. Sci. U. S. A 101, 8443-8448.

Uchida,H., Downing,J.R., Miyazaki,Y., Frank,R., Zhang,J., Nimer,S.D., 1999. Three distinct domains in TEL-AML1 are required for transcriptional repression of the IL-3 promoter. Oncogene 18, 1015-1022.

Uchida,H., Zhang,J., Nimer,S.D., 1997. AML1A and AML1B can transactivate the human IL-3 promoter. J. Immunol. 158, 2251-2258.

van Wijnen,A.J., Stein,G.S., Gergen,J.P., Groner,Y., Hiebert,S.W., Ito,Y., Liu,P., Neil,J.C., Ohki,M., Speck,N., 2004. Nomenclature for Runt-related (RUNX) proteins. Oncogene 23, 4209-4210.

Vangala,R.K., Heiss-Neumann,M.S., Rangatia,J.S., Singh,S.M., Schoch,C., Tenen,D.G., Hiddemann,W., Behre,G., 2003. The myeloid master regulator transcription factor PU.1 is inactivated by AML1-ETO in t(8;21) myeloid leukemia. Blood 101, 270-277.

Venable,M.E., Lee,J.Y., Smyth,M.J., Bielawska,A., Obeid,L.M., 1995. Role of ceramide in cellular senescence. J. Biol. Chem. 270, 30701-30708.

Ventura,A., Kirsch,D.G., McLaughlin,M.E., Tuveson,D.A., Grimm,J., Lintault,L., Newman,J., Reczek,E.E., Weissleder,R., Jacks,T., 2007. Restoration of p53 function leads to tumour regression in vivo. Nature 445, 661-665.

Vijayachandra,K., Lee,J., Glick,A.B., 2003. Smad3 regulates senescence and malignant conversion in a mouse multistage skin carcinogenesis model. Cancer Res. 63, 3447-3452.

Wada,T., Joza,N., Cheng,H.Y., Sasaki,T., Kozieradzki,I., Bachmaier,K., Katada,T., Schreiber,M., Wagner,E.F., Nishina,H., Penninger,J.M., 2004. MKK7 couples stress signalling to G2/M cell-cycle progression and cellular senescence. Nat. Cell Biol. 6, 215-226.

Wahl,G.M., Carr,A.M., 2001. The evolution of diverse biological responses to DNA damage: insights from yeast and p53. Nat. Cell Biol. 3, E277-E286.

Wang,L.C., Swat,W., Fujiwara,Y., Davidson,L., Visvader,J., Kuo,F., Alt,F.W., Gilliland,D.G., Golub,T.R., Orkin,S.H., 1998. The TEL/ETV6 gene is required specifically for hematopoiesis in the bone marrow. Genes Dev. 12, 2392-2402.

Wang,Q., Stacy,T., Binder,M., Marin-Padilla,M., Sharpe,A.H., Speck,N.A., 1996a. Disruption of the Cbfa2 gene causes necrosis and hemorrhaging in the central nervous system and blocks definitive hematopoiesis. Proc. Natl. Acad. Sci. U. S. A 93, 3444-3449.

Wang,Q., Stacy,T., Miller,J.D., Lewis,A.F., Gu,T.L., Huang,X., Bushweller,J.H., Bories,J.C., Alt,F.W., Ryan,G., Liu,P.P., Wynshaw-Boris,A., Binder,M., Marin-Padilla,M., Sharpe,A.H., Speck,N.A., 1996b. The CBFbeta subunit is essential for CBFalpha2 (AML1) function in vivo. Cell 87, 697-708.

Wang,S., Wang,Q., Crute,B.E., Melnikova,I.N., Keller,S.R., Speck,N.A., 1993. Cloning and characterization of subunits of the T-cell receptor and murine leukemia virus enhancer core-binding factor. Mol. Cell Biol. 13, 3324-3339.

Wang,S.W., Speck,N.A., 1992. Purification of core-binding factor, a protein that binds the conserved core site in murine leukemia virus enhancers. Mol. Cell Biol. 12, 89-102.

Wang,W., Chen,J.X., Liao,R., Deng,Q., Zhou,J.J., Huang,S., Sun,P., 2002. Sequential activation of the MEK-extracellular signal-regulated kinase and MKK3/6-p38 mitogen-activated protein kinase pathways mediates oncogenic ras-induced premature senescence. Mol. Cell Biol. 22, 3389-3403.

Wargnier,A., Legros-Maida,S., Bosselut,R., Bourge,J.F., Lafaurie,C., Ghysdael,C.J., Sasportes,M., Paul,P., 1995. Identification of human granzyme B promoter regulatory elements interacting with activated T-cell-specific proteins: implication of Ikaros and CBF binding sites in promoter activation. Proc. Natl. Acad. Sci. U. S. A 92, 6930-6934.

Waterham,H.R., Koster,J., Romeijn,G.J., Hennekam,R.C., Vreken,P., Andersson,H.C., FitzPatrick,D.R., Kelley,R.I., Wanders,R.J., 2001. Mutations in the 3beta-hydroxysterol Delta24-reductase gene cause desmosterolosis, an autosomal recessive disorder of cholesterol biosynthesis. Am. J. Hum. Genet. 69, 685-694.

Weber,J.D., Taylor,L.J., Roussel,M.F., Sherr,C.J., Bar-Sagi,D., 1999. Nucleolar Arf sequesters Mdm2 and activates p53. Nat. Cell Biol. 1, 20-26.

Wei,W., Hemmer,R.M., Sedivy,J.M., 2001. Role of p14(ARF) in replicative and induced senescence of human fibroblasts. Mol. Cell Biol. 21, 6748-6757.

Wei,W., Herbig,U., Wei,S., Dutriaux,A., Sedivy,J.M., 2003. Loss of retinoblastoma but not p16 function allows bypass of replicative senescence in human fibroblasts. EMBO Rep. 4, 1061-1066.

Weller,E.M., Poot,M., Hoehn,H., 1993. Induction of replicative senescence by 5-azacytidine: fundamental cell kinetic differences between human diploid fibroblasts and NIH-3T3 cells. Cell Prolif. 26, 45-54.

Westendorf,J.J., Yamamoto,C.M., Lenny,N., Downing,J.R., Selsted,M.E., Hiebert,S.W., 1998. The t(8;21) fusion product, AML-1-ETO, associates with C/EBP-alpha, inhibits C/EBP-alpha-dependent transcription, and blocks granulocytic differentiation. Mol. Cell Biol. 18, 322-333.

Woolf,E., Xiao,C., Fainaru,O., Lotem,J., Rosen,D., Negreanu,V., Bernstein,Y., Goldenberg,D., Brenner,O., Berke,G., Levanon,D., Groner,Y., 2003. Runx3 and Runx1 are required for CD8 T cell development during thymopoiesis. Proc. Natl. Acad. Sci. U. S. A 100, 7731-7736.

Wotton,S., Stewart,M., Blyth,K., Vaillant,F., Kilbey,A., Neil,J.C., Cameron,E.R., 2002. Proviral insertion indicates a dominant oncogenic role for Runx1/AML-1 in T-cell lymphoma. Cancer Res. 62, 7181-7185.

Wotton,S., Terry,A., Kilbey,A., Jenkins,A., Herzyk,P., Cameron,E., Neil,J.C., 2008. Gene array analysis reveals a common Runx transcriptional programme controlling cell adhesion and survival. Oncogene 27, 5856-5866.

Wotton,S.F., Blyth,K., Kilbey,A., Jenkins,A., Terry,A., Bernardin-Fried,F., Friedman,A.D., Baxter,E.W., Neil,J.C., Cameron,E.R., 2004. RUNX1

transformation of primary embryonic fibroblasts is revealed in the absence of p53. Oncogene 23, 5476-5486.

Wu,C., Miloslavskaya,I., Demontis,S., Maestro,R., Galaktionov,K., 2004. Regulation of cellular response to oncogenic and oxidative stress by Seladin-1. Nature 432, 640-645.

Xue,W., Zender,L., Miething,C., Dickins,R.A., Hernando,E., Krizhanovsky,V., Cordon-Cardo,C., Lowe,S.W., 2007. Senescence and tumour clearance is triggered by p53 restoration in murine liver carcinomas. Nature 445, 656-660.

Yagi,R., Chen,L.F., Shigesada,K., Murakami,Y., Ito,Y., 1999. A WW domain-containing yes-associated protein (YAP) is a novel transcriptional co-activator. EMBO J. 18, 2551-2562.

Yamaguchi,Y., Kurokawa,M., Imai,Y., Izutsu,K., Asai,T., Ichikawa,M., Yamamoto,G., Nitta,E., Yamagata,T., Sasaki,K., Mitani,K., Ogawa,S., Chiba,S., Hirai,H., 2004. AML1 is functionally regulated through p300-mediated acetylation on specific lysine residues. J. Biol. Chem. 279, 15630-15638.

Yamashita,N., Osato,M., Huang,L., Yanagida,M., Kogan,S.C., Iwasaki,M., Nakamura,T., Shigesada,K., Asou,N., Ito,Y., 2005. Haploinsufficiency of Runx1/AML1 promotes myeloid features and leukaemogenesis in BXH2 mice. Br. J. Haematol. 131, 495-507.

Yan,M., Burel,S.A., Peterson,L.F., Kanbe,E., Iwasaki,H., Boyapati,A., Hines,R., Akashi,K., Zhang,D.E., 2004. Deletion of an AML1-ETO C-terminal

NcoR/SMRT-interacting region strongly induces leukemia development. Proc. Natl. Acad. Sci. U. S. A 101, 17186-17191.

Yang,G., Khalaf,W., van de,L.L., Jansen,J.H., Gao,M., Thompson,M.A., van der Reijden,B.A., Gutmann,D.H., Delwel,R., Clapp,D.W., Hiebert,S.W., 2005. Transcriptional repression of the Neurofibromatosis-1 tumor suppressor by the t(8;21) fusion protein. Mol. Cell Biol. 25, 5869-5879.

Yang,Y., Wang,W., Cleaves,R., Zahurak,M., Cheng,L., Civin,C.I., Friedman,A.D., 2002. Acceleration of G(1) cooperates with core binding factor beta-smooth muscle myosin heavy chain to induce acute leukemia in mice. Cancer Res. 62, 2232-2235.

Ye,X., Zerlanko,B., Kennedy,A., Banumathy,G., Zhang,R., Adams,P.D., 2007. Downregulation of Wnt signaling is a trigger for formation of facultative heterochromatin and onset of cell senescence in primary human cells. Mol. Cell 27, 183-196.

Yergeau,D.A., Hetherington,C.J., Wang,Q., Zhang,P., Sharpe,A.H., Binder,M., Marin-Padilla,M., Tenen,D.G., Speck,N.A., Zhang,D.E., 1997. Embryonic lethality and impairment of haematopoiesis in mice heterozygous for an AML1-ETO fusion gene. Nat. Genet. 15, 303-306.

Yuan,Y., Zhou,L., Miyamoto,T., Iwasaki,H., Harakawa,N., Hetherington,C.J., Burel,S.A., Lagasse,E., Weissman,I.L., Akashi,K., Zhang,D.E., 2001. AML1-ETO expression is directly involved in the development of acute myeloid leukemia in the presence of additional mutations. Proc. Natl. Acad. Sci. U. S. A 98, 10398-10403.

Zaidi,S.K., Pande,S., Pratap,J., Gaur,T., Grigoriu,S., Ali,S.A., Stein,J.L., Lian,J.B., van Wijnen,A.J., Stein,G.S., 2007. Runx2 deficiency and defective subnuclear targeting bypass senescence to promote immortalization and tumorigenic potential. Proc. Natl. Acad. Sci. U. S. A 104, 19861-19866.

Zdanov,S., Debacq-Chainiaux,F., Remacle,J., Toussaint,O., 2006. Identification of p38MAPK-dependent genes with changed transcript abundance in H2O2-induced premature senescence of IMR-90 hTERT human fibroblasts. FEBS Lett. 580, 6455-6463.

Zeng,C., van Wijnen,A.J., Stein,J.L., Meyers,S., Sun,W., Shopland,L., Lawrence,J.B., Penman,S., Lian,J.B., Stein,G.S., Hiebert,S.W., 1997. Identification of a nuclear matrix targeting signal in the leukemia and bone-related AML/CBF-alpha transcription factors. Proc. Natl. Acad. Sci. U. S. A 94, 6746-6751.

Zhan,Q., Antinore,M.J., Wang,X.W., Carrier,F., Smith,M.L., Harris,C.C., Fornace,A.J., Jr., 1999. Association with Cdc2 and inhibition of Cdc2/Cyclin B1 kinase activity by the p53-regulated protein Gadd45. Oncogene 18, 2892-2900.

Zhang,D.E., Hetherington,C.J., Meyers,S., Rhoades,K.L., Larson,C.J., Chen,H.M., Hiebert,S.W., Tenen,D.G., 1996. CCAAT enhancer-binding protein (C/EBP) and AML1 (CBF alpha2) synergistically activate the macrophage colony-stimulating factor receptor promoter. Mol. Cell Biol. 16, 1231-1240.

Zhang,H., Cohen,S.N., 2004. Smurf2 up-regulation activates telomere-dependent senescence. Genes Dev. 18, 3028-3040.

Zhang,H., Pan,K.H., Cohen,S.N., 2003a. Senescence-specific gene expression fingerprints reveal cell-type-dependent physical clustering of up-regulated chromosomal loci. Proc. Natl. Acad. Sci. U. S. A 100, 3251-3256.

Zhang,L., Li,Z., Yan,J., Pradhan,P., Corpora,T., Cheney,M.D., Bravo,J., Warren,A.J., Bushweller,J.H., Speck,N.A., 2003b. Mutagenesis of the Runt domain defines two energetic hot spots for heterodimerization with the core binding factor beta subunit. J. Biol. Chem. 278, 33097-33104.

Zhang,L., Lukasik,S.M., Speck,N.A., Bushweller,J.H., 2003c. Structural and functional characterization of Runx1, CBF beta, and CBF beta-SMMHC. Blood Cells Mol. Dis. 30, 147-156.

Zhang,R., Poustovoitov,M.V., Ye,X., Santos,H.A., Chen,W., Daganzo,S.M., Erzberger,J.P., Serebriiskii,I.G., Canutescu,A.A., Dunbrack,R.L., Pehrson,J.R., Berger,J.M., Kaufman,P.D., Adams,P.D., 2005. Formation of MacroH2A-containing senescence-associated heterochromatin foci and senescence driven by ASF1a and HIRA. Dev. Cell 8, 19-30.

Zhang,Y., Xiong,Y., Yarbrough,W.G., 1998. ARF promotes MDM2 degradation and stabilizes p53: ARF-INK4a locus deletion impairs both the Rb and p53 tumor suppression pathways. Cell 92, 725-734.

Zhu,J., Woods,D., McMahon,M., Bishop,J.M., 1998. Senescence of human fibroblasts induced by oncogenic Raf. Genes Dev. 12, 2997-3007.

Zindy,F., Eischen,C.M., Randle,D.H., Kamijo,T., Cleveland,J.L., Sherr,C.J., Roussel,M.F., 1998. Myc signaling via the ARF tumor suppressor regulates p53-dependent apoptosis and immortalization. Genes Dev. 12, 2424-2433.

Ziv,Y., Bielopolski,D., Galanty,Y., Lukas,C., Taya,Y., Schultz,D.C., Lukas,J., Bekker-Jensen,S., Bartek,J., Shiloh,Y., 2006. Chromatin relaxation in response to DNA double-strand breaks is modulated by a novel ATM- and KAP-1 dependent pathway. Nat. Cell Biol. 8, 870-876.